IL
NUOVO CIMENTO
ORGANO DELLA SOCIETÀ ITALIANA DI FISICA
SOTTO GLI AUSPICI DEL CONSIGLIO NAZIONALE DELLE RICERCHE

VOL. II, N. 2 *Serie decima* 1° Agosto 1955

The Evaluation of Transformation Functions by Means of the Feynman Path Integral.

W. K. BURTON and A. H. DE BORDE
Natural Philosophy Department, University of Glasgow

(ricevuto il 6 Maggio 1955)

Summary. — A parametric representation of the Feynman path integral is used to evaluate the transformation function for some simple systems in particle dynamics. The method is used for systems having equations of motion of the first and second orders.

1. – Introduction.

Despite the success of quantum field theory in evaluating radiative corrections in electrodynamics by perturbation methods, difficulties have arisen in applying similar methods to meson fields in view of the stronger coupling involved. Some attention has, therefore, recently been paid to possible alternative formulations which offer the hope of more general methods of calculation. In particular, SCHWINGER (1) has demonstrated that equations governing the behaviour of dynamical systems may be obtained from a variational principle, and in certain cases has succeeded in integrating these equations to obtain the transformation function. DAVISON (2), MATTHEWS and SALAM (3), and POLKINGHORNE (4) have generalized the path integral formalism, originally

(1) J. SCHWINGER: *Phys. Rev.*, **82**, 914 (1951); **91**, 713 (1953).
(2) B. DAVIDSON: *Proc. Roy. Soc.*, A **225**, 252 (1954).
(3) P. T. MATTHEWS and A. SALAM: *Nuovo Cimento*, **12**, 563 (1954).
(4) J. C. POLKINGHORNE: *Proc. Roy. Soc.*, A **230**, 272, (1955).

introduced by FEYNMAN (5) as an alternative formulation of particle dynamics, and thereby obtained commutation relations and field equations equivalent to those of SCHWINGER. In fact, the Schwinger principle may be derived from the path integral formalism, as demonstrated by BURTON (6).

It should now be remarked that calculations of approximate Green's functions by EDWARDS and PEIERLS (7) by integration of the Schwinger equations have led to functional integrals closely resembling those encountered in the path integral.

It is the purpose of this paper to show that the parametric form of Feynman's principle due to DAVISON (2) can be used directly to evaluate transformation functions. The technique is applied here to the free particle, the two-dimensional rigid rotator and the harmonic oscillator. The latter is treated using both second order and first order Lagrangians.

DAVISON expresses Feynman's integral as

$$(1) \qquad (x, t\,|\,x_0, 0) = (m/2\pi i\hbar t)^{\frac{1}{2}} \int_{-\infty}^{\infty} \frac{\mathrm{d}a_1}{\sqrt{i}} \int_{-\infty}^{\infty} \frac{\mathrm{d}a_2}{\sqrt{i}} \ldots \exp\left[\frac{i}{\hbar}\int_0^t L(x(t'), \dot{x}(t'))\,\mathrm{d}t'\right]$$

by expanding the velocity as

$$(2) \qquad \dot{x}(t') = (2\pi\hbar/mt)^{\frac{1}{2}} \sum_{n=0}^{\infty} a_n \varphi_n(t'/t)\,,$$

where $\varphi_n(z)$ form a complete orthonormal sequence of functions in the range $0 < z < 1$, and $\varphi_0(z) = 1$. The expansion for $x(t')$ is obtained by integrating (2) with the initial condition that $x(0) = x_0$. We choose

$$(3) \qquad \varphi_n(z) = \sqrt{2}\cos n\pi z\,, \qquad n > 0.$$

2. – Applications.

a) The free particle. – Here the Lagrangian is given by

$$(4) \qquad L = \tfrac{1}{2}m\dot{x}^2\,.$$

Thus

$$(5) \qquad \frac{i}{\hbar}\int_0^t L\,dt' = i\pi \sum_0^{\infty} a_n^2 = i\pi a_0^2 + i\pi \sum_1^{\infty} a_n^2\,,$$

(5) R. P. FEYNMAN: *Rev. Mod. Phys.*, **20**, 367 (1948).
(6) W. K. BURTON: *Nuovo Cimento*, **1**, 355 (1955).
(7) R. E. PEIERLS and S. F. EDWARDS: *Proc. Roy. Soc.*, A **224**, 24 (1954).

with

$$a_0^2 = (m/2\pi\hbar t)(x - x_0)^2 , \qquad x = x(t). \tag{6}$$

The integrals over a_n with $n > 0$ may be directly performed by using

$$\int_{-\infty}^{\infty} \exp\left[i(\alpha x^2 + kx)\right] \mathrm{d}x = (i\pi/\alpha)^{\frac{1}{2}} \exp\left[-ik^2/4\alpha\right] . \tag{7}$$

Including the factors $\sqrt{i}$ in the denominator of (1), we obtain finally

$$(x, t \,|\, x, 0) = (m/2\pi i\hbar t)^{\frac{1}{2}} \exp\left[\frac{im}{2\hbar t}(x - x_0)^2\right] . \tag{8}$$

b) The two dimensional rigid rotator. – The Lagrangian in this case is $\frac{1}{2}I\dot{\theta}^2$ and the calculation is thus essentially the same as for the free particle. Since, however, θ is a periodic variable we cannot distinguish between θ and $\theta + 2n\pi$ where n is any positive or negative integer. The transformation function will, therefore, be obtained in a more recognizable form if we sum over all indistinguishable values of the final variable. Thus

$$(\theta, t \,|\, \theta_0, 0) = (I/2\pi i\hbar t)^{\frac{1}{2}} \sum_{n=-\infty}^{\infty} \exp\left[\frac{iI}{2\hbar t}(\theta - \theta_0 + 2n\pi)^2\right] . \tag{9}$$

This can be re-expressed in a more convenient form by means of Poisson's summation formula

$$\sum_{n=-\infty}^{\infty} f(2n\pi) = \sum_{k=-\infty}^{\infty} \frac{1}{2\pi} \int_{-\infty}^{\infty} \mathrm{d}y\, f(y) \exp\left[-iky\right] . \tag{10}$$

Thus

$$(\theta, t \,|\, \theta_0, 0) = \frac{1}{2\pi} \sum_{n=-\infty}^{\infty} \exp\left[in(\theta - \theta_0) - in^2\hbar t/2I\right] . \tag{11}$$

Since any transformation function for a system with discrete energy eigenvalue E_n and wave functions $\psi_n(q)$ can be expressed by

$$(q, t \,|\, q_0, 0) = \sum_n \psi_n(q)\psi_n^*(q_0) \exp\left[-iE_n t/\hbar\right], \tag{12}$$

the energy eigenvalues are $E_n = n^2\hbar^2/2I$ and the corresponding eigenfunctions are $(2\pi)^{-\frac{1}{2}} \exp\left[in\theta\right]$ with $n = 0, \pm 1, \pm 2, \ldots$.

c) The harmonic oscillator. – The classical Lagrangian is

$$L = \tfrac{1}{2}m(\dot{x}^2 - \omega^2 x^2) \tag{13}$$

so that

$$\frac{i}{\hbar}\int_0^t L\,\mathrm{d}t' = \frac{imt}{2\hbar}\left\{\frac{(x-x_0)^2}{t^2} - \frac{\omega^2}{3}(x^2 + xx_0 + x_0^2)\right\} + \tag{14}$$

$$+ i\sum_{n=1}^{\infty}\left\{\pi\left(1 - \frac{\omega^2 t^2}{n^2\pi^2}\right)a_n^2 - \left(\frac{\omega t}{n\pi}\right)^2\left(\frac{4\pi m}{\hbar t}\right)^{\frac{1}{2}}(x_0 - (-1)^n x)a_n\right\}.$$

Each integration over a_n is of the form (7). Thus

$$(x, t\,|\,x_0, 0) = (m/2\pi i\hbar t)^{\frac{1}{2}}\left\{\prod_{n=1}^{\infty}\left(1 - \frac{\omega^2 t^2}{n^2\pi^2}\right)^{-\frac{1}{2}}\right\}\cdot \tag{15}$$

$$\cdot\exp\left[\frac{imt}{2\hbar}\cdot\left\{\frac{(x-x_0)^2}{t^2} - \frac{1}{3}\omega^2(x^2 + xx_0 + x_0^2)\right\}\right]\cdot$$

$$\cdot\exp\left[-\frac{im\omega^4 t^3}{\hbar\pi^4}\sum_1^{\infty}\frac{x^2 + x_0^2 - 2xx_0(-1)^n}{n^2(n^2 - (\omega t/\pi)^2)}\right] =$$

$$= \left\{\frac{m\omega}{2\pi i\hbar\sin\omega t}\right\}^{\frac{1}{2}}\exp\left[\frac{im\omega}{2\hbar}\cdot\{(x^2 + x_0^2)\cot\omega t - 2xx_0\,\mathrm{cosec}\,\omega t\}\right],$$

where we have used

$$\begin{cases} \displaystyle\prod_{n=1}^{\infty}\left(1 - \frac{z^2}{n^2}\right) = \frac{\sin\pi z}{\pi z} \\ \displaystyle\sum_{n=1}^{\infty}\frac{1}{n^2(n^2 - z^2)} = \frac{1}{z^2}\left\{\frac{1}{2z^2} - \frac{\pi}{2z}\cot\pi z - \frac{\pi^2}{6}\right\} \\ \displaystyle\sum_{n=1}^{\infty}\frac{(-1)^n}{n^2(n^2 - z^2)} = \frac{1}{z^2}\left\{\frac{1}{2z^2} - \frac{\pi}{2z}\,\mathrm{cosec}\,\pi z + \frac{\pi^2}{12}\right\}. \end{cases} \tag{16}$$

The energy eigenvalues may be obtained as follows. From (12) we find

$$\int \mathrm{d}x\,(x, t\,|\,x, 0) = \sum_{n=0}^{\infty}\exp\left[-iE_n t/\hbar\right] = \tag{17}$$

$$= \left(\frac{m\omega}{2\pi i\hbar\sin\omega t}\right)^{\frac{1}{2}}\int \mathrm{d}x\exp\left[\frac{im\omega x^2}{\hbar}(\cot\omega t - \mathrm{cosec}\,\omega t)\right] =$$

$$= \sum_{n=0}^{\infty}\exp\left[-\left(n + \frac{1}{2}\right)i\omega t\right].$$

Since many of the field equations of quantum mechanics involve only first order time derivatives, it is of interest to examine a Lagrangian which gives first order equations of motion, such as

$$L = \tfrac{1}{2}m\omega(x_1\dot{x}_2 - x_2\dot{x}_1 + \omega(x_1^2 + x_2^2)) \,. \tag{18}$$

The form (1) of DAVISON was based on the assumption that the Lagrangian contains the time derivative in the form $\frac{1}{2}m\dot{x}^2$ and we must be prepared to find that the normalization is no longer correct for a Lagrangian such as (18). It is convenient to set aside all questions of normalization until the x-dependence of the transformation function has been found. The correct normalization factor in the latter (which depends on t) can then be found by demanding that the correct composition law for transformation functions be obeyed.

With this understanding we shall take for the set of paths over which the integration must be performed

$$\left| \begin{array}{l} x_1(t') = x_0 + (x - x_0)(t'/t) + \sum_0^\infty a_n \sin(n\pi t'/t) \\ x_2(t') = \sum_0^\infty b_n \cos(n\pi t'/t) \,. \end{array} \right. \tag{19}$$

It is clear that only one of x_1 and x_2 can be prescribed at the initial and final times, since x_1 and x_2 are classically conjugate. We choose to specify x_1 at both times, and to integrate over all values of x_2. This is the reason for the choice of the second equation of (19). The use the of Lagrangian (18) with (19) leads, on performing the integrations to an indeterminate sum in the exponent. This can be avoided by adding a time derivative to L. With the Lagrangian

$$L' = L - \frac{1}{2}\, m\omega \frac{\mathrm{d}}{\mathrm{d}t}(x_1 x_2) \tag{20}$$

we find

$$\int_0^t L'\,\mathrm{d}t' = \frac{1}{2}\, m\omega \left\{ \frac{1}{3}\,\omega t(x^2 + xx_0 + x_0^2) + \omega t b_0^2 - 2b_0(x - x_0) + \right. \tag{21}$$

$$\left. + \sum_{n=1}^\infty \left[\frac{1}{2}\,\omega t(b_n^2 + a_n^2) - n\pi a_n b_n + \frac{2\omega t}{n\pi}\, a_n(x_0 - (-1)^n x) \right] \right\} .$$

On carrying out the integrations over the a_n and b_n, and absorbing all factors which depend only on t (i.e. independent of x and x_0) into the at present

unknown normalisation factor N, we obtain

$$(22)\qquad \left\{\begin{aligned}(x,t\,|\,x_0,0) &= N\exp\left[\frac{im\omega}{2\hbar}\cdot\left\{\frac{\omega t}{3}(x^2+xx_0+x_0^2)-\frac{(x-x_0)^2}{\omega t}-\right.\right.\\ &\left.\left.-\sum_1^\infty\frac{2\omega t}{n^2\pi^2}\,\frac{x_0-(-1)^n x}{1-(n\pi/\omega t)^2}\right\}\right]=\\ &= N\exp\left[\frac{im\omega}{2\hbar}\cdot\{(x^2+x_0^2)\cot\omega t-2xx_0\operatorname{cosec}\omega t\}\right].\end{aligned}\right.$$

This agrees with (15) if N is chosen to be

$$(23)\qquad N(t)=(m\omega/2\pi i\hbar\sin\omega t)^{\frac{1}{2}}.$$

However, the N is fixed by the composition law up to a factor which may be written $\exp[-iE_0t/\hbar]$, which may be regarded as specifying the zero on the energy scale.

RIASSUNTO (*)

Si fa ricorso a una rappresentazione parametrica dell'integrale di Feynman per calcolare la funzione di trasformazione per alcuni sistemi semplici in dinamica delle particelle. Si applica il metodo a sistemi con equazioni di moto del primo e del secondo ordine.

(*) *Traduzione a cura della Redazione.*

IL NUOVO CIMENTO Vol. II, N. 2 1° Agosto 1955

Covariant One-time Formulation of the Many-body Problem in Quantum Theory.

W. Królikowski

Institute of Physics of the Polish Academy of Sciences - Warsaw

J. Rzewuski

Institute of Physics of the Polish Academy of Sciences - Wroclaw

(ricevuto il 6 Maggio 1955)

Summary. — A covariant one-time formulation of the many-body problem in quantum field theory is obtained by transforming the conventional many-time equations of this problem into other equivalent equations which relate only those values of the wave function and its derivatives which correspond to one space-like hypersurface σ. The transformation is carried out for arbitrary values of the coupling constant λ with exceptions of certain characteristic values λ_k. For small values of λ explicit expressions are given for the kernels of the one-time equations by means of expansions in powers of λ. These kernels are uniquely determined by the kernels of the original many-time equations. In the absence of external forces the kernels of the one-time equations are independent of the time variable. These equations may be treated, therefore, by means of the stationary perturbation methods in contradistinction to the original many-time equations which do not admit stationary treatment.

1. – Introduction.

Many important problems of theoretical physics are formulated in terms of integro-differential equations. In particular the basic equations of the theory of bound states and of the non-local theory of elementary particles are partial integro-differential equations in Minkowski's space containing integrals over

four-dimensional regions of space-time. The equations provide us with a *many-time* description of physical events in the sense that they relate values of the unknown functions and their derivatives corresponding to different values of the time variable. The question arises whether it is possible to construct a mathematical three-dimensional formalism providing an equivalent covariant *one-time* description of the phenomena. Such a one-time description could be of importance as well for the theoretical development of the theory as for the practical problem of determining the solutions. Therefore, several authors (SALPETER (1952), LÉVY (1952), MACKE (1953), KLEIN (1954_1), and recently KURŞUNOĞLU (1954)) investigated the problem of reducing the four-dimensional formalism for bound states (SCHWINGER (1951), BETHE and SALPETER (1951), GÜNTHER (1952, 1954)) to the three dimensional one and of connecting the latter with the three-dimensional Tamm-Dancoff formalism (old: LÉVY (1952), KLEIN (1953), CINI (1953) and new: DYSON (1953), TAYLOR (1954_1)). The effective calculations were based on the assumption of a certain kind of separability of the relative time or relative energy dependence in the four-dimensional wave function, which assumption was only approximately true. Moreover, the relation between the four-dimensional and three-dimensional wave functions allowed in general no clear interpretation. It was even emphasized (KLEIN (1954_1)) that in general an exact covariant one-time formulation of many-time theories described by integro-differential equations is impossible.

It is the aim of the present paper to show, that a covariant partial integro-differential equation in Minkowski's space may be always replaced by another *equivalent* covariant integro-differential equation containing surface integrals over one space-like surface σ only. These surface integrals are independent of the particular position of σ in the considered domain and, therefore, may be chosen in such a way that the resulting equation relates only those values of the unknown function and their derivatives which correspond to points situated on the same surface. Such an equation yields obviously a one-time formulation of the theory, the surface σ being the relativistically invariant generalization of the conception of time.

The proof of this equivalence theorem may be carried out for a wide class of integro-differential equations. To avoid unessential complications, however, we shall confine ourselves to the consideration of a particular type of equations describing a system of two particles with spin $\frac{1}{2}$ interacting by means of a Bose-field. These equations are of particular importance for the theory of bound states. Considerations concerning the same problem in the non-local theories of elementary particles are published elsewhere (RZEWUSKI (1954)). It is an open question how the three-dimensional formalism presented in this paper is related to the new Tamm-Dancoff formalism (DYSON (1953)).

2. – Equivalence Theorem.

Consider the system of two integro-differential equations

$$(2.1) \qquad (\underset{\sim}{\partial}^{(i)} + \varkappa^{(i)})\,\psi(x_1, x_2) = \lambda \int_{\sigma_I}^{\sigma_{II}} G^{(i)}(x_1, x_2; x_1', x_2')\,\psi(x_1', x_2')\,\mathrm{d}x_1'\,\mathrm{d}x_2' \qquad (i = 1, 2)$$

where $\underset{\sim}{\partial}^{(i)} = \gamma_\mu^{(i)}\partial_\mu$, $(\gamma_\mu^{(i)}) = (-i\beta^{(i)}\boldsymbol{\alpha}^{(i)}, \beta^{(i)})$, $\partial_\mu^{(i)} = \partial/\partial x_\mu^{(i)}$, and the unknown function ψ is a function of two points x_1 and x_2 of Minkowski's space with the coordinates $x_\mu^{(1)}$ and $(x_\mu^{(2)}/x^{(i)} = (x_i, ict_i))$. $\mathrm{d}x_1$ and $\mathrm{d}x_2$ are fourdimensional volume elements around these points and the integration is carried out over a domain Ω of space-time contained between two fixed space-like hypersurfaces σ_I and σ_{II} (*) The kernels $G^{(i)}$ of equation (2.1) are given functions of four points. In the case of spin $\frac{1}{2}$, ψ is a second rank bispinor field and $G^{(i)}$ are fourth rank bispinors. λ and $\varkappa^{(i)}$ $(i = 1, 2)$ are parameters.

Equations of the type (2.1) are used for the determination of the wave function $\psi(x_1, x_2)$ in the configurational space of two fermions interacting by means of a Bose-field (cf. BETHE and SALPETER (1951), GÜNTHER (1952, 1954)). This wave function may be interpreted as the probability amplitude of finding two fermions at the points x_1 and x_2 respectively (+) only if the distance $x_\mu^{(1)} - x_\mu^{(2)}$ is space-like. Otherwise the two events are dynamically dependent (causally connected) and the probabilistic interpretation of the conventional quantum theory is impossible. This is due to the fact that the observables x_1 and x_2 do not form a commuting set if one of them lies in the inside of the light cone of the other.

In (2.1) the function $\psi(x_1', x_2')$ appears integrated over the whole domain Ω with respect to x_1' as well as with respect to x_2'. Even if we consider the points x_1 and x_2 occurring on the left hand side of (2.1) to be space-like, on the right hand side of (2.1) time-like distances will appear. In this way values

(*) The considerations of this paper are carried out in such a way that no use is made of the finiteness of the integration domain Ω. Thus in particular, we may also consider equations of the type (2.1) containing integrals over the whole of space-time i.e. we may remove in (2.1) σ_I and σ_{II} into $-\infty$ and $+\infty$ respectively.

(+) When speaking about the interpretation of the wave function in Bethe-Salpeter formalism one ought to keep in mind that « configurational » fermions have for background the vacuum of interacting particles (cf. GÜNTHER (1954)). A similar situation exists in the new Tamm-Dancoff formalysm (DYSON (1953)), while in the old Tamm-Dancoff formalism the background of « configurational » fermions is formed by the vacuum of free particles. In the last case the wave function has the meaning of the probability amplitude in the conventional sense. The wave function of Günther formalism can be specialized for space-like configurations in both above ways.

of the function ψ and their derivatives which admit a probabilistic interpretation are related with those values for which such interpretation is impossible. It is seen that already from the general point of view of statistical interpretation of the theory it is desirable to replace equation (2.1) by an equivalent equation in which only space-like distances would occur.

We are going now to prove the following equivalence theorem: The system (2.1) of integro-differential equations is equivalent with the system

$$(2.2)\qquad (\underset{\sim}{\partial}^{(i)} + \varkappa^{(i)})\,\psi(x_1, x_2) = \\ = \lambda \int\limits_{\sigma_1}\int\limits_{\sigma_2} A^{(i)}[\sigma_1, \sigma_2](x_1, x_2; x_1', x_2')\,\gamma_\mu^{(1)}\gamma_\mu^{(2)}\psi\,(x_1' x_2')\,\mathrm{d}\sigma_\mu^{(1)\prime}\,\mathrm{d}\sigma_\mu^{(2)\prime} \qquad (i = 1, 2)$$

for x_1 and x_2 inside Ω, and if following conditions are satisfied:

1) The kernels $G^{(i)}$ admit unique solutions of (2.4) and (2.10) in particular a solution of (2.4) in the form (2.9);

2) λ does not belong the to the spectrum of characteristic values of these equations.

The equivalence is unterstood in the sense that each solution of (21) satisfies equation (2.2) and vice versa each solution of (2.2) satisfies equation (2.1). The integrations in (2.2) are carried out over two arbitrary space-like surfaces σ_1 and σ_2 of the domain Ω. The kernels $A^{(i)}[\sigma_1, \sigma_2](x_1, x_2; x_1', x_2')$ of equations (2.2) are functions of the points x_1, x_2, x_1', x_2' and functionals of the surfaces σ_1 and σ_2. They are determined by the kernels $G^{(i)}(x_1, x_2; x_1', x_2')$ of the original equations (2.1).

Proof: By means of two arbitrary particular solutions $K^{(1)}(x)$ and $K^{(2)}(x)$ of the two equations:

$$(2.3)\qquad (\underset{\sim}{\partial} + \varkappa^{(i)})K^{(i)}(x) = \delta(x) \qquad (i = 1, 2)$$

it is possible to replace equations (2.1) by the equivalent integral equation

$$(2.4)\qquad \psi(x_1, x_2) = \psi^0(x_1, x_2) + \lambda \int\limits_{\sigma_I}^{\sigma_{II}}\int P(x_1, x_2; x_1', x_2')\,\psi(x_1', x_2')\,\mathrm{d}x_1'\,\mathrm{d}x_2',$$

where $\psi^0(x_1, x_2)$ is the general solution of the set

$$(2.5)\qquad (\underset{\sim}{\partial}^{(i)} + \varkappa^{(i)})\psi^0(x_1, x_2) = 0 \qquad (i = 1, 2)$$

and

$$(2.6)\qquad P(x_1, x_2; x_1', x_2') = \int\limits_{D_f}^{\sigma_{II}} K^{(1)}(x_1 - x_1'')\,\mathrm{d}x_1''\,G^{(1)}(x_1'', x_2; x_1', x_2') \equiv \\ \equiv \int\limits_{\sigma_I}^{\sigma_{II}} K^{(2)}(x_2 - x_2'')\,\mathrm{d}x_2''\,G^{(2)}(x_1, x_2''; x_1', x_2').$$

The second equality in (2.6) is a condition upon $G^{(i)}$ and $K^{(i)}$. Another condition is obtained by differentiation of (2.1):

$$(\underset{\sim}{\partial}^{(1)} + \varkappa^{(1)}) G^{(2)}(x_1, x_2; x_1', x_2') \equiv$$

$$\equiv (\underset{\sim}{\partial}^{(2)} + \varkappa^{(2)}) G^{(1)}(x_1, x_2; x_1', x_2') \underset{Df}{=} \bar{G}(x_1, x_2; x_1', x_2') . \tag{2.7}$$

It is easily seen that both conditions (2.6) and (2.7) are satisfied if the $G^{(i)}$ are of the form

$$\begin{cases} G^{(1)}(x_1, x_2; x_1', x_2') = \int\limits_{\sigma_{\mathrm{I}}}^{\sigma_{\mathrm{II}}} K^{(2)}(x_2 - x_2'') \, \mathrm{d}x_2'' \, \bar{G}(x_1, x_2''; x_1', x_2') , \\ G^{(2)}(x_1, x_2; x_1', x_2') = \int\limits_{\sigma_{\mathrm{I}}}^{\sigma_{\mathrm{II}}} K^{(1)}(x_1 - x_1'') \, \mathrm{d}x_1'' \, \bar{G}(x_1'', x_2; x_1', x_2') . \end{cases} \tag{2.8}$$

Conditions (2.6) and (2.7) are necessary and sufficient for the consistency of the set (2.1). If the $G^{(i)}$ are of the form (2.8) these conditions are satisfied for arbitrary particular solutions $K^{(i)}$ of (2.3). One obtains the equations of GÜNTHER (1952, 1954) and BETHE-SALPETER (1951) by taking for $K^{(i)}$ the retarded or Feynman's solutions of equations (2.3) respectively.

The integral equation (2.4) is equivalent in the domain Ω with the set of integro-differential equations (2.1) in the sense that each solution of (2.1) satisfies equation (2.4) with a properly chosen ψ^0 and inversely the solution of (2.4) satisfies (2.1) if ψ^0 is an arbitrary solution of (2.5). The first part of this statement may be verified by multiplication of (2.1) by $K^{(i)}(x' - x)$ and integration over x, the second part by multiplication of (2.4) with the differential operators $\underset{\sim}{\partial}^{(i)} + \varkappa^{(i)}$ $(i = 1, 2,)$ respectively.

We assume now, that the kernels $G^{(i)}$ admit a unique solution of equations (2.4) in the form

$$\psi(x_1, x_2) = \psi^0(x_1, x_2) + \lambda \int\limits_{\sigma_{\mathrm{I}}}^{\sigma_{\mathrm{II}}} \!\!\!\int R(x_1, x_2; x_1', x_2') \, \psi^0(x_1', x_2') \, \mathrm{d}x_1' \, \mathrm{d}x_2' , \tag{2.9}$$

where the resolving kernel $R(x_1, x_2; x_1', x_2')$ is in general a singular function of the parameter λ (*), the singularities of R determining the spectrum of characteristic values λ_k corresponding to equation (2.4). We assume further that the value of λ occuring in our equations does not belong to this spectrum.

(*) If the kernels $G^{(i)}$ are such that P is quadratically integrable then Fredholm's theorems may be applied and R is a meromorphic function of λ.

Let us introduce now the quantities $A^{(i)}[\sigma_1, \sigma_2](x_1, x_2; x_1', x_2')$ by means of the integral equations

$$
\begin{aligned}
(2.10)\quad A^{(i)}[\sigma_1, \sigma_2](x_1, x_2; x_1', x_2') = \\
= \{G^{(i)}S\}(x_1, x_2; x_1', x_2') + \lambda\{G^{(i)}RS\}(x_1, x_2; x_1', x_2') - \\
- \lambda \int_{\sigma_1}\int_{\sigma_2} A^{(i)}[\sigma_1, \sigma_2](x_1, x_2; x_1'', x_2'')\, \gamma_\mu^{(1)} \gamma_\nu^{(2)} \{RS\} \cdot \\
\cdot (x_1'', x_2''; x_1', x_2')\, \mathrm{d}\sigma_\mu^{(1)''}\, \mathrm{d}\sigma_\nu^{(2)''} \qquad (i = 1, 2)
\end{aligned}
$$

where

$$
(2.11)\qquad S(x_1, x_2; x_1', x_2') = S^{(1)}(x_1 - x_1')S^{(2)}(x_2 - x_2')
$$

is a particular solution of the homogeneous equations (2.5) defined in terms of the well known Jordan-Pauli singular function $\Delta(x)$

$$
(2.12)\qquad S^{(i)}(x) = (\partial + \varkappa^{(i)})\Delta^{(i)}(x)\,,
$$

the upper index « i » in $\Delta^{(i)}$ corresponding to the particular value of $\varkappa^{(i)}$ $(i=1, 2)$ used for the construction of this function. The symbols $\{AB \ldots C\}(x_1, x_2; x_1', x_2')$ occuring in (2.10) are introduced for abbreviation and denote convolutions of the functions inside the bracket. Thus

$$
\begin{aligned}
(2.13)\qquad \{AB \ldots C\}(x_1, x_2; x_1', x_2') = \\
= \int_{\sigma_I}^{\sigma_{II}} \ldots \int_{\sigma_1}^{\sigma_{II}} A(x_1, x_2; \xi_1, \xi_2)\, \mathrm{d}\xi_1\, \mathrm{d}\xi_2 B(\xi_1, \xi_2; \ldots) \ldots C(\ldots; x_1', x_2')\,.
\end{aligned}
$$

We assume that (i) equation (2.10) possess a unique solution for all values of λ with exception of certain characteristic values constituting the spectrum of this equation and (ii) the value of λ occurring in our considerations does not belong to this spectrum.

We notice a well known property of the function S

$$
(2.14)\qquad \psi^0(x_1, x_2) = \int_{\sigma_1}\int_{\sigma_2} S(x_1, x_2; x_1', x_2')\gamma_\mu^{(1)}\gamma_\nu^{(2)}\psi^0(x_1', x_2')\, \mathrm{d}\sigma_\mu^{(1)'}\, \mathrm{d}\sigma_\nu^{(2)'}
$$

according to which an arbitrary solution of equations (2.5) may be expressed in terms of the initial values at two arbitrary space-like surfaces σ_1 and σ_2.

Let us multiply now equation (2.10) by $\gamma_\mu^{(1)}\gamma_\nu^{(2)}\psi^0(x_1', x_2')\, \mathrm{d}\sigma_\mu^{(1)'}\, \mathrm{d}\sigma_\mu^{(2)'}$ and in-

tegrate over σ_1 and σ_2. By virtue of (2.14) and (2.13) one gets easily

$$(2.15)\qquad \iint_{\sigma_1\,\sigma_2} A^{(i)}[\sigma_1, \sigma_2](x_1, x_2; x_1', x_2')\gamma_\mu^{(1)}\gamma_\nu^{(2)}\psi^0(x_1, x_2)\,\mathrm{d}\sigma_\mu^{(1)\prime}\,\mathrm{d}\sigma_\nu^{(2)\prime} =$$

$$= \iint_{\sigma_I}^{\sigma_{II}} [G^{(i)}(x_1, x_2; x_1', x_2') + \lambda\{G^{(i)}R\}(x_1, x_2; x_1', x_2')]\,\psi^0(x_1' x_2')\,\mathrm{d}x_1'\,\mathrm{d}x_2' -$$

$$- \lambda \iint_{\sigma_1\,\sigma_2} A^{(i)}[\sigma_1, \sigma_2](x_1, x_2; x_1'', x_2'')\gamma_\mu^{(1)}\gamma_\nu^{(2)} \iint_{\sigma_I}^{\sigma_{II}} R(x_1'', x_2''; x_1', x_2')\psi^0(x_1', x_2')\,\mathrm{d}\sigma_\mu^{(1)''}\,\mathrm{d}\sigma_\nu^{(2)''}$$

$$(i = 1, 2).$$

According to (2.9) we may write this equation in the form

$$(2.16)\qquad \iint_{\sigma_1\,\sigma_2} A^{(i)}[\sigma_1, \sigma_2](x_1, x_2; x_1', x_2')\gamma_\mu^{(1)}\gamma_\nu^{(2)}\psi(x_1', x_2')\,\mathrm{d}\sigma_\mu^{(1)\prime}\,\mathrm{d}\sigma_\nu^{(2)\prime} =$$

$$= \iint_{\sigma_I}^{\sigma_{II}} G^{(i)}(x_1, x_2; x_1', x_2')\,\psi(x_1', x_2')\,\mathrm{d}x_1'\,\mathrm{d}x_2'\,.$$

But in (2.15) $\psi_0(x_1, x_2)$ may be an arbitrary solution of (2.5). We have therefore, the result that equation (2.16) holds identically in the solutions $\psi(x_1, x_2)$ of equations (2.1) if the quantities $A^{(i)}[\sigma_1, \sigma_2](x_1, x_2; x_1', x_2')$ satisfy the integral equation (2.10). Conversely, going back from (2.16) to (2.15) and using (2.14) and the arbitrariness of the initial values of ψ^0 we get, by virtue of Du Bois Raymond's theorem, equation (2.10). Thus if (2.16) holds identically in the solutions of (2.1) then the quantities $A^{(i)}$ satisfy the integral equation (2.10). Identity (2.16) expresses the identity of the right hand side of equations (2.1) and (2.2) which completes the proof of the equivalence theorem.

For the one-time formulation of the theory it is important to note that the right hand side of equation (2.2) does not depend on σ_1 or σ_2. This is evident from the identity (2.16) in which the right hand side is independent of σ_1 and σ_2 but it may be instructive to verify the above statement directly.

We first notice that, due to the occurance of S functions in equations (2.10), the solutions of those equations satisfy with respect to the dashed variables the equations

$$(2.17)\qquad A^{(i)}[\sigma_1, \sigma_2](x_1, x_2; x_1', x_2')(\overleftarrow{\partial}^{(j)\prime} - \varkappa^{(j)}) = 0 \qquad (i = 1, 2;\ j = 1, 2),$$

where the arrow indicates the direction in which the differentiations are to be carried out. Differentiating now equations (2.10) functionally with respect

to σ_1 at the point x_1'' and using (2.17) we get

$$\frac{\delta A^{(i)}[\sigma_1, \sigma_2](x_1, x_2; x_1', x_2')}{\delta\sigma_1(x_1'')} = \tag{2.18}$$

$$= -\lambda \int_{\sigma_2} A^{(i)}[\sigma_1, \sigma_2](x_1, x_2; x_1'', x_2'')\gamma_\nu^{(2)}(\underset{\sim}{\hat{c}}^{(1)''} + \varkappa^{(1)})\{RS\}(x_1'', x_2''; x_1', x_2')\, \mathrm{d}\sigma_\nu^{(2)''} -$$

$$- \lambda \iint_{\sigma_1\sigma_2} \frac{\delta A^{(i)}[\sigma_1, \sigma_2](x_1, x_2; x_1''', x_2''')}{\delta\sigma_1(x_1'')} \gamma_\mu^{(1)}\gamma_\nu^{(2)}\{RS\}(x_1''', x_2'''; x_1', x_2')\, \mathrm{d}\sigma_\mu^{(1)'''}\, \mathrm{d}\sigma_\nu^{(2)'''}.$$

Introducing solution (2.9) into the left and right hand side of (2.4) and expressing ψ^0 by means of its initial values (2.14) which are arbitrary functions on σ, we get by virtue of the Du Bois Raymond's theorem

$$\{RS\} = \{PS\} + \lambda\{PRS\} \tag{2.19}$$

or, due to (2.3) and (2.6)

$$(\underset{\sim}{\hat{c}}^{(i)} + \varkappa^{(i)})\{RS\} = \{G^{(i)}S\} + \{G^{(i)}RS\}\,. \tag{2.20}$$

Introducing (2.20) into the first integral on the right hand side of (2.18) and using (2.10) we may write equation (2.18) in the form

$$f_1^{(i)}[\sigma_1, \sigma_2](x_1, x_2; x_1', x_2'; x_1'') = \tag{2.21}$$

$$= \lambda \int_{\sigma_1}\int_{\sigma_2} f_1^{(i)}[\sigma_1, \sigma_2](x_1, x_2; x_1''', x_2'''; x_1'')\gamma_\mu^{(1)}\gamma_\nu^{(2)}\{RS\}(x_1''', x_2'''; x_1', x_2')\, \mathrm{d}\sigma_\mu^{(1)'''}\, \mathrm{d}\sigma_\nu^{(2)'''} \quad (i = 1, 2),$$

where

$$f_1^{(i)}[\sigma_1, \sigma_2](x_1, x_2; x_1', x_2'; x_1'') = \frac{\delta A^{(i)}[\sigma_1, \sigma_2](x_1, x_2; x_1', x_2')}{\delta\sigma_1(x_1'')} + \tag{2.22}$$

$$+ \lambda \int_{\sigma_2} A^{(i)}[\sigma_1, \sigma_2](x_1, x_2; x_1'', x_2'')\gamma_\nu^{(2)} A^{(1)}[\sigma_1, \sigma_2](x_1'', x_2''; x_1', x_2')\, \mathrm{d}\sigma_\nu^{(2)''} \quad (i = 1, 2).$$

Equation (2.21) is the homogeneous integral equation corresponding to (2.10). Due to the assumption that λ is not a characteristic value, it posseses only the trivial solution $f_1^{(i)} = 0$. Thus

$$\frac{\delta A^{(i)}[\sigma_1, \sigma_2](x_1, x_2; x_1', x_2')}{\delta\sigma_1(x_1'')} = \tag{2.23}$$

$$= -\lambda \int_{\sigma_2} A^{(i)}[\sigma_1, \sigma_2](x_1, x_2; x_1'', x_2'')\gamma_\nu^{(2)} A^{(1)}[\sigma_1, \sigma_2](x_1'', x_2''; x_1', x_2')\, \mathrm{d}\sigma_\nu^{(2)''} \quad (i = 1, 2).$$

Differentiating (2.10) with respect to σ_2 at the point x_2'' one gets in a similar way

$$\frac{\delta A^{(i)}[\sigma_1, \sigma_2](x_1, x_2; x_1', x_2')}{\delta\sigma_2(x_2'')} = \tag{2.24}$$

$$= -\lambda \int_{\sigma_1} A^{(i)}[\sigma_1, \sigma_2](x_1, x_2; x_1'', x_2'')\gamma_\mu^{(1)} A^{(2)}[\sigma_1, \sigma_2](x_1'', x_2''; x_1', x_2')\, \mathrm{d}\sigma_\mu^{(1)''} \qquad (i = 1, 2).$$

Equations (2.23) and (2.24) enable us to show by a direct calculation that the right hand sides of equations (2.2) do not depend on the surfaces σ_1 and σ_2. Indeed, differentiating e.g. with respect to σ_1 we get due to (2.23), (2.17) and (2.2)

$$\frac{\delta}{\delta\sigma_1(x_1')} \iint_{\sigma_1\,\sigma_2} A^{(i)}[\sigma_1, \sigma_2](x_1, x_2; x_1', x_2')\gamma_\mu^{(1)}\gamma_\nu^{(2)}\psi(x_1', x_2')\, \mathrm{d}\sigma_\mu^{(1)'}\, \mathrm{d}\sigma_\nu^{(2)'} = \tag{2.25}$$

$$= \int_{\sigma_2} A^{(i)}[\sigma_1, \sigma_2](x_1, x_2; x_1', x_2')\gamma_\varrho^{(2)}[(\hat{\varrho}^{(1)'} + \varkappa^{(1)})\psi(x_1', x_2') -$$

$$- \lambda \iint_{\sigma_1\,\sigma_2} A^{(1)}[\sigma_1, \sigma_2](x_1, x_2; x_1'', x_2'')\gamma_\mu^{(1)}\gamma_\nu^{(2)}\psi(x_1'', x_2'')\, \mathrm{d}\sigma_\mu^{(1)''}\, \mathrm{d}\sigma_\nu^{(2)''}]\, \mathrm{d}\sigma_\varrho^{(2)'} = 0 .$$

Using (2.24) one may show in a similar way that the right hand side of (2.2) is independent of σ_2.

These results give us the freedom of choice of the surfaces σ_1 and σ_2 in equations (2.2). Assuming now that the points x_1 and x_2 occurring on the left hand side of these equations are space-like (in this case only it is possible to interpret the function $\psi(x_1, x_2)$ statistically) we may chose σ_1 to coincide with σ_2 and to pass through these points. Equations (2.2) take now the form

$$(\partial^{(i)} + \varkappa^{(i)})\psi(x_1, x_2) = \tag{2.26}$$

$$= \lambda \iint_{\sigma\,\sigma} A^{(i)}[\sigma, \sigma](x_1, x_2; x_1', x_2')\gamma_\mu^{(1)}\gamma_\nu^{(2)}\psi(x_1', x_2')\, \mathrm{d}\sigma_\mu^{(1)'}\, \mathrm{d}\sigma_\nu^{(2)'} \qquad (i = 1, 2),$$

where σ is an arbitrary space-like surface passing through x_1 and x_2. Equations (2.26) correlate only those values of the function $\psi(x_1, x_2)$ which correspond to one space-like surface and which possess therefore a direct statistical interpretation.

By letting σ_1 and σ_2 pass through the points x_1 and x_2 we have introduced a dependence of the threedimensional integration domain in the integrals in (2.26) on x_1 and x_2. This dependence, however, is only apparent. This is seen immediately if one goes over to plane hypersurfaces $t = \text{const}$ or if one

introduces a parametrization of the hypersurfaces σ by means of the parameters u, v, w, τ in such a way that the equations of these surfaces take the form $\tau = \text{const}$ (cf. also (3.8), (3.9) and (4.3)). Equations (2.26) are, in contradistinction to equations (2.1), « one-time » equations in the sense that they contain only one surface σ or, in the case of plane surfaces $t = \text{const.}$, only one value of the time variable t or, finally, in the case of parametrization, only one value of the parameter τ.

The above considerations may be extended immediately to the general case of the m-body problem as formulated by GÜNTHER (1952).

3. – Calculations of the Kernels $A^{(i)}$ for Small Values of λ.

For practical purposes it is important to express the kernels $A^{(i)}[\sigma_1, \sigma_2] \cdot (x_1, x_2; x_1', x_2')$ of equations (2.26) or (2.2) explicitly by means of the kernels $G^{(i)}(x_1, x_2; x_1', x_2')$ of the original equation (2.1). This is possible e.g. for those values of the parameter λ which admit convergent expansions of the quantities $G^{(i)}$, $A^{(i)}$ and R in powers of λ (*)

$$(3.1) \qquad G^{(i)} = \sum_{n=0}^{\infty} \lambda^n G_n^{(i)}, \qquad A^{(i)} = \sum_{n=0}^{\infty} \lambda^n A_n^{(i)} \quad (i = 1, 2), \qquad R = \sum_{n=0}^{\infty} \lambda^n R_n .$$

Introducing (3.1) into (2.10) and equating coefficients in terms containing equal powers of λ we get the following recurrence formulae for the quantities $A_n^{(i)}$ $(i = 1, 2)$:

$$(3.2) \qquad A_n^{(i)}[\sigma_1, \sigma_2](x_1, x_2; x_1', x_2') = \{G_n^{(i)} S\}(x_1, x_2; x_1', x_2') +$$

$$+ \sum_{m=0}^{n-1} \{G_m^{(i)} R_{n-m-1} S\}(x_1, x_2; x_1', x_2') - \sum_{m=0}^{n-1} \int\!\!\int_{\sigma_1 \sigma_2} A_m^{(i)}[\sigma_1, \sigma_2](x_1, x_2; x_1'', x_2'') \gamma_\mu^{(1)} \gamma_\nu^{(2)} \cdot$$

$$\cdot \{R_{n-m-1} S\}(x_1'', x_2''; x_1', x_2') \, \mathrm{d}\sigma_\mu^{(1)''} \, \mathrm{d}\sigma_\nu^{(2)''} \quad (+) \qquad (i = 1, 2; \; n = 0, 1, 2, \ldots),$$

where the expansion coefficients R_n of R may be expressed by $G_n^{(i)}$ by means of equations (2.4), (2.6) and (2.9).

In some cases it may be convenient to carry out the surface integrations in (3.2). This is always possible if the particular solutions $K^{(i)}(x)$ of equat-

(*) So far, the presentation of the kernels $G^{(i)}$ in the form of expansion series in powers of the coupling constant λ is the only one given effectively.

(+) The convention is used here that, for $n = 0$, $\sum_{m=0}^{n-1} = 0$.

ions (2.3) may be written in the form

$$K^{(i)}(x) = \tau[\sigma_x, \sigma_0] S^{(i)}(x) \qquad (i = 1, 2), \tag{3.3}$$

where $\tau[\sigma_x, \sigma_0]$ is a step-functional constant for σ_x different from σ_0 and changing its value discontinuously for $\sigma_x = \sigma_0$. σ_x and σ_0 denote those space-like surfaces of the congruence fillling out the region Ω which pass through the points x and 0 respectively. Functions of the type (3.3) are e.g. the well known retarded and advanced solutions of equations (2.3). To carry out the surface integrations in (3.2) we note that the function $S(x_1, x_2; x_1', x_2')$ satisfies, as a particular solution of the homogeneous equation (2.5) the relation (2.14)

$$S(x_1, x_2; x_1', x_2') = \iint_{\sigma_1 \sigma_2} S(x_1, x_2; x_1'', x_2'') \gamma_\mu^{(1)} \gamma_\nu^{(2)} S(x_1'', x_2''; x_1', x_2') \, \mathrm{d}\sigma_\mu^{(1)''} \, \mathrm{d}\sigma_\nu^{(2)''} . \tag{3.4}$$

Multiplying both sides of this equation by $\tau[\sigma_1, \sigma_{x_1'}] \tau[\sigma_2, \sigma_{x_2'}]$ we get, due to (3.3) and (2.11)

$$\tau[\sigma_1, \sigma_{x_1'}] \tau[\sigma_2, \sigma_{x_2'}] S(x_1, x_2; x_1', x_2') = \tag{3.5}$$

$$= \iint_{\sigma_1 \sigma_2} S(x_1, x_2; x_1'', x_2'') \gamma_\mu^{(1)} \gamma_\nu^{(2)} K^{(1)}(x_1'' - x_1') K^{(2)}(x_2'' - x_2') \, \mathrm{d}\sigma_\mu^{(1)''} \, \mathrm{d}\sigma_\nu^{(2)''},$$

where σ_1 and σ_2 do not in general pass through the points x_1 and x_2 respectively. The functions τ may be introduced under the integral sign since they are constant with respect to integrations over σ_1 and σ_2 respectively. Now the surface integrals occuring in (3.2) are exactly of the form of the right hand side of equations (3.5). Indeed, due to the equations (2.6) and (2.8) the resolving kernel R of equation (2.4) may be written in the form

$$R(x_1, x_2; x_1', x_2') = \iint_{\sigma_{\mathrm{I}}}^{\sigma_{\mathrm{II}}} K^{(1)}(x_1 - x_1'') K^{(2)}(x_2 - x_2'') \, \mathrm{d}x_1'' \, \mathrm{d}x_2'' \bar{R}(x_1'', x_2''; x_1', x_2') \tag{3.6}$$

and, due to (3.2), the quantities $A_m^{(i)}[\sigma_1, \sigma_2](x_1, x_2; x_1', x_2')$ contain on the right hand side a function $S(x_1, x_2; x_1', x_2')$

$$A_m^{(i)}[\sigma_1, \sigma_2](x_1, x_2; x_1', x_2') = \tag{3.7}$$

$$= \iint_{\sigma_{\mathrm{I}}}^{\sigma_{\mathrm{II}}} \tilde{A}_m^{(i)}[\sigma_1, \sigma_2](x_1, x_2; x_1'', x_2'') \, \mathrm{d}x_1'' \, \mathrm{d}x_2'' S(x_1'', x_2''; x_1', x_2') \qquad (i = 1, 2).$$

We may write, therefore, instead of (3.2)

$$(3.8)\qquad A_n^{(i)}[\sigma_1,\sigma_2](x_1,x_2;x_1',x_2') = \{G_n^{(i)}S\}(x_1,x_2;x_1',x_2') +$$

$$-\sum_{m=0}^{n-1}\{G_m^{(i)}R_{n-m-1}S\}(x_1,x_2;x_1',x_2') - \sum_{m=0}^{n-1}\int\!\!\int_{\sigma_I}^{\sigma_{II}} A_m^{(i)}[\sigma_1,\sigma_2](x_1,x_2;x_1'',x_2'')\,\tau[\sigma_1,\sigma_{x_1''}]\cdot$$

$$\cdot\,\tau[\sigma_2,\sigma_{x_2''}]\{R_{n-m-1}S\}(x_1'',x_2'';x_1',x_2')\,\mathrm{d}x_1'\,\mathrm{d}x_2' .$$

Here $\bar{R}_n$ is the n-th approximation of the kernel $\bar{R}$ introduced in (3.6). It may be noticed that the evaluation of surface integrals may be carried out also in the integral equation (2.10) which is not restricted to small values of λ.

One may carry out the surface integrations in (3.2) also in the case, when $K^{(i)}(x)$ has the form

$$(3.3')\qquad K^{(i)}(x) = \tau[\sigma_x,\sigma_0]\Lambda_{\pm}^{(i)}(-i\hbar\overrightarrow{\partial})\,S^{(i)}(x)\,,\quad \begin{cases} \text{« + » for } \sigma_x \text{ later than } \sigma_0, \\ \text{« — » for } \sigma_x \text{ sooner than } \sigma_0, \end{cases}$$

where

$$\Lambda_{\pm}^{(i)}(-i\hbar\overrightarrow{\partial}) = \frac{|H^{(i)}(-i\hbar\overrightarrow{\partial})| \pm H^{(i)}(-i\hbar\overrightarrow{\partial})}{2\,|H^{(i)}(-i\hbar\overrightarrow{\partial})|} \qquad (i=1,2)$$

are operators, which introduced under the integral sign of the Fourier expansion of the function $S(x)$ change into the Casimir's operators.

$$\Lambda_{\pm}^{(i)}(\boldsymbol{p}) = \frac{E^{(i)}(\boldsymbol{p}) \pm H^{(i)}(\boldsymbol{p})}{2E^{(i)}(\boldsymbol{p})} \qquad (i=1,2)\,,$$

where $E^{(i)}(\boldsymbol{p}) = c\sqrt{\boldsymbol{p}^2 + (m^{(i)}c)^2}$. E.g., for $\tau[\sigma_x,\sigma_0] = \varepsilon[\sigma_x,\sigma_0]$, where

$$\varepsilon[\sigma_x,\sigma_0] = \begin{cases} 1 \text{ for } \sigma_x \text{ later than } \sigma_0, \\ -1 \text{ for } \sigma_x \text{ sooner than } \sigma_0, \end{cases}$$

the function given by (3.3') is the Feynman solution of equation (3.2): $K^{(i)}(x) - iS_+^{(i)} = (i/2)S_F^{(i)}(x)$. In order to carry out in this case the surface integrations in (3.2) we multiply both sides of the equation (3.1) by $\Lambda_{\pm}^{(i)}(i\hbar\overleftarrow{\partial}^{(1)'})\cdot\Lambda_{\pm}^{(2)}(i\hbar\overleftarrow{\partial}^{(2)'})\,\tau[\sigma_1,\sigma_{x_1'}]\tau[\sigma_2,\sigma_{x_2'}]$ and we use on the right hand side of (3.4) the relation

$$S(x_1,x_2;x_1',x_2')\Lambda_{\pm}^{(1)}(i\hbar\overleftarrow{\partial}^{(1)'})\Lambda_{\pm}^{(2)}(i\hbar\overleftarrow{\partial}^{(2)'}) = \Lambda_{\pm}^{(1)}(i\hbar\overrightarrow{\partial}^{(1)'})\Lambda_{\pm}^{(2)}(i\hbar\overrightarrow{\partial}^{(2)'})S(x_1,x_2;x_1',x_2') =$$

$$= \Lambda_{\pm}^{(1)}(-i\hbar\overrightarrow{\partial}^{(1)})\Lambda_{\pm}^{(2)}(-i\hbar\overrightarrow{\partial}^{(2)})S(x_1,x_2;x_1',x_2')\,.$$

Then we get, owing to (3.3) and (2.11)

$$(3.5') \qquad S(x_1, x_2; x_1', x_2')\Lambda_{\pm}^{(1)}(i\hbar\overleftarrow{\partial}^{(1)'})\Lambda_{\pm}^{(2)}(i\hbar\overleftarrow{\partial}^{(2)'})\tau[\sigma_1, \sigma_{x_1'}]\tau[\sigma_2, \sigma_{x_2'}] =$$

$$= \int\int_{\sigma_1\sigma_2} S(x_1, x_2; x_1'', x_2'')\gamma_\mu^{(1)}\gamma_\nu^{(2)}K^{(1)}(x_1'' - x_1')K^{(2)}(x_2'' - x_1')\,\mathrm{d}\sigma_\mu^{(1)''}\,\mathrm{d}\sigma_\nu^{(2)''}.$$

Making use of (3.7), (3.6) and (3.5') we may write instead of (3.2)

$$(3.8') \qquad A_n^{(i)}[\sigma_1, \sigma_2](x_1, x_2; x_1', x_2') = \{G_n^{(i)}S\}(x_1, x_2; x_1', x_2') +$$

$$+ \sum_{m=0}^{n-1}\{G_m^{(i)}R_{n-m-1}S\}(x_1, x_2; x_1', x_2') - \sum_{m=0}^{n-1}\int\int_{\sigma_I}^{\sigma_{II}} A_m^{(i)}[\sigma_1, \sigma_2](x_1, x_2; x_1'', x_2'')\Lambda_{\pm}^{(1)}(i\hbar\overleftarrow{\partial}^{(1)''})\cdot$$

$$\cdot\Lambda_{\pm}^{(2)}(i\hbar\overleftarrow{\partial}^{(2)''})\tau[\sigma_1, \sigma_{x_1''}]\tau[\sigma_2, \sigma_{x_2''}]\cdot\{\bar{R}_{n-m-1}S\}(x_1'', x_2''; x_1', x_2')\,\mathrm{d}x_1''\,\mathrm{d}x_2''.$$

The recurrence formulae (3.8) and (3.8') may be considerably simplified if we restrict ourselves to plane surfaces t=const. In this case the functional dependence of $A^{(i)}$ on σ_1 and σ_2 changes into a dependence on the fourth coordinates t_1 and t_2, whereas the functionals $\tau[\sigma_x, \sigma_{x'}]$ become functions of $t - t'$. We may write, therefore, instead of (3.8) and (3.8') respectively

$$(3.9) \qquad A_n^{(i)}[t_1, t_2](x_1, x_2; x_1', x_2') = \{G_n^{(i)}S\}(x_1, x_2; x_1', x_2') +$$

$$+ \sum_{m=0}^{n-1}\{G_m^{(i)}R_{n-m-1}S\}(x_1, x_2; x_1', x_2') - \sum_{m=0}^{n-1}\int\int_{\sigma_I}^{\sigma_{II}} A_m^{(i)}[t_1, t_2](x_1, x_2; x_1'', x_2'')\tau(t_1 - t_1'')\cdot$$

$$\cdot\tau(t_2 - t_2'')\{R_{n-m-1}S\}(x_1'', x_2''; x_1', x_2')\,\mathrm{d}x_1''\,\mathrm{d}x_2''$$

and

(3.9') the same formula but with $\Lambda_{\pm}^{(1)}(i\hbar\overleftarrow{\partial}^{(1)''})\Lambda_{\pm}^{(2)}(i\hbar\overleftarrow{\partial}^{(2)''})$ inserted before the τ's.

4. – Final Remarks.

In view of the one-time equations (2.26) we are particularly interested in the form of $A^{(i)}[\sigma_1, \sigma_2](x_1, x_2; x_1', x_2')$ in the case when $\sigma_1 = \sigma_2 = \sigma$ and when both x_1, x_2 and x_1', x_2' are situated on σ. Chosing for σ the plane surfaces t=const we have, according to (3.9) or (3.9'), the result that $A^{(i)}$ is a function of one time t only. Denoting by $\boldsymbol{x}_1$ and $\boldsymbol{x}_2$ the first three coordinates of the points

x_1 and x_2 we may write this explicitly

$$A^{(i)} = A^{(i)}[t](\boldsymbol{x}_1, \boldsymbol{x}_2; \boldsymbol{x}_1', \boldsymbol{x}_2'; t)\,. \tag{4.1}$$

Multiplying (2.26) by the $hc\gamma_4^{(i)}$ respectively, adding the resulting equations and using (4.1), we may write the one-time equations for the two-particle problem in the form of a Schrödinger equation

$$\left\{\begin{aligned} & i\hbar\,\frac{\partial}{\partial t}\,\psi(\boldsymbol{x}_1, \boldsymbol{x}_2; t) = (H^{(1)} + H^{(2)})\,\psi(\boldsymbol{x}_1, \boldsymbol{x}_2; t) + \\ & \qquad + \iint\limits_V V(\boldsymbol{x}_1, \boldsymbol{x}_2; \boldsymbol{x}_1', \boldsymbol{x}_2'; t)\,\psi(\boldsymbol{x}_1', \boldsymbol{x}_2'; t)\,\mathrm{d}v_1'\,\mathrm{d}v_2'\,, \\ & V(\boldsymbol{x}_1, \boldsymbol{x}_2; \boldsymbol{x}_1', \boldsymbol{x}_2') \equiv \lambda\hbar c[\gamma_4^{(1)} A^{(1)}[t](\boldsymbol{x}_1, \boldsymbol{x}_2; \boldsymbol{x}_1', \boldsymbol{x}_2'; t) + \\ & \qquad + \gamma_4^{(2)} A^{(2)}[t](\boldsymbol{x}_1, \boldsymbol{x}_2; \boldsymbol{x}_1', \boldsymbol{x}_2')]\gamma_4^{(1)}\gamma_4^{(2)}\,, \end{aligned}\right. \tag{4.2}$$

where

$$H^{(i)} = \gamma_4^{(i)}(\hbar c\boldsymbol{\gamma}^{(i)}\vec{\partial}^{(i)} + m^{(i)}c^2) = -\,i\hbar c\boldsymbol{\alpha}^{(i)}\vec{\partial}^{(i)} + \beta^{(i)}m^{(i)}c^2 \qquad (i = 1, 2) \tag{4.3}$$

are the free Hamiltonians of the two particles, ($\boldsymbol{\gamma} = (\gamma_1, \gamma_2, \gamma_3)$, $\vec{\partial} = (\partial_1, \partial_2, \partial_3)$, $\mathrm{d}v = \mathrm{d}x\,\mathrm{d}y\,\mathrm{d}z = i\,\mathrm{d}\sigma_4$, $m = \hbar\varkappa/c$ and v is the domain considered.

The interaction term in the Hamiltonian (4.2) is an integral operator operating on the variables $\boldsymbol{x}_1$ and $\boldsymbol{x}_2$: In the case when the considered system is not acted upon by external forces the kernels of the original equations (2.1) may depend on x_1, x_2, x_1', x_2' only by means of the coordinate differences. This is necessary to secure translational invariance. In this case the kernels $A^{(i)}$ depend also only on coordinate differences (cf. e.g. (3.9) or (3.9′)(and the kernel of equation (4.2) becomes time independent (*)

$$A^{(i)} = A^{(i)}(\boldsymbol{x}_1, \boldsymbol{x}_2; \boldsymbol{x}_1', \boldsymbol{x}_2')\,. \tag{4.4}$$

This is an advantage of the one-time formulation as compared with the many-time formulation (2.1) since it admits the application of stationary methods. Assuming the solution (4.2) in the form

$$\psi(\boldsymbol{x}_1, \boldsymbol{x}_2; t) = \varphi(\boldsymbol{x}_1, \boldsymbol{x}_2)\exp\left[-\,(i/\hbar)Et\right], \tag{4.5}$$

(*) More generally, this kernel is time independent when external forces do not depend on time (invariance for time translations).

we get the stationary Schrödinger equation

$$
(4.6)\qquad \begin{cases} E\varphi(x_1, x_2) = (H^{(1)} + H^{(2)})\varphi(x_1, x_2) + \\ \qquad + \iint_V V(x_1, x_2; x_1', x_2')\varphi(x_1', x_2')\,\mathrm{d}v_1'\,\mathrm{d}v_2', \\ V(x_1, x_2; x_1, x_2) \equiv \lambda\hbar c[\gamma_4^{(1)}A^{(1)}(x_1, x_2; x_1', x_2') + \\ \qquad + \gamma_4^{(2)}A^{(2)}(x_1, x_2; x_1', x_2')]\gamma_4^{(1)}\gamma_4^{(2)}, \end{cases}
$$

to which e.g. the conventional stationary perturbation method may be applied. As the unperturbed Hamiltonian one may use any energy observable with known eigenstates and well approximating the total energy of the system. Generally, for bound states the free Hamiltonian $H^{(1)} + H^{(2)}$ cannot be successfully used as the unperturbed Hamiltonian. The interaction term in equation (4.6) does not depend on the energy E in which it differs from the interaction term obtained by the Tamm-Dancoff method (cf. KLEIN (1954_2), TAYLOR (1954_2)).

It may be noted, that the above considerations may be carried out also in an evidently covariant way by means of an appropriate parametrization of the surfaces σ (cf. end of section 2).

Equations (4.2) as well as (2.26) are equivalent to the original equations (2.1) whenever we consider exact solutions. However, in practical calculations one always uses an approximation method. It is obvious from the above considerations that if we retain in the kernel of (2.1) as well as in the kernel of (4.2) only terms up to the order n in the coupling constant λ and then solve the resulting equations exactly, then solutions will in general differ by terms of the order $n+1$. This difference becomes essential when expansions of solutions in powers of λ are slowly convergent (or divergent) as they usually are for bound states. In the case of equation (2.1) one may try to retain in the kernels $G^{(i)} = \sum_{n=0}^{\infty} \lambda^n G_n^{(i)}$ only the lowest term $G_0^{(i)}$ (the lowest «ladder approximation», cf. BETHE and SALPETER (1951) (and then to solve the approximate equation exactly (cf. GÜNTHER (1955)). The one-time equation (4.2) or (2.26) corresponding exactly to this approximate equation will in general possess a kernel which is an expansion series in powers of λ. Now, one should neglect also in this expansion all higher order terms, as it would be inconsequent to retain in the kernel of (4.2) higher order terms generated by $G_0^{(i)}$ when terms of the same order generated by $G_0^{(i)}$ and so on are not taken into account. It is an open question whether the one-time or the many-time formulation is more practical for explicit calculations. It seems certain, however, that the results will differ essentially whenever an approximate treatment is applied.

Calculations of energy levels in the two-body problem in electrodynamics (SALPETER (1951), KARPLUS and KLEIN (1952), FULTON and MARTIN (1954)) seem to give arguments—in view of the formalism presented in this paper—for that approximative treatment which consists in breaking off the kernel in the one-time equation rather than the kernels in the many-time equations. We note, however, that the procedure of breaking off the kernel in the one-time equation spoils its Lorentz invariance (its independence of σ) in which it differs from the breaking off the kernels in the many-time equations. After this procedure the one-time equation becomes only approximately independent of the hypersurface σ. We hope to come back to that question elsewhere.

Calculating e.g. the kernel of the first order interaction operator (cf. (4.6) and (3.9′))

$$V_1(x_1, x_2; x_1, x_2) = \lambda\hbar c[\gamma_4^{(1)} A_0^{(1)}(x_1, x_2; x_1, x_2) + \gamma_4^{(2)} A_0^{(2)}(x_1, x_2; x_1, x_2)]\gamma_4^{(1)}\gamma_4^{(2)}$$

in the case of electrodynamics, where we have (in Heaviside's units):

$$\lambda G_0^{(1)}(x_1, x_2; x_1', x_2') = \frac{ie^2}{\hbar c}\,\delta(x_1 - x_1')\,S_+^{(2)}(x_2 - x_2')\gamma_\mu^{(1)}\gamma_\mu^{(2)}\,D_+(x_1' - x_2')\,,$$

$$\lambda G_0^{(2)}(x_1, x_2; x_1', x_2') = \frac{ie^2}{\hbar c}\,S_+^{(1)}(x_1 - x_1')\,\delta(x_2 - x_2')\gamma_\mu^{(1)}\gamma_\mu^{(2)}\,D_+(x_1' - x_2')$$

($S_+^{(i)}(x) = \frac{1}{2}S_F^{(i)}(x)$ and $D_+(x) = \frac{1}{2}D_F(x)$ are the Feynman solutions of the equations

$$(\partial^{(i)} + \varkappa^{(i)})\,S_+^{(i)}(x) = -i\,\delta(x) \quad \text{and} \quad \Box D_+(x) = i\,\delta(x))\,,$$

and expanding it in powers of $1/c$ we get for the instantaneous interaction

$$V_1(x_1, x_2; x_1, x_2) = -\frac{e^2}{4\pi}[\Lambda_+^{(1)}(-i\hbar\vec{\partial}^{(1)})\,\Lambda_+^{(2)}(-i\hbar\vec{\partial}^{(2)}) - \Lambda^{(1)}(-i\hbar\vec{\partial}^{(1)})\,\Lambda^{(2)}(-i\hbar\vec{\partial}^{(2)})]\cdot$$
$$\cdot\frac{1 - \boldsymbol{\alpha}^{(1)}\boldsymbol{\alpha}^{(2)}}{|\boldsymbol{x}_1 - \boldsymbol{x}_2|}\cdot\delta(\boldsymbol{x}_1 - \boldsymbol{x}_1')\,\delta(\boldsymbol{x}_2 - \boldsymbol{x}_2')\,.$$

This result is identical with the one obtained by SALPETER (1952). The higher order terms in $1/c$ appear as retardation corrections to this first order instantaneous interaction.

The authors are indebted to Dr. M. GÜNTHER and Dr. J. ŁOPUSZAŃSKI for interesting discussions on this subjects.

The subject of this paper was presented to the Polish Academy of Sciences.

REFERENCES

J. SCHWINGER: *Proc. Natl. Acad. Sci. U.S.*, **37**, 452, 455 (1951).
E. E. SALPETER and H. A. BETHE: *Phys. Rev.*, **84**, 1232 (1951).
M. GÜNTHER: *Phys. Rev.*, **88**, 1411 (1952); **94**, 1347 (1954).
M. LÉVY: *Phys. Rev.*, **88**, 72, 725 (1952).
A. KLEIN: *Phys. Rev.*, **90**, 1101 (1953).
M. CINI: *Nuovo Cimento*, **10**, 526, 614 (1953).
F. J. DYSON: *Phys. Rev.*, **91**, 1543 (1953).
J. C. TAYLOR: *Phys. Rev.*, **95**, 1313 (1954_1).
E. E. SALPETER: *Phys. Rev.*, **87**, 328 (1952).
W. MACKE: *Zeits. Naturforsch.*, **8a**, 599, 615 (1953).
A. KLEIN: *Phys. Rev.*, **94**, 1052 (1954_1).
B. KURŞUNOĞLU: *Phys. Rev.*, **96**, 1690 (1954).
J. RZEWUSKI: *Acta Phys. Pol.*, **13**, 135 (1954); **14**, 123 (1955); *Bull. Acad. Pol. Sci., Cl. III*, **2**, 429 (1954).
A. KLEIN: *Phys. Rev.*, **94**, 195 (1954_2).
J. C. TAYLOR: *Phys. Rev.*, **96**, 1438 (1954_2).
M. GÜNTHER: (1955) (unpublished).
R. KARPLUS and A. KLEIN: *Phys. Rev.*, **87**, 848 (1952).
T. FULTON and P. C. MARTIN: *Phys. Rev.*, **95**, 811 (1954).

RIASSUNTO (*)

Si ricava una formulazione covariante monotemporale del problema di piu corpi nella teoria quantistica dei campi, trasformando le convenzionali equazioni pluritemporali di questo problema in altre equivalenze che contengono solo quei valori della funzione d'onda e le sue derivate che corrispondono a una ipersuperficie σ di tipo spaziale. Si sviluppa la trasformazione per valori arbitrari della costante d'accoppiamento λ ad eccezione di determinati valori caratteristici λ_k. Per piccoli valori di λ si dànno espressioni esplicite per i noccioli delle equazioni monotemporali per mezzo di sviluppi in serie di potenze di λ. Questi noccioli sono univocamente determinati dai noccioli delle originali equazioni pluritemporali. In assenza di forze esterne i noccioli delle equazioni monotemporali sono indipendenti dalla variabile temporale. Queste equazioni si possono, quindi, trattare coi metodi di perturbazione stazionaria in contrapposto alle originali equazioni pluritemporali che non ammettono trattamento stazionario.

(*) *Traduzione a cura della Redazione.*

Detailed Analysis and Discussion of Two Narrow Showers of Pairs of Charged Particles.

A. Debenedetti, C. M. Garelli, L. Tallone and M. Vigone

Istituto di Fisica dell'Università - Torino
Istituto Nazionale di Fisica Nucleare - Sezione di Torino

(ricevuto il 31 Maggio 1955)

Summary. — Detailed experimental data on two events consisting of a narrow shower of pairs of charged particles are reported. An analysis of the common features of the events points out some difficulties in the explanation of the phenomenon as an ordinary cascade shower. Other possible interpretations are suggested.

In a previous work [1] we reported some preliminary results concerning two narrow showers of electron pairs, found in a stack of nuclear emulsions exposed at 80 000 feet.

Purpose of the present work is to collect all the available experimental data on events 1 and 2 and to discuss:

a) the possibility that the phenomenon is due to an ordinary cascade shower produced by the electrons of the first pair.

b) other interpretations.

1. – Experimental Results.

Figs. 1 and 1 bis, show a scheme of the two events and their position in the stack.

[1] A. Debenedetti, C. M. Garelli, L. Tallone, M. Vigone and G. Wataghin: *Nuovo Cimento*, **12**, 954 (1954); see also: *Proc. Rochester Conference on High Energy Physics* 1955, p. 170.

For each pair we measured the distance between its origin and the point at which the two tracks can be resolved. Since the minimum distance we can resolve is about 0,5 μ m, from this measurement we obtain the opening angle of the pair. The radial distances have been measured in the following way: for the pairs of event 1: distance of their points of origin to one track of pair n. 1; for the pairs of event 2: distance from their points of origin to one track of pair n. 2. As the shower passes through several plates (22 plates event 1, 24 plates event 2) the uncertainty in the radial distance increases with the distance from the first pair.

For the interpretation of the phenomenon it would be interesting to know the spatial shape of the shower. To this purpose we projected the pairs origins in a plane perpendicular to the shower

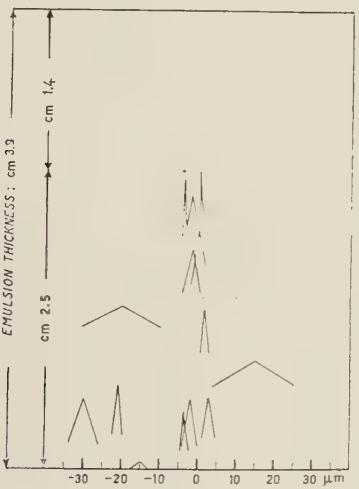

Fig. 1. – Projected points of origin and opening angles of the pairs of event 1. The lateral slow pairs originate on tracks of the preceding pairs that have been deviated.

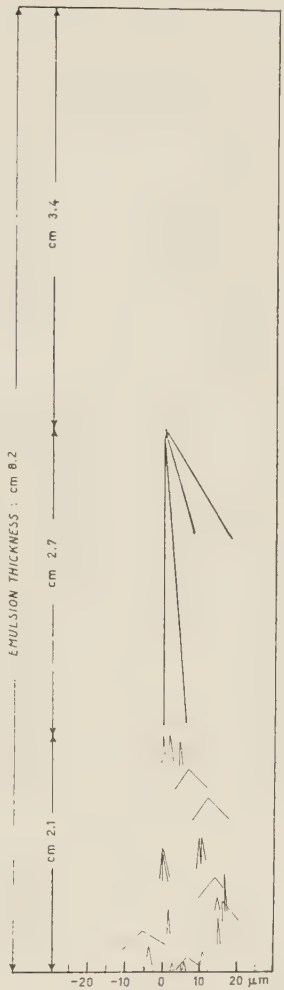

Fig. 1*bis*. – Projected points of origin and opening angles of 23 pairs of event 2. Pair no. 8 is probably a trident on a track of pair no. 2 and it is not drawn in this figure.

axis, but, because of the geometrical position in the stack, the uncertainty in these points is too large to give any useful information. For the same reason we cannot establish if the pairs lie in parallel planes.

We have no conclusive evidence about the identity of the particles constituting the events; however, ionization and scattering measurements on some tracks of the slow pairs indicate that they are probably due to electrons. Moreover, on a track of the second pair of event 2 a slow pair is generated, which is certainly a trident. It seems therefore reasonable to assume that all the observed pairs are electron pairs.

The results of the measurements are collected in tables I and II.

The opening angle of the pair in our case is the only available datum to calculate the energy of the photon. No direct measurements are reliable at so high energies.

A photon of a given energy, in the Coulomb field of a nucleus, originates an electron pair whose opening angle depends both on the energy of the photon and on the momentum transferred to the nucleus. From the distribution of the transferred momentum, given by BETHE-HEITLER ([2]), BORSELLINO ([3]) deduced the distribution of the angle of divergence between the two members of a pair, for several photon energies and for the equipartition of energy (Fig. 2). The most probable opening angle of a pair created by a photon of energy K, given by BORSELLINO, is

$$\omega_p = \frac{4mc^2}{K} . \tag{1}$$

The mean square angle deduced by STEARNS ([4]) under the same assumption is

$$\omega_m = \frac{2mc^2}{K} \ln \frac{K}{2mc^2} . \tag{2}$$

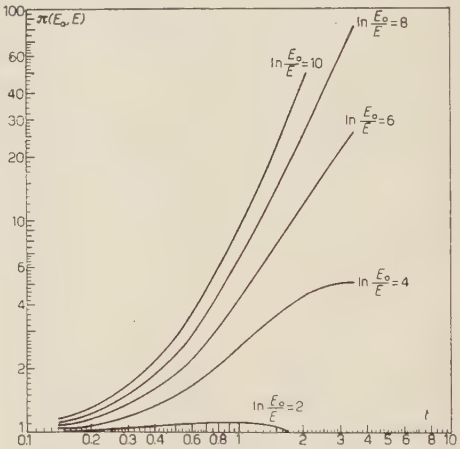

Fig. 2. – Distribution of the angles of divergence ω of a pair for high energy photons (complete screening and equipartition of energy). For $x > 6$, $d\sigma/dx$ has been calculated from formula (11) of BORSELLINO's work.

The energies listed in the tables have been calculated from formula (1). The values obtained from formula (2) are greater by a factor varying from 2 to 5.

The values of the energies are only a rough estimate because of the statistical uncertainty in the opening angle. This fact makes probably unim-

([2]) H. BETHE and W. HEITLER: *Proc. Roy. Soc.*, A **146**, 83 (1934).
([3]) A. BORSELLINO: *Phys. Rev.*, **89**, 1023 (1953).
([4]) M. STEARNS: *Phys. Rev.*, **76**, 836 (1949).

TABLE I. – *Event* 1.

Pair no.	Angle 10^{-3} rad	Energy GeV	Radial distance μm	Distance from the first pair (μm)
1	0.2	10	—	—
2	0.2	10	6	760
3	1	2	2	2 200
4	1	2	< 1	5 030
5	1	2	2.5	6 800
6	10	0.2	35	11 820
7	0.6	3.3	1.5	12 160
8	10	0.2	28	16 560
9	0.6	3.3	30	18 670
10	1	2	3	19 500
11	2	1	35	19 850
12	1	2	2	20 000
13	< 1	> 2	3.5	21 000
14	8	0.25	22	24 500

TABLE II. – *Event* 2.

Pair no.	Angle 10^{-3} rad	Energy GeV	Radial distance μm	Distance from the first pair (μm)
1	1	2	0.5	—
2	0.2	10	0	550
3	1	2	1.5	27 240
4	0.6	3.3	0	27 440
5	2	1	4.5	27 690
6	10	0.2	7	30 510
7	20	0.1	12	32 990
8	25	0.08	63	35 660
9	1	2	11	36 420
10	—	—	11	36 420
11	0.4	5	0	37 240
12	1	2	0	37 290
13	0.1	20	17	39 160
14	25	0.08	24.5	39 560
15	1	2	15	41 210
16	8	0.25	18	41 610
17	0.3	6.6	10	42 460
18	0.8	2.5	15.5	43 010
19	50	0.04	11.5	44 210
20	3	0.66	4.5	45 460
21	2	1	21	45 910
22	50	0.04	27	46 460
23	< 2	> 1	9	46 760
24	< 2	> 1	3.5	46 810

portant the uncertainty due to the scattering of the individual tracks and to the non-equipartition of the energy.

2. – Comparison with the Theory of Soft Showers.

The most striking feature of these events (as well as of Schein's case [5]) is the big number of electron pairs observed in a thickness of emulsion corresponding to about one radiation length, and their strong collimation. This fact suggests the hypothesis that the event has been produced by a narrow shower of photons. However we must first discuss whether it is possible to explain the number of observed pairs and their energy by a multiplicative process of electro-photonic cascade produced by one photon of high energy. We point out that in the event 2, the first pair has an opening angle ten times greater than the opening angle of the second one; moreover its two electrons do not travel in the same direction as the ver. We followed these electrons for 15 mm; their tracks are clearly deviated by Coulomb scattering: in fact, the measure of the opening angle gives different values at different distances from the origin of the pair. Since the variation of the opening angle of pair n. 2 over a distance of 27 mm is very small, it seems reasonable to assume that this pair is more energetic than pair n. 1 and that consequently it cannot derive from pair n. 1 in a process of bremsstrahlung. So that, in this case, we must discuss if the observed shower could be produced by the two electrons of pair n. 2.

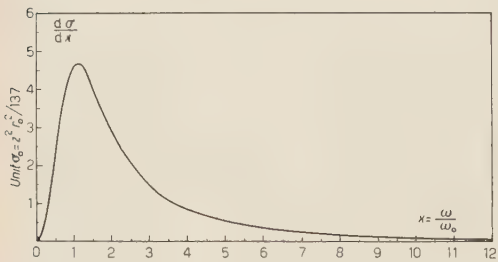

Fig. 3. – t: radiation length. $\prod(E_0; E)$: number of electrons of energy greater than E present in a cascade produced by an electron of energy E_0. The curves are deduced from Arley's theory.

The theoretical predictions of the development of a cascade shower in the first few radiation lengths have been derived by Arley [6] neglecting the energy loss by collisions and the Compton effect. Since the energies involved in our cases are sufficiently high to allow the same approximations, we can compare our experimental data with the results of Arley's calculations. The diagram shown in Fig. 3, deduced from Arley's theory, gives the number of electrons of energy greater that E which are found at a depth t in a shower initiated

[5] M. Schein, D. M. Haskin, and M. G. Glasser: *Phys. Rev.*, **95**, 855 (1954).
[6] N. Arley: *Proc. Roy. Soc.*, **A 168**, 519 (1938).

by an electron of energy E_0. If we assume that the whole phenomenon is due to a single photon, the two electrons of the first pair (or the second pair in event 2) must have produced all the remaining pairs through a cascade process. Taking for E_0 the value 5 GeV (i.e. assuming the equipartition of the energy between the two members of the pair of 10 GeV), and for E the minimum energy of the observed electrons, we would expect:

2,2 pairs in event 1 $\qquad (t = 0{,}84 \quad \ln E_0/E = 4)$

8,5 pairs in event 2 $\qquad (t = 1{,}60 \quad \ln R_0/E = 6)$

instead of the 14 and 23 pairs actually found.

We try to estimate the probability that this discrepancy is due to a fluctuation. Since no exact formula for the fluctuations of the cascade theory has been established so far, we chose in our calculations the formula which gives he highest flucuations, that is the relation of FURRY [7]:

$$P = \frac{1}{\bar{N}}\left(1 - \frac{1}{\bar{N}}\right)^{N-1},$$

(P = probability of finding N pairs instead of the expected $\bar{N}$). We find that the probability for the number of pairs of event 1 to be a fluctuation is:

$$\frac{1}{2.2}\left(1 - \frac{1}{2.2}\right)^{13} = 2 \cdot 10^{-4},$$

and for the number of pairs of the event 2:

$$\frac{1}{8.5}\left(1 - \frac{1}{8.5}\right)^{22} = 8 \cdot 10^{-3}.$$

It is necessary to point out that the number of the pairs, independently of their energy, can be entirely taken into account if we suppose that the energy of the first pair of event 1 has been underestimated by a factor 1 000 (and the energy of the second pair of event 2 by a factor 100), while all the other energies are not higher that the values given in the tables. Also the probability of this occurrence is small, as can be seen from Fig. 2.

Moreover, even in this case, we cannot explain the distribution of the energies of the pairs; in fact, another feature common to the two events, is that the opening angle for most pairs is of the same order as that of the first

---

[7] W. H. FURRY: *Phys. Rev.*, **52**, 569 (1937).

pair. Therefore, in no case the differential energy spectrum has a rate similar to the theoretical previsions. The histograms of figs. 4, 4 bis, 5, 5 bis show the comparison between the experimental data and the theoretical previsions.

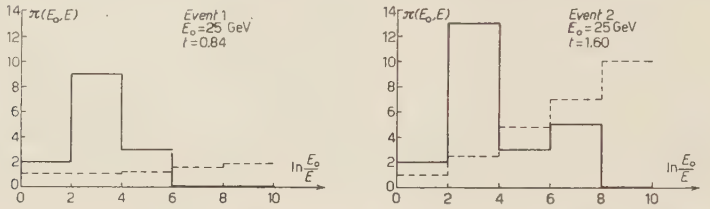

Fig. 4, 4*bis*. – The full line histograms show the experimental energy distribution of the electrons; the dotted line represents the corresponding histograms deduced from Arley's theory.

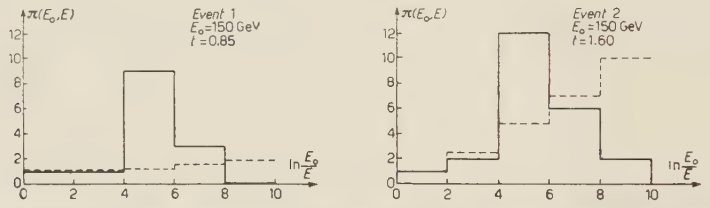

Fig. 5, 5*bis*. The full line histograms show the experimental energy distribution of the electrons; the dotted line represents the corresponding histograms deduced from Arley's theory.

calculated attributing to the first pair two different values of energy, and to the others the energy given in the tables. $E_0 = 25$ GeV (figs. 4, 4 bis) is the minimum value we must attribute to the electrons of the first pair in order to make the explanation in terms of a cascade shower consistent with energy conservation. The excess of high energy pairs and the deficiency of low energy ones, which is evident from this comparison, is not eliminated even if we increase the energy of the first pair to 300 GeV (Figs. 5, 5-bis.)

From the preceding remarks such a fluctuation of an ordinary cascade seems very improbable, chiefly if we consider that several events of the type described above have been observed in quite a short time.

3. – Estimate of the Minimum Number of Incident Photons.

We discuss now separately events 1 and 2.

In case 1 the radial distances between the points of origin of the first three pairs give an additional argument against the hypothesis that one photon is sufficient to explain the whole phenomenon; in effect, in the hypothesis

that pairs n. 2 and n. 3 are the materialization of photons radiated by the electrons of pair n. 1, these photons would make with the direction of pair n. 1 angles of at least $5 \cdot 10^{-3}$ rad and 10^{-3} rad respectively, whereas the opening angle of the first pair is 10^{-4} rad. The distribution law of the angle between the electron and the photon in the process of bremsstrahlung is the same as that of the angle between the photon and the positron in the pair production (BETHE-HEITLER (2)). It is improbable that an electron of a pair whose opening angle is 10^{-4} rad should radiate a photon with an angle ten times larger. Therefore we must think that at least the three photons materialized in the first 2 mm of emulsion do not derive from each other according to a scheme of cascade generation; we shall refer to them as « incident photons ».

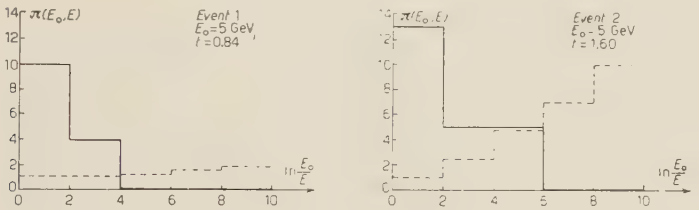

Fig. 6, 6*bis*. – The full line histograms show the differential energy spectrum of the electrons, if we attribute to each pair the most probable energy given in the tables. The dotted line represents the energy distribution of the cascade electrons which may have been produced by the electrons of the first pair.

However the interpretation of the event as the materialization and the successive multiplication of three photons gives rise to two difficulties: some of the following pairs have a too high energy, and the total number of pairs is still too large. The experimental data are best explained if we suppose that three or four pairs more are the result of the materialization of « incident photons ». The energy of these « incident photons » should vary in the range from 2 to 10 GeV, to account for the peak of experimental energy (see Fig. 6). Moreover such an assumption is in agreement with the experimental « number of pairs versus distance » curve (see Fig. 7). It is important to point out that the same number of photons chosen to account for the total number of pairs observed at a thickness $t = 0.84$ gives a satisfactory agreement with the number of pairs observed at different values of t.

Analogous considerations can be done for event 2: only eight or nine of the 22 pairs which we find in the last 2 cm of emulsion can have been generated by the electrons of pair n. 2 (see Fig. 6-bis). We must think that almost all the remaining pairs are the materialization of incident photons, according to the fact that their multiplication is insignificant because of the small thickness of traversed emulsion (less than 0.54 radiation lengths). If we assume

that ~ 11 pairs are not secondary production (pairs n. 1 and n. 2 and 9 of the last 22 pairs) we find a good agreement with the experimental data (see Fig. 8).

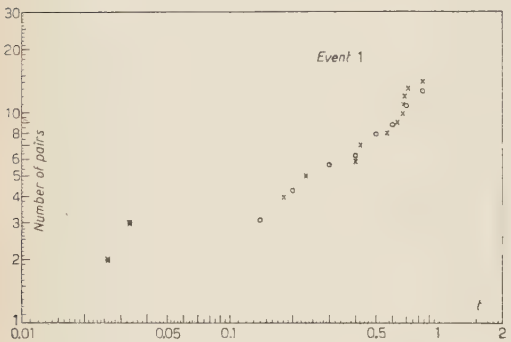

Fig. 7. – Experimental number of pairs versus radiation length. ○ expected number of pairs, calculated under the assumption that 7 high energy pairs (no. 1, 2, 3, 4, 5, 7, 9) are due to incident photons, and each of them multiplicates according to Arley's previsions.

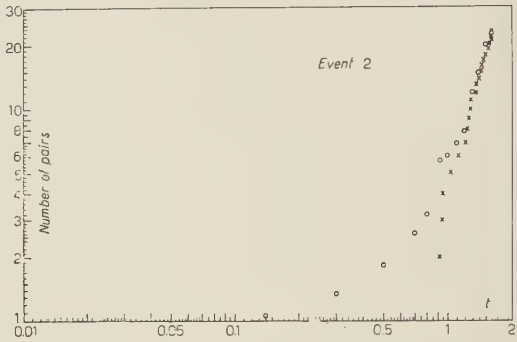

Fig. 8. – Experimental number of pairs versus radiation length. ○ expected number of pairs, calculated under the assumption that 11 incident photons corresponding to pairs no. 1, 2, 3, 4, 9, 11, 12, 13, 15, 17, 18, multiplicate according to Arley's previsions.

4. – Conclusions.

From the preceding considerations, the main features of the events available for a tentative interpretation are the following:

a) the position in the stack;

b) the angular collimation;

c) the energy of the individual pairs;

d) the minimum number of photons necessary to account for the whole phenomenon.

First we wish to investigate whether the photons can derive from the decay of some π^0-mesons. As the points of origin of all the observed pairs are contained in a cone whose opening angle is of the order of 10^{-3} rad, it seems reasonable to assume that the maximum angle between the two photons arising from the decay of the same π^0-meson must be of the same order. Since, under the assumption of the approximate equipartition of energy between the two photons, the energy of the π^0-meson and the angle θ between its two

decay products are related by the formula:

$$\gamma \sim \frac{2}{\theta}$$

(where $\gamma = E/m_\pi c^2$), we calculate that the energy of the supposed π^0-meson must be at least of 270 GeV. This means that the hypothesis of π^0-mesons is consistent with our data only if our energies are underestimated.

Let us accept for a moment the π^0 hypothesis and try to determine their origin. Because of the position of the events in the stack, the π^0 cannot have been produced outside the emulsion. In fact, a π^0-meson with $\gamma = 2\,000$ will travel only 2 or 3 mm and it is very unlikely that the remaining emulsion thickness should have been traversed by several photons without materializing. A careful scanning along the shower axis in the backward direction yielded no nuclear interaction of such an energy as to be correlated with the described events; therefore the supposed π^0-mesons do not belong to a meson shower, in which also charged particles would be present.

We cannot exclude that the events are due to the decay in some π^0-mesons of a neutral unstable particle, with a lifetime of the order of 10^{-10} s; but the mass of this particle cannot be smaller than the mass of a heavy meson, and consequently its energy must be of the order of 10^{12} eV, that is an improbably high energy with respect to the measured energies.

It seems to us that an interpretation more consistent with the actual angular collimation and the most probable values of the energies can be given in terms of a purely electromagnetic process. In this case, we must think that the production of photons, with respect to the theoretical previsions, is considerably increased, at least at high energies, by some unknown process, for example multiple photon production. An anomalous trident production at high energies cannot account for the whole phenomenon. In fact, in each event there are at most two or three energetic pairs whose points of origin are not clearly resolvable from some tracks.

Another possible explanation is that a light neutral unstable particle should disintegrate directly in several photons.

We wish also to point out that an additional difficulty arises from the large gap between the second and the third pair observed in event 2. This feature suggests that either the number of incident photons has been overestimated, and the event presents an extreme fluctuation, or the photon production is not simultaneous. In the last case, a supposed excited particle could have decayed by steps.

Since our data do not give conclusive evidence for any of the possible interpretations a richer statistics of events of this type is necessary to give a more precise explanation.

We wish to express our gratitude to Professor G. WATAGHIN for his constant encouragement and his valuable suggestions, and to Dr. R. ASCOLI for useful discussions.

RIASSUNTO

Si descrivono dettagliatamente due casi di sciami di coppie di particelle cariche, e si danno i risultati delle misure sperimentali. Una analisi delle caratteristiche comuni ai due eventi rende difficile la loro interpretazione come normali cascate elettrofotoniche. Si suggeriscono altre possibili interpretazioni.

IL NUOVO CIMENTO Vol. II, N. 2 1° Agosto 1955

On the Motion of Charged Particles in General Relativity.

B. Bertotti

Dublin Institute for Advanced Studies

(ricevuto il 1° Giugno 1955)

Summary. — In this paper two things are done: *a*) the procedure for obtaining the self-reaction terms according to Einstein's method [see (1)] is expounded and greatly abbreviated by a dimensional consideration; *b*) the problem of the motion of two charged particles is solved with the aid of the «*geodesic method*» [see (7)].

1. – The " New Approximation Method ".

The equations of motion for charged particles follow necessarily from the field equations of general Relativity:

$$G_{\mu\nu} + 8\pi E_{\mu\nu} = 0 \,, \tag{1}$$

where $G_{\mu\nu}$ is Einstein's tensor, and

$$E_{\mu\nu} = \frac{1}{4\pi}\left(-F_{\mu\alpha}F_{\nu}^{\alpha} + \frac{1}{4}\, g_{\mu\nu}F_{\alpha\beta}F^{\alpha\beta}\right) \tag{2}$$

the energy-momentum tensor of the electromagnetic field $F_{\alpha\beta}$. A particle is represented by a field singularity, avoiding in this way the problem of its internal structure and of the form of the matter tensor.

Einstein's «new approximation method» (1) for solving the gravitational equations has been applied by L. Infeld and P. Wallace (2) to the equation (1);

(*) On leave of absence from the Istituto Nazionale di Fisica Nucleare, Sezione di Milano.

(1) See A. Einstein, L. Infeld and B. Hoffman: *Ann. of Math.*, **39**, 66 (1938). An improved version is contained in: A. Einstein and L. Infeld: *Can. Jour. of Math.*, **1**, 209 (1949), here quoted as EI.

(2) L. Infeld and P. Wallace: *Phys. Rev.*, **57**, 797 (1940).

they neglected cross-terms between electromagnetic and gravitational fields and non-linear combinations of the latter, and report, that by a laborious procedure one gets, in this approximation, precisely the equation proposed by DIRAC [3]. It is worth while to recall the main features of the method and to add a dimensional consideration, which will make the task much simpler. In passing we should like to stress the fact that the « new approximation method » is the only one known for solving a non-linear tensorial equation like (1) to any degree of accuracy.

The fundamental tensor will be expanded in a series, the parameter being the reciprocal of the speed of light. This allows the splitting of the equations (1) in successive linear sets. We assume *quasi-stationary* conditions, i.e. we regard the time-derivative of any quantity as small compared with its space-derivatives. The mass of the particle arises merely as a constant of integration, and is assumed a priori to be *positive*.

The auxiliary variables

$$\gamma_{\mu\nu} = h_{\mu\nu} - \tfrac{1}{2}\eta_{\mu\nu}\eta^{\alpha\beta}h_{\alpha\beta} \quad [4] \tag{3}$$

inserted in (1) yield the following linear terms:

$$\tfrac{1}{2}\eta^{\varrho\sigma}(\gamma_{\mu\nu,\varrho\sigma} - \gamma_{\mu\varrho,\nu\sigma} - \gamma_{\nu\varrho,\mu\sigma} + \eta_{\mu\nu}\eta^{\alpha\beta}\gamma_{\alpha\varrho,\beta\sigma}) .$$

Grouping the equations in (1) according to their order of magnitude, and denoting by $S_{\mu\nu}$ the non-linear terms in $G_{\mu\nu}$, we get the equations:

$$\gamma_{00,ss} = \gamma_{sr,sr} + 2S_{00} + 16\pi E_{00} \equiv B_{00} \tag{4a}$$

$$\gamma_{0i,ss} - \gamma_{0s,si} = -\gamma_{00,0i} + \gamma_{is,s0} + 2S_{0i} + 16\pi E_{0i} \equiv B_{0i} \tag{4b}$$

$$\gamma_{ij,ss} - \gamma_{is,js} - \gamma_{js,is} + \delta_{ij}\gamma_{sr,sr} =$$
$$= -\gamma_{i0,j0} - \gamma_{j0,i0} + 2\delta_{ij}\gamma_{0s,0s} + \gamma_{ij,00} - \delta_{ij}\gamma_{00,00} + 2S_{ij} + 16\pi E_{ij} \equiv B_{ij} . \tag{4c}$$

The first equation to be solved is (4*a*) at its lowest order; next comes (4*b*), and afterwards (4*c*); again (4*a*) at the next order, and so on. One can see that all the right-hand sides, denoted by $B_{\mu\nu}$, are always known from the

[3] P. A. M. DIRAC: *Proc. Roy. Soc.*, A **167**, 148 (1938).

[4] Greek indices range from 0 to 3; Latin from 1 to 3. The flat metric (1, −1, −1, −1) is denoted by $\eta_{\mu\nu}$ (or $\eta^{\mu\nu}$), and the deviations from it by $h_{\mu\nu}$:

$$g_{\mu\nu} = \eta_{\mu\nu} + h_{\mu\nu} .$$

A comma indicates partial differentiation, and a dot an ordinary time-derivative.

previous equations (or zero). Now it can be shown that for the integration of equations of the types (4*b*) and (4*c*) it is required that the following relations hold at each step (the reason is that the unknown left hand sides of (4*b*) and (4*c*) satisfy *identically* the same relations):

I.

$$B_{0i,j} = 0\,, \tag{5a}$$

$$B_{ij,j} = 0\,. \tag{5b}$$

Does this actually happen? Yes, because the B quantities are built up with solutions of the previous approximations (this is shown by the same line of reasoning used in EI (§ 7), observing that $E_{\mu\nu}$ has by definition vanishing divergence).

II. The surface integrals

$$C_0 = -\frac{1}{16\pi}\int_1 B_{0j}n^j\,\mathrm{d}s \tag{6a}$$

$$C_i = -\frac{1}{16\pi}\int_1 B_{ij}n^j\,\mathrm{d}s \tag{6b}$$

have to vanish. By n^j we mean the ordinary euclidean outward normal to the surface of integration, which is *any* surface enclosing only (say) the first singularity (by (5), and Gauss' theorem, the integrals are independent of its shape). We make the first integral C_0 vanish by adding to γ_{00} at a previous step a suitable harmonic, *pole-type* function, solution of the homogeneous equation corresponding to (4*a*); by adding a dipole field, we could also make C_i vanish. But since a dipole solution is inconsistent with a positive mass, we exclude dipoles and the three conditions

$$C_i = 0 \tag{7}$$

are, at each stage of approximation, differential conditions imposed on the world line of the singularity; when we sum up the contributions coming from the different orders we obtain the equations of motion for the particle.

2. – The Self-Reaction Force.

Since we will be dealing in the second part of the paper with the external force, we may here confine ourselves to the self-reaction, to wit to the con-

tributions to the integrals C_i depending only on the charge of the enclosed particle.

We choose gravitational units, in which mass and charge have the dimension of a length (for the electron e.g., $m \cong 6.7 \cdot 10^{-56}$ cm; $e \cong 1.4 \cdot 10^{-34}$ cm) and the speed of light is unity. We will neglect in this part of the work:

— cross terms between m and e;

— powers of e higher than the third (notice that, since $E_{\mu\nu}$ is a quadratic in $F_{\alpha\beta}$, only even powers of e can occur).

The first allows us to solve separately the equations for the parts of the field depending on m and on e only; they will be linked at each step of approximation by the integral conditions (7). The numerical factor in (6*b*) is chosen in such a way that the terms linear in m give rise to the product mass times acceleration, with a minus sign. Also, we may compute the energy-momentum tensor (2) just as in restricted Relativity.

We call

$$x^i = y^i(x^0) \tag{8}$$

the path of the particle. The calculation will be greatly simplified by taking a Lorentz frame in which the body is at rest at the moment we consider, say $x^0 = 0$:

$$\dot{y}^i(0) = 0 \,. \tag{9}$$

Consider now that the whole approximation procedure is such that the integrals (6) are polynomials in $\ddot{y}^i$ and its derivatives; and that in our units the force is dimensionless. This and the fact that no other length except e (actually only e^2) is involved is enough for averring that the only possible term *is the one with three time-derivatives*, i.e.

$$e^2 \dddot{y}^i \,, \tag{10}$$

apart from a numerical factor. No term can contain four time-derivatives, for the only dimensionally possible would be a quadratic form in $\ddot{y}^i$; but no three-vector can be built in such a way.

To confirm that in (10) the factor is actually the well-know $\frac{2}{3}$, we will use a development in series of the *retarded* potentials given by EDDINGTON (5),

(5) A. EDDINGTON: *The mathematical theory of relativity* (Cambridge, 1924), p. 253.

whose relevant terms read:

$$A_0 = e\left[\frac{1}{r} + \frac{1}{2}\ddot{r} - \frac{1}{6}\frac{\mathrm{d}^3}{\mathrm{d}x^{03}}(r^2) + \ldots\right] \tag{11a}$$

$$A_i = e\left[-\frac{1}{r}\dot{y}^i + \ddot{y}^i - \frac{1}{2}\frac{\mathrm{d}^2}{\mathrm{d}x^{02}}(r\dot{y}^i) + \ldots\right], \tag{11b}$$

r being the ordinary distance from the particle. The electromagnetic tensor

$$F_{\mu\nu} = A_{\mu,\nu} - A_{\nu,\mu} \tag{12}$$

is then:

$$F_{0i} = e\left[-\frac{1}{r^2}r_{,i} + \frac{1}{2}\ddot{r}_{,i} + \frac{\mathrm{d}}{\mathrm{d}x^0}\left(\frac{1}{r}\dot{y}^i\right) - \frac{1}{3}\frac{\mathrm{d}^3}{\mathrm{d}x^{03}}(r\,r_{,i}) - \dddot{y}^i \ldots\right] \tag{13a}$$

$$F_{ij} = e\left[\frac{1}{r^2}(r_{,j}\dot{y}^i - r_{,i}\dot{y}^j) + \frac{1}{2}\frac{\mathrm{d}^2}{\mathrm{d}x^{02}}(r_{,i}\dot{y}^j - r_{,j}\dot{y}^i) + \ldots\right]. \tag{13b}$$

These formulae, inserted in (2) allow us to split the gravitational equations (1) in the various orders, according to the number of time-derivations coming in. We want to know the explicit expression of B_{ij} at the stage in which *three* time-differentiations occur. From (4*c*) we see that for this we need the parts of γ_{00} and γ_{ij} with one time-derivation, and the parts of γ_{0i} with two time-derivations. We should then solve the corresponding field equations. But now to avoid ambiguity, we decide to choose the null solution when the B quantities are zero in the equation we are dealing with. Then, counting the number of time-derivations coming in the corresponding components of $E_{\mu\nu}$ [see (2)] and carefully examining the form of the right-hand sides of (4), we easily see that all the above parts of the γ's are zero. Thus we are left with the integrals [see (6*b*) and (4*c*)]:

$$-\int_{S_1} E_{ij}n^j \mathrm{d}S. \tag{14}$$

We take as the surface of integration a sphere S_1, with its centre in y_1^i; and we notice also that, since the result is independent of the radius, only terms singular as r^{-2} will contribute.

The explicit formula for E_{ij} is, from (2):

$$E_{ij} = \frac{1}{4\pi}\left(F_{ik}F_{jk} - F_{0i}F_{0j} + \frac{1}{2}\delta_{ij}F_{0k}F_{0k} - \frac{1}{4}\delta_{ij}F_{kh}F_{kh}\right). \tag{15}$$

From (13*b*) we see that the magnetic field F_{ij} contributes nothing. A short computation confirms that the *relevant* terms are:

$$E_{ij} \sim -\frac{1}{4\pi}\frac{2}{3}\frac{1}{r^2}\left(r_{,i}\dddot{y}^j + r_{,j}\dddot{y}^i - \delta_{ij}r_{,s}\dddot{y}^s\right). \tag{16}$$

To compute the integrals (14) we notice that, for considerations of symmetry

$$\int_{S_1}\frac{1}{r^2}\,r_{,i}n^i\,\mathrm{d}S = \frac{4\pi}{3}\,\delta_{ij}\,. \tag{17}$$

Thus the above integral (14) gives just the required term

$$\tfrac{2}{3}e^2\ddot{y}^i\,. \tag{18}$$

It is also easily established that if we take instead of (11) the developments corresponding to the *retarded* potentials, we get instead of (18)

$$-\tfrac{2}{3}e^2\dddot{y}^i\,. \tag{18'}$$

Since (18) [or (18′)] is the only possible term containing e^2, this result is valid for *any* velocity of the particle.

The general form of the reaction force in this approximation can be obtained from (18) [or (18′)] by a Lorentz transformation.

3. – The Interaction of Two Charges.

An answer to the problem of the motion of more charged particles, up to the first relativistic corrections, could be obtained by undertaking an enormous computational work according to EI's pattern. But we can avoid that. D. M. Chase (6) proved that the motion of a *test charged particle* (which is defined by taking the limit when m and e tend both to zero, but their ratio does not) is described by the law, derived from the field equations (1):

$$\frac{\mathrm{d}^2x^\mu}{\mathrm{d}s'^2} + \left\{\begin{matrix}\mu\\ \varrho\sigma\end{matrix}\right\}'\frac{\mathrm{d}x^\varrho}{\mathrm{d}s'}\frac{\mathrm{d}x^\sigma}{\mathrm{d}s'} = -\frac{e}{m}\,F'^\mu{}_\nu\,\frac{\mathrm{d}x^\nu}{\mathrm{d}s'}\,; \tag{19}$$

where any dashed quantity refers to the *background* field, obtained by putting

(6) D. M. Chase: *Phys. Rev.*, **95**, 243 (1954).

$m = e = 0$. Using a very plausible method, which gives the right result in the case of a purely gravitational field (7), we will apply the formula (19) to solve the problem of the mutual action of two charged particles.

Our approximation will consist in regarding both the Newtonian (m/r) and Coulombian (e/r) potentials of the second order; we propose to evaluate the fourth order equations of motion for the first particle. We indicate by the suffixes 1 and 2 the two particles, whose euclidean distance is r. We will follow closely the same procedure used in G, and we beg to refer to it for any detail lacking.

The metric field of a charged particle (the second) permanently at rest at the origin can be described by (8):

$$(20)\quad ds^2 = \left(1 - 2\frac{m_2}{r'} + \frac{e_2^2}{r'^2}\right)dx^{0^2} - \left(1 - 2\frac{m_2}{r'} + \frac{e_2^2}{r'^2}\right)^{-1} dr'^2 - r'^2\, d\theta^2 - r'^2 \sin^2\theta\, d\varphi^2 .$$

For all g-quantities except g_{00}, the second order will suffice:

$$(20')\qquad ds^2 = \left(1 - 2\frac{m_2}{r'} + \frac{e_2^2}{r'^2}\right)dx^{0^2} - \left(1 + 2\frac{m_2}{r'}\right)dr'^2 - r'^2\, d\theta^2 - r'^2 \sin^2\theta\, d\varphi^2 .$$

The change in the radial coordinate

$$(21)\qquad r' = r + m_2 + \frac{1}{4}\frac{m_2^2}{r} - \frac{1}{4}\frac{e_2^2}{r}$$

carries (20′) into the *isotropic* form

$$(22)\qquad ds^2 = (1 - 2\varphi + 2\varphi^2 + V^2)\,dx^{0^2} - (1 + 2\varphi)\,dx^i\,dx^i ,$$

$$(\varphi = m_2/r;\ V = e_2/r)$$

which is required by physical considerations. Also, the electromagnetic field of a charge at rest is, exactly (8):

$$(23)\qquad F_{0i} = V_{,i} ; \qquad F_{ij} = 0 .$$

A simple computation shows then that in this coordinate frame the equa-

(7) We call it the « *geodesic method* »: B. Bertotti: *Nuovo Cimento*, **12**, 226 (1594) (here quoted as G).

(8) A. Eddington: *The mathematical theory of relativity* (Cambridge, 1924), p. 185. We use electrostatic units of charge.

tions of motion (19) read, up to the fourth order:

$$\ddot{y}_1^i - \varphi_{,i} + e_1/m_1 V_{,i} = \varphi_{,i}(\dot{y}_1^s \dot{y}_1^s - 4\varphi) - 4\varphi_{,s}\dot{y}^s \dot{y}^i + \tag{24}$$
$$+ e_1/m_1[V_{,i}(\tfrac{1}{2}\dot{y}_1^s \dot{y}_1^s + 3\varphi) + V_{,s}\dot{y}_1^s \dot{y}_1^i] - V V_{,i} .$$

When the first body also has finite mass and charge, it will impart to the second—which we may take still *momentarily at rest* at the origin—an acceleration, whose main part is:

$$\ddot{y}_2^i = -\left(\frac{m_1}{r}\right)_{,i} + \frac{e_2}{m_2}\left(\frac{e_1}{r}\right)_{,i} . \tag{25}$$

To compute the $g_{\mu\nu}$-field for this «accelerated particle at rest», we read (22) as the field of 2 in an instantaneously co-moving frame, and we apply to it a Lorentz transformation to the frame actually used. The same reasoning used in G shows that the only new relevant terms are

$$h_{0i} = 4\varphi \dot{y}_2^i \tag{26}$$

which, by (25), produce the supplementary terms

$$-4\varphi_{,i}\frac{m_1}{r} + 4V_{,i}\frac{e_1}{r} \tag{27}$$

to be added to the right-hand side of (24). Also the electromagnetic field changes with the Lorentz transformation. The four potential becomes $(V, -V\dot{y}_2^i)$, which gives a supplement

$$V\ddot{y}_2^i$$

to F_{0i}. By (25) and (19) this causes (27) to change in

$$-4\varphi_{,i}\frac{m_1}{r} + 5V_{,i}\frac{e_1}{r} - \frac{e_1}{m_1}\frac{e_2}{m_2}V_{,i}\frac{e_1}{r} . \tag{27'}$$

Finally, we have to take into account the *retardation* of the field. To this end we have only to replace in the left-hand side of (24) $1/r$ by

$$\frac{1}{r} + \frac{1}{2}\ddot{r} \tag{28}$$

as one can see, for instance, from the direct considerations used in G. Any,

other correction is irrelevant in our approximation; and it does not make any difference to use *advanced* instead of retarded potentials. By (25) the corrected term (28) reads:

$$\frac{1}{r} - \frac{1}{2}\frac{m_1}{r^2} + \frac{1}{2}\frac{e_2}{m_2}\frac{e_1}{r^2}. \tag{28'}$$

The equation (24) becomes then, with the corrections (27') and (28'):

$$\ddot{y}_1^i - \varphi_{,i} + \frac{e_1}{m_1} V_{,i} = \varphi_{,i}\left(\dot{y}_1^s \dot{y}_1^s - 4\varphi - 5\frac{m_1}{r}\right) - 4\varphi_{,s}\dot{y}_1^s \dot{y}_1^s + \tag{29}$$

$$+ \frac{e_1}{m_1}\left[V_{,i}\left(\frac{1}{2}\dot{y}_1^s \dot{y}_1^s + 3\varphi - 2\frac{e_2}{m_2}\frac{e_1}{r}\right) + V_{,s}\dot{y}_1^s \dot{y}_1^i\right] - V_{,i}\left(V - 7\frac{e_1}{r}\right).$$

The problem is essentially solved. It remains now to get rid of the particular frame we assumed by a Lorentz transformation. By this we mean to replace any quantity occurring in (29)—distances, velocities, accelerations—by its expression in the frame we actually use, in which the second body moves with the velocity $\dot{y}_2^i$. Just for the sake of completeness, we give now the complicated formula one gets.

$$\ddot{y}_1^i - \varphi_{,i} + \frac{e_1}{m_1} V_{,i} = \varphi_{,i}\left[(\dot{y}_1^s - \dot{y}_2^s)(\dot{y}_1^s - \dot{y}_2^s) + \dot{y}_2^s \dot{y}_2^s - 2\dot{y}_1^s \dot{y}_2^s - 4\varphi - 5\frac{m_1}{r}\right] - \tag{30}$$

$$- \varphi_{,s}\left[4(\dot{y}_1^s - \dot{y}_2^s)(\dot{y}_1^i - \dot{y}_2^i) + \dot{y}_2^s \dot{y}_1^i\right] - \frac{1}{2}\left(m_2 - \frac{e_1}{m_1}e_2\right)\frac{\partial}{\partial y_1^i}\left(\frac{y_1^s y_1^j}{r^3}\right)\dot{y}_2^s \dot{y}_2^j - V_{,i}\left(V - 7\frac{e_1}{r}\right) +$$

$$+ \frac{e_1}{m_1}\left\{V_{,i}\left[\frac{1}{2}(\dot{y}_1^s - \dot{y}_2^s)(\dot{y}_1^s - \dot{y}_2^s) - \dot{y}_2^s \dot{y}_2^s + 2\dot{y}_1^s \dot{y}_2^s + 3\varphi - 2\frac{e_2}{m_2}\frac{e_1}{r}\right] + \right.$$

$$\left. + V_{,s}\left[(\dot{y}_1^s - \dot{y}_2^s)(\dot{y}_1^i - \dot{y}_2^i) + \dot{y}_2^s \dot{y}_1^i\right]\right\}.$$

Notice that the magnetic force $e_1/m_1 \; \boldsymbol{v} \wedge \boldsymbol{H}$, being of the fourth order, is « hidden » in the second member.

4. – Conclusion.

Since the geodesic method consists in describing the *mutual* action of the two bodies, its failure to yield the self-reaction term (18) is quite explained; and for a complete description of the motion one has to supplement (29) by (18).

Among the complicated supplementary terms in (29), we wish to draw attention to the 7th in the second member, which is proportional to the spe-

cific charges of the *other* body, and may become relevant when this is very light. Of course, with the orders of magnitude occurring both in microscopic and macroscopic cases, all the correction terms seem to be far below the experimental threshold.

* * *

I wish to express my gratitude to Professor E. SCHRÖDINGER for valuable discussions.

RIASSUNTO

Il presente lavoro comprende due parti: *a*) il procedimento per ottenere la forza di reazione secondo il metodo di EINSTEIN [vedi (1)] è esposto e grandemente semplificato mediante una considerazione dimensionale; *b*) il problema del moto di due particelle cariche è risolto con l'aiuto del « *metodo della geodetica* » [vedi (7)].

Assorbimento di ultrasuoni in miscele di gas contenenti idrogeno.

S. PETRALIA

Istituto di Fisica dell'Università - Bologna

(ricevuto il 1° Giugno 1955)

Riassunto. — Si riferisce su misure di assorbimento di ultrasuoni in idrogeno puro e in miscele di idrogeno e argon, idrogeno e ossigeno, condotte allo scopo di studiare l'influenza di gas estranei sul tempo di rilassamento rotazionale dell'idrogeno, e di verificare insieme se la teoria di Kohler sull'assorbimento di tipo classico, valevole per miscele di gas monoatomici, si può estendere al caso in cui queste contengono gas biatomici. Si trova una diminuzione del tempo di rilassamento dell'idrogeno per effetto dell'impurità, presente in forte concentrazione. Tale diminuzione non supera il 10% nel caso dell'argon, è molto maggiore nel caso dell'ossigeno. Qui il tempo di rilassamento decresce in modo continuo dal valore competente all'idrogeno a quello competente all'ossigeno. Si determina un valore del tempo di rilassamento dell'ossigeno, che risulta inferiore a quello dato da THALER, ma che è in accordo con il risultato di un calcolo teorico di Brout. Infine sembra si possa concludere che la teoria di Kohler non è senz'altro applicabile al caso delle miscele qui studiate.

1. – Introduzione.

Nel corso di misure sull'assorbimento di ultrasuoni in miscele di gas, intese a studiare l'influenza dei fenomeni di diffusione sull'assorbimento stesso, si è presentato il problema, per il caso di miscele contenenti idrogeno — gas dispersivo a frequenze ultrasonore elevate — di determinare se si altera e come l'assorbimento molecolare di questo gas, per l'aggiunta di gas estranei. È ben nota la grande influenza che sui processi di rilassamento acustico, interessanti le vibrazioni interne delle molecole di un gas, esercitano le impurità, anche se in piccola concentrazione. Per quanto riguarda gli stati di energia rotazionale, che sono responsabili del rilassamento nell'idrogeno, si può prevedere, che un effetto di gas estranei sul tempo di rilassamento possa aver luogo solo

quando questi sono presenti in grande concentrazione, tale cioè che, il tempo necessario perchè avvenga un urto tra una molecola di idrogeno e una molecola dell'impurità sia dello stesso ordine o più piccolo del tempo di rilassamento. Ora per l'idrogeno quest'ultimo è dell'ordine di 10^{-8} s [1], per cui l'impurità deve essere in proporzione superiore a 1 %, affinchè influisca sulla frequenza di rilassamento rotazionale.

Qui si è misurato l'assorbimento di ultrasuoni di frequenza di 3 MHz in miscele di idrogeno con argon e con ossigeno, a diversa concentrazione dei componenti. Si è scelta come una delle impurità l'argon, perchè esso si comporta come gas inerte e d'altra parte essendo monoatomico, è privo di stati di energia rotazionale, per cui si può prevedere che la sua influenza sul tempo di rilassamento dell'idrogeno deve risultare piccola. L'altra impurità, l'ossigeno, è un gas che può reagire chimicamente con l'idrogeno, condizione questa che, secondo A. Eucken [2], determinerebbe un più rapido scambio di energia tra i gradi di libertà di traslazione e i gradi interni della molecola; inoltre esso ha stati di rotazione, che rilassano a frequenze ultrasonore superiori a quelle per le quali è forte l'assorbimento molecolare nell'idrogeno. La miscela idrogeno-ossigeno risulta quindi composta di due gas entrambi dispersivi, con tempi di rilassamento diversi, e c'è da attendersi che essa costituisca una specie molecolare con tempo di rilassamento variabile, a seconda della concentrazione dei componenti, tra i tempi estremi caratteristici per l'idrogeno e per l'ossigeno. Il comportamento potrebbe essere analogo a quello dell'aria, studiata recentemente da C. Ener, A. F. Gabrysh e J. C. Hubbard [3], la quale ha un tempo di rilassamento acustico intermedio ai tempi corrispondenti ai gas principali che la compongono.

Dal confronto dei risultati sperimentali con la teoria dell'assorbimento ultrasonoro di origine molecolare nei gas, si è cercato poi di vedere se l'espressione stabilita da M. K. Kohler [4] per l'assorbimento classico vale anche per le miscele qui esaminate, contenenti almeno un gas biatomico. Di recente la teoria di Kohler, che in più della teoria classica di G. G. Stokes e G. Kirchhoff contiene dei termini dovuti alla diffusione e alla termodiffusione, è stata da me [5] verificata per miscele di gas monoatomici.

[1] E. S. Stewart e J. L. Stewart: *Journ. Acoust. Soc. Am.*, **24**, 194 (1952).

[2] A. Eucken e R. Becker: *Zeits. Phys. Chemie*, B **27**, 235 (1934).

[3] C. Ener, A. F. Gabrysh e J. C. Hubbard: *Journ. Acoust. Soc. Am.*, **24**, 474 (1952).

[4] M. K. Kohler: *Ann. der Phys.*, **39**, 209 (1941).

[5] S. Petralia: *Nuovo Cimento*, **1**, 351 (1955).

2. – Metodo di misura.

Per la misura dell'assorbimento si è fatto uso di un interferometro precedentemente descritto ([6]), tenuto a temperatura di 25 °C. Generalmente la sorgente sonora vibrava sulla frequenza di 3 MHz; qualche misura è stata fatta con un quarzo vibrante sulla frequenza di 0.6 MHz. Ogni sorgente era accoppiata con una propria camera interferometrica. I quarzi venivano alimentati da un oscillatore ad accoppiamento elettronico, e le reazioni acustiche venivano osservate con un voltmetro elettronico. Le misure del coefficiente d'assorbimento dell'ampiezza sonora per lunghezza d'onda sono state eseguite col metodo di H. C. HARDY ([7]).

L'idrogeno era ottenuto da bombole del commercio e veniva purificato per passaggio attraverso trappole, raffreddate con azoto liquido. L'argon era anch'esso ottenuto da bombola, e, per purificarlo, lo si lasciava per qualche tempo a contatto con calcio metallico, alla temperatura di 550 °C. L'ossigeno infine era preparato per riscaldamento di permanganato di potassio, e quindi condotto nell'apparecchiatura attraverso trappole, raffreddate con miscela di anidride carbonica solida e acetone.

Le concentrazioni dei gas nelle miscele erano determinate in base alle loro pressioni parziali. La pressione iniziale della miscela era di circa una atmosfera; essa veniva ridotta nelle misure successive, ponendo la camera interferometrica in comunicazione, attraverso un largo rubinetto, con un recipiente preventivamente vuotato e attendendo per alcune ore, onde assicurare con una completa diffusione la costanza della composizione della miscela. Si sono realizzati valori del rapporto f/p, tra la frequenza e la pressione del gas, compresi tra 1.5 e 45 MHz/atmosfere.

3. – Risultati sperimentali.

I risultati delle misure sono raccolti nelle tabelle I-IV. Nella tabella I sono posti a confronto i coefficienti d'assorbimento per lunghezza d'onda $\alpha\lambda_{sp}$ nell'idrogeno puro, determinati da me, con quelli determinati da I. F. ZARTMAN ([8]) e da E. S. STEWART e J. L. STEWART ([1]). Le misure effettivamente sono state eseguite, nei tre casi, a temperature diverse e cioè a 25 °C, a 36,5 °C e a 0 °C rispettivamente. Non è noto in modo preciso quale è la dipendenza di $\alpha\lambda_{sp}$ dalla temperatura; trattandosi qui di temperature poco discoste le une dalle altre, si è ritenuto di poter fare il confronto tra le tre determinazioni.

([6]) S. PETRALIA: *Nuovo Cimento*, **10**, 817 (1953).
([7]) H. C. HARDY: *Journ. Acoust. Soc. Am.*, **15**, 91 (1943).
([8]) I. F. ZARTMAN: *Journ. Acoust. Soc. Am.*, **21**, 171 (1949).

TABELLA I. – *Coefficienti di assorbimento per lunghezza d'onda nell'idrogeno.* Misure di I. F. ZARTMAN ($t = 36.5$ °C), E. S. STEWART e J. L. STEWART ($t = 0$ °C) e dell'Autore ($t = 25$ °C).

ZARTMAN		STEWART		AUTORE	
f/p (MHz/atm)	$\alpha\lambda_{sp}$	f/p (MHz/atm)	$\alpha\lambda_{sp}$	f/p (MHz/atm)	$\alpha\lambda_{sp}$
2.13	0.135	2.0	0.099	2.96	0.146
2.39	0.182	2.5	0.12	4.09	0.166
2.80	0.193	3.0	0.135	6.05	0.232
3.34	0.168	4.0	0.182	8.04	0,280
4.22	0.231	7.9	0.29	10.25	0.336
5.68	0.315	16	0.30	13.45	0.361
10.95	0.388	30	0.30	18.73	0.345
14.25	0.368	60	0.33	27.10	0.320
16.77	0.326	—	—	—	—
26.12	0.186	—	—	—	—

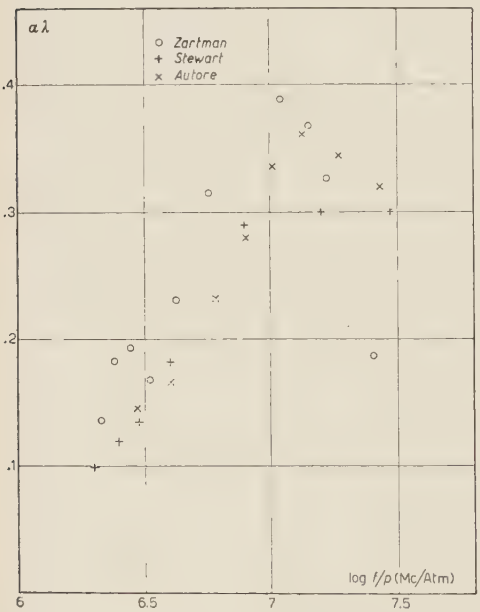

Fig. 1. – Valori di $\alpha\lambda_{sp}$ per l'idrogeno, secondo ZARTMAN, STEWART e l'Autore, per diversi f/p.

Si può notare che a parità del rapporto f/p i valori di $\alpha\lambda_{sp}$ a 25 °C sono compresi tra i valori determinati alle temperature estreme. La disposizione interferometrica usata permette quindi di ottenere risultati attendibili. Comunque il buon funzionamento di essa è stato verificato con misure di assorbimento nell'argon, a varie pressioni, ritrovando sempre il valore classico per il rapporto α/f^2 relativo a tale gas.

Nelle tabelle II e III sono elencati, per le varie miscele realizzate con le due coppie di gas, in funzione del rapporto f/p, il coefficiente d'assorbimento per lunghezza d'onda sperimentale, $\alpha\lambda_{sp}$, il coefficiente d'assorbimento dell'ampiezza sonora α_{sp}, il corrispondente coefficiente d'assorbimento classico α_{cl}, adottato nei calcoli, il rapporto α_{sp}/α_{cl} e il coefficiente $\alpha\lambda_{rl} = \alpha\lambda_{sp} - \alpha\lambda_{cl}$, che rappresenta quella parte del coefficiente d'assorbimento per lunghezza d'onda, che è dovuta ai processi di assorbimento molecolare. Nella tabella IV compaiono il tempo tra due collisioni di una molecola τ_c, il

tempo di rilassamento τ_r, la frequenza ultrasonora di massimo assorbimento f_m e il numero medio n di urti richiesti per uno scambio di energia tra gli stati di rotazione e di traslazione di una molecola.

Le misure sono state eseguite in circostanze diverse; non tutte hanno lo stesso grado di precisione. La causa più importante di errore risiede nella alterazione, che può subire di volta in volta la composizione delle miscele, soprattutto per effetto di gas estranei, che possono svilupparsi nella apparecchiatura.

TABELLA II. – *Coefficienti di assorbimento in miscele di idrogeno-argon.* $t = 25$ °C.

Concentrazione	f/p (MHz/atm)	$\alpha\lambda_{sp}$	α_{sp} (cm^{-1})	α_{cl} (cm^{-1})	α_{sp}/α_{cl}	$\alpha\lambda_{rl}$
90.5% H_2	3.00	0.163	6.09	0.89	6.84	0.140
9.5% A	5.00	0.273	10.01	1.48	6.75	0.234
	7.10	0.329	11.94	2.12	5.64	0.273
	9.40	0.365	13.07	2.79	4.67	0.291
	11.51	0.390	13.81	3.41	4.04	0.300
	15.27	0.43	15.28	4.53	3.37	0.32
	17.12	0.47	16.62	5.09	3.26	0.34
	20.24	0.50	17.57	5.99	2.93	0.34
	26.40	0.54	18.81	7.85	2.39	0.33
80.4% H_2	1.76	0.091	0.90	0.198	4.54	0.071
19.6% A	3.00	0.158	7.64	1.69	4.52	0.124
	4.15	0.207	9.95	2.33	4.26	0.159
	4.86	0.235	11.39	2.73	4.17	0.182
	5.75	0.255	12.15	3.26	3.73	0.188
	7.09	0.304	14.56	3.97	3.66	0.222
	7.97	0.311	14.76	4.48	3.29	0.219
	11.09	0.355	16.53	6.23	2.65	0.227
	15.46	0.415	18.99	8.68	2.19	0.237
	21.44	0.47	20.88	12.04	1.73	0.22
	29.72	0.54	24.05	16.99	1.44	0.20
60.2% H_2	1.83	0.086	1.11	0.28	3.95	0.065
39.8% A	2.99	0.138	8.87	2.30	3.86	0.102
	4.11	0.176	11.23	3.16	3.55	0.127
	5.68	0.222	14.04	4.37	3.21	0.154
	7.85	0.265	16.53	6.03	2.74	0.172
	10.90	0.317	19.62	8.40	2.33	0.187
	15.15	0.37	22.61	11.65	1.94	0.19
	21.24	0.43	25.83	16.33	1.58	0.18
	29.5	0.49	29.13	22.70	1.28	0.14
31% H_2	1.50	0.052	0.835	0.245	3.41	0.037
69% A	2.51	0.074	1.20	0.407	2.94	0.049
	3.03	0.096	1.55	0.49	3.15	0.066
	4.17	0.137	10.94	3.37	3.24	0.095

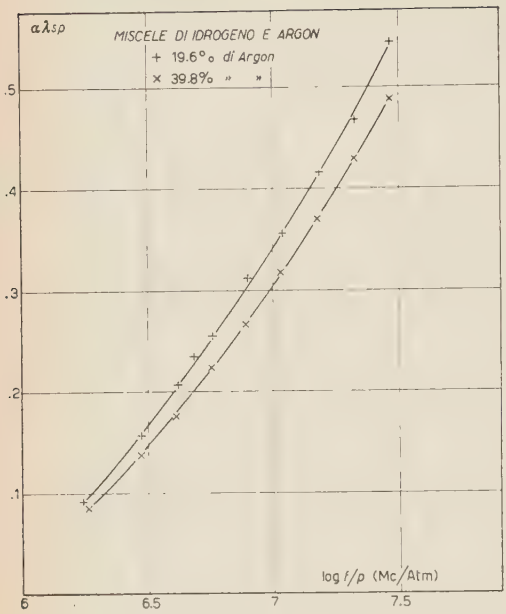

Fig. 2. – Parametro $\alpha\lambda_{sp}$ per due miscele di idrogeno-argon, in funzione di f/p.

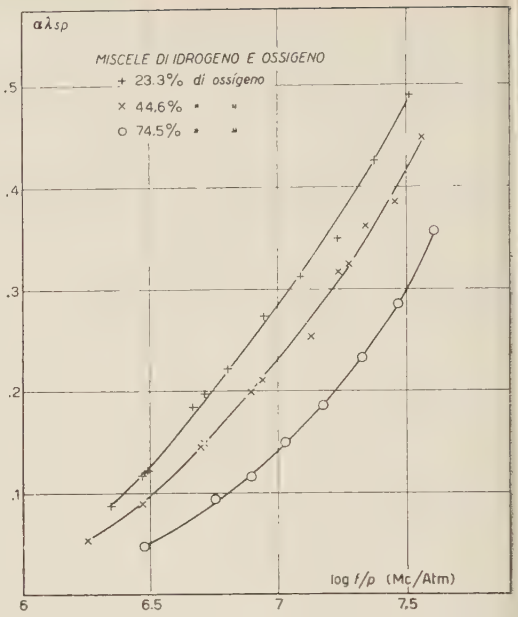

Fig. 3. – Parametro $\alpha\lambda_{sp}$ per tre miscele di idrogeno-ossigeno, in funzione di f/p.

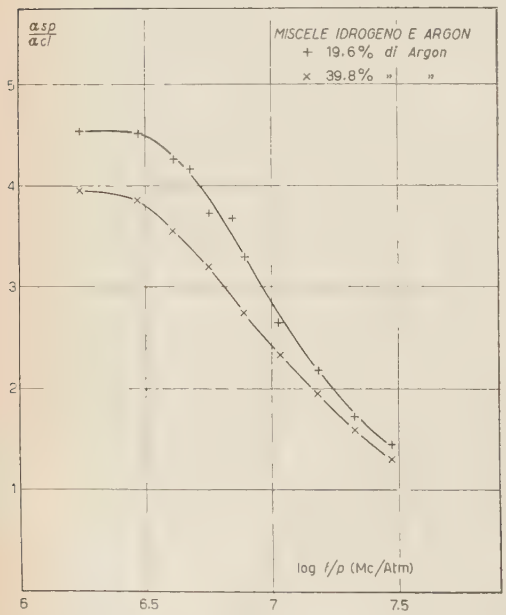

Fig. 4. – Rapporto α_{sp}/α_{cl} per due miscele di idrogeno-argon; variabile f/p.

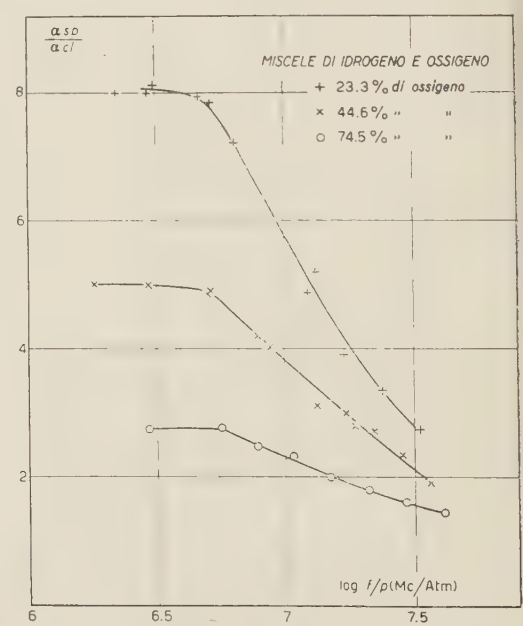

Fig. 5. – Rapporto α_{sp}/α_{cl} per tre miscele di idrogeno-ossigeno; variabile f/p.

TABELLA III. – *Coefficienti di assorbimento in miscele di idrogeno-ossigeno.* $t = 25$ °C.

Concentrazione	f/p (MHz/atm)	$\alpha\lambda_{sp}$	α_{sp} (cm^{-1})	α_{cl} (cm^{-1})	α_{sp}/α_{cl}	$\alpha\lambda_{rl}$
90% H_2	3.12	0.138	4.95	0.40	12.37	0.127
10% O_2	5.13	0.201	7.18	0.66	10.87	0.183
	5.92	0.231	8.17	0.76	10.75	0.210
	7.70	0.278	9.80	0.99	9.89	0.251
	8.74	0.291	10.16	1.13	8.99	0.260
	12.85	0.355	12.29	1.65	7.45	0.309
	14.67	0.364	12.55	1.89	6.64	0.312
	20.76	0.46	15.70	2.67	5.88	0.39
	32.03	0.50	16.79	4.12	4.07	0.38
76.7% H_2	2.21	0.087	0.83	0.104	8.00	0.076
23.3% O_2	2.97	0.117	5.58	0.70	7.99	0.102
	3.12	0.122	5.98	0.74	8.11	0.106
	4.66	0.184	8.75	1.10	7.94	0.161
	5.19	0.198	9.63	1.23	7.85	0.172
	6.42	0.233	10.96	1.52	7.22	0.201
	8.90	0.273	12.76	2.11	6.05	0.229
	12.39	0.312	14.31	2.93	4.88	0.250
	17.20	0.350	15.90	4.07	3.90	0.275
	23.90	0.42	19.04	5.65	3.36	0.30
	32.90	0.49	21.56	7.79	2.77	0.32
55.4% H_2	1.80	0.054	0.682	0.133	5.10	0.044
44.6% O_2	2.98	0.089	5.55	1.10	5.04	0.072
	5.01	0.146	9.09	1.86	4.88	0.117
	5.13	0.149	9.34	1.90	4.91	0.119
	7.86	0.200	12.32	2.92	4.22	0.154
	8.74	0.211	13.10	3.24	4.04	0.160
	13.37	0.254	15.47	4.96	3.12	0.175
	17.36	0.317	19.36	6.44	3.00	0.214
	18.79	0.325	19.60	6.97	2.81	0.214
	22.18	0.362	22.30	8.23	2.71	0.238
	24.43	0.38	22.80	9.69	2.35	0.23
	36.38	0.45	25.94	13.49	1.92	0.24
25.5% H_2	2.97	0.047	3.78	1.38	2.74	0.030
74.5% O_2	5.64	0.093	7.32	2.63	2.78	0.060
	7.84	0.115	9.05	3.65	2.48	0.069
	10.75	0.149	11.67	5.01	2.33	0.087
	14.95	0.186	14.25	7.00	2.03	0.099
	21.05	0.23	17.93	9.82	1.82	0.11
	29.14	0.29	22.03	13.60	1.62	0.12
	40.6	0.36	27.30	18.90	1.45	0.13

(*segue* TABELLA III).

Concentrazione	f/p (MHz/atm)	$\alpha\lambda_{sp}$	α_{sp} (cm^{-1})	α_{cl} (cm^{-1})	α_{sp}/α_{cl}	$\alpha\lambda_{rl}$
18% H_2 82% O_2	1.79	0.025	0.412	0.169	2.43	0.015
	2.99	0.033	2.76	1.39	1.98	0.016
	5.00	0.059	4.93	2.36	2.09	0.031
	8.71	0.102	8.43	4.10	2.06	0.053
	14.39	0.150	12.39	6.78	1.83	0.069
	18.10	0.179	14.74	8.53	1.73	0.077
	23.59	0.23	18.61	11.11	1.67	0.09
	32.95	0.30	24.35	15.53	1.57	0.11
	44.59	0.38	30.94	21.01	1.47	0.13

Per valori elevati di f/p altra causa di errore, nella misura dell'assorbimento e delle lunghezze d'onda, è il piccolo numero delle reazioni acustiche che si possono osservare. Per quei dati, cui si attribuisce maggiore attendibilità, sono stati costruiti dei grafici (fig. 1-5).

TABELLA IV. – *Tempi di rilassamento, frequenze di massimo assorbimento, rapporto τ_r/τ_c per l'idrogeno e le varie miscele. $t = 25$ °C, $p = 1$ atm.*

Miscela	$\tau_c \cdot 10^{10}$ s	$\tau_r \cdot 10^9$ s	$f_m \cdot 10^{-6}$ s^{-1}	$n = \tau_r/\tau_c$
100 % H_2	0.689	21.0	11.5	305
90.5 % H_2 – 9.5 % A	1.046	20.5	11.6	195
80.4 % H_2 – 19.6 % A	1.178	19.0	12.0	161
60.2 % H_2 – 39.8 % A	1.493	18.9	11.2	126
31 % H_2 – 69 % A	1.677	18.6	10.0	111
90 % H_2 – 10 % O_2	0.983	16.5	14.6	168
76.7 % H_2 – 23.3 % O_2	1.224	12.8	19.1	105
55.4 % H_2 – 44.6 % O_2	1.412	8.4	28.4	60
25.5 % H_2 – 74.5 % O_2	1.560	4.1	58.6	26
18 % H_2 – 82 % O_2	1.576	3.3	73.8	21

4. – Discussione dei risultati.

Secondo la teoria di O. H. KNESER [9] sull'assorbimento molecolare degli ultrasuoni nei gas, teoria formulata per i gradi di libertà di oscillazione della molecola, e che si suppone possa estendersi anche ai gradi di libertà di rota-

[9] O. H. KNESER: *Ann. der Phys.*, **16**, 337 (1933).

zione, si può scrivere per la parte del coefficiente d'assorbimento per lunghezza d'onda dovuta al rilassamento

$$\alpha\lambda_{rl} = \pi \frac{(Q^2 - 1)N}{1 + Q^2N^2} \tag{1}$$

con

$$N = \frac{f}{f_w}, \qquad f_w = \frac{C_v}{2\pi(C_v - C')\tau_r}, \qquad Q^2 = \frac{V_\infty^2}{V_0^2} = \frac{1 + R/(C_v - C')}{1 + R/C_v} \tag{2}$$

dove f_w è la frequenza ultrasonora cui corrisponde un punto di flesso nella curva di dispersione della velocità di propagazione, V_0 e V_∞ sono i valori della velocità per frequenza zero e infinito, C_v il calore specifico a frequenza zero, C' il calore specifico rotazionale, τ_r il tempo di rilassamento.

Con i dati sperimentali relativi all'idrogeno puro, si ottiene, nell'approssimazione in cui si possa trascurare Q^2N^2 rispetto all'unità, $\tau_r = 2.1 \cdot 10^{-8}$ s a pressione atmosferica, in buon accordo con le determinazioni fatte da altri Autori. Infatti nella letteratura si trova che τ_r per l'idrogeno è compreso tra $2.3 \cdot 10^{-8}$ s e $2 \cdot 10^{-8}$ s; il valore più attendibile è $2.3 \cdot 10^{-8}$ s e le differenze possono attribuirsi alla presenza di lievi impurità nei vari campioni di idrogeno.

Una rielaborazione delle espressioni (1) e (2) permette di scrivere per il rapporto tra il coefficiente d'assorbimento sperimentale e il coefficiente d'assorbimento classico

$$\frac{\alpha_{sp}}{\alpha_{cl}} = 1 + \frac{RC'\tau}{2C_p(C_v - C')B}(1 - \omega^2\tau^2) \tag{3}$$

essendo $\omega = 2\pi f$, R costante dei gas perfetti, $C_p = C_v + R$ e

$$\tau = \frac{C_v - C'}{C_v}\tau_r, \qquad B = \frac{\alpha_{cl}V_0}{\omega^2}. \tag{4}$$

Per frequenze basse alle quali si possa ritenere $\omega^2\tau^2 \ll 1$, la (3) diviene

$$\frac{\alpha_{sp}}{\alpha_{cl}} = 1 + \frac{RC'\tau}{2C_p(C_v - C')B} \tag{3'}$$

e da questa si può ricavare τ e quindi τ_r.

Per poter valutare il rapporto α_{sp}/α_{cl}, occorre scegliere un valore opportuno per il coefficiente di assorbimento classico. Tale coefficiente, nel caso che a noi interessa di miscele di gas, si può calcolare o in base all'espressione di Stokes-Kirchhoff ([10]), oppure in base all'espressione più generale data da

([10]) Vedi L. Bergmann: *Der Ultraschall* (Zürich, 1954).

Kohler [4]. Questa ultima espressione vale

$$(5) \qquad \frac{\alpha}{f^2} = \frac{2\pi^2}{V^3}\left\{\frac{4}{3}\frac{\eta}{\varrho} + \frac{\gamma-1}{\gamma}\frac{\Lambda}{c_v\varrho} + \frac{\gamma-1}{\gamma}\frac{\nu'_{12}\nu_{12}}{c_v\varrho} + \gamma D_{12}c_1c_2\left(\frac{M_2-M_1}{M_0}\right)^2 + \right.$$
$$\left. + 2(\gamma-1)\nu'_{12}c_1c_2\frac{M_2-M_1}{M_0}\right\}$$

ed è stata stabilita per miscele di gas monoatomici; la sua estensione al caso di miscele di gas a struttura molecolare più complessa può non essere lecita.

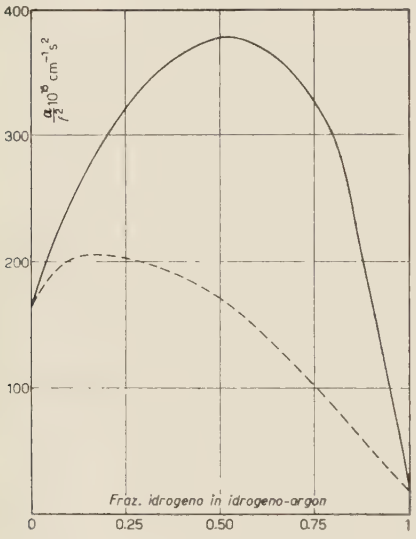

Fig. 6. – Valori classici del parametro α/f^2 per le miscele di idrogeno-argon, calcolati secondo la teoria di Stokes-Kirchhoff (-----) e secondo la teoria di Kohler (——).

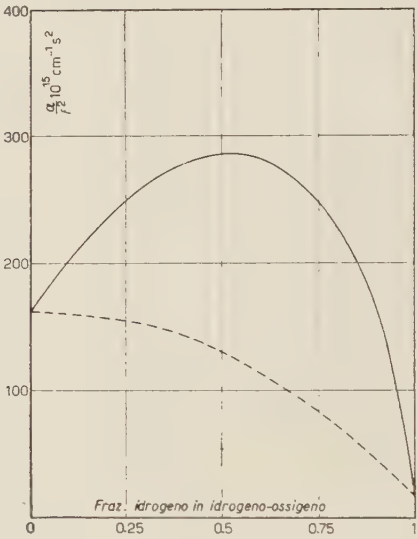

Fig. 7. – Valori classici del parametro α/f^2 per le miscele di idrogeno-ossigeno, calcolati secondo la teoria di Stokes-Kirchhoff (-----) e secondo la teoria di Kohler (——).

Nelle fig. 6 e 7 sono riportati i valori di α/f^2, in funzione della concentrazione di idrogeno nelle due miscele, derivati o dalla espressione di Stokes-Kirchhoff (curva a tratti) o dalla espressione di Kohler (curva continua).

Qui il valore di α_{cl} è stato scelto per tentativi, assumendo o quello di Stokes-Kirchhoff o quello di Kohler o un valore intermedio, col criterio che i valori che si possono dedurre, in base a tale scelta, per gli $\alpha\lambda_{rl}$ si accordino il più possibile con quelli prevedibili con la (1) di Kneser, soprattutto per le misure fatte a bassi f/p, che sono più precise e in base alle quali si è proceduto al calcolo di τ_r. Le fig. 8 e 9 mostrano l'andamento teorico di $\alpha\lambda_{rl}$ in funzione di f/p, per una miscela di idrogeno-argon, ove si è preso per α_{cl} un valore medio tra quelli estremi di Stokes-Kirchhoff e di Kohler, e per una miscela

di idrogeno-ossigeno ove si è preso per α_{cl} il valore di Stokes-Kirchhoff; vi sono segnati anche i punti sperimentali. L'accordo sembra molto buono nel primo caso, meno nel secondo; dal segno delle divergenze bisogna concludere però, che si debba trattare di errori nelle determinazioni di $\alpha\lambda_{sp}$, che possono essere notevoli per f/p elevati. Divergenze si notano anche per le altre miscele, ove, per valori elevati di f/p, si possono avere, a seconda dei casi, valori superiori o inferiori degli $\alpha\lambda_{rl}$, dedotti dall'esperienza, rispetto a quelli teorici.

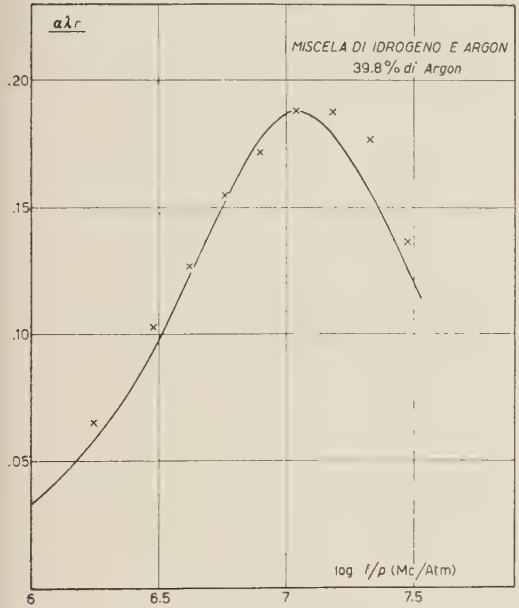

Fig. 8. – Valori sperimentali (×) e teorici (——) di $\alpha\lambda_{rl}$ per una miscela di idrogeno-argon, in funzione di f/p.

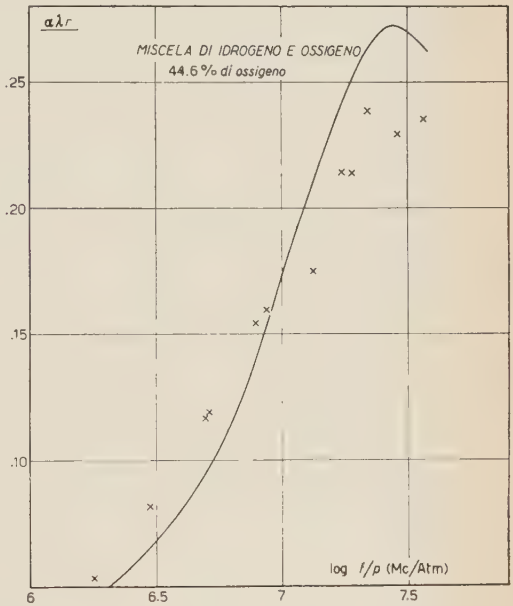

Fig. 9. – Valori sperimentati (×) e teorici (——) di $\alpha\lambda_{rl}$ per una miscela di idrogeno ossigeno, in funzione di f/p.

Fissato il valore di α_{cl}, si è calcolato il rapporto α_{sp}/α_{cl}, che compare nelle tabelle II e III. Si nota che tale rapporto per bassi f/p si può ritenere costante. La media dei valori di α_{sp}/α_{cl}, che si hanno a bassa frequenza, viene utilizzato nella (3′). Per le miscele costituite da idrogeno e ossigeno, entrambi biatomici, si è preso $C_v = (5/2)R$, $C_p = (7/2)R$, $C' = R$. Inoltre secondo KOHLER [11] il cociente di viscosità η dei gas vale

$$\eta = 1.271 p \tau_c \,, \tag{6}$$

[11] M. K. KOHLER: *Zeits. f. Phys.*, **5**, 715 (1949).

mentre il coefficiente di conduzione termica Λ, secondo EUCKEN [12], si esprime con

$$\Lambda = K\eta C_v \,. \tag{7}$$

La (3′) con tali valori numerici assume la forma

$$\frac{\alpha_{sp}}{\alpha_{cl}} = 1 + 0.067\,\frac{\tau_r}{\tau_c}\,, \tag{8}$$

dove τ_r/τ_c rappresenta il numero medio n di urti necessari per la disattivazione di uno stato energetico rotazionale.

Per le miscele contenenti idrogeno e argon si è fatto uso della (3′) per determinare τ; le costanti V_0, C_v, C', che in essa compaiono, sono state calcolate con le usuali regole [13] di composizione valevoli per miscugli di sostanze.

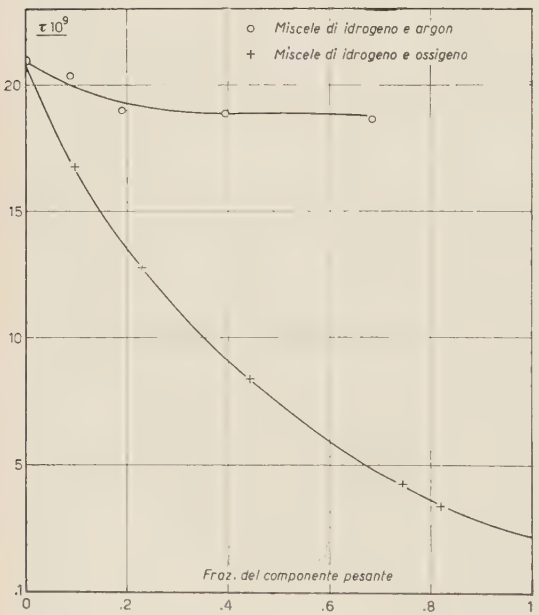

Fig. 10. – Tempo di rilassamento acustico delle miscele idrogeno-argon (○) e idrogeno-ossigeno (+), in funzione della concentrazione dell'argon e dell'ossigeno.

Determinato τ_r, dalle (2) si ha f_w, e da questa si ottiene la frequenza di massimo assorbimento f_m, essendo

$$f_m = f_w \cdot V_0 / V_\infty \,.$$

Nella fig. 10 è riportato l'andamento del tempo di rilassamento τ_r per le due miscele, in funzione della concentrazione del componente più pesante. È interessante osservare che anche l'argon influisce sul tempo τ_r dell'idrogeno, riducendolo di circa il 10 %, quando esso raggiunge la concentrazione molecolare del 20 %. Aumentando ancora la concentrazione molecolare, l'effetto sembra attenuarsi e si può dire che il valore di τ_r si mantiene costante, almeno fino alla concentrazione del 69 % di argon qui realizzata. Nelle miscele idrogeno-ossigeno τ_r diminuisce regolarmente col crescere della concentrazione di ossigeno, ogni

[12] A. EUCKEN: *Phys. Zeits.*, **12**, 1101 (1911); **14**, 324 (1913).

[13] Vedi J. R. PARTINGTON: *An Advanced Treatise on Physical Chemistry*, Vol. I (Longmans, 1949).

miscela avendo un proprio tempo di rilassamento. Prolungando la curva, che riunisce i punti segnati in fig. 10, fino alla concentrazione del 100% in ossigeno, si trova come tempo di rilassamento per l'ossigeno puro il valore di $2.2 \cdot 10^{-9}$ s. Esso rappresenta un valore di τ_r ottenuto per estrapolazione da un gas impuro — la miscela idrogeno con ossigeno — e quindi può risultare più piccolo del valore, che si potrebbe avere da una misura in ossigeno puro. Una tale determinazione è stata fatta da W. J. THALER [14], il quale ha trovato $\tau_r = 5.24 \cdot 10^{-9}$ s, notevolmente superiore. Ci sono ancora altre due determinazioni di τ_r per l'ossigeno. Una è dovuta a J. G. PARKER, C. E. ADAMS e R. M. STAVSETH [15]; essa è stata fatta a frequenze ultrasonore comprese tra 60 e 70 kHz e a pressioni variabili da 1 a 10 mm Hg, e fornisce $\tau_r = 4.95 \cdot 10^{-10}$ s. Secondo gli autori una così notevole differenza con il valore di τ_r dato da THALER potrebbe forse spiegarsi, ammettendo una influenza della frequenza usata sulla misura del tempo di rilassamento.

Una indicazione sul valore probabile di τ_r per l'ossigeno risulta dagli esperimenti di E. F. GREENE e D. F. HORNING [16] sulla propagazione di onde di urto in tale gas. Secondo GREENE e HORNING i livelli rotazionali dell'ossigeno non rilassano così lentamente, come risulterebbe dalle misure di THALER; in altri termini si dovrebbe avere un tempo di rilassamento più piccolo di quello indicato da quest'ultimo Autore. Sembra anzi che dovrebbero attribuirsi alla molecola di ossigeno almeno due tempi di rilassamento, entrambi più corti del valore di $5.24 \cdot 10^{-8}$ s di THALER.

Conviene ricordare ancora una ricerca teorica di R. BROUT [17], secondo la quale la probabilità di disattivazione degli stati rotazionali, per molecole biatomiche simmetriche, si può esprimere con

$$P = \frac{1}{2}\left(\frac{d_0}{r_0}\right)^2, \tag{10}$$

d_0 essendo la distanza internucleare e r_0 il diametro di collisione. Essa probabilità quindi non varierebbe sensibilmente da una specie molecolare all'altra, quando il peso molecolare supera 20 e si è a temperatura ordinaria. Per l'ossigeno risulterebbe $P = 0.057$, sono necessarie cioè 17 collisioni per la disattivazione, da cui si ricava $\tau_r = 2.7 \cdot 10^{-9}$ s. Questo valore è abbastanza prossimo a quello qui estrapolato.

Si conclude pertanto che:

---

[14] W. J. THALER: *Journ. Acoust. Soc. Am.*, **24**, 15 (1953).

[15] J. G. PARKER, C. E. ADAMS e R. M. STAVSETH: *Journ. Acoust. Soc. Am.*, **25**, 263 (1953).

[16] E. F. GREENE e D. F. HORNING: *Journ. Chem. Phys.*, **21**, 617 (1953).

[17] R. BROUT: *Journ. Chem. Phys.*, **22**, 1189 (1954).

1) Il tempo di rilassamento nell'idrogeno è influenzato dalla presenza di gas estranei, che vi siano mescolati in forte percentuale. Ciò avviene in modo diverso per l'argon e per l'ossigeno, quali impurità. Col primo gas si ha una lenta diminuzione di τ_r, che può arrivare fino al 10% del valore che compete all'idrogeno puro, per una concentrazione di argon di circa 20%, mentre per concentrazioni superiori τ_r sembra rimanere costante. Con l'ossigeno il tempo di rilassamento diminuisce, in maniera più rapida inizialmente, dal valore che compete all'idrogeno fino al valore relativo all'ossigeno.

2) La teoria di Kohler sull'assorbimento ultrasonoro di tipo classico nelle miscele, non è senz'altro estendibile ai casi in cui di queste entrano a far parte gas biatomici, anche se leggeri come l'idrogeno.

3) Il tempo di rilassamento per l'ossigeno, con molta probabilità, è inferiore al valore stabilito da THALER, e ciò in accordo con altre determinazioni sperimentali e con i risultati teorici di BROUT.

SUMMARY (*)

The Author refers on absorption measures of ultrasonics in pure hydrogen and in mixtures of hydrogen and argon, hydrogen and oxygen performed in order to study the influence of extraneous gases on the rotational relaxation time of hydrogen and to verify if Kohler's theory of the classical type of absorption, holding for mixtures of monoatomic gases, can be extended also to the case of presence of biatomic gases. The effect of the presence of biatomic impurities in strong concentration is to shorten the relaxation time of hydrogen. This shortening does not exceed 10% for argon, and is much greater for oxygen. Here the relaxation time decreases continually from the value competing to hydrogen to that competing to oxygen. The author determines a relaxation time for oxygen which is shorter than that given by THALER, but which agrees with the result of a theoretical calculation by BROUT. It seems finally that the conclusion may be drawn that Kohler's theory does not immediately apply to the mixtures studied in this paper.

(*) *Editor's Translation.*

IL NUOVO CIMENTO Vol. II, N. 2 1° Agosto 1955

On the Meaning of Bilocalizability.

J. Rayski

Institute of Theoretical Physics, Nicolas Copernicus University - Toruń

(ricevuto il 3 Giugno 1955)

Summary. — An analysis of the foundations of quantum mechanics shows that two distinct procedures are involved therein: quantization of space-time, and the linking of a mechanical model to the quantized space-time (Q.S.T.). The former is called l-quantization, the latter h-quantization for reasons to be explained in the text. The point model of elementary particle is found to be rather unnatural while a bipoint model fits naturally into the framework of Q.S.T. Among the possible bi-point models a rotator model is preferable fitting smoothly to the covariance properties of Q.S.T.. The rest mass of the bi-point particle is no more a parameter introduced ad hoc but is determined by the momenta of the internal motion of the particle. A bilocal field theory based on the bi-point (rotator) model of the elementary physical entity is constructed: field equations are set up as well as the current four-vector, energy-momentum tensor, and angular momentum tensor densities satisfying differential conservation laws. The bilocal field may be quantized and describes a whole set (family) of particle sorts with higher spins and masses corresponding to the excited states of the underlying rotator model. There is a one-to-one correspondence between the particle types forming a family and the irreducible unitary representations of the group of rotations which fact exhibits an intimate and complete connection between space and matter. The particle families may be classified according to single- or double-valuedness of field quantities, according to the type of symmetry with respect to inversions, and according to the order of the field equation. A comparison with the present experimental evidence about elementary particles (rest-mass values, decay schemes, etc.) seems promising.

1. – Quantization of Space-Time.

In the usual exposition of the foundations of quantum theory too little stress has been laid on a clear separation of concepts: some having rather a general character, may be regarded as geometrical of origin, and some being rather specific, depend upon the special physical model assumed. We do not mean to say that this conceptual differentiation is something very fundamental. We like rather the idea that in a satisfactory future theory of elementary physical systems, every basic assumption will be equally fundamental, i.e. no room will be left for specific models with accidental properties. On the contrary, the properties of elementary physical systems should follow from some quite general principles and the differentiation into geometry, (or kinematics), and dynamics will become spurious. Nevertheless, the separation of concepts into these of geometrical character and those concerned with the dynamical model may be helpful for heuristic reasons. It may facilitate to find out which of our assumptions are rather accidental, or oversimplified, and can be removed or replaced by more refined conceptions.

Let us start with a brief recapitulation of those concepts (inherent more or less explicitly in any course of lectures on quantum theory) which seem to be quite general, i.e. independent of the special model of quantized system. We shall see that these concepts are closely connected with the structure of space-time itself, and may be called « quantization of space-time ».

The manifold of points $(x_1, x_2, x_3, x_4) \equiv x_\mu \equiv (\boldsymbol{x}, ix_0)$ whose transformations onto itself form the Loretz group, is the Minkowski space. This space may be generalized (quantized) by regarding the quantities x_μ as operators $\underline{\underline{x}}_\mu$ ($\boldsymbol{x}$ are real operators, x_4 is an imaginary operator) with the infinitesimal displacement operators $\underline{\underline{d}}_\mu$, satisfying the commutation relations

$$[\underline{\underline{x}}_\mu, \underline{\underline{d}}_\nu] = \delta_{\mu\nu}\,, \tag{1}$$

as their counterparts. From (1) it follows that $\underline{\underline{\boldsymbol{d}}}$ are imaginary operators, $\underline{\underline{d}}_4$ is a real operator. If the time scale is chosen so that the velocity of light is $c = 1$, the dimension of $\underline{\underline{d}}_\mu$ is cm^{-1}. It will be natural and convenient to introduce, besides c, another constant l with dimension of lenght, and investigate the operators $\underline{\underline{x}}_\mu$ and $il^2\underline{\underline{d}}_\mu$. The natural kinematic units are $c = l = 1$.

The operators $\underline{\underline{x}}_\mu$ and $il^2\underline{\underline{d}}_\mu$ are subject to a non-commutative algebra. They span a space being a generalization of the Hilbert space. We may consider canonical transformations replacing $\underline{\underline{x}}_\mu$ and $il^2\underline{\underline{d}}_\mu$ by other quantities being functions of the former and preserving the relations (1) or rather

$$[\underline{\underline{x}}_\mu, il^2\underline{\underline{d}}_\nu] = il^2\delta_{\mu\nu}\,. \tag{1'}$$

In particular, we may limit ourselves to linear transformations preserving the four-vector character of these quantities. An example of such a transformation is

$$(2)\qquad \begin{cases} \underline{\underline{x}}'_\mu = \dfrac{1}{\sqrt{2}}\,(\underline{\underline{x}}_\mu - il^2\underline{\underline{d}}_\mu) \\ il^2\underline{\underline{d}}'_\mu = \dfrac{1}{\sqrt{2}}\,(\underline{\underline{x}}_\mu + il^2\underline{\underline{d}}_\mu)\,. \end{cases}$$

In order to be canonical, such real transformations with two row and column matrices must be unimodular (Det = 1) but do not need to be unitary. Later on we shall have to do with the subgroup of canonical transformations consisting of matrices

$$(3)\qquad \begin{pmatrix} 1 & \\ & 1 \end{pmatrix},\quad \begin{pmatrix} & a^2 \\ -a^{-2} & \end{pmatrix},\quad \begin{pmatrix} -1 & \\ & -1 \end{pmatrix},\quad \begin{pmatrix} & -a^2 \\ a^{-2} & \end{pmatrix}.$$

It is the group of reciprocal transformations (Born transformations). al (or in natural units simply a) may be called the rate of reciprocity. The matrices (3) are not unitary unless the rate of reciprocity is $(a) = 1$. The corresponding group of unitary transformations

$$(3')\qquad \begin{pmatrix} 1 & \\ & 1 \end{pmatrix},\quad \begin{pmatrix} & 1 \\ -1 & \end{pmatrix},\quad \begin{pmatrix} -1 & \\ & -1 \end{pmatrix},\quad \begin{pmatrix} & -1 \\ 1 & \end{pmatrix}$$

is a normal divisor of the group of all real, unitary, unimodular transformations preserving the four-vector character of the operators $\underline{\underline{x}}_\mu$ and $il^2\underline{\underline{d}}_\mu$.

From the abstract scheme of operators we may go over to matrices by introducing a frame of reference connected with the eigenvectors of a complete set of operators, e.g. $|x'\rangle$. In this x-representation we have

$$(4)\qquad \langle x'|\,\underline{\underline{x}}_\mu\,|x''\rangle = x'_\mu\,\delta(x'-x'')\,,\qquad \langle x'|\,\underline{\underline{d}}_\mu|x''\rangle = -\frac{\partial}{\partial x'_\mu}\,\delta(x'-x'')\,.$$

Together with $\underline{\underline{x}}_\mu$ and $\underline{\underline{d}}_\mu$ any operator $\underline{\underline{F}}$, being their function, becomes a matrix. With the aid of (4) we may easily verify the following relations

$$(5)\qquad \langle x'|\,\underline{\underline{F}}\,\underline{\underline{d}}_\mu|x''\rangle = \frac{\partial}{\partial x''_\mu}\langle x'|\,\underline{\underline{F}}\,|x''\rangle\,,\qquad \langle x'|\,\underline{\underline{d}}_\mu\underline{\underline{F}}\,|x''\rangle = -\frac{\partial}{\partial x'_\mu}\langle x'|\,\underline{\underline{F}}\,|x''\rangle\,,$$

$$(6)\qquad \langle x'|\,\underline{\underline{x}}_\mu\underline{\underline{F}}\,|x''\rangle = x'_\mu\langle x'|\,\underline{\underline{F}}\,|x''\rangle\,,\qquad \langle x'|\,\underline{\underline{F}}\,\underline{\underline{x}}_\mu|x''\rangle = x''_\mu\langle x'|\,\underline{\underline{F}}\,|x''\rangle\,.$$

Thus, all the characteristic features of quantization (replacement of c-numbers by operators, Hilbert space, representations, canonical transformations) appear as purely geometrical concepts without any connection to dynamics of physical systems. The above generalization of the notion of Minkowski's space is just a quantization of space-time. We are sceptical as to whether any other alternative of quantizing space-time (attempted recently by some authors), may be fruitful.

2. – The Point Model of Elementary Particle and the Corresponding Field Model.

In order to throw a bridge between geometry and physics (or between the concepts of space-time and the dynamics of physical systems) a model of a dynamical system is unavoidable. The simplest model is a material point. In this particular case it is possible to throw a bridge between the geometry and the model in the following way: the operators $\underline{\underline{x}}_\mu$ are to be assigned to the physical notion of position of the material point in space-time while the operators $-i\underline{\underline{d}}_\mu$ (multiplied by Planck's constant) to the physical notion of its momentum and energy. In the units $c = l = 1$ the Planck's constant (*) h has a dimension of mass. The natural physical units are $c = l = h = 1$. c and l are purely geometrical (kinematical) units, while h, (or rather h/cl) is a dynamical unit enabling to establish a connection between geometry and the mechanical model.

There appears a difficulty in assigning the operators $-ih\underline{\underline{d}}_\mu$ to the momentum and energy of the material point p_μ since there exists a physical relation between the p_μ's (e.g. the relation (8)) while the d_μ's are independent. This difficulty is circumvented in the following way: $-ih\underline{\underline{\boldsymbol{d}}}$ is simply identified with $\boldsymbol{p}$ while the equality between $-ihd_4$ and p_4 is regarded as a condition upon the state vector:

$$(7') \qquad -ih\underline{\underline{\boldsymbol{d}}}\,\psi = \boldsymbol{p}\,\psi\,,$$

$$(7'') \qquad -ihd_4\,\psi = p_4\,\psi\,.$$

(7″) is nothing else but the Schrödinger equation. On account of a physical relation between p_4 and $\boldsymbol{p}$, and in consequence of the weaker attachment (7″), the operator d_0 does not enter explicitly into observables and therefore its canonical conjugate $\underline{\underline{x}}_0$ may be treated simply as a parameter. Thus, the Hilbert space necessary for a dynamical description of the material point appears to be spanned merely on the operators $\underline{\underline{\boldsymbol{x}}}$ and $\underline{\boldsymbol{d}}$.

(*) We denote by h the Planck's constant divided by 2π.

The above exposure differs from the traditional one chiefly by regarding the canonical quantization of a physical system rather as a secondary fact: a linking of the physical notions characterizing a particular model to the more fundamental geometrical notions of the quantized space-time.

The quantization of systems with more degrees of freedom is a straightforward generalization of the procedure of quantization of the material point while the connection between the physical system and the quantized space-time is established via the conception of a configuration space.

Another important generalization is accomplished by a transition to the field theory. Taking as a starting point the classical connection between the momenta of the material point

$$p_\mu^2 + m^2 = 0 \,, \tag{8}$$

a bridge connecting it with the quantized space-time may be established by using a possible realization of the momenta $-ih\underline{\partial}_\mu = p_\mu$ by

$$p_\mu = -ih\frac{\hat{c}}{\partial \underline{x}_\mu} \tag{9}$$

in conformity with (1). In this way the left hand side of (8) becomes an operator acting upon functions of $\underline{x}_\mu$. In this way we are led to the Schrödinger-Gordon equation

$$(\Box - m^2)\psi(\underline{x}) = 0 \,, \tag{10}$$

i.e. we go over to the field theory. It is remarkable that by this transition the operator (or matrix) character of the position variables has been lost entirely. Now, the $\underline{x}_\mu$'s may be trated again as c-numbers x_μ. This feature seems to be suspicious. It may be regarded as brought about by the use of an oversimplified model (material point). This model seems to be too classical: it deprives the quantized space-time of its most characteristic quantic features. The question is whether it is possible to liberate oneself of the point model and devise other models of elementary physical systems fitting better into the framework of quantized space time.

3. – h- and l- Quantization of Fields.

Although the Schrödinger-Gordon equation has been arrived at by combining the notion of the point model with the notions of the quantized space-time, it possesses an autonomous meaning of a classical field model. Such

a field model may be subjected to a procedure of quantization and this has been done several years ago (second quantization). However, the question is whether this traditional procedure of quantization (being a straightforward generalization of the canonical quantization for systems with infinitely many degrees of freedom) is the only alternative deserving the name of a field quantization. From the exposure of section 1 this may be doubted: the canonical quantization (h-quantization) appears to be a secondary procedure while primary is rather the quantization of space-time, i.e. the introduction of the displacement operators $\underline{\underline{d}}_\mu$ (or rather $il^2\underline{\underline{d}}_\mu$) on equal footing with the position operators $\underline{\underline{x}}_\mu$. The Planck's constant h is strange to the quantized space-time, this last being connected rather with a constant l. Thus, the most straightforward and natural procedure seems to be a field quantization in the spirit of the space-time quantization (l-quantization to be distinguished from the canonical h-quantization). In other words, we have to assume that the field variable ψ is not a mere function of position variables but an operator constructed of the elements of the quantized space-time

$$\psi = \psi(\underline{\underline{x}}_\mu,\ il^2\underline{\underline{d}}_\nu)\ . \tag{11}$$

This assumption is nothing else but the starting point of the non-local formalism proposed by YUKAWA (1950). Going over to the x-representation the field variable becomes a non-diagonal matrix

$$\psi = \langle x' \,|\, \psi \,|\, x'' \rangle\ . \tag{11'}$$

A diagonal matrix would be obtained only in the special case: if ψ were independent of $\underline{\underline{d}}_\nu$, or in the limit $l \to 0$.

Such a procedure of field quantization (l-quantization) seems to the author very natural. It is not inconsistent with the traditional h-quantization. It seems plausible that the grave difficulties encountered in the traditional quantum field theory have been brought about by the fact that the l-quantization of fields has been overlooked. We hope that a full (and only a full) quantization, being a union of the l- and h-quantization, may provide a satisfactory (divergence-free) field theory able to explain the existence of such a great variety of new unstable particles.

4. – Bipoint Model of Elementary Particle.

In order to formulate a field theory with a generalized conception of field quantity (11), we may ask about the corresponding model of an elementary physical system. It is obvious that the model underlying a bilocal field quantity (11') cannot be a material point but a bipoint.

Let us consider a bipoint, i.e. a physical entity characterized by a pair of points x' and x'' in space-time, and introduce the canonically conjugate momenta p' and p''. Similarly as in the theory of a monopoint there should exist a relation between the momenta somewhat analogous to (8).

The bipoint being not a pair of material points but a new physical entity, the expected relation is something new, unknown to the traditional physics, and has to be introduced as a postulate. We shall try the simplest relation of this type

$$p'_\mu p'_\mu + p''_\mu p''_\mu = 0 \tag{12}$$

$$(\text{or} \quad p'_\mu p'_\mu + p''_\mu p''_\mu = -m^2)\,. \tag{12'}$$

Introducing Yukawa's variables by means of a canonical transformation

$$x_\mu = \tfrac{1}{2}(x'_\mu + x''_\mu)\,, \qquad r_\mu = x'_\mu - x''_\mu\,, \tag{13}$$

$$p_\mu = p'_\mu + p''_\mu\,, \qquad k_\mu = \tfrac{1}{2}(p'_\mu - p''_\mu) \tag{13'}$$

the relation (12) becomes

$$p_\mu p_\mu + 4k_\mu k_\mu = 0\,. \tag{14}$$

The bipoint suggests the following interpretation: it represents a particle with a structure. r_μ are the internal structure variables while x_μ are the coordinates of the particle regarded as a whole. p_μ represents the momentum and energy of the particle while $4k_\mu k_\mu$ should play the role of the square of the rest mass. Thus, an explicit introduction of a rest mass m by (12') seems to be useless for a bipoint model. It seems rather satisfactory that the rest mass be not introduced as a foreign element but appears automatically as an intrinsic property of the model. The relativity tought us (through the relation $m = \sqrt{\boldsymbol{p}^2 + m_0^2}$) that the mass is not a mere parameter but a function of the momentum of the particle. It is only natural to expect that also the rest mass is not a mere parameter but a function of some momenta. In this case it is the momentum k_μ of an internal motion of the particle. The rest mass appears to be a manifestation of the internal movement of the particle.

The bipoint model of an elementary particle fits better into the framework of quantized space-time characterized by two sets of operators x_μ and $\underset{=}{d}_\mu$, or, in the x-representation, by a double manifold of points x'_μ and x''_μ. Therefore, the bipoint model may be regarded as a quantum model of an elementary physical entity in contradistinction to the classical mono-point model.

5. – Correspondence Requirement and Supplementary Conditions.

The traditional point model of elementary particle may be regarded as a special case of the bipoint model restricted by four supplementary conditions

$$r_\mu = 0 \,. \qquad (\mu = 1, \ldots 4) \tag{15}$$

These conditions may be regarded as constraints reducing the number of (eight) degrees of freedom x'_μ, x''_μ (or x_μ, r_μ) to four x_μ. In this case the subsidiary momenta k_μ may be eliminated whereby (14) reduces to $p_\mu p_\mu = 0$. In this way we arrive at a point model with a vanishing rest mass. A non-vanishing rest mass could be introduced only by the alternative starting point (12′).

The supplementary conditions (15) obviously constitute an unsound over-simplification. They violate the idea of a quantized space-time by reducing any matrix $\langle x' | F | x'' \rangle$ connected with the model of the particle to a diagonal form $F(x')\delta(x' - x'')$. On the other hand, we cannot do without any supplementary conditions. Above all we have to guarantee that the square of the rest mass be positive. For correspondence reasons we have to look for new supplementary conditions containing (15) as a limiting case.

Supplementary conditions reduce the number of degrees of freedom of the elementary physical system, i.e. extract from the geometry of the quantized space-time another geometry (a physical « Spielraum ») with a reduced number of dimensions. But supplementary conditions should not violate the properties of the quantized space-time. On the contrary, they have to exhibit the intrinsic covariance properties of the quantized space-time itself. As remarked previously the « points » of the quantized space-time may be subjected to the Lorentz transformations and to the canonical transformations. The supplementary conditions have to be covariant with respect to both (they will fit well to the covariance properties of the quantized space-time if they will be not only covariant but invariant against a subgroup of the group of quantized space-time transformations). The following supplementary conditions

$$[(al)^2 p_\mu + r_\mu]^2 = 0 \,, \qquad [(al)^2 p_\mu - r_\mu]^2 = 0 \tag{16}$$

or, equivalent

$$p_\mu r_\mu = 0 \,, \qquad (al)^4 p_\mu^2 + r_\mu^2 = 0 \tag{16′}$$

satisfy the above requirement. They are invariant with respect to Lorentz transformations and also with respect to reciprocal transformations

$$\begin{cases} (al)^2 p_\mu \to r_\mu \,, & r_\mu \to -(al)^2 p_\mu \,, \\ (al)^2 k_\mu \to x_\mu \,, & x_\mu \to -(al)^2 k_\mu \,. \end{cases} \tag{17}$$

For a particle with a non-vanishing rest mass M we get from (16′) in the system of rest

$$r_0 = 0\,, \qquad \boldsymbol{r}^2 = (al)^4 M^2, \tag{18}$$

so that the internal structure variables reduce to two angles on a sphere with radius $(al)^2 M$. The elementary particle is represented by a pair of points separated by a space-like interval. In the system of rest the two points lie on a hypersurface $t = \text{const}$ with a distance $(al)^2 M$. These two points may rotate about their centre so that we have to do here with a rotator model of elementary particle.

The supplementary conditions (16) may be taken explicitly into account by eliminating the subsidiary coordinates and momenta. For a particle at rest these are r_0, $r = |\boldsymbol{r}|$, and k_0, k_r respectively. Since the momenta k_0 and k_r have to drop out from (14) we are left with

$$p_4^2 + 4\frac{S^2}{r^2} = 0 \qquad [\boldsymbol{p} = 0,\ r_4 = 0,\ r = (al)^2 M] \tag{19}$$

where S^2 is the squared angular momentum of the internal motion of the bipoint. From (19) the rest mass of the bipoint follows

$$M = \frac{1}{al}\sqrt[4]{4S^2}\,. \tag{20}$$

As is seen from (18) the requirement of correspondence with the point model is satisfied: in the limit $l \to 0$ the bipoint degenerates into a monopoint. But the transition $l \to 0$ in (20) is not permissible. This shows clearly a singular character of the traditional local theory.

6. – First Quantization of the Bipoint (Rotator) Model.

A bridge between the bipoint model and the quantized space-time will be completed by identifying the momenta p'_μ, p''_μ canonically conjugate to x'_μ, x''_μ with the corresponding partial derivatives, or, in terms of Yukawa variables

$$p_\mu \to -i\frac{\partial}{\partial x_\mu}\,, \tag{21′}$$

$$k_\mu \to -i\frac{\partial}{\partial r'_\mu}\,, \tag{21″}$$

(in the units $c = l = h = 1$). Now, (19) should be interpreted as a condition upon a field quantity

$$\left(p_4^2 + 4\frac{S^2}{r^2}\right)\Psi(x, r) = 0 \qquad [\boldsymbol{p}\Psi = 0,\ r_4\Psi = 0,\ (r^2 + (al)^4 p_\mu^2)\Psi = 0]\,. \tag{22}$$

and may be readily generalized for arbitrary eigenvalues of p

$$\left(p_\mu^2 + 4\left\{k_\mu^2 + \frac{1}{r_0^2}[(al)^4(p_\mu k_\mu)^2 - r_\mu r_\nu k_\mu k_\nu + 2ir_\mu k_\mu]\right\}\right)\Psi(x, r) = 0 \tag{23}$$

$$[r_\mu p_\mu \Psi = 0,\ (r_\mu^2 + (al)^4 p_\mu^2)\Psi = 0]\,.$$

(23) may be regarded as a generalization of the Schrödinger-Gordon equation for the case of a bipoint (more exactly: of a rotator) model of the elementary particle. The additional terms appearing in (23) may be understood as a consequence of the reaction forces brought about by the constraints.

The above field equation seems rather complicated but still it is the simplest example of a field equation (except for the traditional local field equation) since the rotator is a simplest structure (except for the point model).

Of course, it is also possible to investigate the partly quantized (approximative) versions of the model by quantizing only the translational degrees of freedom (22′) and regarding the internal momenta k_μ as classical or vice versa. In the former case we would get a classical rotator whose movement (as a whole) is governed by the wave mechanics of a particle with a rest mass given by (20). In this case the particle could assume any value of the rest mass and could change it continuously in the course of time provided an interaction with external fields be present influencing the angular momentum of the internal motion. In the latter case we would get a quantized rotator whose centre moves classically. In consequence of the quantization (22″) of the internal degrees of freedom the model possesses, in this case, a quantized spin whose square determines, at the same time, the rest mass of the whole physical entity

$$M_n = \frac{1}{al}\sqrt[4]{4n(n+1)}\,, \qquad n = 0, 1, 2, \ldots\,. \tag{24}$$

Thus, the first h-quantization of the internal degrees of freedom is equivalent to a spin and mass quantization. In consequence of a suitable perturbation by external fields the particle may change its state of spin and mass (« discontinuously »). The higher states of mass and spin may be regarded either as excited states of the same particle, or as different particles forming a particle family. The choice between the two alternatives is merely a matter of taste.

7. – Group-Theoretical Virtues of the Rotator Model.

Bipoint models of elementary physical entities offer a possibility of investigating the corresponding bilocal fields where a single bilocal field quantity describes a whole family of particles with a given mass spectrum. The problem is to find, among the various possibilities, the model corresponding best to the experimental evidence. Obviously, we could investigate, besides the rotator model, other bipoint models e.g. an oscillator model of elementary particle. In this case a suitable starting point would be an alternative connection between the momenta

$$p_\mu^2 - C(k_\mu^2 + l^{-4} r_\mu^2) = 0 ,$$

with an auxiliary condition $p_\mu r_\mu = 0$ reducing the four-dimensional oscillator to a three-dimensional (space-like) one. This model seems less satisfactory than the rotator model. First of all it introduces an inexplicable potential energy for the internal motion. Secondly, it deprives the excited states of the particle of any connection with higher spins. A close connection between spin and mass in the case of a rotator model seems very satisfactory: it shows that there exists a one-to-one correspondence between all the particle sorts forming a family and all irreducible unitary representations of the group of rotations. This correspondence may be interpreted as a manifestation of a very intimate connection between space and matter. Physical space is characterized, above all, by the group of rotations (being equivalent to the totality of its irreducible unitary representations). Therefore, to every irreducible unitary representation there should correspond (at least) one particle sort, otherwise the connection between space and matter would be incomplete and therefore accidental. Accepting the rotator model of elementary physical entity it becomes at once understandable that matter is not an intruder in space-time but both are connected intimately to each other. On the other hand, the traditional field theories (as well as e.g. the bilocal theory constructed upon the oscillator model) are rather unsatisfactory in this respect. Here, some field quantities, belonging to a few irreducible (single or double valued) representations, are taken into account while the remaining are ignored. This constitutes an inexplicable discrimination of some representations against the others, a fact hardly acceptable from a group-theoretical viewpoint.

8. – Conservation Laws.

As the supplementary conditions (16) involve the momenta p, it will be convenient to work in the p-space instead of the x-space. We introduce the

Fourier transform of the field quantity

$$\Psi(x, r) = \frac{1}{(2\pi)^2}\int \mathrm{d}^4p\, \Psi(p, r) \exp[ip_\mu x_\mu] \tag{25}$$

and take account of the supplementary conditions by putting

$$\Psi(p, r) = \varphi(p, r) N\, \delta(r_\mu p_\mu)\, \delta(r_\mu^2 + (al)^4 p_\mu^2), \tag{26}$$

where N is a normalizing factor

$$1/N = \int \mathrm{d}^4r\, \delta(r_\mu p_\mu)\, \delta(r_\mu^2 + (al)^4 p_\mu^2), \tag{27}$$

while $\varphi(p, r)$ is a function of only two independent of the four variables r_μ. $\Psi(p, r)$ may be called « field distribution » while $\varphi(p, r)$ may be called « field skeleton ». Denoting by $\underline{\underline{M}}^2$ the operator

$$\underline{\underline{M}}^2 = 4\left\{k_\mu^2 - \frac{1}{p_\varrho^2}(p_\mu k_\mu)^2 - \frac{1}{r_\varrho^2}(r_\mu r_\nu k_\mu k_\nu - 2ir_\mu k_\mu)\right\}, \tag{28}$$

the generalized Schrödinger equation (23) is equivalent to

$$(p_\mu^2 + \underline{\underline{M}}^2)\Psi(p, r) = 0 \qquad \text{or} \qquad (p_\mu^2 + \underline{\underline{M}}^2)\varphi(p, r) = 0\,. \tag{29}$$

$$[p_\mu r_\mu = 0, \quad r_\mu^2 = (al)^4 p_\mu^2]$$

The same equations hold for the complex conjugates since M^2 is a real operator.

The field equation (23) or (29) is invariant with respect to translations and rotations in space-time as well as to gauge transformations of the first type which secures the existence of conservation laws for energy, momentum, angular momentum, and charge. We shall show that the conservation laws may be put in the traditional form of continuity equations. To this end we construct explicitly a symmetric energy-momentum-stress tensor $T_{\mu\nu}(x)$ and a charge-current vector $j_\mu(x)$ satisfying the continuity equations

$$\partial_\mu T_{\mu\nu}(x) = \partial_\nu T_{\mu\nu}(x) = 0\,, \qquad \partial_\mu j_\mu(x) = 0\,. \tag{30}$$

The existence of an angular momentum tensor density satisfying a differential conservation law follows from the symmetry of $T_{\mu\nu}$.

First of all we construct the following sub-densities

$$(31)\qquad T_{\mu\nu}(p, q, r) =$$
$$= \varphi^*(p+q, r)\left\{2q_\mu q_\nu + (q_\mu p_\nu + q_\nu p_\mu - \delta_{\mu\nu} q_\lambda p_\lambda)\left[1 + \frac{1}{p_0^2}(\underset{\leftarrow}{\underline{M}}^2 - \underset{\rightarrow}{\underline{M}}^2)\right]\right\}\varphi(q, r),$$

$$(32)\qquad j_\mu(p, q, r) = \varphi^*(p+q, r)\left\{2q_\mu + p_\mu\left[1 + \frac{1}{p_0^2}(\underset{\leftarrow}{\underline{M}}^2 - \underset{\rightarrow}{\underline{M}}^2)\right]\right\}\varphi(q, r),$$

where the arrow below M^2 denotes that this operator acts to the left or to the right hand side

$$(33)\qquad \varphi^* \underset{\leftarrow}{\underline{M}}^2 \varphi \equiv (\underline{M}^2\varphi^*)\varphi\,, \qquad \varphi^* \underset{\rightarrow}{\underline{M}}^2 \varphi \equiv \varphi^*(\underline{M}^2\varphi)\,.$$

With the aid of (29) the conservation laws for the sub-densities

$$(34)\qquad p_\mu T_{\mu\nu}(p, q, r) = 0\,, \qquad p_\mu j_\mu(p, q, r) = 0\,,$$

follow easily. The expressions (31) and (32) are quite similar to their local counterparts (independent of r_μ) and differ merely by the terms involving the operator $\underline{M}^2$. But in the traditional field theory M^2 is a c-number so that the additional terms drop out.

The densities may be obtained from the sub-densities by integrating the latter over the (two independent of the four) r_μ's and over the q_μ's

$$(35)\qquad T_{\mu\nu}(p) = \int \mathrm{d}^4 q N \int \mathrm{d}^4 r\, \delta(r_\mu q_\mu)\, \delta(r_\mu^2 + (al)^4 q_\mu^2)\, T_{\mu\nu}(p, q, r)$$

with a similar expression for the current.

As is seen from (26) it will be more elegant to use $\Psi(q, r)$ instead of $\varphi(q, r)$ in (31) and (32) so that the basic sub-densities are of the form of products of a field skeleton by a field distribution

$$(36)\qquad F_{\mu\nu\ldots}(p, q, r) = \varphi^*(p + q, r) f_{\mu\nu\ldots} \Psi(q, r)\,,$$

which may be also symmetrized, e.g.

$$(36')\qquad F(p, q, r) = \tfrac{1}{2}(\varphi^*(p + q, r) f \Psi(q, r) + \Psi^*(p + q, r) f \varphi(q, r)).$$

The product of the field quantities taken at different points q, and $q - p$ with a subsequent integration over q is well known in the operator calculus as convolution.

Obviously the densities of the type (35) satisfy the relations of the type (34) whence their Fourier transforms

$$(37)\qquad \begin{cases} T_{\mu\nu}(x) = \dfrac{1}{(2\pi)^2}\int \mathrm{d}^4p\, T_{\mu\nu}(p)\exp\left[ip_\mu x_\mu\right] \quad \text{and} \\ j_\mu(x) = \dfrac{1}{(2\pi)^2}\int \mathrm{d}^4p\, j_\mu(p)\exp\left[ip_\mu x_\mu\right] \end{cases}$$

satisfy the continuity equations (30).

By integrating the densities (37) over the three-dimensional x-space we get the expressions for the total energy, momentum, and charge. These expressions are identical with the expressions given in a previous paper (RAYSKI, 1955 *a*). Their physical meaning is clear since they split into a series of usual expressions for local fields describing particles with masses M_n and spin n. These fields may be quantized separately by the usual methods of second quantization.

9. – Other Alternatives of Field Equations.

Until now we were concerned with a generalized Schrödinger-Gordon equation. But a similar formalism may be constructed for a generalized Dirac equation

$$(38)\qquad \gamma_\mu \frac{\partial}{\partial x''_\mu}\langle x'|\Psi|x''\rangle = 0\,, \qquad \left(\text{and} \quad \frac{\partial}{\partial x'_\mu}\langle x'|\overline{\Psi}|x''\rangle\gamma_\mu = 0\right)$$

or, in terms of Yukawa variables

$$(39)\qquad \gamma_\mu(p_\mu - 2k_\mu)\Psi(x, r) = 0\,.$$

In consequence of the constraints (16) the k_4 and k_r have to be eliminated again by supplementing (39) with suitable reaction forces. In this way we get a spin-rotator model of elementary particles, with the operator S^2 replaced by the well known operator J of Dirac. In this case the mass spectrum is

$$(40)\qquad M_n = \frac{1}{al}\sqrt{2(n+1)}$$

for particles with spin $n + \frac{1}{2}$ (compare RAYSKI, 1955 *b*).

It seems to be possible to construct also a family of bosons described by a first order wave equation with the γ_μ's replaced by the Duffin-Kemmer ma-

trices β_μ with five rows and columns. In this case the mass spectrum for particles with spin n is given by (40). On the other hand, we may describe fermions by a Schrödinger-Gordon equation. In this case we would obtain a family with the mass spectrum (24) while spin is given by $n - \frac{1}{2}$. Using a second order wave equation and two-component spinors we get the usual number of independent states (the same as for the four-component spinors satisfying the Dirac equation). When using, alternatively a second order wave equation and four-component spinors the number of states is doubled. This alternative seems as well of physical interest since in this way we could describe fermions with opposite charges which are not related as particles to antiparticles (each possessing an antiparticle of its own). It seems that the hyperons $\Lambda^{\pm}$ with mass about 2320 are just of this type.

10. – A General Classification of Families.

The question is how many families of elementary particles are expected to exist in Nature and what are their distinctions? Following the idea put forward in section 7 we propose the following postulate: to each (single or double valued) irreducible unitary representation of the group of rotations and inversions in the 3-dimensional euclidean space there should correspond (at least) one type of elementary particle. Consequently, we may expect the esistence of two families of bosons: a tensor and a ps-tensor family described by a scalar and a ps-scalar bilocal field quantity respectively. Furthermore, three families of fermions according to the type of transformation law against inversions: two families of the type $(\pm i)$, and $(\mp i)$, and one family of the type $(\pm)$. The alternative $(\mp)$ is just realized by the respective antiparticle (Yang and Tiomno, 1952).

The above classification takes advantage only of the representations of the group of transformations in the 3-dimensional euclidean space. This is quite understandable for particles with a non-vanishing rest mass since their intrinsic properties should manifest themselves also in the state of rest, and thus, have nothing to do with the time variable. On the other hand, it is not at all obvious whether such a classification is sufficient for particles with a vanishing rest mass. (This is perhaps the reason why photons and gravitons do not fit into our scheme).

Another possibility of classification is offered by the existence of the alternatives: of a first or a second order wave equation. This last possibility may be regarded as a classification with respect to the time variable. Thus, the number of expected families may be doubled: four families of bosons and six families of fermions according to the types of parity and the order of field equations.

11. – A Confrontation with the Experimental Evidence.

Let us discuss briefly whether our formalism may be reconciliated with the present experimental evidence. There are three kinds of mesons satisfying Bose statistics: pion, meson τ, and meson θ. The first two are ps-scalar, the last is probably scalar. As the mass of the pion (273) is much smaller than that of τ and θ (~ 966) we may assume that pion is the lowest member of a ps-tensor family described by a second order wave equation. From (24) its theoretical mass ($n = 0$) is zero which may be interpreted in the following way: it possesses no mechanical mass but only a field mass brought about by the interaction (chiefly with virtual nucleons). On the other hand, τ and θ may be described by a Kemmer equation, i.e. possess a mechanical mass according to (40) for $n = 0$.

The approximative equality of their masses shows that the rate of reciprocity a is the same for both families. This is gratifying. No evidence exists for the lowest member of the fourth family: scalar with a vanishing mechanical mass.

Going over to fermions we notice the existence of an absolute selection rule: the law of conservation of the number of particles (minus antiparticles) for nucleons (together with hyperons). This may be accounted for by assuming that nucleons and hyperons are of the types $\pm$ while lighter fermions are of the types $\pm i$. In order to account for the lightest fermions ν, e, μ, whose masses are merely field masses, we have to assume a second order wave equation leading to the mass spectrum (24). Most probably electron has an opposite relative parity to that of muon and neutrino. The heavy mesons K satisfying Fermi statistics are either the next members of the electron or muon families (with spins $\frac{3}{2}$) or the lowest members of the remaining families of the types $\pm i$ satisfying a first order equation (spin $\frac{1}{2}$).

A little more details are known about hyperons. Besides the best known hyperon Λ^0 with mass $2\,181 \pm 1$ decaying into a nucleon and a pion, there exist charged hyperons with a similar decay scheme and mass about 2320. They seem to be nothing else but charged counterparts of Λ^0 in spite of a large mass difference. We denote them $\Lambda^{\pm}$. Most probably Λ^- is not an antiparticle to Λ^+. Next we have the cascade hyperon Υ^- with mass $2\,582 \pm 10$ decaying into Λ^0 and a pion. This hyperon is always negatively charged. There is an increasing evidence for the existence of still heavier hyperons with mass either close to 2900 or close to 3160. At least a part of them decays with the emission of a K-meson.

The fact that the hyperon $\Lambda^{\pm}$ appears with both signs of charge distinguishes it sharply from the proton (and from the cascade hyperon Υ^-). The-

refore we may expect that the nucleon and the cascade hyperon belong to one family while Λ^0 and $\Lambda^{\pm}$ to quite another family. The easiest way to account for the two signs of charge of Λ is to assume that it is described by a four-component spinor satisfying a second order wave equation while the nucleon together with the cascade hyperon are described by a four component spinor satisfying a Dirac equation.

If it is so, the nucleon family possesses a mass spectrum (40) while the Λ-family possesses a mass spectrum (24). By adjusting a from the value of the nucleonic mass $M_0 = 1836$ we get from (30) the next masses

$$M_1 = 2597, \quad M_2 = 3180, \quad \text{etc.}.$$

We notice that these values are close to the experimental values 2582 and 3160. Now, with the same value a, we get from (24)

$$M_0 = 0, \quad M_1 = 2183, \quad M_2 = 2860, \quad \text{etc.}.$$

and notice a remarkable agreement of the value M_1 with the experimental value 2181 ± 1 for the hyperon Λ^0.

A difficulty appears in connection with the value zero for $n = 0$. In order to prevent a decay of nucleons and hyperons into this fermion the state $n = 0$ has to be excluded by an extra assumption (beyond the formalism itself). The value M_0 being excluded in this way or other, the remaining selection rules follow from the formalism. In particular the combined laws of conservation of parity and angular momentum secure that the decay $Y^- \to N + \pi^-$ be possible only if the decay products form a D-state, (i.e. carry off an orbital angular momentum 2). On the other hand, the decay $Y^- \to \Lambda^0 + \pi^-$ may occur in an S-state provided Λ has an opposite relative parity ($\pm$) to that of Y ($\mp$). Thus, the cascade type of decay of the hyperon Y is strongly favoured.

The mass 2320 of the charged hyperons $\Lambda^{\pm}$ is not found among the theoretically predicted values, and the difference $2320 - 2180$ is to be explained as a self mass of electromagnetic origin. At the first sight such a large electromagnetic self mass seems inexplicable, but the fact that in this case the number of states is doubled may facilitate the understanding of this anomaly. Since Λ^- is not antiparticle to Λ^+ they have to be described by two separate solutions $\psi^{(-)}$ and $\psi^{(+)}$. Now, it is possible that there exists a coupling between the two by a Pauli term of the form

$$(\bar{\psi}^{(+)}\gamma_{[\mu,\nu]}\psi^{(-)} + \bar{\psi}^{(-)}\gamma_{[\mu,\nu]}\psi^{(+)})F_{\mu\nu}\,.$$

Such a coupling yields a quadratically divergent self energy term (non-compensating to a logarithmic divergence in the sense of Weisskopf). In a corresponding future (convergent) theory of interaction such a term may yield a contribution to the (finite) self energy much larger than the usual terms.

It may be expected that a similar shift will occur for the higher members of the Λ-family too, whence the charged counterparts of the next hyperon belonging to this family may have a mass shifted from 2860 to about 3000. A hyperon of this type seems to have been observed by FRIEDLANDER.

It seems that our classification may be reconciled with the present status of experimental evidence but the agreement is far from being decisive. However, the fact that the best known hyperons Λ^0 and Y^- fit qualitatively and quantitatively into our scheme seems promising.

REFERENCES

M. BORN: *Rev. Mod. Phys.*, **21**, 463 (1949).
J. RAYSKI: *Proc. Phys. Soc.*, **64**, 957 (1951).
J. RAYSKI: *Acta Phys. Pol.*, **14**, (1955*a*).
J. RAYSKI: *Acta Phys. Pol.*, **14**, (1955*b*) (in the press).
H. YUKAWA: *Phys. Rev.*, **77**, 219 (1950).
H. YUKAWA: *Phys. Rev.*, **91**, 415 (1953).

RIASSUNTO (*)

L'analisi dei fondamenti della meccanica quantistica mostra che essa comprende due procedimenti distinti: la quantizzazione dello spazio-tempo e il collegamento di un modello meccanico allo spazio-tempo quantizzato (Q.S.T.). Per ragioni spiegate nel testo, il primo di questi procedimenti si dice quantizzazione *l*, il secondo quantizzazione *h*. Si trova che per le particelle elementari il modello puntiforme non risulta naturale, mentre un modello bipuntuale si inserisce naturalmente nel quadro della Q.S.T. Tra i possibili modelli bipuntuali è preferibile un modello a rotatore che si adatta docilmente alle proprietà di covarianza della Q.T.S. La massa a riposo della particella bipuntuale non è più un parametro introdotto espressamente ma è determinata dalle quantità di moto derivanti dai moti interni della particella. Si costruisce una teoria di campo bilocale basata sul modello bipuntuale (rotatore) dell'entità fisica elementare: si impostano equazioni di campo, nonchè le densità del quadrivettore corrente, del tensore energia-quantità di moto, e del tensore momento angolare, densità che soddisfano leggi di conservazione differenziali. Il campo bilocale può essere quantizzato e descrive un'intera serie (famiglia) di specie di particelle con spin d'ordini superiori e masse corrispondenti agli stati eccitati del modello a rotatore preso per base. Si ha corrispondenza biunivoca tra i tipi di particelle che formano una famiglia e le rappresentazioni unitarie irriducibili del gruppo di rotazioni, il che dimostra un'intima e completa connessione tra spazio e materia. Le famiglie di particelle si possono classificare a seconda della mono o bivalenza delle grandezze di campo, a seconda del tipo di simmetria rispetto alle inversioni, e a seconda dell'ordine dell'equazione di campo. Il confronto con i dati sperimentali disponibili sulle particelle elementari (valori di massa a riposo, schemi di decadimento, ecc.) sembra dare risultati promettenti.

(*) *Traduzione a cura della Redazione.*

Radioactivity of ^{134}Cs.

G. Bertolini, M. Bettoni and E. Lazzarini

Istituto di Fisica Sperimentale del Politecnico - Milano

(ricevuto il 4 Giugno 1955)

Summary. — The β decays of ^{134}Cs and the γ decays of ^{134}Ba have been investigated with an intermediate image β spectrometer and a scintillation spectrometer. From β-γ coincidences a new β decay of 335 keV endpoint has been revealed and the existence of a weak β decay on the 1 350 keV level of barium has been confirmed. From β-γ and γ-γ coincidences and from internal conversion coefficients, the relative intensity of the β decays and the multipolarity of γ transitions have been investigated. The five excited states of ^{134}Ba are assumed having energies of 795, 1 350, 1 395, 1 700 and 1 949 keV. Their spins and parities are 2+, 2+, 3+ or 4+, 3+ or 4+ and 4+.

1. – Introduction.

According to the Table of Isotopes of Hollander, Perlman and Seaborg [1] the ^{134}Cs disintegrates to ^{134}Ba with a scheme as shown in Fig. 1.

β spectrometer and scintillation techniques have been used to investigate this scheme. The first measurements with β-rays spectrometer [2-4] reveal two β-decays with endpoints of 90 keV and 650 keV approximately. Waggoner and coll. [5] first reveal at the end of the Kurie plot of the high energy spectrum a slight convexity toward the energy axis. This curvature could not be ac-

[1] J. M. Hollander, I. Perlman and G. T. Seaborg: *Rev. Mod. Phys.*, **25**, 469 (1953).

[2] L. G. Elliot and R. E. Bell: *Phys. Rev.*, **72**, 979 (1947).

[3] K. Siegbahn and M. Deutsch: *Phys. Rev.*, **73**, 410 (1948).

[4] C. L. Peacock and J. L. Brand: *Phys. Rev.*, **83**, 484 (1951).

[5] M. A. Waggoner, M. L. Moon and A. Roberts: *Phys. Rev.*, **80**, 420 (1950).

counted for on the basis of the effect of the conversion electron of the 560 and 600 keV γ-rays which occur in this region. SCHMIDT and KEISTER ([6]) afterwards observed that the continuous spectrum showed two high energy components whose endpoints differ by 30-40 keV. We do not know the reason why a β-decay on the 1.831 MeV level of ^{134}Ba was included in the scheme. Perhaps it may be found in the attempt to include a γ transition of 1.037 MeV which otherwise could not be inserted unless the possibility of a K-capture branch or an impurity is admitted. However, in comparing the height of the conversion lines of 1.037 and 1.360 MeV over a period of four months, WAGGONER and coll. ([5]) excluded the hypothesis of impurities. More over they placed an upper limit of 4% on the K-electron capture by ^{134}Cs. The same limit was placed by SIEGBAHN and DEUTSCH ([3]), who investigated the Xe K X-rays using a proportional counter. Recently CORK and coll. ([7]) proposed a more complicated decay scheme, with continuous components of 80, 210, 410, 657 and 2 400 keV endpoints. A β^+ decay of the ^{134}Cs has been excluded by MIMS and HALBAN ([8]) who placed an upper limit of 0.009 percent on positron emission.

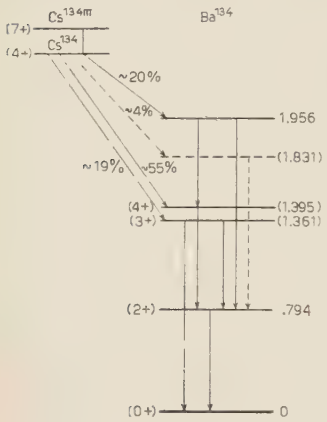

Fig. 1. – Decay scheme of ^{134}Cs according to Table of Isotopes.

The energies of the γ-rays of the ^{134}Ba have been measured by several researches by means of secondary electron spectra obtained by internal ([4-6]) and photoelectric ([2,3,7,9]) conversion, and by scintillation spectrometers ([10]). The multipole order of the 560, 600, 800 and 1360 keV γ-rays has been determined by measurements of internal conversion coefficients ([3-6]). Measurements of angular correlation and polarization-directional correlation ([11-15]) permit the assignment of the spins and parities to the levels. Such assignment is consistent with the measurement of angular moment of ^{134}Cs using the mag-

([6]) F. H. SCHMIDT and G. L. KEISTER: *Phys. Rev.*, **86**, 632 (1955) (A).

([7]) J. M. CORK, J. M. LE BLANC, W. H. NESTER, D. W. MARTIN and M. K. BRICE: *Phys. Rev.*, **90**, 444 (1953).

([8]) W. MIMS and H. HALBAN: *Proc. Phys. Soc.*, A **64**, 311 (1951).

([9]) M. C. JOSHI and B. V. THOSAR: *Phys. Rev.*, **86**, 1022 (1954).

([10]) D. LU and M. L. WIEDENBECK: *Phys. Rev.*, **94**, 501 (1954).

([11]) F. METZGER and M. DEUTSCH: *Phys. Rev.*, **78**, 551 (1950).

([12]) E. L. BRADY and M. DEUTSCH: *Phys. Rev.*, **78**, 558 (1950).

([13]) B. L. ROBINSON and L. MADANSKY: *Phys. Rev.*, **84**, 604 (1951).

([14]) B. L. ROBINSON and L. MADANSKY: *Phys. Rev.*, **88**, 1065 (1952).

([15]) R. M. KLOEPPER, S. E. LENNOX and M. L. WIEDENBECK: *Phys. Rev.*, **88**, 695 (1952).

netic resonance method ([16]) and with the allowed shape of the β spectra of 90 and 650 keV. A summary of the experimental values is given in Table I.

We have investigated the decay of ^{134}Cs in order to study the energy and the intensity of the different β decays, the energy and multipole order of the associated γ-rays.

TABLE I.

Reference		(2)	(3)	(5)	(4)	(6)	(7)	(9)
β decay	β_1	90 (28%)	—	—	92 (25%)	~79 (~24%)	—	—
energy	β_2	658 (72%)	—	651	648 (75%)	$\beta_3 - \beta_2 =$	—	—
in keV	β_3	—	—	—	—	~ 30-40 keV	—	—
γ decay	γ_1	—	—	—	—	—	202.5	
energy	γ_2	—	—	—	—	—	475.0	467
in keV	γ_3	—	—	—	—	561.5	563.0	553
	γ_4	568	566	560	558	566.5	569.7	571
	γ_5	602	603	602	600	601.2	605.4	607
	γ_6	—	—	—	—	—	662.7	—
	γ_7	794	798	799	800	793.1	796.8	794
	γ_8	—	—	—	—	—	822.6	—
	γ_9	—	—	1 037	—	1 037.2	1 039	1 027
	γ_{10}	—	—	1 170	—	1 164.4	1 168	1 164
	γ_{11}	—	1 350	1 363	—	1 365.7	1 368	1 368
Conversion coeffic.	α_4	—	$\alpha_4+\alpha_5 =$ $4.4\cdot10^{-3}$	$8.2\cdot10^{-3}$ / $6.7\cdot10^{-3}$	$9.05\cdot10^{-3}$	—	—	—
	α_5	—	—	$5.31\cdot10^{-3}$ / $5.06\cdot10^{-3}$	$5.67\cdot10^{-3}$	$5.7\cdot10^{-3}$	—	—
	α_7	—	$2.4\cdot10^{-3}$	$2.55\cdot10^{-3}$ / $2.41\cdot10^{-3}$	$3.02\cdot10^{-3}$	$2.1\cdot10^{-3}$	—	—
	α_{11}	—	—	$6.20\cdot10^{-4}$ / $6.20\cdot10^{-4}$	—	—	—	—

2. – Sources.

^{134}Cs, 5.6 mC/g specific activity was supplied from Harwell. It was mounted on nylon film of 0.16 mg/cm^2 and, in order to study carefully the β spectrum shape, it was evaporated under vacuum on Al foil 1 μm thick.

To investigate the β spectrum, a source of $\sim 1\ \mu$C was used; a source of $\sim 10\ \mu$C was used for γ-γ and β-γ coincidences and for internal and photoelectric conversion.

([16]) V. JACCARINO, B. BEDERSON and H. H. TSTROKE: *Phys. Rev.*, **87**, 676 (1952).

3. – Experimental Apparatus.

A high-transmission intermediate image β-spectrometer type SLÄTIS and SIEGBAHN ([17]) was used to investigate the β spectrum and the secondary electron spectrum. The Geiger-Müller counter used had a nylon window of

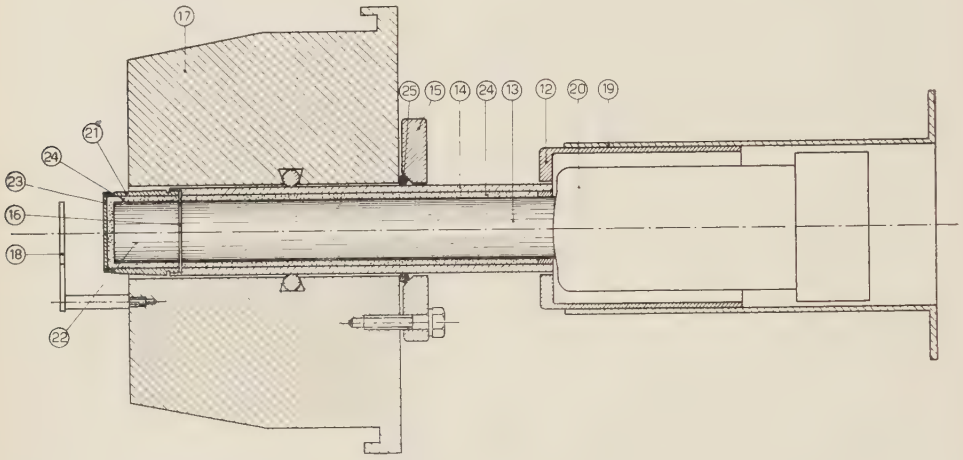

Fig. 2. – Arrangement for γ detection. (13) plexiglas light pipe, (16) optical joint (17) β spectrograph pole shoe, (18) source holder, (20) 5819 phototube, (22) NaI(Tl) crystal, (24) magnesium oxide.

0.16 mg/cm² thickness. The baffles in the spectrometer were adjusted for a transmission of ~ 4%. β-γ coincidences were realized with the method described by A. C. G. MITCHELL in the SIEGBAHN book ([18]). γ-rays were detected by a cylindrical NaI(Tl) crystal 1″ diameter × 1″ long mounted behind the source. A light pipe realised with plexiglas surrounded by magnesium oxide was in optical joint with the crystal and a 5819 multiphotoplier (Fig. 2).

β-rays were detected by an anthracene cylindrical cristal ½″ diameter × ½″ long directly in contact with a light pipe (Fig. 3). Contrary to the former, the latter light pipe is not surrounded by magnesium oxide and its functioning is due to the angle of incidence of most of the light emitted by a single flash being greater than the critical angle. This pipe revealed an efficiency lower than that with magnesium oxide. The surface of the anthracene crystal facing the source was covered with 0.1 μm of Al by vacuum evaporation. The evaporation method appeared better than that of covering the crystal with Al foil

([17]) G. BOLLA, S. TERRANI and L. ZAPPA: *Nuovo Cimento*, **12**, 875 (1954).
([18]) K. SIEGBAHN: *β- and γ-Ray Spectroscopy* (Amsterdam, 1955), p. 221.

1 μm thick (the thinnest at our disposal) both in order to reveal low energy particles and to avoid distorsions in the monochromatic electron peaks.

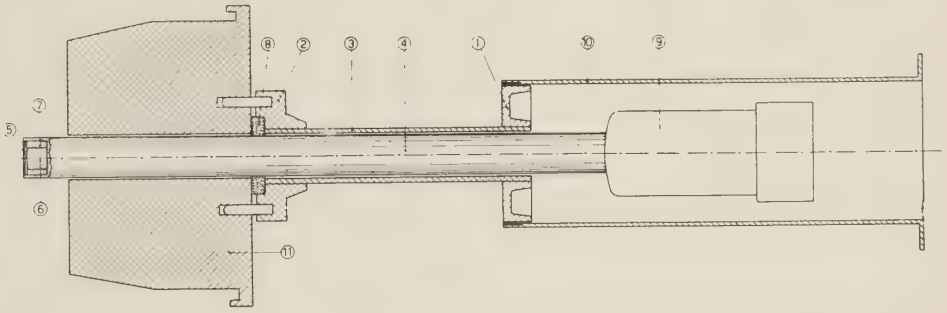

Fig. 3. – Arrangement for β detection. (1) (3) (10) Armco iron, (4) plexiglas light pipe, (5) lead, (6) anthracene crystal, (7) magnesium oxide, (9) 5819 phototube, (11) spectrograph pole shoe.

The pulses from the photomultiplier were sent to a coincidence with 0.5 μs resolution time ([19]), through two similar chains formed by a preamplifier, amplifier and discriminator type BELL and JORDAN ([20]), (Fig. 4).

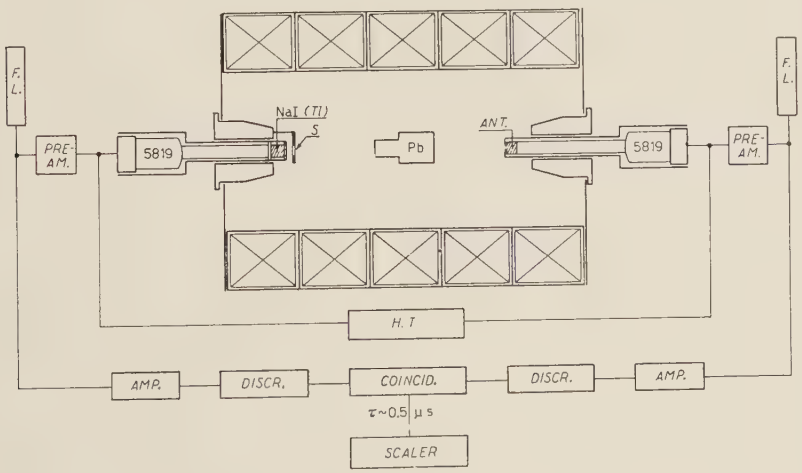

Fig. 4. – β-γ coincidences arrangement.

The γ spectrum of ^{134}Cs was analyzed with a cylindrical crystal of NaI(Tl) $1'' \times 1''$ and a single channel analyser ([21]). It is shown in Fig. 6.

([19]) B. SMALLER and E. AVERY: *Rev. Sci. Instr.*, **22**, 341 (1951).
([20]) W. H. JORDAN and P. R. BELL: *Rev. Sci. Instr.*, **18**, 703 (1947).

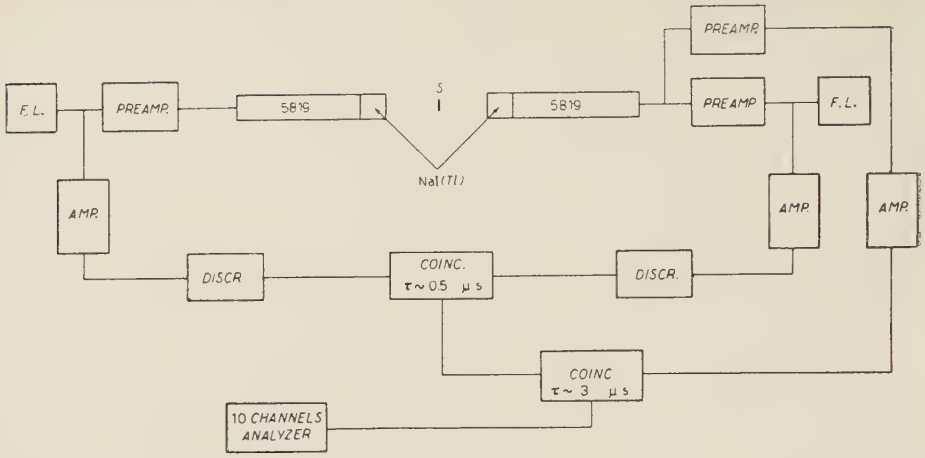

Fig. 5. – γ-γ coincidences arrangement.

The γ-γ coincidences were performed by the same chain used for the β-γ coincidences. The output pulse was sent to a ten channel analyser ([22]) (Fig. 5).

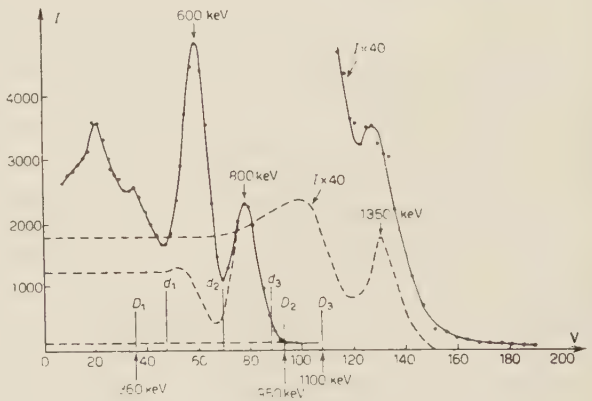

Fig. 6. – Single channel scintillation spectrum, D_1, D_2, D_3 represent the bias of the discriminator of the γ detector chain in β-γ coincidences measurement. d_1, d_2, d_3 represent the bias of the discriminator in γ-γ coincidences measurements.

4. – Experimental Technique.

In order to analyse the γ spectrum of ^{134}Cs and the results of the γ-γ coincidences, it is necessary to know the response of the crystal to every single energy considering the geometry used during the experiments. This is necessary in order to know exactly the number of γ-rays of a single energy and the ratio, for a single γ energy, between the voltage pulses higher and lower than the discriminator level. To realise this, spectra of ^{203}Hg (279 keV), ^{137}Cs (661 keV), ^{65}Zn (1.14 MeV) and ^{22}Na (0.51 and 1.28 MeV) were taken. The

source was placed at the same distance as for the intensity and coincidence measurements of ^{134}Cs ($d = 7.6$ cm).

The response of the NaI(Tl) crystal to the different energies is shown in Fig. 7. From the same spectra it is possible to obtain the experimental ratio

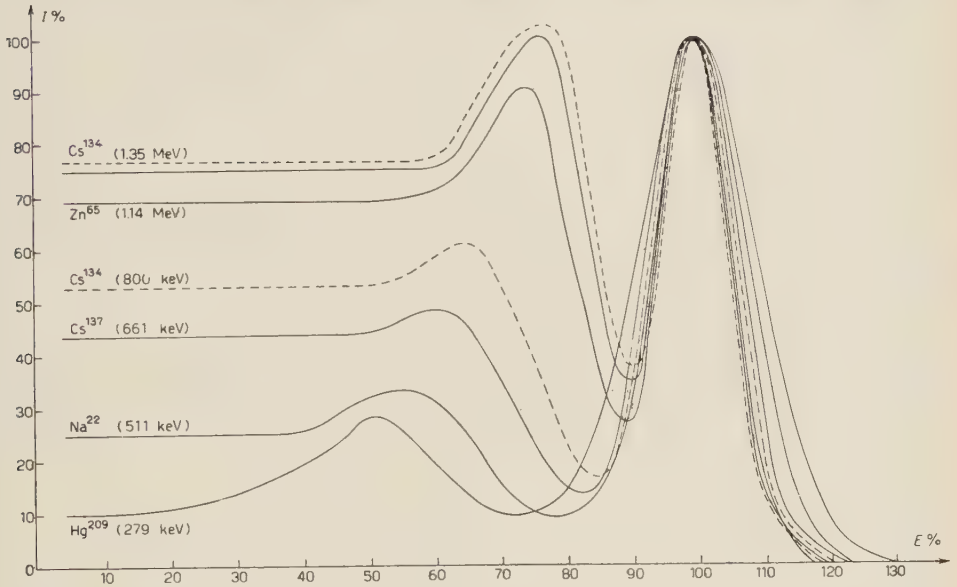

Fig. 7. – γ spectra percentually plotted relatively to the position and intensity of the photo peak for energies of 279, 510, 661, 1 140 and 1 280 keV. A NaI((Tl) cylindrical crystal 1″ diam. × 1″ long at 7.6 cm from the source was used. The back-scattering has been subtracted. The dotted lines represent the response of the crystal to 800 and 3 350 keV rays constructed from above curve.

of photo-peak pulses to the total number of pulses, assuming a flat experimental Compton distribution at low energies for γ-rays of energy higher than 500 keV. This assumption cannot be verified for all the energies because of the presence of the backscattering peak. Experimentally it is verified for the ^{137}Cs until 32 keV and the ratio photo-peak total number of pulses is found in agreement with the value of MÄDER and coll. ([23]) and with the theoretical results obtained by Dr. BERTOLINI in collaboration with Dr. BRACCI of the C.I.S.E. laboratory of Milan (*).

([21]) J. I. FRANCIS Jr., P. R. BELL and J. C. GUNDLACH: *Rev. Sci. Instr.*, **22**, 133 (1951).

([22]) E. GATTI: *Nuovo Cimento*, **11**, 153 (1954).

([23]) D. MAEDER, R. MÜLLER and V. WINTERSTEIGER: *Helv. Phys. Acta*, **27**, 3 (1954).

(*) This evaluation has been done with the Montecarlo Method taking into con-

Using the absorption coefficients reported by MÄDER and coll. ([23]), the counting efficiency of a $1'' \times 1''$ cylindrical crystal of NaI(Tl) was calculated for small sources placed at various distances from the crystal surface along the axis of the cylinder.

In Fig. 9 the percentage of γ-rays absorbed in the crystal as a function of the energy and the crystal-source distance is shown.

5 – γ Spectrum.

Fig. 6 shows the γ spectrum of ^{131}Cs. The peak at 600 keV includes the γ-rays of 560 and 600 keV. γ-rays of low energy are hidden by the Compton distributions and backscattering peaks at 600 and 800 keV. The small peaks of the 1.03 and 1.17 MeV γ-rays are also hidden by the tail of the peak at 800 keV and by the Compton distribution of the 1.35 MeV γ-rays.

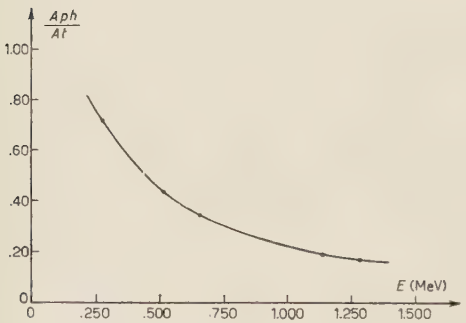

Fig. 8. – Experimental photo peak pulses to the total number of pulses for a NaI(Tl) cylindrical crystal 1″ diam. × 1″ long at 7.6 cm from the source.

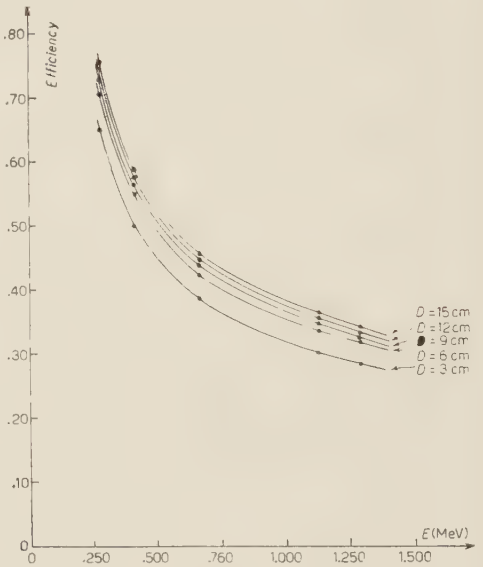

Fig. 9. – Theoretical efficiency of a NaI(Tl) cylindrical crystal 1″ diam. × 1″ long for various γ ray energies and source distances.

The relative intensities of the 800 keV and 1.35 MeV γ-rays are derived from the graph of Fig. 7 by constructing their Compton distribution. The 600 keV photoelectric peak deduced from these evaluations and the plot of

sideration the possibility of two Compton effects for a single γ-ray before escaping from the crystal. Three thousand γ-rays have been used. A ratio photopeak/total counts = 0.3 was obtained.

Fig. 8 permit us to obtain the 600 keV γ-rays intensity. Fig. 6 shows this procedure. It can be noted that the intensity of the Compton distribution of the 600 keV γ transition respecting the intensity of the photoelectric peak obtained with the above method is less than that obtainable from Fig. 7 (26 % against 38 %). For this reason it is preferable to plot the smallest number of Compton distributions and evaluate the γ-rays intensities from the photoelectric peak Fig. 8. Table II shows the intensities obtained for the γ transitions. The intensities of 560 and 600 keV γ-rays, that are not resolved with the scintillation spectrograph, were obtained from γ-γ coincidences measurements.

TABLE II.

γ-ray energy in keV	560 + 600	800	1 350
intensity	56.100	39.150	597

6. – γ-γ Coincidences.

γ-γ coincidences, realised by the experimental apparatus of Fig. 5, were set up for investigating coincidences between γ-rays of 560 and 600 keV, 560 (or 600) and 800 keV, 560 (or 600) and 1350 keV, and 800 and 1350 keV. The 10 channels used to analyse the coincidence pulses were able to contain the full peak at 600 or 800 keV. The area of the photoelectric peak was evaluated for different bias of the discriminators. A single run was made to last one hour. The random coincidences were evaluated during a measurement that also lasted one hour. Table III shows the average experimental results of three measurements.

TABLE III.

	d_{1B}	d_{2B}	d_{3B}
d_{1A}	$C_1 = 8\,884 \pm 142$	$C_2 = 2\,720 \pm 75$	$C_3 = 194 \pm 23$
d_{2A}	$C_1' = 2\,069 \pm 72$	—	$C_3' = 17 \pm 6.4$

Let the two detecting chains of the γ-γ coincidences be A and B. C_3 and the differences $C_2 - C_3$ and $C_1 - C_2$ are the pulses of the A spectrum (Fig. 6)

between d_{1A} and d_{2A} in coincidence with the pulses of the B spectrum between d_{3B} and ∞, d_{2B} and d_{3B}, d_{1B} and d_{2B} (Fig. 6). C_3 is the coincidence number between 560 (or 600) keV and 1.35 MeV γ-rays. $C_2 - C_3$ is the coincidence number between 560 (or 600) keV and 800 keV γ-rays assuming that the number of coincidences between 800 keV γ-rays having a voltage pulse between d_{1A} and d_{2A}, and 1.35 MeV γ-rays is negligible.

$C_1 - C_2$ must be corrected to a long extent in order to obtain the effective number of 560-600 keV coincidences. The correction is carried out according to formula:

$$N_{C\,560\text{-}600} = C_1 - C_2 - A_{\text{Compt } 8A}\,\omega\varepsilon_{6B}\left(\frac{A_{ph}}{A_t}\right)_{6B} - A_{6B}\omega\varepsilon_{8A}\left(\frac{A_c}{A_t}\right)_{8A}$$

where:

$A_{\text{Compt } 8A}$ = area of the 800 keV Compton distribution contained between d_{1A} and d_{2A} in the A spectrum;

ω = solid angle subtended by the crystal;

ε_{6B} and ε_{8B} = efficiencies of the crystal for 600 keV and 800 keV γ-rays respectively;

$(A_{ph}/A_t)_{6B}$ = ratio between the photoelectric area and total area of 600 keV γ-rays for B spectrum;

$(A_c/A_t)_{8A}$ = ratio between Compton area containd between d_{1A} and d_{2A} and the total area of 800 keV γ-rays for the A crystal.

In Table IV are shown the corrected results.

TABLE IV.

$N_{C560\text{-}600}$	$N_{C600\text{-}800}$	$N_{C600\text{-}1350}$	$N_{C800\text{-}1350}$
2285 ± 192	$2\,526 \pm 79$	194 ± 23	17 ± 6.4

The detectors were placed at 180° and an analogous measurement carried out with the detectors at 90° is in agreement with that at 180° within the experimental errors.

7. – β-Spectrum.

The β spectrum shows clearly two components with endpoints of 86 ± 15 and 645 ± 10 keV. The form of the Fermi plot obtained for both components

is linear. At the end of the spectrum appear the conversion lines corresponding to the γ-radiation of 560 and 600 keV and for this reason it is not possible to observe the existence of a low intensity component of higher energy. Fig. 10 shows a Fermi plot for the source evaporated under vacuum.

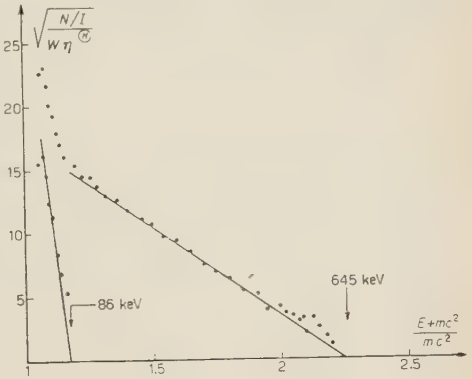

Fig. 10. – ^{134}Cs Fermi plot.

8. – β-γ Coincidences.

β spectra in coincidence with γ-rays were investigated with the apparatus described in the above paragraphs. By varying the bias of the discriminator associated with the γ-rays detector it was possible to investigate β spectra in coincidence with γ-rays of different energies. The measurements were made with the bias at three different values: $D_1 = 360$ keV, $D_2 = 950$ keV and $D_3 = 1\,100$ keV (see Fig. 6).

The bias D_1 permitted the detection of coincidences between β-rays and γ-rays of whatever energy. The relative Fermi plot is shown in Fig. 11 (*a* curve). It is a straight line analogous to that shown in Fig. 10. The spectrum obtained with the bias D_3 (*c* curve) evidences a β-spectrum with endpoint of 335 keV ([24]). This spectrum, and a second one with endpoint of about 650 keV, which obviously cannot be that revealed by the *a* curve, are in coincidence with γ-rays of high energy, i.e. with 1.35 MeV γ-rays.

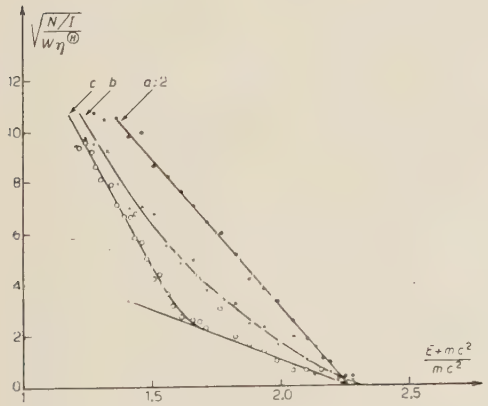

Fig. 11. – ^{134}Cs Fermi plot in coincidences with γ rays of energies higher that D_1 (*a* curve), D_2 (*b* curve), D_3 (*c* curve) (see Fig. 6).

The Fermi plot performed with bias D_2 (*b* curve) is an intermediate state between the *a* curve and the *c* curve. In this plot three β components are probably present: the two

([24]) G. Bertolini, M. Bettoni and E. Lazzarini: *Nuovo Cimento*, **1**, 746 (1955).

components in coincidence with the 1.35 MeV γ-rays and a small portion of the mean component ascribed to coincidences with 800 keV γ-rays which give voltage pulses higher that D_2. We think that the β spectrum evidenced by the coincidence measurements is the same as that indicated by SCHMIDT and coll. in their abstract ([6]).

9. – Photo Spectrum.

The γ-rays energies were investigated by photoelectric and internal conversion. Fig. 12 shows the secondary electron spectrum from a lead converter ~ 4 μm thick with a spectrometer resolving power of 3%. Table V shows the energies obtained for the γ-rays.

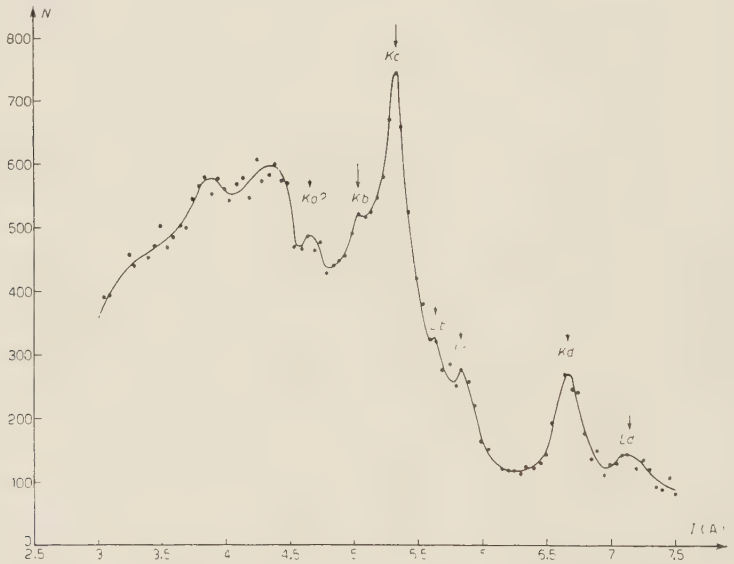

Fig. 12. – Photo spectrum of ^{134}Cs with a lead converter 4 μm thick.

TABLE V.

	γ_a	γ_b	γ_c	γ_d	γ_e	γ_f	γ_g
Photoelectric conversion	504.8 ± 4.2	558 ± 3.6	601 ± 1	795 ± 1			
Internal conversion		559.7 ± 4	598.5 ± 3	795 ± 1.5	1 039 ± 12	1 163 ± 12	1 350 ± 7

10. – Decay Scheme.

The proposed decay scheme of ^{134}Cs is shown in Fig. 13. γ_6 is a probable weak transition between 1949 and 1700 keV level. It was detected in the secondary electron spectrum taken with high resolving power.

γ_5 was not revealed but there is no doubt to its existence because of the coincidences of β_3 with γ_7. On the other hand the γ_7 transition is a transition to ground state as confirmed by the γ-γ coincidences which revealed coincidences of γ_7 with $\sim$ 600 keV γ-rays (γ_1) but not with 800 keV γ-rays (γ_8). (Table IV). The small number of coincidences revealable in the former case can be attributed to coincidences between γ_9 and γ_8.

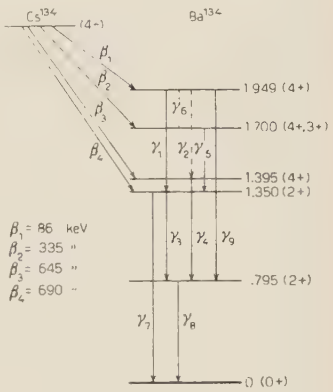

Fig. 13. – Proposed decay scheme of ^{134}Cs.

γ_2 transition has been assumed negligible in respect to γ_1. This hypothesis permits us to obtain, as it will appear further, the relative intensities for β_1, β_2, β_3 and β_4 which makes possible to obtain the internal conversion coefficients in agreement with those calculated with values obtained from absolute measurements with scintillation and β spectrometer.

It is not possible to place the 1.039 MeV γ-ray in the decay scheme. Its assignment to a K-capture branch was taken into account, but an investigation on the Xe K-X-rays using a proportional counter and NaI(Tl) crystal does not give evidence of this decay.

The relative intensities of the β_1, β_2, β_3 and β_4 decays are determined by the following scheme.

a) Calculation of the γ_7 decay probability in respect to γ_3 decay. This is determined from the ratio between $N_{\substack{C556\\600}-1350}$ (coincidence number of 559 (or 600) keV with 350 keV γ-rays) and $N_{C\,559-600}$ (coincidence number of 559 keV with 600 keV γ-rays).

$$\frac{N_{\substack{C559\\600}-1350}}{N_{C\,559-600}} = \frac{I_{\beta_1}\omega^2\varepsilon_6\varepsilon_{1350}\left(\frac{A_{ph}}{A_{Compt}-A_{ph}}\right)_6\left(\frac{A_{higher}}{A_t}\right)_{1350}\frac{N_{\gamma_1}}{N_{\gamma_1}-N_{\gamma_2}}\frac{N_{\gamma_7}}{N_{\gamma_3}+N_{\gamma_7}}}{2I_{\beta_1}\omega^2\varepsilon_6^2\left(\frac{A_{ph}}{A_{Compt}+A_{ph}}\right)_6^2\left(\frac{N_{\gamma_2}}{N_{\gamma_1}+N_{\gamma_2}}+\frac{N_{\gamma_1}}{N_{\gamma_1}+N_{\gamma_2}}\frac{N_{\gamma_7}}{N_{\gamma_3}+N_{\gamma_7}}\right)}$$

where:

I_{β_1} = β_1 decay intensity;

ω = solid angle subtended by the crystal in 4π units;

ε_6 = crystal efficiency for 600 keV γ-rays for the solid angle ω;

ε_{1350} = crystal efficiency for 1.35 MeV γ-rays for the solid angle ω;

$\left(\frac{A_{ph}}{A_{Compt}+A_{ph}}\right)_6$ = ratio of photoelectric peak/total number of pulses 0f 600 keV γ-rays spectrum;

$\left(\frac{A_{higher}}{A_t}\right)_{1350}$ = ratio between the spectrum area higher than the bias of the discriminator and the total area of the 1.35 MeV γ-rays spectrum;

$\frac{N_{\gamma_1}}{N_{\gamma_1}+N_{\gamma_2}}$ = probability of the γ_1 transition;

$\frac{N_{\gamma_2}}{N_{\gamma_1}+N_{\gamma_2}}$ = probability of the γ_2 transition;

$\frac{N_{\gamma_7}}{N_{\gamma_3}+N_{\gamma_7}}$ = probability of the γ_7 transition;

$\frac{N_{\gamma_3}}{N_{\gamma_3}+N_{\gamma_7}}$ = probability of the γ_3 transition;

Assuming $N_{\gamma_2} \ll N_{\gamma_1}$ it is $\frac{N_{\gamma_7}}{N_{\gamma_3}+N_{\gamma_7}} = 0.0752$.

b) Determination of the 559 keV γ-rays in respect to 600 keV γ-rays intensity

$$\frac{N_{C\,559-600}}{N_{559+600}} = \frac{2N_{559}}{N_{559+600}}\left\{\omega\varepsilon_6\left(\frac{A_{ph}}{A_{Compt}+A_{ph}}\right)_6\right\}$$

and by neglecting the contribution of β_4 decay $N_{600}/N_{559} = 4.16$.

From this ratio, the following relation is derived

$$\frac{I_{\beta_3}}{I_{\beta_1}} = \frac{I_{\beta_1}}{I_{\beta_1}}\,3.85 - 2.85\ .$$

c) From the equation

$$\frac{N_{C\,559-600}}{N_{559+600}} = \frac{2I_{\beta_1}\omega\varepsilon_6\left(\frac{A_{ph}}{A_{Compt}+A_{ph}}\right)_6 \frac{N_{\gamma_3}}{N_{\gamma_3}+N_{\gamma_7}}}{I_{\beta_1}\left(1+\frac{N_{\gamma_3}}{N_{\gamma_3}+N_{\gamma_7}}\right)+I_{\beta_2}\frac{N_{\gamma_3}}{N_{\gamma_3}+N_{\gamma_7}}+I_{\beta_3}+I_{\beta_4}\frac{N_{\gamma_3}}{N_{\gamma_3}+N_{\gamma_7}}}$$

and assuming that γ_7 is negligible in respect to γ_3 one obtains $I_1 = 24\,\%$.

d) From β-γ coincidences (Fig. 11, *c* curve) $I_{\beta_2}/I_{\beta_4} = 2.7$.

From *a*), *b*), *c*) and *d*) the relative intensities of β decays are obtained: $I_{\beta_1} = 24\%$; $I_{\beta_2} = 2.7\%$; $I_{\beta_3} = 72.3\%$; $I_{\beta_4} = 1\%$.

11. – Conversion Coefficients.

The internal conversion lines are shown in Fig. 13. By the β decays intensities and by comparing the peak areas with β spectrum total area, the internal conversion coefficients are obtained. They are shown in Table VI. In the same table are given the conversion coefficients obtained by comparing absolute measurements of γ intensities taken with scintillation spectrograph and conversion electrons with β-spectrograph.

TABLE VI.

	α_{559}	α_{600}	α_{800}	α_{1350}
β spectrograph measurements	$6.45 \cdot 10^{-3}$ ± 0.90	$3.50 \cdot 10^{-3}$ ± 0.25	$2.50 \cdot 10^{-3}$ ± 0.20	$7.7 \cdot 10^{-4}$ ± 0.9
β spectrograph and scintillation spectrograph measurements	$8.7 \cdot 10^{-3}$ ± 1	$4.7 \cdot 10^{-3}$ ± 0.34	$1.49 \cdot 10^{-3}$ ± 0.20	—
Theoretical values:				
ED	$2.25 \cdot 10^{-3}$	$\sim 2 \cdot 10^{-3}$	$1.06 \cdot 10^{-3}$	$3.87 \cdot 10^{-4}$
EQ	6.17 »	5.25 »	2.63 »	8.5 »
MD	9.75 »	8.13 »	4.12 »	13 »
EO	15.40 »	12 »	6 »	18 »
MQ	20 »	20 »	—	—

12. – log *Ft* Values, Spin and Parities.

The log *Ft* values calculated assuming for the ^{134}Cs a half life of 2.3 y are 6.52, 9.44, 8.94 and 10.92 respectively for the decays β_1, β_2, β_3 and β_4. The β_4 decay seems to be a second forbidden ($\Delta J = 2$, no). It is not possible to judge this from the spectrum shape because of the statistical errors in the coincidence measurements.

This assignment is substantiated by the angular momentum and parity of the ^{134}Cs level and by the half life of the 1350 keV level which is presumed to be < 0.5 μs. The classification 3 – of the 1350 keV level reported in the Table of Isotopes should indicate a half life of ~ 200 μs according

to $M3$ transition ([25]). Moreover the $2+$ assignment to the third level indicates that the 1.35 MeV γ-rays are electric quadrupole transitions in accordance with the measurements of the internal conversion coefficient. The assignment $0+$, $2+$, $2+$, and $4+$ to first four ^{134}Ba excited levels is the most probable.

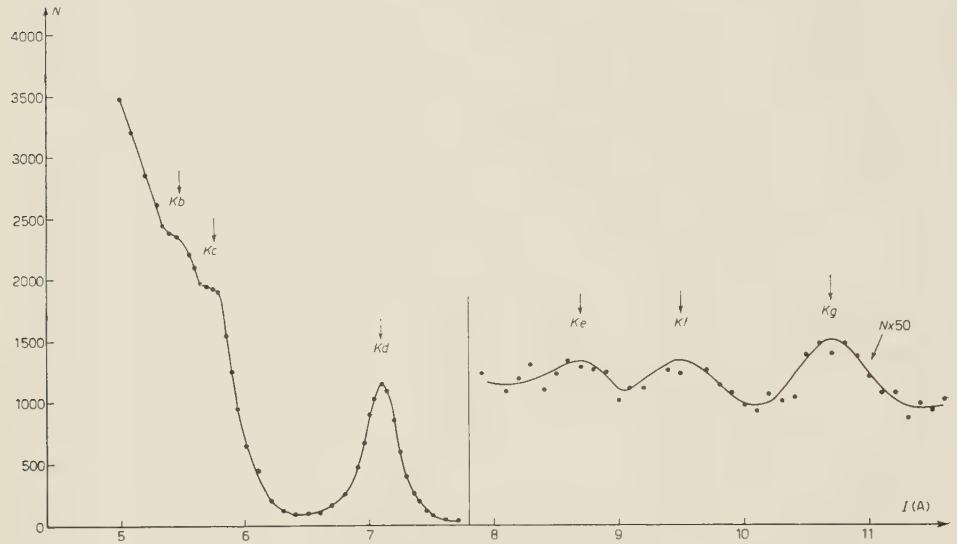

Fig. 14. – Internal conversion lines of ^{134}Cs.

Coincidences β-γ between β-rays and 1.35 MeV γ-rays (measurements carried out by R. HOLLANDER and reported by WAGGONER and coll. ([5])) and between β_1-rays and γ-rays ([2,26]) seem incompatible with a $5+$ 1949 keV level as established by ROBINSON and MADANSKY ([14]) by polarisation - directional correlation. If the assignment $2+$ to the second excited level is correct the spin 3 or 4 and parity plus seems to be the most probable.

When this work was already finished and ready for publication we learnt of the work of KEISTER and coll. ([27]) that appeared on an issue of the Physical Review which was not received by us through an oversight on the part of the distributors.

The intensities of the γ-rays and relative internal conversion coefficients observed in our measurements are in agreement with the values of KEISTER and coll.. A disagreement exists in the evaluation of the β decays intensities.

([25]) V. F. WEISSKOPF: *Phys. Rev.*, **83**, 1073 (1951).
([26]) J. L. MEEM Jr. and F. MAIENSCHEIN: *Phys. Rev.*, **76**, 328 (1949).
([27]) G. L. KEISTER, E. B. LEE and F. H. SCHMIDT: *Phys. Rev.*, **97**, 451 (1955).

in the assignment of the energy of the first excited level of the ^{134}Ba, in the assignment of the spin and parity at 1365 keV level and in the position of 1.367 MeV γ transition.

We have derived the β decays intensities from β-γ and γ-γ coincidence measurements. In this measurements are involved two errors: the evaluation of the shape of the pulse spectrum of NaI(Tl) crystal to a single γ energy and the evaluation of the β_2/β_4 ratio in β-γ coincidences because of the back-scattering of the source and of a probable decay of the 1700 keV going to the ground state without passing through the 1350 keV level.

From β-γ coincidences it is evident that the 1350 keV level can go directly to the ground state and its half life is less that 0.5 μs; γ-γ coincidences show that the probability of the decay is 0.0≤1. The above consideration and the internal conversion coefficient of the 1350 keV γ-rays consistent with $E2$ radiation, cannot be in agreement with an assignment (3 –) at the 1350 keV level. Moreover the coincidence measurements of KEISTER and coll. indicating that more low energy β-decays are followed by 600 keV γ-rays than by 795 keV γ-rays, are consistent with our decay scheme.

* * *

We are grateful to Prof. G. BOLLA for his encouragement of this work and to Prof. A. GAMBA of the Turin University for a helpful discussion on the selection rules in the decay of ^{134}Cs. One of the authors, G. BERTOLINI, wishes to thank Dr. J. RUTHERGLEN and his coworkers of the University of Glasgow for useful notices about the γ scintillation spectra.

RIASSUNTO

È stato studiato il decadimento β del ^{134}Cs e il decadimento γ del ^{134}Ba con spettrografo β a immagine intermedia e con spettrografo a scintillazione. Misure di coincidenze β-γ hanno messo in evidenza un decadimento γ di energia massima 335 keV e hanno confermato l'ipotesi di un decadimento β molto debole sul livello di 1350 keV del ^{134}Ba. Le intensità relative dei decadimenti β e le multipolarità delle transizioni γ sono state ricavate da misure combinate di coincidenze β-γ, coincidenze γ-γ e coefficienti di conversione. Si propone uno schema di decadimento con stati eccitati del bario di 795, 1350, 1395, 1700 e 1949. I loro spin e parità risultano essere 2+, 2+, 3+ o 4+, 3+ o 4+, e 4+.

On the Energy Distribution and the Emission Probability of Internal Bremsstrahlung in $^{71}_{32}$Ge.

A. Bisi, E. Germagnoli (*), L. Zappa and E. Zimmer (*)

Istituto di Fisica Sperimentale del Politecnico - Milano
Laboratori CISE - Milano (*)

(ricevuto il 4 Giugno 1955)

Summary. — The continuous γ spectrum due to bremsstrahlung associated with the orbital electron capture in $^{71}_{32}$Ge has been investigated with a scintillation spectrometer. The intensity distribution of the spectrum in the energy range between 50 keV and the upper limit of energy ($E_{max} = 220 \pm 3$ keV) was found to agree closely with the one calculated according to the theory developed by Morrison and Schiff. The ratio of the total number of bremsstrahlung quanta to the number of K-captures in the interval of energy between 70 keV and the upper limit was $(2.3 \pm 0.5) \cdot 10^{-5}$, which also is in satisfactory agreement with the theoretical value. The half life of $^{71}_{32}$Ge was checked and found to be 12.5 ± 0.1 days. The type of transition is briefly discussed according to nuclear shell model. Some results concerning the decay of $^{77}_{32}$As which have been obtained during the present measure are also reported.

1. – Introduction.

Several activities are known to be produced when isotopes of Ge are irradiated with slow neutrons: some of them have been investigated in detail [1,2]. In particular, a few hours after the irradiation of a sample of natural Ge, three activities are still important: two of them are due to the radioactive chain:

$$^{77}_{32}\mathrm{Ge} \xrightarrow[12.8\ \mathrm{h}]{\beta^+} {}^{77}_{33}\mathrm{As} \xrightarrow[39\ \mathrm{h}]{\beta^-} {}^{77}_{34}\mathrm{Se}$$

[1] J. M. Hollander, I. Perlman and G. T. Seaborg: *Rev. Mod. Phys.*, **25**, 469 (1953).

[2] R. W. King: *Rev. Mod. Phys.*, **26**, 307 (1954).

while the third one has to be attributed to $^{71}_{32}$Ge, which decays by pure orbital electron capture towards the ground state of $^{71}_{31}$Ga, its half life being about 12 days.

The β and γ spectrum emitted from $^{77}_{32}$Ge is rather complicated and has been recently investigated by SMITH [3] and by BURSON *et al.* [4] by means of magnetical lens spectrometers and scintillation spectrometers and with the aid of β-γ and γ-γ coincidences techniques.

The activity due to $^{77}_{33}$As has also been examined during the last years and will shortly be considered in the next section.

The aim of the present work is an investigation of the energy spectrum of continuous γ-radiation emitted in the decay of $^{71}_{32}$Ge (internal bremsstrahlung). The results concerning this topic published so far do not satisfactorily agree with one -another nor with the theoretical predictions of MORRISON and SCHIFF [5] and consequently a further analysis of this spectrum was attempted.

Internal bremsstrahlung, when associated with orbital electron capture, is a comparatively improbable process and therefore a rather weak emission of photons takes place. It is very important in this case to make sure that spurious activities due to even very weak radioactive impurities are not present in the sample under investigation. Consequently it seemed worth while to start the measurement with a careful study of γ radiations emitted from the sample: their decay has been watched in order to decide about the importance of possible impurities and in order to carry out, if necessary, a chemical separation. A sample of GeO_2, containing about 5 mC of $^{71}_{32}$Ge was supplied by A.E.R.E. (Harwell) and was first examined by means of a single crystal scintillation spectrometer during a period of four days, beginning one day after the end of the irradiation. In this interval the short-lived activities were already negligible and the γ spectrum associated with the decay of $^{77}_{32}$Ge was predominantly observed. Although the energy resolution of a single crystal spectrometer is not sufficient for drawing definite conclusions about a rather complicated γ spectrum, our results, which are not described here, showed a satisfactory agreement with the results of the above mentioned authors [2,4].

2. – γ-Rays Emitted from $^{77}_{33}$As.

In the past $^{77}_{33}$As was assumed to be a pure β^- emitter and only recently it has been pointed out by several authors that the β spectrum is not a simple one and that in two or three percent of the disintegrations the emission of

---

(3) A. B. SMITH: *Phys. Rev.*, **86**, 98 (1952).
(4) S. B. BURSON, W. C. JORDAN and J. M. LE BLANC: *Phys. Rev.*, **96**, 1555 (1954).
(5) P. MORRISON and L. SCHIFF: *Phys. Rev.*, **58**, 24 (1940).

β-rays having a maximum energy lower than the energy corresponding to the transition between the ground states of $^{77}_{33}$As and $^{77}_{34}$Ge is possible. γ-rays are simultaneously emitted ([6-10]).

The energies of γ lines and the decay schemes which have been proposed by some of the above mentioned authors substantially agree. However some particulars concerning the existence as well as the intensity of a few weak γ lines are still uncertain. An accurate measurement of the energies and of the relative intensities of γ-rays emitted from $^{77}_{33}$As was possible during our investigation of the decay of the irradiated sample of GeO_2; the results are given in Table I. The continuous background due to internal bremsstrahlung of $^{71}_{32}$Ge was not so intense as to distort seriously the shape of the examined γ spectrum and could be easily subtracted. Therefore a chemical separation of $^{77}_{33}$As was not considered necessary for such a purpose. The energy values

TABLE I.

Energy (keV)	Number of unconverted γ-rays (arbitrary units)
86	10.7
161	4.9
243	100
525	30.5

quoted in Table I resulted from a comparison with the γ lines of $^{109}_{48}$Cd (87 keV), $^{203}_{80}$Hg (279 keV), $^{22}_{11}$Na (positron annihilation γ line of 511 keV) and $^{137}_{55}$Cs (662 keV); their accuracy is better than 1%.

The relative intensities of the four lines have been obtained from a measurement of the areas under their photopeaks; the probability of a γ quantum losing its entire energy within the NaI(Tl) crystal (cubic 2.5 cm side) either through photoelectric absorption or after multiple Compton scatterings, has been taken into account. The accuracy of the quoted values is 5% or thereabout.

It was not possible to investigate carefully with the scintillation spectrometer the shape of the spectrum in the energy region less than 30 keV owing

---

([6]) S. A. REYNOLDS, G. W. LEDDICOTTE and H. A. MAHLMAN: *Phys. Rev.*, **91**, 333 (1953).

([7]) M. E. BUNKER, R. J. PRESTWOOD and J. W. STARNER: *Phys. Rev.*, **91**, 1021 (1953).

([8]) F. RASETTI and E. C. BOOTH: *Phys. Rev.*, **91**, 1192 (1953).

([9]) B. L. SARAF, J. VARMA and C. E. MANDEVILLE: *Phys. Rev.*, **91**, 1216 (1953).

([10]) H. LANGEVIN: *Journ. Phys. et Rad.*, **16**, 238 (1954).

to the very intense background due to K X-rays characteristic of Ga. This interval of energies was however examined by means of a proportional counter: evidence was found that no line having an appreciable intensity exists between 20 and 30 keV.

As far as the four observed γ lines are concerned, the agreement with the results of the above mentioned authors is quite good, particularly with LANGEVIN's ([10]), if, as it looks likely from an examination of her results, the numerical values of the relative intensities of the two lines of lowest energy have to be interchanged.

Finally, we tried to find evidence of the line at about 282 keV corresponding to the transition between the levels at 525 keV and 243 keV of $^{77}_{34}$Se. This line was observed, although with a good deal of uncertainty, by BUNKER *et al* ([7]); according to our results its intensity must be less than $4 \cdot 10^{-3}$ of the intensity of the 243 keV line.

3. – Activity Due to the Decay of $^{71}_{32}$Ge.

It is well known that $^{71}_{32}$Ge decays only by orbital electron capture and that the continuous γ radiation which is simultaneously emitted has to be attributed to internal bremsstrahlung. The interest in an analysis of this spectrum lies in the fact that it is possible to deduce from it the energy involved in the decay $^{71}_{32}\mathrm{Ge} \rightarrow {}^{71}_{31}\mathrm{Ga}$ and also to check the validity of the theory of bremsstrahlung from K capture, which was firstly enunciated by MORRISON and SCHIFF ([5]).

In fact it is comparatively simple to investigate a spectrum of internal bremsstrahlung, when the decay of a nucleus is due to electron capture only because there are none of the experimental difficulties which have to be faced when competitive processes (either positron or electron emission) take place also.

A critical review of the theoretical and experimental situation relative to bremsstrahlung processes has been recently published by C. S. WU and the whole work published up to and including 1954 was collected therein ([11]).

Bremsstrahlung in $^{71}_{32}$Ge has been investigated also by SARAF ([9,12]) and by LANGEVIN ([13]).

The upper limit of the energy of γ-rays associated with the orbital electron capture in $^{71}_{32}$Ge has been measured by SARAF ([9,12]) by means of a crystal spectrometer and was found to be 225 ± 12 keV; his most recent results seem however to show a disagreement with the theoretical shape of the spectrum.

([11]) C. S. WU in K. SIEGBAHN: *Beta- and Gamma-ray Spectroscopy* (Amsterdam, 1955), p. 649.

([12]) B. L. SARAF: *Phys. Rev.*, **95**, 97 (1954).

([13]) M. LANGEVIN: *Compt. Rend. Ac. Sci.*, **238**, n. 26, 2518 (1954).

Actually, the theory developed by MORRISON and SCHIFF gives for bremsstrahlung from K-capture, if the transition is allowed, the energy distribution:

$$N(E)\,\mathrm{d}E = C(E)\,\frac{\alpha}{\pi m_0^2 c^4}\,\frac{E}{E_0^2}\,(E_0 - E)^2\,\mathrm{d}E\,, \tag{1}$$

where $N(E)\,\mathrm{d}E$ is the number of photons in the energy interval between E and $E+\mathrm{d}E$

$C(E)$ can be considered as a constant, at least at not-too-low energies;

α is the fine structure constant;

m_0 is the mass of the electron;

c is the velocity of light;

E_0 is the upper limit of the photon energy.

It is to be expected that for $^{71}_{32}$Ge (allowed transition, according to nuclear shell model) the spectrum given by (1) is valid and therefore it should be possible to derive a linearized plot according to the formula

$$\left[\frac{N(E)}{C(E)E}\right]^{\frac{1}{2}} = K(E_0 - E)\,, \tag{2}$$

where K is a constant.

According to the results given by SARAF, this seems to be possible only for energies higher than about 100 keV, while at lower energies a remarkable excess of the number of photons is evident.

A further study of this spectrum was carried out by LANGEVIN ([13]), whose results agreed with those obtained by SARAF as long as a recently irradiated sample was used, and showed moreover that the theory is verified also at lower energies ($\sim$ 50 keV). A remarkable distortion in the linearized plot was however observed when the measurements were repeated about one month later. These results were interpreted as due to the presence of a second bremsstrahlung spectrum, whose upper limit of energy should be about 160 keV; this activity was supposed to be due to an isomeric state of $^{71}_{32}$Ge, the half life of which should be considerably longer than 12 days.

A measurement of the spectrum of internal bremsstrahlung was made by us firstly after the γ activity due to the transition $^{77}_{33}\mathrm{As} \rightarrow {}^{77}_{34}\mathrm{Se}$ had become completely negligible (about fifteen days after the irradiation of GeO_2) and without making any preliminary chemical separation.

Eq. (1) was found to be valid down to rather low energies ($\sim$ 50 keV), in satisfactory agreement with the previous results of SARAF *et al.* ([9]) and of LANGEVIN ([13]). Later on an excess in the number of photons was noticed at low ($\lesssim$ 100 keV) and high ($\gtrsim$ 200 keV) energies, but this circumstance is

considered to be due to some weak impurities within the source. Actually after a chemical separation it was possible to find the previous shape of the linearized plot again.

The decay of the source was then followed for about three half lives and in this period no evidence was found of the second transition due to electron capture observed by LANGEVIN. Only when the source became very weak, the influence of the same previously separated impurity was noticed, but it was felt that a further purification would not be useful, because a sufficiently reliable evidence had been had that the transition $^{71}_{32}\mathrm{Ge} \rightarrow {}^{71}_{31}\mathrm{Ga}$ was a simple one and did not involve the presence of a complex spectrum (*).

Experimental results are discussed in the following sections.

4. – Experimental Results.

4·1. *Half life.* – The half life of $^{71}_{32}\mathrm{Ge}$ has been measured following the time decrease of the intensity of K X-rays emitted from a source which had been located within a proportional counter. The decay curve is shown in Fig. 1 and hence a half life of 12.5 ± 0.1 days can be deduced.

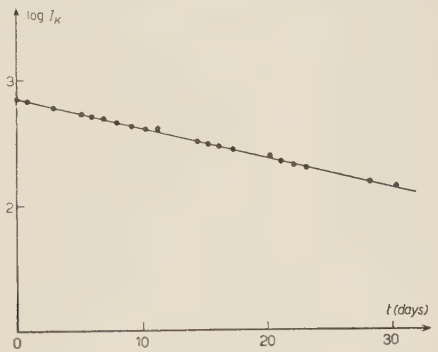

Fig. 1. – Time dependence of the intensity of K X-rays from the transition $^{71}_{32}\mathrm{Ge} \rightarrow {}^{71}_{31}\mathrm{Ga}$.

4·2. *The Spectrum of Internal Bremsstrahlung.* – The continuous γ spectrum emitted from $^{71}_{32}\mathrm{Ge}$ has been studied by means of a single crystal spectrometer. The NaI(Tl) crystal, cubic in shape (2.5 cm side) was optically coupled to the photocathode of a Du Mont 6292 photomultiplier. The side of the crystal facing the source was covered with an Al reflector and with a mica window, the thickness being 9 mg cm^{-2}.

The γ source was located on the crystal itself and was shielded with a suitable Al layer in order to absorb most of the 9.2 keV K X-rays. Several measurements have been carried out with Al layers the thicknesses of which ranged between 30 and 100 mg cm^{-2}. The dependence of the shape of the spectrum upon the diameter and the thickness of the source has been investigated making

(*) No serious attempt has been made to identify the spurious, long lived activity of which was showed evidence during our measurements; a study of the emitted γ, spectrum suggests that it is $^{75}_{34}\mathrm{Se}$.

use of sources 10 mg cm^{-2} and 70 mg cm^{-2} thick with diameters between 2 and 10 mm.

Within the limits of the previously indicated dimensions, the continuous γ spectrum showed always the same intensity distribution. We suppose that such a distribution is the true one, at least for energies higher than 100 keV, if we leave some not very important corrections out. These corrections will be discussed later.

The pulses given by the scintillation spectrometer were amplified by means of a conventional chain and analyzed with a 20 channel fast pulse analyzer ([14]). The width of the channels has been set to equal 2 volts: this width is, in the range of investigated energies, three or four times less than the width of a monochromatic γ line.

The above described scintillation spectrometer shows, in the energy range covered by the bremsstrahlung spectrum, a rather intense continuous background due to cosmic radiation. A pronounced peak can be readily noticed at about 90 keV. When the spectrometer had been shielded with about 2.5 cm of Pb the cosmic background was reduced to a tenth within the investigated range of energy.

The sources of $^{71}_{32}$Ge were chemically separated and purified as K_2GeF_6 according to the method described by BRAUER ([15]). β and γ activity due to $^{40}_{19}$K was completely negligible.

4·3. *Corrections to the Spectra.* – The experimental intensity distributions of the bremsstrahlung spectrum were corrected as follows to take into account the causes of distortion:

a) Cosmic background was subtracted.

b) The finite resolution of the spectrometer: according to a formula given by PALMER and LASLETT ([16,17]) the corrected spectrum $N_T(E)$ is given by

$$N_T E = N_e(E) - KN'_e(E) - \tfrac{1}{2}KEN''_e(E) ,$$

where $N_e(E)$, $N'_e(E)$, $N''_e(E)$ are respectively the intensity of the observed spectrum, its first and its second derivative.

([14]) E. GATTI: *Nuovo Cimento*, **11**, 153 (1954).

([15]) G. BRAUER: *Handbuch der präparativen anorganischen Chemie* (Stuttgart-1954), p. 544.

([16]) J. P. PALMER and L. J. LASLETT: *A.E.C.U.*, 1220 (March 14, 1951).

([17]) T. B. NOVEY: *Phys. Rev.*, **89**, 672 (1953).

K is given by:

$$K = \frac{W^2(E)}{0.693 \cdot 2E}$$

where $W(E)$ is the half width of a monochromatic line corresponding to photons having energy E.

The half widths $W(E)$ have been measured in the same experimental conditions which were adopted to study the bremsstrahlung spectrum. The γ lines used for deriving the function $W(E)$ are listed in Table II.

TABLE II.

Isotope	γ-ray energy (keV)
$^{137}_{55}Cs$	662
$^{22}_{11}Na$	511
$^{203}_{80}Hg$	279
$^{195}_{79}Au$	97
$^{109}_{48}Cd$	87
$^{210}_{82}Pb$ (RaD)	46.7

c) The correction for the efficiency of the crystal, rather unimportant except for higher energies, was made using the graphs given by BELL ([18]). The contribution of Compton distribution of detected photons has been neglected: this is certainly a good approximation for low energies and for a crystal with 2.5 cm side because the intensity of the spectrum falls rapidly to zero at the upper limit of energy and the most probable energy is about 75 keV.

d) The absorption of γ-rays within the Al absorbers interposed between the source and the detector and the self-absorption within the source itself have been calculated making use of the absorption coefficients given by VICTOREEN ([19]). This calculation has been checked measuring the intensity attenuation undergone by some γ lines of low energy ($E < 100$ MeV) in the absorbers. The agreement between the calculated and measured attenuation is quite satisfactory.

e) The escape probability of K X-rays of iodine from the crystal has been taken into account making use of the data reported by BELL ([18]).

([18]) P. R. BELL in K. SIEGBAHN: *Beta- and Gamma-Ray Spectroscopy* (Amsterdam, 1955), p. 133.

([19]) J. A. VICTOREEN: *Journ. Appl. Phys.*, **20**, 1141 (1949).

4·4. *Energy Associated to the Transition.* – The spectrum of internal bremsstrahlung in $^{71}_{32}$Ge is given in Fig. 2 and hence the deduced linearized plot is

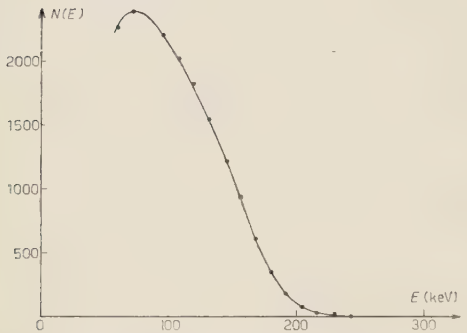

Fig. 2. - Spectrum of internal bremsstrahlung γ-rays associated with the decay of $^{71}_{32}$Ge.

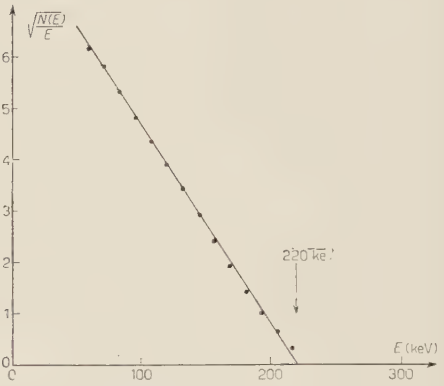

Fig. 3. - $^{71}_{32}$Ge linearized plot of continuous γ spectrum.

shown in Fig. 3. The upper limit energy was found to be:

$$E_{\max} = 220 \pm 3 \text{ keV} .$$

Consequently, if the binding energy of K-electron is added, we obtain for the energy associated to the transition $^{71}_{32}\text{Ge} \rightarrow {}^{71}_{31}\text{Ga}$ (difference between atomic masses):

$$E_0 = 231 \pm 3 \text{ keV} .$$

4·5. *Emission Probability of a Bremsstrahlung Photon.* – The probability of the emission of a bremsstrahlung photon has been obtained measuring by means of the scintillation spectrometer the ratio between the intensity of the continuous γ spectrum (N_γ) and the intensity of Ga K X-rays (I_K). For this purpose the intensity of the K X-line has been measured with several Al absorbers interposed between the source and the crystal. The area under the peak, plotted as a function of the thickness of Al, has been extrapolated to zero thickness and then corrected for self-absorption. As a test of the obtained value the measurement has been repeated with a known fraction of the same source. The agreement between the two obtained values was satisfactory.

As far as the portion of the continuous γ spectrum between 70 keV and the upper limit is concerned, and after correction for K fluorescence yield of

Ga ($\omega_K = 0.51$) ([20]), we found that

$$\frac{N_\gamma}{N_K} = (2.3 \pm 0.5) \cdot 10^{-5}$$

where $N_K = I_K/\omega_K$.

The value which can be calculated according to the theory of MORRISON and SCHIFF ([5]) is:

$$\left(\frac{N_\gamma}{N_K}\right)_{\text{th}} = 2.5 \cdot 10^{-5} .$$

5. – Discussion.

From the above mentioned ([1,12,13]) measurements, and from ours, it can be inferred that the transition ${}^{71}_{32}\text{Ge} \rightarrow {}^{71}_{31}\text{Ga}$ takes place between the ground states of both nuclei. Spin and magnetic moment of ${}^{71}_{31}\text{Ga}$ have been measured ([21]), and its ground state orbital was found to be $p_{\frac{3}{2}}$. According to the nuclear shell model the ground state orbital of ${}^{71}_{32}\text{Ge}$ is $p_{\frac{1}{2}}$. Consequently the considered transition may be classified as an allowed one ($\Delta I = 0, 1$; no). According to sistematics discussed by MAYER, MOSZKOWSKI and NORDHEIM ([22]) for odd A nuclei, $\log ft < 6$. If the values here measured for transition energy and half life are used, and omitting L capture we get:

$$\log ft = 4.3 .$$

It can therefore be concluded that only s-electrons are important in the orbital electron capture in ${}^{71}_{32}\text{Ge}$. The ratio between the probability of L_{I}-capture and the probability of K-capture can be easily calculated ([23,24]) and we obtain:

$$\frac{P_{L_{\text{I}}}}{P_K} = 0.10 .$$

Consequently, in a first order approximation at least, the emission of bremsstrahlung photons is associated with K-capture processes only, and in this case a test of the shape of bremsstrahlung spectrum, as it can be calculated

([20]) I. BERGSTRÖM, in K. SIEGBAHN: *Beta- and Gamma-Ray Spectroscopy* (Amsterdam, 1955), p. 624.

([21]) J. E. MACK: *Rev. Mod. Phys.*, **22**, 64 (1950).

([22]) M. GOEPPERT-MAYER, S. A. MOSZKOWSKI and L. W. NORDHEIM: *Rev. Mod. Phys.*, **23**, 315 (1951).

([23]) E. R. MARSHAK: *Phys. Rev.*, **61**, 431 (1942).

([24]) M. E. ROSE and J. L. JACKSON: *Phys. Rev.*, **76**, 1540 (1949).

([25]) M. LANGEVIN: *Compt. Rend. Acad. Sci.*, **239**, n. 23, 1625 (1954).

according the theory developped by MORRISON and SCHIFF under the hypothesis of a K-capture process and of an allowed transition, is particularly expressive.

Our measurements suggest that for internal bremsstrahlung from $^{71}_{32}$Ge the intensity distribution in the energy range between 50 keV and the upper limit is in close agreement with the theoretical one.

We wish finally to point out that the ratio between the probability of L-capture and the probability of K-capture in $^{71}_{32}$Ge has been recently measured by LANGEVIN ([25]) and that the obtained value ($P_L/P_K = 0.30 \pm 0.02$) does not agree with the theoretical expectations. This value however depends rather critically upon the assumed value of K-shell fluorescence yield of Ga. With the most recent values of fluorescence yields which have been discussed by BERGSTRÖM ([20]) the result obtained by LANGEVIN may be corrected into $P_L/P_K = 0.18$. It seems consequently reasonable to suppose that such a disagreement cannot be attributed to serious shortcoming of the actual theories.

* * *

We wish to express our thanks to Prof. G. BOLLA for his interest in the present work.

RIASSUNTO

Con uno spettrometro a scintillazione si è studiato lo spettro γ continuo, dovuto alla bremsstrahlung interna, che accompagna la cattura elettronica orbitale del $^{71}_{32}$Ge. È stato trovato che la distribuzione d'intensità di tale spettro è in buon accordo con quella calcolata in base alla teoria di Morrison e Schiff per energie comprese tra circa 50 keV e il limite superiore ($E_{max} = 220 \pm 3$ keV). La probabilità di emissione di un quanto di bremsstrahlung, relativamente all'intervallo di energia dello spettro continuo compreso tra 70 keV e l'energia massima, è risultato essere $N_\gamma/N_K = (2.3 \pm 0.5) \cdot 10^{-5}$ che è pure in buon accordo con quella prevista. Il periodo di dimezzamento del $^{71}_{32}$Ge è stato trovato uguale a 12.5 ± 0.1 giorni. La natura della transizione $^{71}_{32}\text{Ge} \rightarrow {}^{71}_{31}\text{Ga}$ è brevemente discussa in base al modello nucleare a shell. Alcuni dati relativi al decadimento $^{77}_{32}\text{As} \rightarrow {}^{77}_{34}\text{Se}$, ricavati nel corso della presente misura, vengono riportati.

On the Measurement of Ionization in Nuclear Plates.

C. Castagnoli G. Cortini and A. Manfredini

Istituto di Fisica dell'Università - Roma
Istituto Nazionale di Fisica Nucleare - Sezione di Roma

(ricevuto il 4 Giugno 1955)

Summary. — Using an apparatus previously described, measurements of the number of gaps $\bar{n}$, total length of gaps $\bar{x}$, mean gap length $\bar{w} = \bar{x}/\bar{n}$, and number of « long » gaps $\bar{n}_\varepsilon$, were made on a large number of tracks. Proton, π-meson and μ-meson tracks coming to rest in the stack of pellicles (the no. 29 stack of Sardinian Expedition 1953) were employed. A rather large velocity interval has been investigated ($0 < v/c < 0.80$). Our experimental results have been compared with the different theories which have been proposed to describe the formation of tracks of ionizing particles in nuclear emulsions. The problem of choosing the parameter which must be measured in the different velocity intervals in order to obtain the best value of the mass is discussed. It turns out that the best parameters are: in the near minimum region $\bar{w}$, and in the « clogged » region $\bar{x}$.

1. – Introduction.

The idea of measuring ionization by the « grain density » g, where

(1) $g =$ number of developed grains per unit length of track,

in order to determine the velocity v of ionizing particles (of charge $Z = 1$), is as old as the nuclear emulsion technique. In the last few years, several authors have investigated this type of measurement.

In order to get the most precise and reliable value of v it was proposed that (besides or instead of g) a number of different variables should be measured:

(2) $\bar{n}$ = blob density ([1-5]) = number of blobs per unit lenght = n_0 = = number of gaps per unit length ([6-8]).

(3) $\bar{n}_\varepsilon$ = « long » gap density, a « long » gap being one whose length is $> \varepsilon$ ([9,10]).

(4) $\bar{x}_\varepsilon$ = total length of « long » gaps per unit length of track. In the following we shall put $\bar{x}_0 = \bar{x}\,(\varepsilon = 0) = \bar{x}$ ([11-15]).

(5) $\bar{w}_\varepsilon = \bar{x}_\varepsilon/\bar{n}_\varepsilon$ = mean length of the « long » gaps. Also, we put for $\varepsilon = 0$, $\bar{w}_0 = \bar{w}$ ([7,16,17]). $\bar{w}$ is the variable officially recommended by the Padna Conference, 1954 ([18]).

For tracks ending in the emulsion also the integrals of the variables (1), (3) and (4), with respect to the residual range R

$$(1') \qquad G = \int_0^R g\,\mathrm{d}R\,; \qquad (3') \quad N_\varepsilon = \int_0^R n_\varepsilon\,\mathrm{d}R\,; \qquad (4') \quad X_\varepsilon = \int_0^R x_\varepsilon\,\mathrm{d}R$$

were considered. Variable (1), while abandoned by most workers, is still being investigated by some authors ([8,19,20]).

([1]) L. Voyvodic: *Conf. Bristol*, 1951, p. 16.
([2]) A. H. Morrish: *Phil. Mag.*, **43**, 533 (1952).
([3]) A. H. Morrish: *Phys. Rev.*, **91**, 423 (1953).
([4]) R. R. Daniel and D. H. Perkins: *Proc. Roy. Soc.*, A **221**, 351 (1954); see also *Congr. Bagnères*, 1953, p. 159.
([5]) M. G. K. Menon and C. O'Ceallaigh: *Proc. Roy. Soc.*, A **221**, 292 (1954).
([6]) G. Kayas: *Compt. Rend.*, **238**, 2153 (1954).
([7]) G. Kayas: *Journ. Phys. et Rad.*, **15**, 34 (1954); *Suppl. Nuovo Cimento*, **1**, 200 (1955).
([8]) A. Orkin-Lecourtois, G. Kayas and T. F. Hoang: *Suppl. Nuovo Cimento*, **12**, 398 (1954).
([9]) P. H. Fowler and D. H. Perkins: *Suppl. Nuovo Cimento*, **12**, 236 (1954).
([10]) R. M. Tennant: *Ph. D. Thesis, London University*, 1953.
([11]) P. E. Hodgson: *Phil. Mag.*, **41**, 725 (1950).
([12]) G. Belliboni and M. Merlin: *Nuovo Cimento*, **8**, 349 (1951).
([13]) C. O'Ceallaigh: *Phil. Mag.*, **42**, 1032 (1951).
([14]) M. Renardier, H. Moucharafieh and M. Morand: *Compt. Rend.*, **231**, 848, (1950).
([15]) D. M. Ritson: *Phys. Rev.*, **91**, 1572 (1953).
([16]) C. O'Ceallaigh: *Conf. Bagnères*, 1953, p. 73.
([17]) C. O'Ceallaigh: *CERN Secr. St. Meas.*, no. 11 (1954); see also: R. H. W. Johnston and C. O'Ceallaigh: *Phil. Mag.*, **45**, 424 (1954); *Nuovo Cimento*, **1**, 468 (1955).
([18]) Ambrosen *et al.*: *Suppl. Nuovo Cimento*, **11**, 228 (1954).
([19]) L. Jaunean and F. Hug-Bousser: *Journ. Phys. et Rad.*, **13**, 465 (1952).
([20]) T. F. Hoang: *Compt. Rend.*, **238**, 1790 (1954); *Suppl Nuovo Cimento*, **1**, 186 (1955).

Considerable work has also been done on the problem of the formation of tracks in nuclear emulsions. This process can be separated into two quite distinct steps.

1) *The first step* takes place when the particle traverses the emulsion and leads to the formation of a latent image in a number of AgBr crystals. The mean number of affected crystals along the trajectory is determined by the ionizing power of the particle. Here several factors are involved, such as the knock-on electrons, the Čerenkov radiation, the finite dimensions of the AgBr crystals, the mechanism of latent image formation (see for instance GOLDSCHMIDT-CLERMONT [21]) and the quoted bibliography), the strength of the developing agents and so on.

2) *The second step* takes place during the processing. The developable crystals grow (essentially by physical development) and some of them coalesce to form developed grains or blobs. The factors involved here are: the diameter of the developed grains, and the arrangement of crystals and of grains along the track. These factors are important from the point of view of the practical use of emulsions because the coalescence of grains determines the well known underfluctuations [4,22] of ionization measurements in emulsions. Thus in order to get well founded estimates of statistical errors in these measurements, it is first necessary to have a satisfactory picture of this second step. In fact, a recent paper by BLATT [23] which gives a very powerful and general mathematical treatment of this problem, shows that the fluctuations depend on the ionization (as has already been found experimentally [4]), and are different for the different models used to represent a particle track. Several such models have been recently suggested [17,24-27].

The aim of the present work is:

1) To investigate the validity of these different models, particularly of two of them [17,26] which have extreme characteristics, are rather simple, yield easily workable formulas, and give definitely different results.

2) To study the behaviour of variables (1) to (4) in a range of velocity as large as possible and to decide on the best variable to be employed in practice in the different v intervals.

[21] Y. GOLDSCHMIDT-CLERMONT: *Ann. Rev. Nucl. Sci.*, **3**, 141 (1953).
[22] P. E. HODGSON: *Brit. Journ. Appl. Phys.*, **3**, 11 (1952).
[23] J. M. BLATT: Private communication, 1954.
[24] M. DELLA CORTE, M. RAMAT and L. RONCHI jr.: *Nuovo Cimento*, **10**, 509 (1953).
[25] M. DELLA CORTE, M. RAMAT and L. RONCHI jr.: *Nuovo Cimento*, **10**, 958 (1953).
[26] A. J. HERZ and G. DAVIS: Private communication, 1954.
[27] W. W. HAPP, T. E. HULL and A. H. MORRISH: *Canad. Journ. Phys.*, **30**, 699 (1952).

It is to be remarked that the photometric methods, on which much valuable work has been done in the last few years, are not discussed in this paper. We also do not consider the apparatus recently proposed by BONETTI *et al.* [28] which is intended to obtain the maximum possible information from the tracks but requires an effort that is probably only worthwhile for very important tracks.

2. – Experimental results.

The measurement of the quantities (1) to (4) requires considerable work. A number of papers have recently been published [15,17,29 33] in which an experimental device was proposed to make the measurements simpler and faster. Among them we use systematically the one suggested by RITSON [15] and improved in this laboratory [30]. The Ritson apparatus gives only the value of $n = n_0$ while the Rome method enables one to get the values of $n = n_0$, r_0 (and therefore w_0) and n_ε (for a given value of ε) simultaneously, at a rate of 2.4 mm of track per hour.

Thanks to this method it was possible to make a systematic and extensive investigation (otherwise very difficult) on the behaviour of all these different variables in a rather large interval of v ($0 < v/c < 0.80$, that is $0 < T < \sim 600$ MeV for protons). It is to be noted that with the method described we explored some « new » v-intervals: for instance, the behaviour of w in the near-minimum range had never been investigated, previously. Some 100 tracks were measured, for a total number of 1775 cells.

The results of the measurements are shown in Fig. 1, where $\bar{n}$, $\bar{n}_\varepsilon$ (for $\varepsilon = 0.7$ μm), $\bar{x}$ and $\bar{w}$ values are plotted against the variable $r = R/M$, expressed in microns/electron mass.

The following types of tracks were used to obtain the experimental points of Fig. 1:

a) For $r < 30$ μm/m_e: proton, π^+-meson and μ-meson tracks ending in the emulsion and suffering decay at rest. Any point in this region is the mean of the measurements done on several meson or proton-tracks. 200 μm is the fixed value of the cell-length employed [30].

b) For $r > 30$ μm/m_e: π^+-tracks ending in the emulsion and π^--tracks ending in the emulsion and associated with stars. Each point is obtained *from*

[28] A. BONETTI, C. C. DILWORTH, M. LADU and G. OCCHIALINI: *Atti Acc. Naz. Lincei*, **17**, 311 (1954).
[29] M. DELLA CORTE: *Nuovo Cimento*, **12**, 28 (1954).
[30] G. BARONI and C. CASTAGNOLI: *Suppl. Nuovo Cimento*, **12**, 364 (1954).
[31] J. E. HOOPER and M. SCHARFF: *CERN Secr. St. Meas.*, no. 12 (1954).
[32] M. RENARDIER and Y. AVIGNON: *Compt. Rend.*, **233**, 393 (1951).
[33] H. M. MAYER, *CERN Secr. St. Meas.*, no. 20 (1955).

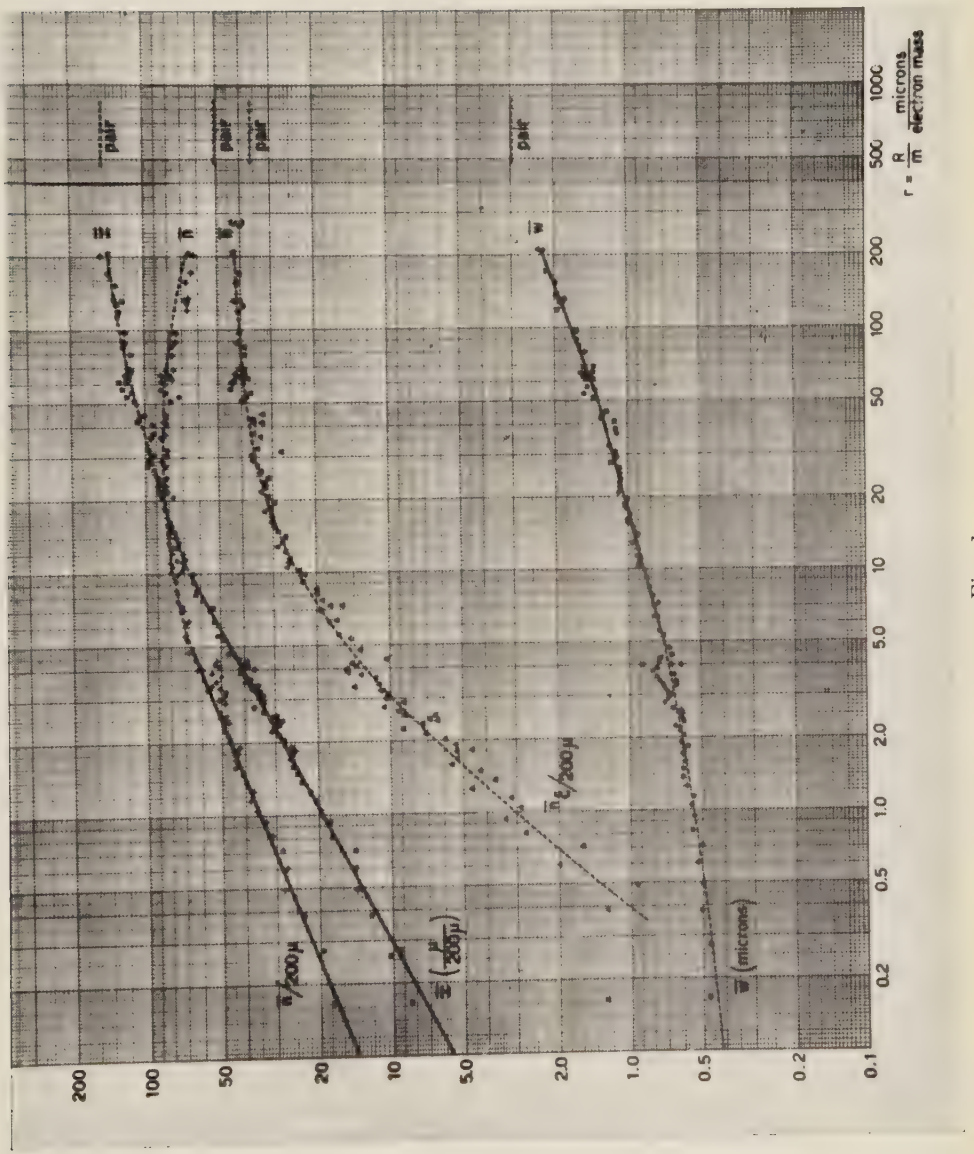
pair
pair
pair
pair
$\bar{n}/200\mu$
$\bar{n}\,\epsilon/200\mu$
$\bar{w}$ (microns)
200
100
50
20
10
5.0
2.0
1.0
0.5
0.2
0.1
0.2
0.5
1.0
2.0
5.0
10
20
50
100
200
500
1000
$r = \frac{R}{m}\ \frac{\text{microns}}{\text{electron mass}}$

Fig. 1.

a single track, and precisely from a number δ of 200 μm-cells, so chosen that the corresponding $\Delta R = 200 \cdot \delta$ μm was not larger than the straggling, while the total blob number was greater than 300.

All tracks were taken from a single 40 plate stack from the 1953 Sardinian Expedition ([34]) that is from a volume of 360 cm³. The processing of the stack was done in this laboratory. Only a few microns of thickness near the surface were discarded from each plate. The dip angle of the tracks employed was $< \sim 10^{\circ}$.

A number of grain density measurements on « thin » tracks ($g < 4\ g_{\text{plateau}}$) was also done by the conventional grain counting method. The results are shown in Fig. 2*a*, in comparison (Fig. 2*b*) with results of $\overline{w}$ measurements performed *on the same tracks*.

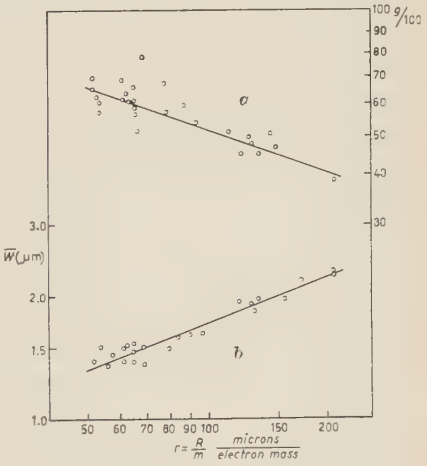

Fig. 2.

Finally a number of tracks associated with energetic pairs or tridents were measured (for a total number of 186 cells), in order to obtain « plateau » values for each one of the considered variables. These values are indicated in Fig. 1 by horizontal dotted lines.

3. – Comparison with two different models of nuclear tracks.

The two considered models can be summarized as follows.

The « C » model. – This model, proposed by O'Ceallaigh ([17]), corresponds to a particular case of the model worked out by Happ *et al.* ([27]). Its basic assumption is that the centres of the AgBr crystals along the track are randomly distributed. The frequency distribution function of gap lengths is then exponential ($\sim \exp[-\Lambda w]$): this point has been tested by the Author in a direct experiment, performed on *near minimum tracks*. The ionizing power of the particle determines, through rather complex phenomena (see introduction) the mean gap length:

$$\overline{w} = \frac{\int_0^\infty \exp[-\Lambda w] w \, dw}{\int_0^\infty \exp[-\Lambda w] \, dw} = \frac{1}{\Lambda}; \qquad \overline{w}_\varepsilon = \frac{1}{\Lambda} + \varepsilon . \tag{6}$$

([34]) J. Davies and C. Franzinetti: *Suppl. Nuovo Cimento*, **12**, 480 (1954).

Under these assumptions one gets [23]:

$$\bar{n}_\varepsilon = A(t - 2\gamma - \varepsilon) \exp\left[-A(2\gamma + \varepsilon)\right], \tag{7}$$

where γ is the (constant) radius of developed grains, and t is the cell length. An important feature of this model is that $\bar{w}$ is independent of γ, that is, on the degree of development. That is why the Author suggests a systematic use of this parameter as a measure of the ionization.

The « H.D. » model. – This model, suggested by HERZ and DAVIS [26], is an extension of the model previously proposed by other authors [24,25,29]. Its basic idea is that since the AgBr crystals occupy a considerable fraction of the total volume of the emulsion their centres cannot be in any way considered as randomly distributed. To take into account the « graininess » of the emulsion, the H.D. model takes the most radical point of view, as follows. A track can be considered as a juxtaposition of equal segments (of length β). Each of these contains an AgBr crystal. The ionizing power of the particle determines the probability p that an AgBr becomes developable.

During the processing the developable crystals, through physical development, grow to a fixed diameter 2γ. The degree of coalescence is determined by the largest integer Γ less than $2\gamma/\beta$.

One gets easily [23,26]

$$\bar{w}_\varepsilon = \beta\left(\Gamma + \frac{1}{p}\right) - (2\gamma + \varepsilon), \tag{6'}$$

$$\bar{n}_\varepsilon = p(1-p)^\Gamma \frac{t}{\beta}. \tag{7'}$$

The formulae are correct in the limiting case $t \gg 2\gamma$. Under this condition (which is well satisfied in our measurements: $t = 200$ μm) in both models we have

$$\bar{x}_\varepsilon = \bar{w}_\varepsilon \cdot \bar{n}_\varepsilon. \tag{8}$$

In the limiting case $\bar{w} \gg \beta$, $p \ll 1$, that is for near minimum tracks, the H.D. model becomes identical with the « C » model [23], the mathematical condition to get the same formulae being the validity of the approximation $\log(1-p) = -p$. So, *for near minimum tracks*, we can in any case accept O'CEALLAIGH's statement, according to which *w does not depend on the processing.*

In order to make a comparison with experimental results it is necessary to fix the values of the emulsion-dependent parameters in the two models, that is:

γ for the C-model,

γ and β for the H.D.-model.

The radius γ of the developed grains can be directly measured ([27]). Obviously it depends on the processing. From rather rough measurements we get, for our stack:

$$0.70 \leqslant 2\gamma \leqslant 0.78 \ \mu\text{m} . \tag{9}$$

The characteristic length β of the H.D.-model is more difficult to define. Perhaps the most reasonable estimate of it is the reciprocal number of the AgBr crystals crossed by a straight line of length 1. Then, if d is the mean diameter of the AgBr crystals, it would be ([35,36]):

$$\beta = \frac{1}{0.455} \cdot \frac{2}{3} d = 1.466 d , \tag{10}$$

where 0.455 is the fraction occupied by AgBr crystals in the volume of the emulsion. In any case some uncertainty remains about this purely geometrical method of getting β, as well as about the value of d, which seems to be between 0.2 and 0.3 μm ([37,38]).

However, the β-value to be inserted in the formulae is easily determined starting from the H.D.-model, as follows. Formula (7′) gives $\bar{u}/t$ as a function only of β, p and Γ. For any reasonable value of Γ ($\Gamma = 1, 2, 3$) the maximum value that $\bar{n}\, t$ can attain when p varies in the interval (0. 1) is easily calculated, and the parameter must be adjusted so as to give the experimental maximum value of $\bar{n}/t$, that is (see Fig. 1) $85/200 = 0.425$ gap/micron.

We get in this way the β values listed in Table I and, by means of (10), the corresponding d values. The 4th and 5th rows of Table I indicate the corresponding limiting values of 2γ, as deduced from the meaning of Γ.

Once β is fixed, it is easy from (6′) and (7′) to calculate corresponding pairs of values of $\bar{w}$ and $\bar{n}$ (two independent parameters), and to compare

TABLE I. – (All length in microns).

$\Gamma =$	1	2	3
$\beta =$	0.59	0.35	0.25
$d =$	0.40	0.24	0.17
$2\gamma <$	1.18	1.05	1.00
$2\gamma >$	0.59	0.70	0.75
$2\gamma =$	0.70	0.70	0.75

([35]) A. ZHDANOV: *Journ. Phys. et Rad.*, **6**, 233 (1935).
([36]) L. M. BROWN: *Phys. Rev.*, **90**, 95 (1953).
([37]) G. BARONI and C. CASTAGNOLI: *Nuovo Cimento*, **7**, 364 (1950).
([38]) E. PICKUP: *Canad. Journ. Phys.*, **31**, 898 (1953).

them with experimental pairs deduced from Fig. 1. The result is shown in Fig. 3; 2γ has been adjusted for any value of Γ so as to obtain the best fit (see the last row of Table I). It is seen that the H.D. model gives satisfactory

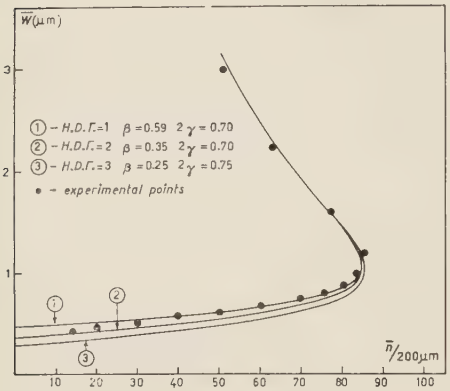

Fig. 3.

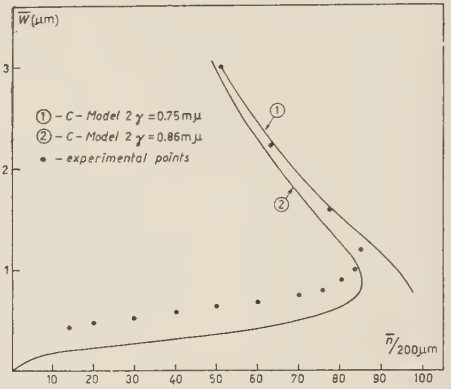

Fig. 4.

agreement with experiment, with 2γ values agreeing with (9) and (particularly for $\Gamma = 2$) a reasonable value of β.

The same comparison can be made for the C-model (Fig. 4). Grain radius γ has been adjusted so as to obtain, in one case the best fit for minimum tracks, and in the other case the right value for the maximum of $\bar{n}$. Both curves give rather good agreement with experiment in the near minimum region, where the C-model *coincides* with the H.D.-model, and where it was directly tested by the Author. On the contrary we have a definite discrepancy in the high ionization region. Besides, the 2γ value used in the curve 2, Fig. 4, is too high, and it does not fit eq. (9).

So, we are induced to discard the C-model, and to look for other means of testing the H.D.-model. The comparison between exprimental points and H.D. curves, in Fig. 3 allows one to state a relation between $r = R/M$ and the probability p. Thus we can plot the curves of $\bar{n}$, $\bar{w}$ and $\bar{n}_\varepsilon$ deduced from (6′), (7′), versus p, and compare the experimental points with these curves. We see from Fig. 5 and 6 that the H.D.-model gives a rather satisfactory account also of our n_ε points, if $\Gamma = 1$ or 2.

In conclusion, we can consider the H.D.-model—though very rough—as having satisfied the above control, and accept it provisionally. Therefore we must calculate the standard fluctuations from the formulae derived by BLATT [39] for the H.D.-model. The more reliable values of the integer Γ to be inserted in the formulae are 1 and 2. The corresponding values of β and 2γ are listed in Table I and in Figures 2 and 3.

Of course, the model must be further tested, for instance, by measuring n_ε for a number of values of ε, or by testing the fluctuation formulae. While

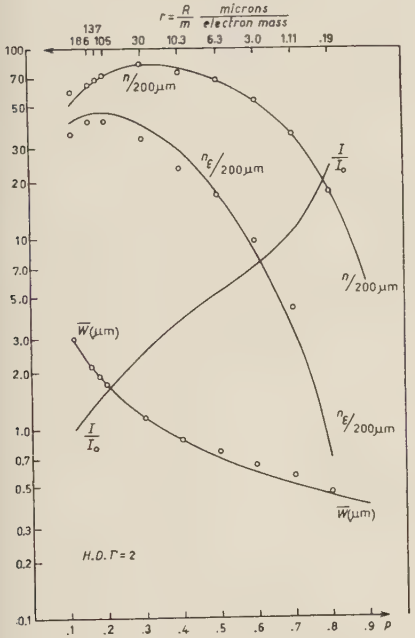

Fig. 5.

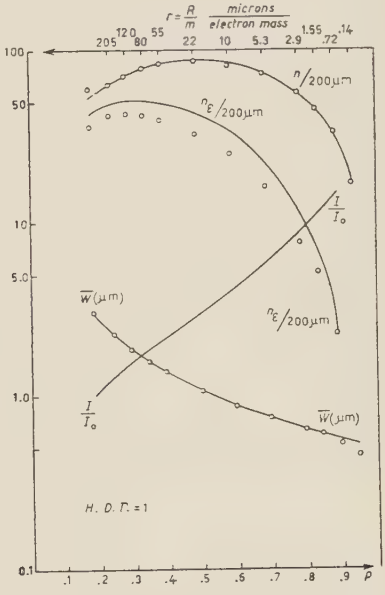

Fig. 6.

the first method is a powerful one in order to determine the value of Γ, the second method is not very useful in this respect.

Indeed, if

$$\sigma_n = \frac{\mu_n}{\sqrt{N}}\,\bar{n} \tag{11}$$

is the standard fluctuation of $\bar{n}$ for N counted gaps, the Blatt formula for the factor μ_n can be put in the form [39]

$$\mu_n^2 = \left[1 - (2\Gamma + 1)\frac{\beta}{t}\,\bar{n}\right],$$

and, for every pair of Γ and β values of Table I, we get

$$\mu_n \sim \sqrt{1 - 1.75\bar{n}/t}\,. \tag{12}$$

[39] Ref. [23]. See also G. LOVERA: *Nuovo Cimento*, **12**, 154 (1954).

For « plateau » tracks, we have (Fig. 1) $\bar{n}= 50$ for $t = 200$, so that

$$\mu_n = 0.75 , \tag{12'}$$

while in the maximum region, $\bar{n} = 85$, we have

$$\mu_n \cong 0.50 . \tag{12''}$$

It is to be noted that for a good test of fluctuation formulae, measurements on much shorter cells than those employed in this experiment should be made.

Finally it is perhaps worthwhile to remark that, if a reliable value of β could be determined, the knowledge of the probability p for a traversed crystal to be affected as a function of the ionizing power (Figs. 5 and 6) could be a good starting point of new investigations on the mechanism of the latent image formation in nuclear emulsions.

4. – Best parameters to use in mass measurements.

First we want to point out that among the functions of the velocity, the variable $r = R/M$ (used as abscissa in Fig. 1) is very convenient to use for tracks ending in the emulsion. R is a quantity easily and precisely measured, so that M, the interesting physical quantity, can be determined from r:

$$M = \frac{R}{r} \tag{13}$$

in a straighforward way, without using any theoretical or empirical relation involving other variables.

Also, if a track goes out of the emulsion but the grain density changes appreciably along it, one can measure the variation Δr of r, and ΔR of R, and get the mass from

$$M = \frac{\Delta R}{\Delta r} .$$ [40]

In the first case, neglecting the error in the measurement of R, the error of M can be derived by eq. (13) as:

$$\frac{\sigma_M}{M} = \frac{\sigma_r}{r} = \sigma(\log r) .$$

[40] An example of how this can be applied if a number of measurements of r is available, will soon be given elsewhere (C. CASTAGNOLI, G. CORTINI and A, MANFREDINI: K–*meson and hyperon events, Nuovo Cimento,* in press).

Therefore the « sensitivity » of the parameters (1) to (4), is well evaluated by the slope of the corresponding curves, if their logarithms are plotted against $\log r$, as in Fig. 1. Then, a significant factor in selecting the best variables will be:

1) *The ratio of this slope to the relative standard fluctuation* of the variable considered (for a given length of measured track). Other significant elements will be:

2) *Objectivity* (small dependence on the observer), and

3) *Small dependence on the degree of development.*

Another very important factor would be the rapidity of measurements, but as our apparatus gives *all the variables* (excepted g) at the same time, this factor becomes unimportant.

On this basis, we can select the best variables to use in the measurements for the different intervals of r. Table II summarizes our main conclusions:

TABLE II. – *Best variables to use in different intervals of* $r=R/m$.

Interval of r ($\mu m/m_e$)	Best variables	r_0 (*)	a (*)	b (*)
0–5	n	2.00	1.670 ± 0.005	0.404 ± 0.015
	x	2.50	1.499 ± 0.003	0.532 ± 0.008
5–10	x			
	$\overline{w}$	12.0	-0.042 ± 0.002	0.270 ± 0.009
10–50	$\overline{w}$			
50–300	$\overline{w}$	65.00	0.165 ± 0.004	0.377 ± 0.014

(*) a, b and r_0 are the constants in the analytical expression:

$$\lg_{10}\left\{\begin{matrix} n \\ x \\ w \end{matrix}\right\} = a + b \lg_{10}\left(\frac{r}{r_0}\right)$$

They were obtained from the experimental points using the least square method (solid lines in fig. 1 and 7).

A) In the near-minimum region ($r > 25$) we definitely prefer the O'CEALLAIGH variable $\overline{w}$, for the following reasons:

1) It is independent of development (to a first approximation).

2) It presents, as a function of r, a higher slope than the blob number n (Fig. 1). The higher slope overcompensates the moderate underfluctuation of $\bar{n}$ (see formulae (11), (12)) to be compared with the normal fluctuation σ_w of $\bar{w}$, that is (5):

$$\sigma_{\bar{w}} = \frac{\bar{w}}{\sqrt{N}} . \tag{14}$$

3) It is much more reproducible and objective than the grain number g. Fig. 2 gives a comparison which makes this point clear.

Points 1) and 3) were directly tested by measuring the fluctuations of some 40 experimental points (Fig. 7) with respect to the least square straight line, in the $r > 25$ region. Each point corresponds to a single and different track. Measurements were made on different plates and *no reference to a fixed* (minimum *or* « *plateau* ») *value was made*. The distribution of differences between experimental and least square values (see Fig. 7) was in agreement with the

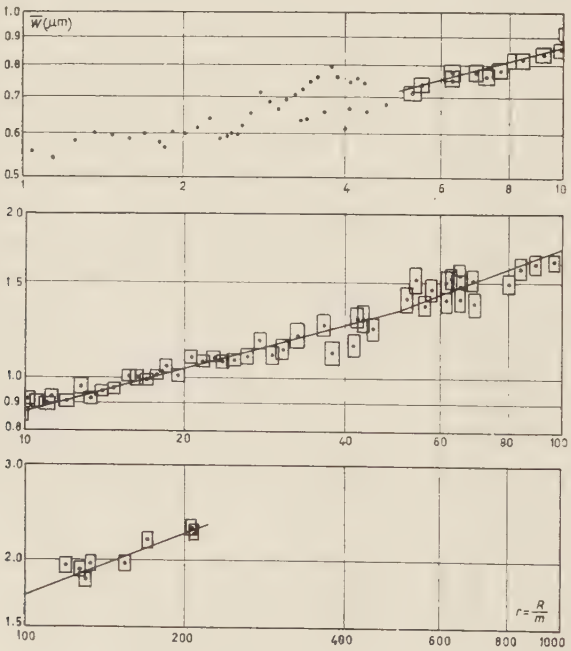

Fig. 7.

normal distribution defined by eq. (14). A χ^2-test gave a probability of 0.35. Thus, the fluctuations must be due essentially to purely statistical reasons.

B) In the clogged region ($r < 10$). – The O'CEALLAIGH variable does not seem to be convenient for $r < 10$, although its use was recommended by the Author specifically for tracks at the end of their ranges. The reasons are:

1) Since, in the clogged region the O'Ceallaigh model is no longer valid, there is no reason to think that $\overline{w}$ is still independent of γ. On the contrary the approximate validity of the H.D.-model leads one to think that $\overline{w}$ will depend on γ rather strongly in this region (see eq. (6′)).

2) The slope of the curve is very much smaller than that of the other variables ($\overline{n}$ and $\overline{x}$).

So we must turn to the variables $\overline{n}$ and $\overline{x}$. Our results seem to suggest that $\overline{n}$ is more dependent on development than is $\overline{x}$ ([41]).

Moreover, $\overline{x}$ has the advantage of a larger slope than n. Thus we decided to use the x-variable in the clogged region. We do not follow the rather general trend to use the integrated parameter (4′); by means of the straight line of Fig. 1, we can deduce at once a value of r and therefore of M *for every measured cell*. In this way a frequency distribution of mass values deduced from any single cell can be obtained so providing a powerful test of the internal consistency of the method. Further work on this line is still in progress.

C) In the intermediate region ($10 < r < 25$). – We do not see any definite reason to prefer $\overline{w}$ or $\overline{x}$. In this region $\overline{n}$ is practically constant so that $\overline{w}$ and $\overline{x}$ have the same slope. An extensive examination of the fluctuations of these two variables and of their dependence on processing is still to be made. We provisionally use the $\overline{w}$ variable, as suggested by the Padau Conference.

([41]) If the H.D.-model formulae are to be taken literally, a reason for this could be found in the fact that for the $\Gamma=2$ assumption, the value of 2γ is just the least possible one (see Table I). Now for a fixed β, and rather high p, the H.D.-formulae give a strong discontinuity in $\overline{w}$ and $\overline{n}$, when Γ jumps 1 unit, while the $\overline{x}$ variable does not suffer any discontinuity.

RIASSUNTO

Mediante un apparato già descritto è stata eseguita una serie molto estesa di misure sulle « lacune » delle tracce in emulsioni nucleari. Sono state misurate: la densità $\overline{n}$, la lunghezza totale $\overline{x}$, la lunghezza media $\overline{w} = x/\overline{n}$ delle lacune e la densità $\overline{n}_\varepsilon$ delle sole lacune « lunghe ». Sono state impiegate tracce di protoni e di mesoni π e μ terminanti il loro percorso entro un pacco di pellicole esposto durante la campagna di lanci svolta a Cagliari nel 1953. È stato studiato un intervallo di velocità notevolmente esteso ($0 < v/c < 0.80$). I risultati sperimentali vengono paragonati con i modelli di traccia proposti finora da diversi autori. Si discute la scelta del parametro che, in ogni intervallo di velocità, risulta il più conveniente per risalire alla massa della particella. Risulta che nella regione prossima al minimo è preferibile il parametro $\overline{w}$, mentre nella zona di alta ionizzazione è più conveniente usare il parametro $\overline{x}$.

Sulla relazione fra la teoria di Tomonaga-Schwinger e quella di Dirac-Fock-Podolsky.

P. Bocchieri

Istituto di Scienze Fisiche dell'Università - Milano
Istituto Nazionale di Fisica Nucleare - Sezione di Milano

A. Loinger

Istituto di Fisica dell'Università - Pavia

(ricevuto il 7 Giugno 1955)

Riassunto. — Si dimostra, mediante una opportuna estensione covariante di un metodo proposto da Becker e Leibfried, che, per particelle tutte di un solo tipo, la teoria di Dirac-Fock-Podolsky è equivalente a una formulazione della teoria di Tomonaga-Schwinger relativa ad un numero finito di particelle.

1. – Com'è noto, uno dei risultati fondamentali della meccanica quantistica non relativistica è l'equivalenza tra la descrizione ondulatoria (« Wellenbild ») e quella corpuscolare (« Partikelbild ») (1).

Il metodo più noto per dimostrare tale equivalenza è quello di Fock (2). Un metodo assai più semplice e diretto e che rende particolarmente evidente come la teoria della descrizione corpuscolare non sia altro che una trascrizione matematica della teoria della descrizione ondulatoria è stato successivamente esposto da Becker e Leibfried (3).

In questa nota esporremo una estensione covariante di quest'ultimo metodo: precisamente faremo vedere come per particelle tutte di *un solo* tipo la « many-

(1) Vedi, per esempio, W. Heisenberg: *I principi fisici della teoria dei quanti* (Torino, 1953).

(2) V. Fock: *Zeits. f. Phys.*, **75**, 622 (1932); **76**, 852 (1932).

(3) R. Becker e G. Leibfried: *Phys. Rev.*, **69**, 34 (1946); *Zeits. f. Phys.*, **125**, 347 (1948).

time theory », *nella formulazione originaria di* DIRAC-FOCK-PODOLSKY [1], sia completamente equivalente ad una teoria di campo di TOMONAGA-SCHWINGER [5] relativa ad un numero *finito* di particelle [6], nella quale di conseguenza non vengono escluse transizioni a stati di energia negativa [7].

Il presente lavoro ha un interesse principalmente metodologico, in quanto sia la « many-time theory » che la formulazione suddetta della teoria di Tomonaga-Schwinger hanno evidentemente un significato fisico assai limitato.

Il procedimento matematico adoperato è tuttavia interessante, in quanto non è da escludersi che esso possa rendere agevole una trascrizione covariante configurazionale (rispetto agli elettroni ed ai positroni) della usuale teoria di campo, nella quale il numero delle particelle non è conservato.

Le funzioni d'onda così ricavabili ammettono una interpretazione probabilistica.

2. – Si considerino le equazioni fondamentali della teoria di Tomonaga-Schwinger:

$$i\hbar c\,\frac{\delta\Psi[\sigma]}{\delta\sigma(z)} = -\frac{1}{c}\,j^{\mu}(z)A_{\mu}(z)\Psi[\sigma]\,; \tag{1}$$

ove

$$j^{\mu}(x) = iec\,\bar{\psi}(x)\,\gamma^{\mu}\psi(x);$$

$$\left[\frac{\partial A_{\mu}}{\partial x^{\mu}} - \int_{\sigma} D(x-z)\,\frac{1}{c}\,j^{\mu}(z)\,d\sigma_{\mu}\right]\Psi[\sigma] = 0\,; \tag{2}$$ [8]

$$(d\sigma_{\mu} = (dz_2\,dz_3\,dz_0,\ dz_1\,dz_3\,dz_0,\ dz_1\,dz_2\,dz_0,\ -i\,dz_1\,dz_2\,dz_3))$$

$$\Box A_{\mu} = 0\,; \qquad [A_{\mu}(x),\ A_{\nu}(x')] = i\hbar c\,\delta_{\mu\nu}\,D(x-x')\,; \tag{3}$$

$$\{\psi_{\alpha}(x),\ \bar{\psi}_{\beta}(x')\} = -iS_{\alpha\beta}(x-x'); \tag{4}$$

e tutti gli altri anticommutatori uguali a zero. Qui e nel seguito x è un punto generico dello spaziotempo, mentre z appartiene alla superficie σ di tipo spaziale.

---

(1) Vedi, per esempio, P. A. M. DIRAC: *The Principles of Quantum Mechanics*, Second Edition (Oxford, 1935), p. 286 e segg..

(5) Vedi, per esempio, W. PAULI: *Ausgewählte Kapitel aus der Feldquantisierung* (Zürich, (1951).

(6) Vedi, per esempio, op. cit. in (5), p. 6 e segg..

(7) M. GÜNTHER (*Phys. Rev.*, 88, 1411 (1952)) ha dimostrato questa equivalenza con un metodo abbastanza complicato, il quale costituisce una estensione del metodo di Fock citato in (2).

(8) L'assumere, invece della (2), la più corretta condizione supplementare di GUPTA e BLEULER, non porterebbe alcuna difficoltà.

Definiremo al modo seguente l'operatore N, numero di particelle del campo materiale:

$$N = i\int_{\sigma} \bar{\psi}(z)\gamma^{\mu}\psi(z)\,d\sigma_{\mu}\,. \tag{5}$$

Valgono allora, se $|N'\rangle$ è uno stato con N' particelle, le seguenti equazioni:

$$N|N'\rangle = N'|N'\rangle\,; \tag{6}$$

$$N\psi_{\alpha}(z)|N'\rangle = (N'-1)\,\psi_{\alpha}(z)|N'\rangle\,; \tag{7}$$

$$N\bar{\psi}_{\alpha}(z)|N'\rangle = (N'+1)\bar{\psi}_{\alpha}(z)|N'\rangle\,. \tag{8}$$

La dimostrazione delle ultime due è immediata quando si tenga conto delle:

$$\psi(x) = \int_{\sigma} S(x-z)\gamma^{\mu}\psi(z)\,d\sigma_{\mu}\,;$$

$$\bar{\psi}(x) = \int_{\sigma} \bar{\psi}(z)\gamma^{\mu}S(z-x)\,d\sigma_{\mu}\,.$$

(Si osservi inoltre che per un qualsiasi spinore $\varphi(x)$ valgono le:

$$\varphi(z') = \int_{\sigma} S(z'-z)\gamma^{\mu}\varphi(z)\,d\sigma_{\mu}\,;$$

$$\bar{\varphi}(z') = \int_{\sigma} \bar{\varphi}(z)\gamma^{\mu}S(z-z')\,d\sigma_{\mu}).$$

Dalle (6), (7), (8) segue (9) l'esistenza di uno stato $\rangle_0$ tale che

$$\psi_{a}(z)\rangle_0 = 0\,,$$

che diremo stato di vuoto e che supporremo normalizzato: ${}_0\langle\,\rangle_0 = 1$.

Tale stato di vuoto *non* è lo stato di minima energia, ma è lo stato che corrisponde ad assenza completa di particelle.

(Se avessimo supposto gli stati di energia negativa occupati dal « mare » e avessimo definito il vuoto come lo stato di minima energia, avremmo avuto la « teoria dei buchi » (6), la quale è ovviamente equivalente alla usuale formu-

(9) Vedi, per esempio, P. A. M. Dirac: *The Principles of Quantum Mechanics*, Third Edition (Oxford, 1947), p. 136.

lazione con elettroni e positroni: la trascrizione configurazionale di tale formulazione fornirebbe una teoria diversa dalla « many-time theory »).

Ovviamente lo stato:

$$\overline{\psi}_{\alpha_1}(z_1')\,\overline{\psi}_{\alpha_2}(z_2')\ldots\overline{\psi}_{\alpha_f}(z_f')\rangle_0\,,$$

è un autostato di N appartenente all'autovalore f.

Lo stato generico (che supporremo normalizzato) corrispondente alla presenza di f particelle è manifestamente:

$$\Psi_f[\sigma]=(f!)^{-\frac{1}{2}}\int_\sigma \overline{\psi}(z_1')\ldots\overline{\psi}(z_f')\rangle_0\gamma_1^{\mu_1}\ldots\gamma_f^{\mu_f}\Phi(z_1',\ldots,z_f')\,\mathrm{d}\sigma_{1,\mu_1}\ldots\mathrm{d}\sigma_{f,\mu_f}\,.$$

Si noti che in virtù delle regole di anticommutazione la Φ è antisimmetrica. Il fattore $(f!)^{-\frac{1}{2}}$ è inserito per ragioni di normalizzazione. Si ha infatti:

$${}_0\langle\psi_{\beta_g}(z_g'')\ldots\psi_{\beta_1}(z_1'')\overline{\psi}_{\alpha_1}(z_1')\ldots\overline{\psi}_{\alpha_f}(z_f')\rangle_0=\delta_{fg}(-i)^f\sum_p(-1)^p S_{\beta_1\alpha_1}(z_1''-z_1')\ldots S_{\beta_f\alpha_f}(z_f''-z_f'),$$

ove la somma va estesa a tutte le permutazioni dei primi indici β e dei primi argomenti z'' e va preso il segno positivo o quello negativo a seconda che la permutazione considerata sia di classe pari o dispari rispetto alla fondamentale $1, 2, \ldots, f$. Pertanto, se si vuole che il prodotto di due vettori di stato normalizzati $\Psi_f[\sigma]$ e $\Psi_f'[\sigma]$, sia:

$$\langle\Psi_f'|\Psi_f\rangle=(-i)^f\int_\sigma\overline{\Phi}'(z_f',\ldots,z_1')\gamma_f^{\mu_f}\ldots\gamma_1^{\mu_1}\Phi(z_1',\ldots,z_f')\,\mathrm{d}\sigma_{1,\mu_1}\sigma\ldots\mathrm{d}\sigma_{f,\mu_f}\,,$$

bisognerà prendere come ket fondamentale:

$$(f!)^{-\frac{1}{2}}\overline{\psi}_{\alpha_1}(z_1')\ldots\overline{\psi}_{\alpha_f}(z_f')\rangle_0\,.$$

Lo stato più generale corrispondente ad un numero indefinito di particelle sarà allora:

$$\Psi[\sigma]=c_0\rangle_0+\sum_1^\infty{}_f\,c_f\Psi_f[\sigma]\,,$$

dove c_0 e c_f non dipendono da σ.

Con qualche calcolo è ora facile rendersi conto che:

$$\frac{\delta}{\delta\sigma(z)}\underbrace{\int_\sigma \dots \int_\sigma}_{f} \overline{\psi}(z_1') \dots \overline{\psi}(z_f') \rangle_0 \gamma_1^{\mu_1} \dots \gamma_f^{\mu_f} \Phi(z_1', \dots z_f') \, \mathrm{d}\sigma_{1,\mu_1} \dots \mathrm{d}\sigma_{f,\mu_f} =$$

$$= \sum_1^f{}_k (z_k' \to z) \underbrace{\int_\sigma \dots \int_\sigma}_{f \quad 1} \overline{\psi}(z_1') \dots \overline{\psi}(z_k') \dots \overline{\psi}(z_f') \rangle_0 \gamma_1^{\mu_1} \dots \gamma_{k-1}^{\mu_{k-1}} \cdot$$

$$\cdot \gamma_{k+1}^{\mu_{k+1}} \dots \gamma_f^{\mu_f} \left(\frac{m_0 c}{\hbar} + \gamma_k^{\mu_k} \frac{\partial}{\partial z_k'^{\mu_k}} \right) \Phi(z_1', \dots, z_k', \dots, z_f') \cdot$$

$$\cdot \mathrm{d}\sigma_{1,\mu_1} \dots \mathrm{d}\sigma_{k-1,\mu_{k-1}} \mathrm{d}\sigma_{k+1,\mu_{k+1}} \dots \mathrm{d}\sigma_{f,\mu_f} ;$$

ed inoltre è:

$$(9) \quad \overline{\psi}(z)\gamma^\mu \psi(z) \underbrace{\int_\sigma \dots \int_\sigma}_{f} \overline{\psi}(z_1') \dots \overline{\psi}(z_f') \; {}_0\gamma_1^{\mu_1} \dots \gamma_f^{\mu_f} A_\mu(z) \cdot$$

$$\cdot \Phi(z_1', \dots, z_f') \, \mathrm{d}\sigma_{1,\mu_1} \dots \mathrm{d}\sigma_{f,\mu_f} = (-i) \sum_1^f{}_k (z_k' \to z) \underbrace{\int_\sigma \dots \int_\sigma}_{f-1} \overline{\psi}(z_1') \dots \overline{\psi}(z_k') \dots \overline{\psi}(z_f') \rangle_0 \cdot$$

$$\cdot \gamma_1^{\mu_1} \dots \gamma_{k-1}^{\mu_{k-1}} \gamma_{k+1}^{\mu_{k+1}} \dots \gamma_f^{\mu_f} \gamma^\mu A_\mu(z) \, \Phi(z_1', \dots, z_k', \dots, z_f') \cdot$$

$$\cdot \mathrm{d}\sigma_{1,\mu_1} \dots \mathrm{d}\sigma_{k-1,\mu_{k-1}} \mathrm{d}\sigma_{k+1,\mu_{k+1}} \dots \mathrm{d}\sigma_{f,\mu_f} .$$

Nel ricavare la (9) si è tenuto presente che:

$$\psi(z) \, \psi(z_1') \dots \overline{\psi}(z_f') \rangle_0 = -i \sum_1^f{}_k (-1)^{k-1} S(z - z_k') \, \overline{\psi}(z_1') \dots \overline{\psi}(z_{k-1}') \, \overline{\psi}(z_{k+1}') \dots \overline{\psi}(z_f') \rangle_0 .$$

Pertanto, sostituendo in (1):

$$i\hbar c \sum_1^\infty{}_f c_f (f!)^{-1/2} \sum_1^f{}_k (z_k' \to z) \underbrace{\int_\sigma \dots \int_\sigma}_{f-1} \overline{\psi}(z_1') \dots \overline{\psi}(z_f') \rangle_0 \gamma_1^{\mu_1} \dots \gamma_{k-1}^{\mu_{k-1}} \cdot$$

$$\cdot \gamma_{k+1}^{\mu_{k+1}} \dots \gamma_f^{\mu_f} \left[\frac{m_0 c}{\hbar} + \gamma_k^{\mu_k} \left(\frac{\partial}{\partial z_k'^{\mu_k}} - \frac{ie}{\hbar c} A_{\mu_k}(z_k') \right) \right] \Phi(z_1', \dots z_f') \cdot$$

$$\cdot \mathrm{d}\sigma_{1,\mu_1} \dots \mathrm{d}\sigma_{k-1,\mu_{k-1}} \mathrm{d}\sigma_{k+1,\mu_{k+1}} \dots \mathrm{d}\sigma_{f,\mu_f} = 0 ;$$

moltiplicando a sinistra per ${}_0\langle \psi(z_n'') \dots \psi(z_1'')$, si ha:

$$\sum_1^n{}_k (z_k' \to z)(-i)^n \sum_p (-1)^p S(z_k'' - z_k') \left[\frac{m_0 c}{\hbar} + \gamma_k^{\mu_k} \left(\frac{\partial}{\partial z_k'^{\mu_k}} - \right. \right.$$

$$\left. \left. - \frac{ie}{\hbar c} A_{\mu_k}(z_k') \right) \right] \Phi(z_1'', \dots, z_k', \dots, z_n'') = 0 ;$$

da cui facilmente

$$\left[\gamma_k^\mu\left(\frac{\partial}{\partial z_k^\mu}-\frac{ie}{\hbar c}A_\mu(z_k)\right)+\frac{m_0 c}{\hbar}\right]\Phi(z_1,\ldots,z_n)=0\,,\qquad (k=1,\ldots,n) \tag{10}$$

che sono le equazioni fondamentali della teoria di Dirac-Fock-Podolsky.

Consideriamo ora la (2). Con calcoli del tutto simili a quelli fatti per giungere alla (10) essa diviene:

$$\left[\frac{\partial A_\mu}{\partial x^\mu}-e\sum_1^n{}_k D(x-z_k)\right]\Phi(z_1,\ldots,z_n)=0\,,$$

la quale è la condizione supplementare della teoria di Dirac-Fock-Podolsky.

Le equazioni (3) sono comuni alle due teorie. La Φ che si ottiene col nostro procedimento è normalizzata in quanto per essa vale la

$$(-i)^n\int_\sigma \overline{\Phi}(z_n',\ldots,z_1')\gamma_n^{\mu_n}\ldots\gamma_1^{\mu_1}\Phi(z_1',\ldots,z_n')\,\mathrm{d}\sigma_{1,\mu_1}\ldots\mathrm{d}\sigma_{n,\mu_n}=1\,,$$

che è la condizione di normalizzazione (riferita alla superficie σ) della teoria di Dirac-Fock-Podolsky.

Abbiamo in tal modo completamente dimostrato l'equivalenza esistente tra una teoria di Tomonaga-Schwinger relativa ad un numero *finito* di particelle tutte di *un solo* tipo e la teoria di Dirac-Fock-Podolsky.

Come è chiaro, questa equivalenza non è limitata all'elettrodinamica, ma è valida anche per tutte le teorie mesoniche.

* * *

Ringraziamo cordialmente il prof. P. Caldirola per l'interessamento dimostratoci.

SUMMARY

In this paper a covariant generalization of a method due to Becker and Leibfried [3] is exposed. It is shown that, for identical particles, the many-time theory, as formulated by Dirac-Fock-Podolsky [1], is equivalent to a non-physical formulation of the field theory of Tomonaga-Schwinger, concerning a *finite* number of particles.

LETTERE ALLA REDAZIONE

(La responsabilità scientifica degli scritti inseriti in questa rubrica è completamente lasciata dalla Direzione del periodico ai singoli autori)

A Simple Theory of the $^7Li(\gamma, {}^3H)\,^4He$ Reaction.

W. Czyż

Physical Institute, Jagiellonian University - Cracow (Poland)

(ricevuto il 27 Maggio 1955)

The results of recent experimental investigations [1-5] do not supply a complete pattern of the reaction $^7Li(\gamma,{}^3H)\,^4He$. Nevertheless, the following simple theory may give some contribution to the understanding of the mechanism of this reaction.

We assume a two body model of the ^7Li-nucleus composed of a triton and an α-particle. This model is based on following considerations.

1) The energy threshold of the $^7Li(\gamma, t)\alpha$ reaction is comparatively low (2.465 MeV), whereas the threshold energies for (γ, n) and (γ, p) reactions are 7.15 MeV and 9.5 MeV respectively.

2) It is known, that ground state of ^7Li-nucleus is $P_{\frac{3}{2}}$. This state is easily obtainable from the t-α model.

3) A system composed of a triton (magnetic moment 2.9789) and an α-particle (magnetic moment 0) must possess in its ground state $P_{\frac{3}{2}}$ (with orbital magnetic moment 0.405) a magnetic moment equal to 3.3839 nuclear magnetons. When compared to the experimental value of 3.2559 nuclear magnetons it exhibits a rather small difference of 3.8%.

In preliminary calculations we assume the interaction between a triton and an α-particle as a square well potential of radius r_0 and depth V. V is a function of the orbital angular momentum of the t-α system. The Coulomb interaction between t and α is neglected. Most important transitions are the electric dipole $P \rightarrow S$ and $P \rightarrow D$ ones. The cross-sections σ_{PS}, σ_{PD} of the $^7Li(\gamma, t)\alpha$ reaction were evaluated in analogy with the calculations of Guth and Mullin [6]. Therefore we restrict ourselves to results represented in Fig. 1.

The values of σ_{PS} and σ_{PD} for $r_0 = 5 \cdot 10^{-13}$ cm and $V_P = -8.45$ MeV, $V_S = -1$ MeV and $+4$ MeV. $V_0 = +4$ MeV (the index indicates the angular momentum of the t-α system) are plotted against the γ-ray energy. V_P is determined by the binding energy -2.465 MeV (for fixed r_0), V_S and V_D are fitted to the experimental results [1-5].

[1] Erdös, Stoll, Wächter and V. Wataghin: *Nuovo Cimento*, **12**, 639 (1954).

[2] Stoll: *Helv. Phys. Acta*, **27**, 395 (1954).

[3] Titterton and Brinkley: *Proc. Phys. Soc.*, A **66**, 579 (1953).

[4] Stoll and Wächter: *Nuovo Cimento*, **10**, 374 (1954).

[5] Nabholz, Stoll and Wäffler: *Helv. Phys. Acta*, **25**, 701 (1952).

[6] Guth and Mullin: *Phys. Rev.*, **76**, 234 (1949).

The angular distributions of tritons in the $P \rightarrow D$ transition may be represented by $1 - 0.375 \cos^2 \theta$, where θ is the angle between the direction of the outgoing

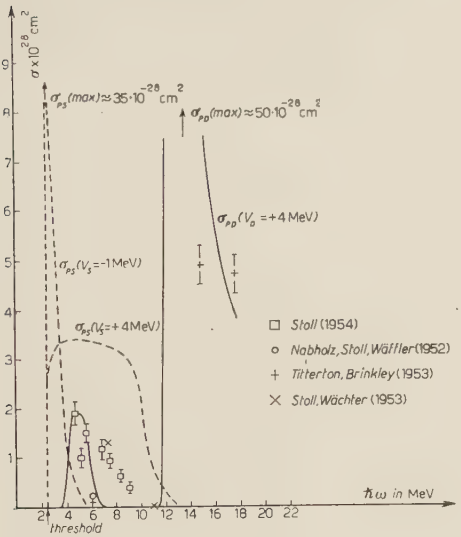

Fig. 1.

triton and that of incident photon beam. The angular distribution of tritons in the $P \rightarrow S$ transition is isotropic.

As it was found by STOLL [2] the angular distribution for incident photons of the energy of 4.7 MeV is approximatively proportional to $1 - 0.5 \cos^2 \theta$. It may be seen from the Fig. 1 that the assumption of the same t-α interaction in S- and D-state gives a wrong angular distribution for $\hbar\omega = 4.7$ MeV. This suggests the necessity of the assumption of attraction in t-α systems in the S-state, and repulsion in the D-state. The assumption of attraction in the D-state leads to cross-sections being in complete disagreement with the experiment. A value of $V_S = -1$ MeV was chosen, since it may be calculated that already for $V_S = -1.2$ MeV a bound state of the t-α system is obtained not known for the ^{7}Li-nucleus. In the neighbourhood of the threshold energy for this reaction σ_{PS} exhibits a sharp maximum. Then, it may be supposed, that the cross-section for γ-ray energy exceeding $\hbar\omega \approx 4$ MeV is determined by the $P \rightarrow D$ transition.

In the following some details of the shape of the cross-section curve in the energy regions 4 MeV $\lesssim \hbar\omega \lesssim$ 10 MeV and $\hbar\omega \lesssim 4$ MeV are considered. In the region $4 \lesssim \hbar\omega \lesssim 10$ MeV, the results obtained by STOLL [2] reveal a few resonances, not shown in fig. 1. These resonances may be obtained for the considered model only from magnetic dipole, electric quadrupole and still higher multipole-transitions. It is doubtful whether in this very rough model these resonances may be really obtained. Nevertheless we believe, that the principal form of the cross-section is given by the $P \rightarrow D$-transition, and its mechanism is well described by the t-α model of the ^{7}Li-nucleus. We may suppose that besides this « two-body mechanism » there exists another mechanism of the ^{7}Li(γ, t)α reaction (which may be a compound nucleus mechanism), from which the « fine structure » of the cross-section curve in the region $4 \lesssim \hbar\omega \lesssim$ $\lesssim 10$ MeV may be obtained.

It seems that ref. [1,2] do not give satisfactory answer to the question what is the cross-section for $\hbar\omega \lesssim 4$ MeV. This fact is probably due to insufficient development technique of the tracks of the disintegration products of such small energy ($E_t + E_\alpha \lesssim 1.5$ MeV). If our model were valid for the all γ-quanta of energy greather than the threshold energy (2.465 MeV) $P \rightarrow S$ transition wold give a sharp maximum in neighbourhood of the reaction threshold. However it is not impossible that the pattern of the reaction cross section in the energy domain $\hbar\omega \lesssim 4$ MeV may be considerably changed if the lifetime of the α-particle in the ^{7}Li-nucleus were sufficiently short. E.g. it may be supposed that any of the both constituents of the ^{7}Li-nucleus are not distinguished from one another, since a proton is

frequently exchanged between the triton and the α-particle. If the lifetime of the α-particle (denoted by T) in a ^{7}Li-nucleus is shorter than the period of electromagnetic vibration of the incident photon, then for this photon the electric dipole moment of the ^{7}Li-nucleus vanishes and consequently the electric dipole transitions vanish too. On assuming $T \approx 10^{-21}$ s (lower limit of Wheeler's estimation (7)) the critical energy for which the electric dipole moment of the ^{7}Li-nucleus becomes important may be estimated as follows:

$$\hbar\nu_{\text{crit}} = \hbar\omega_{\text{crit}} \approx 0.66 \cdot 10^{-21}\,\text{MeV s} \cdot \cdot 2\pi \cdot 10^{-21}\,\text{s}^{-1} \approx 4\ \text{MeV}\ .$$

It is then possible that further measurements might give negligibly malls values of the cross-section for the energy $\hbar\omega \lesssim 4$ MeV.

Besides the measurements of the angular distribution of the tritons for the energy 14 MeV $\lesssim \hbar\omega \lesssim$ 18 MeV might give valuable informations concerning the mechanism of the ^{7}Li$(\nu, t)\alpha$ reaction. It is hoped that the resulting experimental distribution would confirm our distribution $1 - 0.375 \cos^2\theta$ characteristic for the $P \to D$ transition.

The proper magnitude of the Coulomb corrections neglected in the preceding considerations is still not known to the author of this note.

A more complete report of the present investigations will be published in *Acta Physica Polonica*.

I wish to thank Professor H. Niewodniczański and Professor J. Weyssenhoff for their interest to this work and encouragements during its creation.

(7) Wheeler: *Phys. Rev.*, **52**, 1083 (1937).

Moments magnétiques des noyaux legers.

F. J. Wiśniewski
Lodz - Polonia

(ricevuto il 4 Giugno 1955)

Dans des notes antérieures (1) on a montré que les noyaux atomiques se comportent comme des corps solides en rotation autour d'un axe fixe.

En tenant compte de ce fait on cherchera maintenant d'établir une théorie des moments magnétiques des noyaux et de la confronter avec les données expérimentales. On déduira l'expression mathématique pour les moments magnétiques en se basant sur les quatres hypotheses suivantes:

1) Le moment magnétique total d'un noyau est la somme géometrique des moments magnétiques des nucléons constituant le noyau et du moment magnétique du a la rotation du noyau autour d'un axe fixe.

2) Les divers moments magnétiques cités plus haut ont un axe commun (axe de rotation) sur lequel il peuvent être dirigés dans le même sens ou bien dans le sens contraire.

3) Le moment résultant d'un nombre pair de nucléons de même nature est nul.

4) Le moment résultant d'un nombre impair de nucléons de même nature est égal au moment magnétique d'un seul d'entre eux.

Avant d'appliquer ces hypothèses au calcul des moments magnétiques on passera à la déduction de l'expression du moment magnétique du à la rotation du noyau en le traitant comme un corps solide.

Moment magnetique d'un solide électrisé en rotation. - Soit Δ l'axe de rotation d'un ensemble de particules dont une certaine partie est chargée tandis que la partie restante est neutre au point de vue électrique.

Désignons par g_z la distance de l'axe de rotation Δ d'une particule chargée. Si $\dot{\varphi}$ est la vitesse angulaire autour de Δ le moment magnétique dû à la rotation autour de Δ de cette particule est:

$$e\varrho_z^2\dot{\varphi}/2c\,.$$

Le moment magnétique total s'obtient en faisant la somme de l'expression précédente pour toutes les particules chargées électriquement. On obtient ainsi

$$\mu = \frac{e}{2c}\sum{}'\varrho_z^2\dot{\varphi} = \frac{e}{2c}\dot{\varphi}\sum{}'\varrho_z^2\,,$$

ou $\sum'$ désigne la sommation par rapport aux particules électrisées. Le moment d'inertie J est par definition

$$J = m\sum\varrho_A^2$$

(1) *Compt. Rend. Ac. Paris*, **235**, 364 (1952); **236**, 1483 (1953); **237**, 1222 (1953).

ou $\sum$ désigne la sommation par rapport a toutes les particules chargées ou non au nombre de A.

Posons:

$$\frac{\sum' \varrho_z^2}{\sum \varrho_A^2} = \omega ,$$

alors

$$\mu = \frac{e}{2mc} \omega \dot{\varphi} \sum m \varrho_A^2 = \frac{e}{2mc} \omega J \dot{\varphi} .$$

Or (2)

$$J\dot{\varphi} = \frac{h}{2\pi} (n + \tfrac{1}{2}) , \tag{1}$$

donc

$$\mu = \frac{eh}{4\pi mc} (n + \tfrac{1}{2}) \omega . \tag{2}$$

Si le solide est formé d'un anneau de particules lourdes de rayon ϱ on a

$$\varrho = \varrho_A \mp \varrho_z$$

et

$$\omega = \frac{Z'}{N' + Z'} = \frac{Z'}{\overline{A}} \leqslant 1 \tag{3}$$

où Z' est le nombre de particules chargées et N' le nombre de particules neutres sur l'anneau circulaire.

$\widetilde{\omega}$ est alors une fraction rationnelle.

D'après la remarque faite plus haut $\widetilde{\omega}$ est égal au rapport du nombre Z' de protons situés sur l'anneau au nombre $\overline{A}$ de nucléons qui forment l'anneau.

$$\begin{cases} \omega = \dfrac{Z'}{\overline{A}} = \dfrac{Z'}{N' + Z'} ; \\ \overline{A} = N' + Z' < A . \end{cases} \tag{4}$$

En désignant par Z le nombre total de protons dans le noyau on doit avoir

$$Z' \leqslant Z . \tag{5}$$

(2) F. J. WIŚNIEWSKI: *Annali di matematica pura e applicata*, **10** (1931-2).

Comme le nombre $(Z - Z')$ de protons situés au centre de l'anneau ne peut depasser le nombre total $A - \overline{A}$ de nucléons qui sont situés au centre de l'anneau on doit avoir l'inégalité

$$Z - Z' \leqslant A - \overline{A} ; \quad Z' \geqslant Z + \overline{A} - A . \tag{6}$$

En tenant compte des inégalités (5) et (6) on obtient a partir de (4) les inégalités suivantes:

$$\frac{Z + \overline{A} - A}{\overline{A}} \leqslant \widetilde{\omega} \leqslant \frac{Z}{\overline{A}} , \tag{7}$$

$$\overline{A} \leqslant \frac{A - Z}{1 - \omega} ; \qquad \overline{A} \leqslant \frac{Z}{\omega} ; \quad \overline{A} \leqslant A . \tag{8}$$

Toute valeur de ω doit satisfaire les inégalités (7) et (8).

Le moment magnétique d'un noyau. - On doit distinguer trois cas différents:

1) Le nombre de protons est impair et le nombre de neutrons est pair. Conformement aux hypothèses faites plus haut on obtient pour le moment magnétique résultant les deux formules possibles

$$(A_1) \qquad \mu = \mu_{p_r} + \omega k ,$$
$$(A_2) \qquad \mu = \mu_{p_r} - \omega k . \qquad k = n + \tfrac{1}{2}$$

2) Le nombre de protons est pair et le nombre de neutrons impair.

Alors on a

$$(B_1) \qquad \mu = \mu_n + \omega k ,$$
$$(B_2) \qquad \mu = \mu_n - \omega k . \qquad k = n + \tfrac{1}{2}$$

3) Le nombre de protons et le nombre de neutrons est impair.

$$(C_1) \qquad \mu = \mu_{p_r} + \mu_n + \omega k ,$$
$$(C_2) \qquad \mu = \mu_{p_r} + \mu_n - \omega k . \qquad k = n + \tfrac{1}{2}$$

μ_{p_r} désigne ici le moment magnétique du proton et μ_n le moment magnétique du neutron.

Les moments magnétiques sont exprimés en unités du magnéton nucléaire.

Comme base de calcul on admettra le modèle annulaire solide décrit dans

TABLE I. – $\mu_{p_T} = 2.7925$; $\mu_n = -1.9128$; $\mu_{p_T} + \mu_n = 0.8797$.

	Z	N	A	$\bar{A}$	form	spin	k	ω	μ calc.	μ exp.	$\lvert\Delta\rvert$
^{3}H	1	2	3	3	(A_1)	1/2	1/2	1/3	2.9591	2.9785 (+)	0.019
^{3}He	2	1	3	2	(B_2)	1/2	1/2	1/2	− 2.163	− 2.1274 (+)	0.035
									− 1.4128		
^{5}He	2	3	5	4	(B_1)	3/2	3/2	1/4	− 1.554	− 1.59 (−)	0.036
								1/2	− 1.179		
^{7}Li	3	4	7	6	(A_1)	3/2	3/2	1/3	3.292	3.253 (+)	0.039
								1/2	3.54		
^{7}Be	4	3	7	6	(B_1)	1/2	1/2	2/3	− 1.580	− 1.59 (−)	0.01
								1/2	− 1.683		
^{9}Be	4	5	δ	8	(B_1)	3/2	3/2	1/2	− 1.162	− 1.761 (+)	0.014
								3/8	− 1.351		
^{10}B	5	5	10	8	(C_1)	3	5/2	3/8	1.818	1.800 (+)	0.018
								4/8	2.1297		
								5/8	2.4422		
^{11}B	5	6	11	8	(A_2)	3/2	1/2	3/8	2.603	2.6283 (+)	0.025
								2/8	2.666		
								4/8	2.543		
								5/8	2.481		
^{11}C	6	5	11	9	(B_2)	3/2	3/2	5/9	− 1.080	− 1.1 (−)	0.02
								6/9	− 0.913		
^{14}N	7	7	14	7	(C_2)	1	1/2	1	0.38	0.40 (+)	0.02

La dernière colonne contient la valeur absolue des différences entre les valeurs expérimentales des moments magnétiques et leurs valeurs calculées. Les différences ne sont pas notables.

Dans la colonne des moments magnétiques calculés on a introduit les moments magnétiques qui correspondent aux différentes valeurs numériques de ω qui satisfont l'inégalité (7). Ces valeurs sont possibles mais ne furent pas observées.

(+) J. E. MACK: *Rev. Mod. Phys.*, **64**, 22 (1950).

(−) E. F. KÜLTZ, W. W. KUNTZ et W. G. HARTMAN: *Uspehi Fizičeskih Nauk*, **55**, 535 (1955), (en russe).

une des notes citées plus haut. Le nombre $\bar{A}$ de nucléons qui forment l'anneau est tiré de la même note. Pour ω on prend une fraction rationnelle qui satisfait les inégalités (7).

Pour les noyaux a nombre impair de nucléons, k sera pris égale au spin du noyaux ou bien au spin moins un comme dans le cas de ^{11}B.

Pour les noyaux a nombre impair de protons et neutrons on posera k égal au spin moins $\frac{1}{2}$ car k est par définition une fraction rationnelle avec dénominateur 2 et spin entier.

La structure de ^{7}Li, ^{9}Be, ^{10}B, ^{11}B, ^{14}N, est donnée dans la note citée. Quant à ^{3}H et ^{3}He on leur attribuera les deux structures possibles formées de trois nucléons. On admettra que ^{3}H est formé par un anneau de trois nucléons et ^{3}He sera representé par une barre formée par trois nucléons.

Dans la table sont reunis: 1) les valeurs numériques des moments magnétiques de ^{7}Li, ^{9}Be, ^{10}B, ^{11}B, ^{14}N calculés par l'une des formules (E), (B), (C), et 2) les valeurs numériques déterminées expérimentalement.

Il suit qu'entre les valeurs possibles des moments magnétiques qui correspondent aux formules (A), (B), (C) et aux différentes valeurs de ω conformement à l'inégalité (7) il y a pour les noyaux mentionnés une valeur proche de la valeur déterminée expérimentalement.

Il faut remarquer que non seulement les moments magnétiques des noyaux légers peuvent être répresentés par les expressions (A), (B), (C), mais que c'est aussi le cas pour les moments magnétiques des noyaux plus lourds.

Il est à remarquer qu'une même valeur de ω correspond à plusieurs noyaux comme il résulte de la Table II. On peut donc grouper les noyaux suivant les valeurs de ω. Il en suit que tous les noyaux qui ont la même valeur numérique de ω doivent avoir une structure identique.

TABLE II. – $\mu_{p_T} = 2.792$; $\mu_n = -1.913$; $\mu_{p_T} + \mu_n = 0.879$.

		Z	N	A	form.	spin	k	ω	μ calc.	μ exp.	$\lvert\Delta\rvert$
a)	^{19}F	9	10	19	(A_2)	1/2	1/3	1/3	2.627	2.628	0.001
	^{22}Na	11	11	22	(C_2)	3	5/2	1/3	1.712	1.713	0.001
	^{27}Al	13	14	27	(A_1)	5/2	5/2	1/3	3.671	3.641	0.03
	^{81}Br	35	46	81	(A_2)	3/2	3/2	1/3	2.291	2.269	0.022
b)	^{23}Na	11	12	23	(A_2)	3/2	3/2	3/8	2.229	2.217	0.012
	^{25}Mg	12	13	25	(B_1)	5/2	5/2	3/8	— 0.976	— 0.96	0.016
	^{63}Cu	29	34	63	(A_2)	3/2	3/2	3/8	2.230	2.226	0.014
	^{121}Sb	51	70	121	(A_1)	5/2	5/2	3/8	3.729	3.7	0.00
c)	^{59}Co	27	32	59	(A_1)	7/2	7/2	1/2	4.54	4.648	0.108
	^{69}Ga	31	38	69	(A_2)	3/2	3/2	1/2	2.042	2.016	0.026
	^{153}Eu	63	90	153	(A_2)	5/2	5/2	1/2	1.542	1.5	0.042
d)	^{45}Sc	21	24	45	(A_1)	7/2	7/2	4/7	4.792	4.8	0.012
	^{85}Rb	37	48	85	(A_2)	5/2	5/2	4/7	1.364	1.353	0.011
e)	^{55}Mn	25	30	55	(A_1)	5/2	5/2	1/4	3.417	3.468	0.051
	^{79}Se	34	45	79	(B_1)	7/2	7/2	1/4	— 1.038	— 1.015 [2]	0.023
	^{91}Zr	40	51	91	(B_1)	5/2	5/2	1/4	— 1.288	— 1.30 [3]	0.012
	^{151}Eu	63	88	151	(A_1)	5/2	5/2	1/4	3.417	3.40	0.017
f)	^{49}Ti	22	27	49	(B_2)	7/2	7/2	3/13	— 1.106	— 1.102 [1]	0.004
	^{73}Ge	32	41	73	(B_2)	9/2	9/2	3/13	— 0.875	— 0.876 [1]	0.001
g)	^{47}Ti	22	25	47	(B_1)	5/2	5/2	5/11	— 0.777	— 0.787 [4]	0.01
	^{79}Br	35	44	79	(A_2)	3/2	3/2	5/11	2.110	2.105	0.005

[1] C. D. JEFFREIES: *Phys. Rev.*, **92**, 1262 (1953).
[2] W. A. HARDY, G. SOLVEY et C. H. TOWNES: *Phys. Rev.*, **92**, 1532 (1953).
[3] S. SAWA: *Journ. Phys. Soc. Japan*, **8**, 784 (1953).
[4] Toutes les valeurs des moments magnétiques non citeés sous (1), (2), (3), sont citeés d'après J. E. MACK: *Rev. Mod. Phys.*, **64**, 22 (1950).

On the Approximate Thomas-Fermi Function for a Compressed Neutral Atom.

T. TIETZ

Department of Theoretical Physics University Łódz - Łódz (Poland)

(ricevuto il 9 Giugno 1955)

Let us put the Thomas-Fermi function (1) for a compressed neutral atom with atomic radius x_0 (measured in Thomas-Fermi units μ) in the form

$$\Phi(x) = \Phi_0(x) + \delta(x) , \tag{1}$$

$\Phi_0(x)$ being the Thomas-Fermi function for the free neutral atom. According to FERMI (1) we have for $\delta(x)$ the differential equation

$$\delta'' = \tfrac{3}{2}(\Phi_0/x)^{\frac{1}{2}}\delta , \tag{2}$$

subject to the boundary conditions

$$\begin{cases} \delta(0) = 0 , \\ \Phi'(x_0) = \Phi(x_0)/x_0 . \end{cases} \tag{3}$$

SAUVENIER (2) for the well-known SOMMERFELD (3) asymptotic formula for $\Phi_0(x)$ previously gave the approximate formula

$$\Phi(x) = \Phi_0(x)\left[1 + \frac{4z_0 + 1}{(\lambda_1 - 4)z_0 - 1}\left(\frac{1 + z}{1 + z_0}\right)^{\lambda_1/\lambda}\right] \tag{4}$$

(where $z = x^{\lambda}\,144^{-\lambda/3}$, $z_0 = x_0^{\lambda}\,144^{-\lambda/3}$), from which follows the boundary value relation useful for the equation of state of metals

$$\Phi(x_0)/\Phi_0(x_0) = 2.060 z_0/(z_0 - 0.2651) , \tag{5}$$

as UMEDA (4) has noticed. UMEDA (4) has pointed out, that this formula has however,

(1) E. FERMI: *Mem. R. Accad. d'Italia*, **1**, 149 (1930); P. GOMBAS: *Die statistische Theorie des Atoms und ihre Anwendungen* (Wien, 1949).
(2) H. SAUVENIER: *Bull. Soc. Roy. Lieges*, **8**, 313 (1939).
(3) A. SOMMERFELD: *Zeits. f. Phys.*, **78**, 283 (1932).
(4) K. UMEDA: *Journ. Phys. Soc. Japan*, **9**, 291 (1954).

several drawbacks, as follows

$$(6)\quad \begin{cases} a) \text{ for } 0 < z_0 < 0.2651,\ (0 < x_0 < 0.9389),\ \Phi(x_0) < 0 \text{ while } \Phi(x) \text{ must by nature be always positive;} \\ b) \text{ at } z_0 = 0.2651\ (x_0 = 0.9389) \text{ instead of origin, } \Phi(x_0) = \infty; \\ c) \text{ at } z_0 = \infty\ (x_0 = \infty)\ \Phi(x_0)/\Phi_0(x_0) = 2.060 \text{ instead of 1.} \end{cases}$$

We shall now investigate, whether these drawbacks could be avoided, if for $\Phi_0(x)$, other approximate formulae were adopted. First, the MARCH [5] approximate formula of Sommerfeld type comes into consideration. It only leads however, to the same boundary value relation as the above equation (5). UMEDA using the Kerner approximate solution $\Phi_0(x) = 1/(1 + cx)$, which is very simple and of a relatively high degree of approximation, has found for a compressed neutral atom the following formula [6]

$$(7)\qquad \Phi(x) = \Phi_0(x)\left[1 + 4\left(\frac{x}{x_0}\right)^{\frac{1}{2}} \frac{I_1(X)}{X_0 I_0(X_0) - 2I_1(X_0)}\right],$$

where $X = 6^{\frac{1}{2}}C^{-\frac{1}{2}}x^{\frac{1}{2}}$ and $I_n(x) =$ Bessel function of purely imaginary argument. The Kerner-Umeda formula (7) is free from the drawbacks mentioned above. Accordingly, we take our formula [7]

$$(8)\qquad \Phi_0(x) = \frac{1}{(1 + ax)^2} \qquad a = 1/1.75661\,,$$

which is very simple and of a high degree of approximation as prouved in a preceding note by the author [8]. Equation (2) takes the form

$$(9)\qquad \delta'' = \frac{3}{2}\,\frac{\delta}{x^{\frac{1}{2}}(1 + ax)} \approx \frac{3}{2}\,\frac{\delta}{ax^{\frac{3}{2}}}\,.$$

Equation (9) becomes asymptotically an equation of Bessel type.
Since $\delta(x)$ must be a monotonously increasing function and $\delta(0) = 0$ then

$$(10)\qquad \delta(x) = AX^2 I_2(X); \qquad X = \frac{4\sqrt{3}}{\sqrt{2a}}\,x^{\frac{1}{4}}\,,$$

where $I_n(x) =$ Bessel function of purely imaginary argument and A is a disposable coefficient. The boundary condition $\Phi'(x_0) = \Phi(x_0)/x_0$ determines the coefficient A: we obtain

$$(11)\qquad A = 4\,\frac{1 + 3ax_0}{(1 + ax_0)^3}\,\frac{1}{X_0^2[X_0 I_1(X_0) - 4I_2(X_0)]}\,.$$

[5] N. H. MARCH: *Proc. Camb. Phil. Soc.*, **46**, 356 (1950).
[6] See reference [4].
[7] T. TIETZ: *Journ. Chem. Phys.*, **22**, 2094 (1954); *Ann. d. Phys.*, **15**, 955, 968 (1955).
[8] T. TIETZ: *Nuovo Cimento*, **1**, 955, 968 (1955).

The approximate formula corresponding to the equation (7) is in our case

$$\Phi(x) = \Phi_0(x)\left[1 + 12\left(\frac{x}{x_0}\right)^{\frac{1}{2}} \frac{I_2(X)}{[X_0 I_1(X_0) - 4I_2(X_0)]}\right]. \tag{12}$$

The equation corresponding to equation (5) is

$$\Phi(x_0)/(\Phi_0(x_0) = 1 + 12 \frac{1}{X_0 \frac{I_1(X_0)}{I_2(X_0)} - 4}. \tag{13}$$

This formula is free from the drawbacks mentioned above as follows:

1) at $x_0 = 0$ by virtue of the series expansions of the Bessel functions $I_1(x)$ and $I_2(x)$ for (13) we have

$$\Phi(x_0)/\Phi_0(x_0) \approx 1 + \frac{48}{X_0^2} \to \infty;$$

2) at $x_0 = \infty$ the asymptotic expansion for $I_1(x)$ and $I_2(x)$ gives in our case

$$\Phi(x_0)/\Phi_0(x_0) \approx 1 + \frac{12}{X_0} \to 1.$$

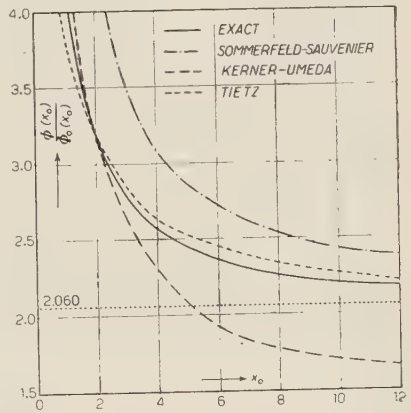

Fig. 1.

In fig. 1 we have boundary values of the exact as well as approximate Thomas-Fermi functions for the compressed neutral atom as a function of the atomic radius x_0 c.f. eqs. (5), (7) for $x = x_0$ and (13). Equation (13) seems to be more favorable for the values considered in fig. 1 than eqs. (5) and (7).

The author wishes to express his gratitude to Professor Dr. K. Umeda for his reprints on this field and for precious advice.

A Note on the Strength of Field Equations.

F. E. Mauger
King's College - London

(ricevuto il 26 Giugno 1955)

In Appendix II of the 1953 edition of « The Meaning of Relativity » Einstein showed how the field equations of different theories may be compared. For example, the method is applied to Maxwell's equations in the following manner. In terms of the six-vector F_{kl} we have the equations

$$V_{klm} \equiv F_{kl,m} + F_{lm,k} + F_{mk,l} = 0 , \tag{1}$$

$$U_k \equiv F_{kl,l} = 0 , \tag{2}$$

together with the identities

$$U_{k,k} = 0 , \qquad \text{and} \qquad V_{ikl,m}\eta^{iklm} = 0 ;$$

where η^{iklm} is the tensor density of Levi-Civita. We expand F_{kl} in a Taylor series:

$$F_{kl} = \underset{0}{F}_{kl} + \underset{1}{F}_{kla}x^a + \underset{2}{F}_{klab}x^a x^b + \dots ;$$

there are then $6\binom{4}{n}$ coefficients in the term of degree n where

$$\binom{4}{n} = \frac{4 \cdot 5 \cdot 6 \dots n + 3}{1 \cdot 2 \cdot 3 \dots n} .$$

Differentiating (1) and (2) $n - 1$ times gives $4\binom{4}{n-1}$ and $4\binom{4}{n-1}$ equations to determine the $6\binom{4}{n}$ coefficients but as (1) and (2) are not independent we must subtract $\binom{4}{n-2}$ and $\binom{4}{n\ \ 2}$, corresponding to the identities obtained by differentiating the original identities $n-2$ times. Thus the strength is given by

$$\Omega_n = 6\binom{4}{n} - 8\binom{4}{n-1} + 2\binom{4}{n-2} \sim \binom{4}{n}\frac{12}{n} \quad \text{for large } n .$$

If, on the other hand, the potentials A_k are used instead of the six-vector, together with the equations

$$L_i \equiv A_{i,ss} = 0 , \tag{3}$$

$$B \equiv A_{s,s} = 0 , \tag{4}$$

and the identity

$$L_{i,i} \equiv B_{,ss} = 0 ,$$

then the strength is given by

$$\Omega_n = 4\binom{4}{n} - 4\binom{4}{n-2} - \binom{4}{n-1} + \binom{4}{n-3} \sim \binom{4}{n}\frac{18}{n} \text{ for large } n .$$

Thus equations (3) and (4) are weaker, as one would expect, since the A_k are not completely determined in terms of the six-vector.

In this note we shall compare the strength of Einstein's generalized field equations in the form given by EINSTEIN [1] with that given by STEPHENSON [2].

As a further example the determination of the strength of Dirac's electrodynamics [3] is discussed.

If one applies the method to comparing Einstein's field equations with the modified form deduced by Stephenson a similar result to that for Maxwell's equations is obtained. The strength of the former set

$$\underset{+-}{g_{ik;l}} = 0 ,$$

$$\Gamma_i = 0 ,$$

$$\underset{-}{R_{ik}} = 0 ,$$

$$\underset{\vee}{R_{ik,l}} + \underset{\vee}{R_{kl,i}} + \underset{\vee}{R_{li,k}} = 0 ,$$

together with the Bianchi and two further identities is given by

$$\Omega_n = \left\{16\binom{4}{n} + 64\binom{4}{n-1}\right\}\left\{64\binom{4}{n-1} + 4\binom{4}{n-1} - 10\binom{4}{n-2} + 4\binom{4}{n-3}\right\} +$$

$$+ 4\binom{4}{n-3} + \binom{4}{n-2} + \binom{4}{n-4} - 4\binom{4}{n} - 3\binom{3}{n} - 2\binom{2}{n} - 1 ,$$

where the last four terms are due to the restrictions which may be applied to the

(1) A. EINSTEIN: *The Meaning of Relativity* (Princeton, 1953), Appendix II.
(2) G. STEPHENSON: *Nuovo Cimento*, **12**, 279 (1954).
(3) P. A. M. DIRAC: *Proc. Roy. Soc.*, A **291**, 291 (1951).

g_{ik} by suitable choice of the coordinate frame. Thus

$$\Omega_n \sim \binom{4}{n} \frac{45}{n} .$$

Now consider Shepenson's set

$$g_{i\ \underline{k};l} = 0 ,$$

$$R_{\underline{ik}} = 0 ,$$

$$T^s_{\underset{\vee}{mn}|s} = 0 ,$$

where the vertical bar denotes covariant differentiation with respect to the symmetric connection $\Gamma^s_{\underline{mn}}$, and $T^s_{\underset{\vee}{mn}}$ is defined by:

$$-\Gamma^s_{\underset{\vee}{mn}} = \tfrac{1}{3}(\delta^s_m T_n - \delta^s_n T_m) + T^s_{\underset{\vee}{mn}} . \tag{5}$$

The corresponding strength is

$$\Omega_n = \left\{16\binom{4}{n} + 64\binom{4}{n-1}\right\} - \left\{64\binom{4}{n-1} + 10\binom{4}{n-2} + 6\binom{4}{n-2} + 4\binom{4}{n-3}\right\} - \left\{4\binom{4}{n} + 3\binom{3}{n} + 2\binom{2}{n} + 1\right\} \sim \binom{4}{n}\frac{51}{n} .$$

Thus this set is weaker than Einstein's field equations which suggests that in equation (5) the $T^s_{\underset{\vee}{mn}}$ are not completely determined in terms of the $\Gamma^s_{\underset{\vee}{mn}}$. This, in fact, turns out to be the case, for if we define

$$T'^s_{\underset{\vee}{mn}} = T^s_{\underset{\vee}{mn}} + \delta^s_m \varphi_n - \delta^s_n \varphi_m ,$$

where φ_n is an arbitrary vector, then

$$\Gamma'^s_{\underset{\vee}{mn}} = \Gamma^s_{\underset{\vee}{mn}} .$$

Dirac's equations ([3]) for a field with sources are

$$A^\mu A_\mu = k^2 , \tag{6}$$

$$\frac{\partial}{\partial x_\nu}\left\{\frac{\partial A_\mu}{\partial x^\nu} - \frac{\partial A_\nu}{\partial x^\mu}\right\} = \lambda A_\mu . \tag{7}$$

Here there are five equations and five field variables λ, A_μ, so we expect no identities. The strength is therefore given by

$$\Omega_n = 5\binom{4}{n} - \binom{4}{n} - 4\binom{4}{n-2} ,$$

$$\sim \binom{4}{n}\frac{24}{n} .$$

The variable λ, which appears in an undifferentiated form in (6) and (7), may be eliminated and we obtain the four equations

$$\frac{\partial}{\partial x_\nu}\left\{\frac{\partial A_\mu}{\partial x^\nu} - \frac{\partial A_\nu}{\partial x_\mu}\right\} = \frac{1}{k^2} A^\alpha \frac{\partial}{\partial x_\nu}\left\{\frac{\partial A_\alpha}{\partial x^\nu} - \frac{\partial A_\nu}{\partial x^\alpha}\right\} A_\mu ,$$

for the four field variables A_μ. The strength is then given by

$$\Omega_n = 4\binom{4}{n} - 4\binom{4}{n-2} \sim \binom{4}{n}\frac{24}{n} ;$$

the same as previously. Thus Dirac's equations are weaker than the classical Maxwell equations.

My thanks are due to Dr. C. W. KILMISTER for whose assistance I am extremely grateful.

Modulation of the Electrical Conductivity by Surface Charges in Metals.

G. Bonfiglioli and E. Coen

Istituto Elettrotecnico Nazionale G. Ferraris - Torino

R. Malvano

Istituto di Fisica dell'Università Torino

(ricevuto il 28 Giugno 1955)

In the present paper we report some preliminary measurements on the effect of conductivity modulation by electrical charges brought, by a transverse electric field, at the surface of a thin flat metal specimen: (T.E. field effect).

In the early stages of the transistor developement the same effect was discovered in semiconductors (Germanium, Silicon): evidently the low density of current carriers made the experiment very easy to be carried on: the physical information gained in this case was concerned with the density of carriers and the existence of « surface states » [1-3]. Quite apart from the much greater experimental difficulties, that minimize the effect to be expected (due to the enormous density of carriers) there is no reason why such an effect could not be detected in metals.

Fig. 1 shows the circuit used in our experiment.

The specimen, of resistence R, is mounted on an arm of a high sensitivity ($\sim 10^{-6}$), good precision Wheatstone bridge. The regulable H.V. power supply

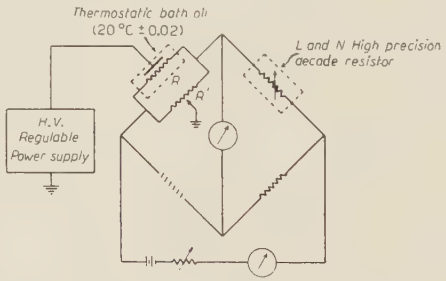

Fig. 1.

provides a transverse electric field sufficient to induce, on the specimen, a suitable surface charge density to get a measurable effect of conductivity variation.

The used specimen (thin metallic films in order to handle so little an amount of material to be able to sensibly alter the average carrier density on it) were formed by evaporation in vacuum ($\sim 10^{-5}$ mm Hg) of the metal on a suitable insulating support. As support we

[1] W. Schockley: *Electrons and holes in semiconductors* (New York, 1950), pp. 29 ff.

[2] W. Schockley and G. L. Pearson: *Phys. Rev.*, **74**, 232 (1948).

[3] E. Low: *Proc. Phys. Soc.*, B **68**, 10 (1954).

used the best quality white mica which bears very high electric field intensity ($\sim 10^6$ V/cm) sufficient to get measurable effects.

The metals tested belonged to widely different groups (Au, Bi, Sb).

The average thicknesses (100...2 000Å) of the evaporated layers were evaluated using a spectrophotometric titration against specimens of known metal content.

remark that in this case the effect is:

a) not linear;

b) not completely reversible.

Since the interpretation of the above preliminary results is not an easy matter, a complete discussion of the experiment will appear elsewhere (4).

Anyway, as a tentative conclusion, we may say that the transverse electric

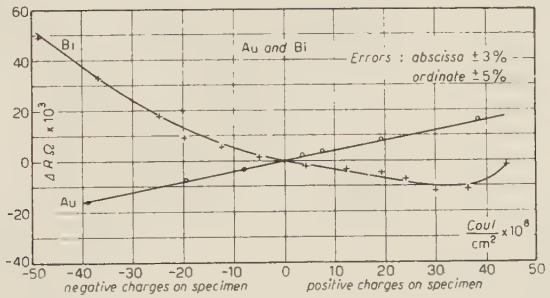

Fig. 2.

As an example we report in fig. 2 the experimental results for specimens of Bi and Au.

The main results obtained may be summarized as follows:

1) in Au, noble monovalent metal, with purely electronic conduction (negative Hall effect), due to nearly free electrons, an increment of the electron density causes the conductivity σ to *increase linearly*;

2) in Sb, multivalent semimetal, with electrons + holes conduction, and a very high Hall effect (normally positive, as in our specimens), an increase of the electron density causes σ to *increase linearly*, as in the Au case;

3) in Bi, multivalent semimetal, with electrons + holes conduction, and very high, impurity sensitive, Hall effect (normally negative, in our case positive), an increment of the electron density causes σ *to decrease*. Besides we must

field effect in metal seems to be almost a purely surface phenomenon, the electrical charges brought at the surface of the specimen moving along the metal surface with a mobility quite different from the bulk ones. Its value has been calculated for each specimen combining the value of the resistence with the value of the Hall effect coefficient measured in a conventional manner (5). Furthermore in the case of Bi the conductivity modulation does not seem to be a purely electronic phenomenon; but it seems also complicated by some lattice distorsion, that takes place possibly at the true metal surface, and may be caused by the changed electronic density, and responsible of the irreversibility and non linearity of the T.E. field effect.

(4) G. Bonfiglioli, E. Coen and R. Malvano: in press in the *Phys. Rev.*

(5) G. Bonfiglioli, E. Coen and R. Malvano: in press in the *J.A.P.*

Energy Measurements with a Plastic Scintillator.

F. Boreli and B. Grimeland (*)

Institute of Nuclear Sciences « Boris Kidrich » - Belgrade, Yugoslavia

(ricevuto il 1° Luglio 1955)

For organic scintillators the pulse height due to heavy particles is not a linear function of the particle energy ([1,2]). Birks ([2]) has given the following formula for the connection between the specific fluorescence $\mathrm{d}S/\mathrm{d}r$ and the specific energy loss $\mathrm{d}E/\mathrm{d}r$:

$$\frac{\mathrm{d}S}{\mathrm{d}r} = \frac{A\,\mathrm{d}E/\mathrm{d}r}{1 + kB\,\mathrm{d}E/\mathrm{d}r}. \tag{1}$$

According to Birks' theory $A\,\mathrm{d}E/\mathrm{d}r$ represents the number of ionised or excited molecules per unit length capable of primary photon emission, and $kB\,\mathrm{d}E/\mathrm{d}r$ represents the probability of quenching by molecular interaction etc., relative to the probability of primary photon emission. If $\mathrm{d}E/\mathrm{d}r$ is small, which is the case for electrons, one can write:

$$\frac{\mathrm{d}S}{\mathrm{d}r} = \frac{\mathrm{d}E}{\mathrm{d}r}, \tag{2}$$

or

$$S = AE. \tag{3}$$

For electrons, therefore, the pulse height should be a linear function of the energy, and this has been found experimentally to be the case for anthracene ([3]). For α-particles, on the other hand, $\mathrm{d}E/\mathrm{d}r$ is great and ([1]) may be written:

$$\frac{\mathrm{d}S}{\mathrm{d}r} = \frac{A}{kB}, \tag{4}$$

or

$$S = \frac{Ar}{kB}. \tag{5}$$

The pulse height for α-particles should, therefore, be proportional to the range of the particles in the scintillator, and this has also been verified experimentally for anthracene ([2]). The constant A is given by

$$A = \frac{S_{\mathrm{el}}}{E_{\mathrm{el}}}. \tag{6}$$

E_{el} is the electron energy and S_{el} is the electron pulse height which is usually measured in volts. The magnitude of A will depend upon the amplification used

(*) On leave from the Joint Establishment of Nuclear Energy Research, Kjeller per Lillestrom, Norway.

([1]) C. J. Taylor, W. K. Jentschke, M. E. Remley, F. S. Eby and P. G. Kruger: *Phys. Rev.*, **84**, 1034 (1951).

([2]) J. B. Birks: *Phys. Rev.*, **84**, 364 (1951); *Proc. Phys. Soc.*, A **64**, 874 (1951) and *Scintillation Counters* (London, 1953).

([3]) J. I. Hopkins: *Phys. Rev.*, **77**, 406 (1950); *Rev. Scient. Instr.*, **22**, 29 (1951).

and has no general interest. kB may be determined when measurements are made with both electrons and α-particles under the same conditions. One has then

$$kB = \frac{S_{el} E_{\alpha}}{S_{\alpha} E_{el}} . \tag{7}$$

kB is a constant for the scintillating material, and does not depend upon the amplification, voltage on the PM tube etc. Under the assumption that the stopping power of the scintillator relative to air does not vary with energy, an assumption which is only approximately correct, kB may be expressed in cm of air per MeV. BIRKS [2] measured this constant for anthracene and found a value of 7.15 cm/MeV. It is supposed that the constant will have approximately this value for all solid organical scintillators in crystalline form, and measurements by HARRISON [4] and REYNOLDS [5] on terphenyl in solutions also gave values very similar to that obtained by BIRKS. As far as is known to the authors, no values have as yet been published for plastic scintillators, and in order to use such a scintillator for measurements of proton energies it was necessary to determine the constant kB for this scintillator.

The plastic scintillators used consisted of tetraphenyl-1-1-4-4 butadiene-1-3 dissolved in polystyrene, and they were made in France [6]. A Polonium α source gave a collimated beam of α-particles and the distance between the source and the scintillator could be varied continuously. It can be seen from fig. 1 that the pulse height is in this case a linear function of particle range. No source of monoenergetic electrons was available when the experiments were carried out, and it was necessary, therefore, to use Compton electrons. Sources of ^{137}Cs and ^{65}Zn were used. ^{137}Cs emits a γ-ray with an energy of 0.663 MeV and ^{65}Zn emits a γ-ray with an energy of 1.11 MeV. This corresponds to maximum energies of the Compton electrons

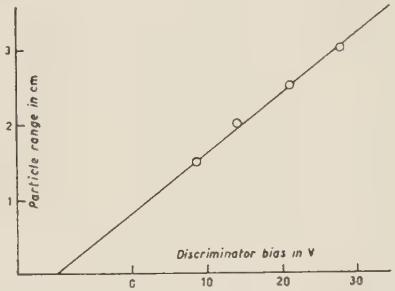

Fig. 1. – Connection between pulse height and particle range for α-particles in plastic scintillator.

of 0.478 MeV and 0.900 MeV respectively. The Compton peaks obtained for ^{137}Cs and ^{65}Zn are shown in fig. 2. The middle point of the steep slope of the curves is taken to correspond to the maximum energy of the Compton electrons. A straight line through the two points obtained also goes through the true zero point of the discriminator, and this indicates the linear relation between pulse height and energy. To obtain a further check of the linearity, measurements were made with a cobalt source. Cobalt emits two γ-lines, with energies of 1.33 MeV and 1.17 MeV. The corresponding maximum energies for Compton electrons are 1.117 MeV and 0.965 MeV. Obviously one does not obtain two distinct Compton peaks in this case, and the most reasonable procedure seems to be, therefore, to suppose the middle point of the steep slope to correspond to the mean energy, that is to 1.04 MeV. The result obtained in this way, once more bears out the linear relation between energy and pulse height.

In this way the value of the constant kB for the plastic scintillator was determined to be 10.5 cm/MeV. To check the method used, the same mea-

(4) F. B. HARRISON: *Nucleonics*, **10** (1952), no. 6, 40.

(5) G. T. REYNOLDS: *Nucleonics*, **10** (1952), no. 7, 46.

(6) L. PICHAT and Y. KOECHLIN: *Journ. Chim. Phys.*, **48**, 225 (1951).

surements were made with an anthracene crystal, and in this case a value of 6.80 cm/MeV was obtained, which agrees reasonably well with Birks' value. It is quite clear, therefore, that the constant B has a higher value for the plastic scintillator than for anthracene, and this indicates that relatively more molecules are damaged in the plastic scintillator as a result of the irradiation. It is known that plastic materials which are exposed to strong irradiation in nuclear reactors may change completely some of their physical properties, and perhaps there is a certain connection between this two phenomena.

In the last years scintillation counters have been used on many occasions to measure the energy of neutrons [7-11].

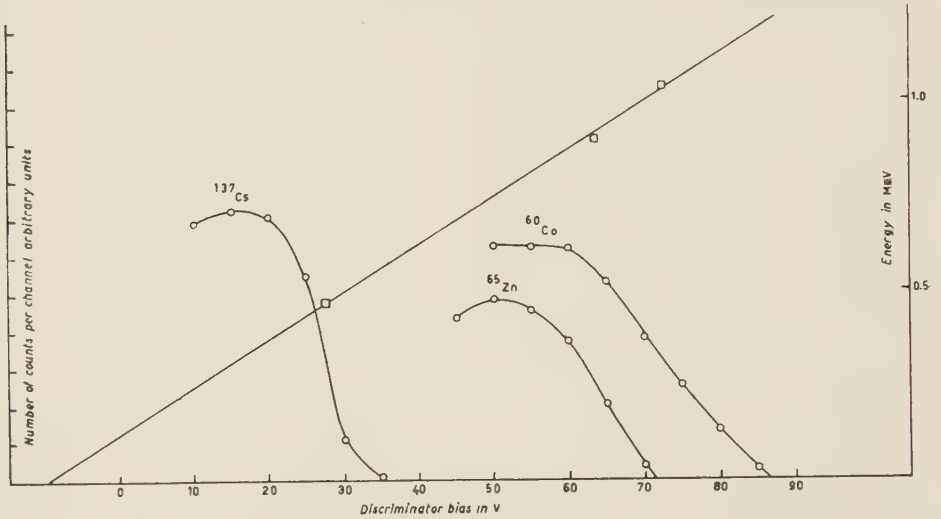

Fig. 2. – Measurements on Compton electrons. The ordinate scale for the bias curves marked ^{137}Cs, ^{65}Zn and ^{60}Co is on the left side, the energy scale for the straight line is on the right side.

What is actually measured is the energy spectrum of the recoil protons. In order to do this, the relation between pulse height and energy for protons must be known, and this relation can be derived from [1]. One has:

$$dS = A \frac{dE}{1 + kB\,dE/dr}, \tag{9}$$

or

$$dS = Af(E). \tag{10}$$

To determine $f(E)$, dE/dr must be known as a function of energy, and this is given in « Experimental Nuclear Physics I », edited by E. Segrè [12]. The functions $f(E)$ and $F(E) = \int_0^E f(E)\,dE$ is plotted in fig. 3 with $kB = 10.5$ cm/MeV — plastic scintillator and $kB = 7.0$ cm/MeV — anthracene. The relation between pulse height and energy is given by

$$S = AF(E), \tag{11}$$

(7) R. A. Allen, L. E. Beghian and J. M. Calvert: *Proc. Phys. Soc.*, **65**, 295 (1952).

(8) M. S. Poole: *Proc. Phys. Soc.*, **65**, 453 (1952).

(9) P. Shapiro, V. E. Scherrer, B. A. Allison and W. R. Faust: *Phys. Rev.*, **95**, 751 (1954).

(10) R. E. Segel, C. D. Swartz and G. E. Owen: *Rev. Sci. Instr.*, **25**, 140 (1954).

(11) E. A. Eliot, D. Hicks, L. E. Beghian and H. Halban: *Phys. Rev.*, **94**, 144 (1954).

(12) E. Segrè: *Experimental Nuclear Physics* (New York, 1953), p. 188.

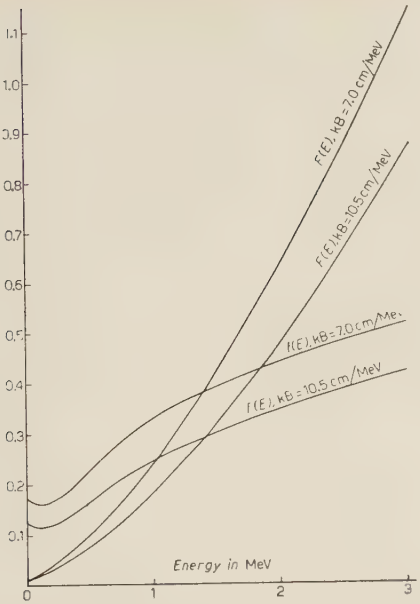

Fig. 3. – $f(E)$ and $F(E)$ for plastic scintillator and anthracene crystal.

where A must be determined from measurements on electrons. If the pulse height distribution of the recoil protons is given by $N(S)$, their energy distribution will be given by

$$N_1(E) = N(S)Aj(E) . \tag{12}$$

In the present experiments neutrons from the (D, D) reaction were used. The deuterons had an energy of 150 KeV, which gives an energy of 2.5 MeV to the neutrons which leave the target normal to the deuteron beam. The target consisted of heavy ice. Different pieces of the plastic scintillator were tried. They were all cylindrical, and the largest had a diameter of 3.4 cm and a height of 4.5 cm. The pulse height distribution and the corresponding energy distribution obtained with this large scintillator are given in fig. 4. It is reasonable to assume the middle point of the steep slope of the curve to correspond to the maximum proton energy. This again equals the neutron energy which in this case is known to

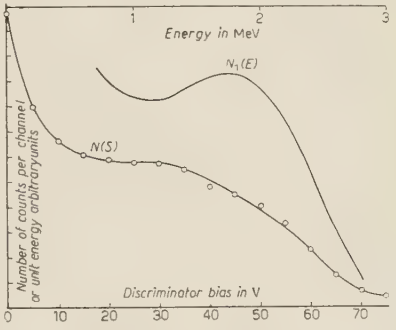

Fig. 4. – Pulse height distribution $N(S)$ for protons in plastic scintillator. The energy distribution $N_1(E)$ according to formula (12) is also given.

be 2.5 MeV, and this agrees reasonably well with the energy distribution curve. Curves obtained with an anthracene crystal are shown in fig. 5. kB was taken

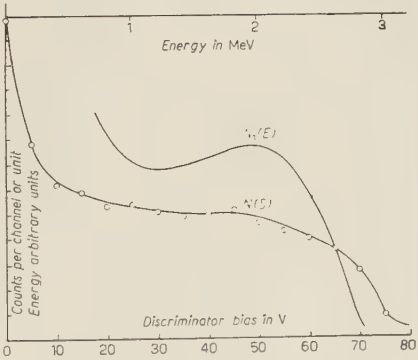

Fig. 5. – Pulse height distribution $N(S)$ for protons in anthracene crystal. The energy distribution $N_1(E)$ according to formula (12) is also given.

to be equal to 7.0 cm/MeV. The resolution is better with anthracene, but the plastic scintillators on the other hand can be obtained in much larger sizes, and when the number of neutrons is small, this may offer an advantage.

The Fast Ionization Chamber in the Study of α-Radioactivity in Air.

U. Facchini and A. Malvicini
Laboratori C.I.S.E. - Milano

(ricevuto il 5 Luglio 1955)

In a recent paper [1] we studied the behaviour of argon nitrogen mixtures as filling gas of fast ionization chambers and we showed that the electron collection in these mixtures is not practically influenced by small quantities of oxygen.

With such mixtures it is possible to operate a fast ionization chamber easily and quickly thus avoiding the necessity of the good vacuum and the careful purification of gases required when using unmixed pure gases, such as argon or nitrogen. The linearity of the chamber α-particle spectra measurements is as good as in the case of pure gases.

The chamber used in these experiments is the same described in [1]. The chamber is filled and operate in the same way.

The air, which is under examination is sucked through an electrical discharge between a few scores of sharp points and an aluminum plate; in this way most of the radioactive contaminations contained in the air are deposited on the plate in a thin layer. This method of collecting radioactive products of the air has been described and extensively studied by G. Aliverti [2].

The plate is quickly put in the ionization chamber and the energy spectrum of α-particles is measured at different times.

The results obtained with ordinary air are shown in fig. 1 (*a*, *b*, *c*) the quantity of air under examination being 1 cubic metre and the time of flow about 20 min. The air was taken in the basement of our laboratory.

The spectrum taken between the 22-nd and 30-th minute after the beginning of the flow is shown in fig. 1*a* where the line of RaA (5.99 MeV) and of RaC′ (7.68 MeV) can be noted. The spectrum in fig. 1*b* was taken between the 40-th min and 50-th. It can be seen that the RaA line has disappeared and the small peak at 6.05 MeV is due to the ThC; the ThC′ line at 8.77 MeV is clearly visible.

In fig. 1*c*, corresponding to a time between the 200-th min and the 460 min, it is noted that the RaC′ line has decayed while the ThC′ lines have maintained a stationary intensity.

The figures are in agreement with the

(1) U. Facchini, A. Malvicini: *Nucleonics*, **13**, no. 4, 36 (1955); *Nuovo Cimento*, **1**, 1255 (1955).

(2) G. Aliverti: *Nuovo Cimento* (1931-32); *Zeits. f. Geophys.*, **9**, 16 (1933).

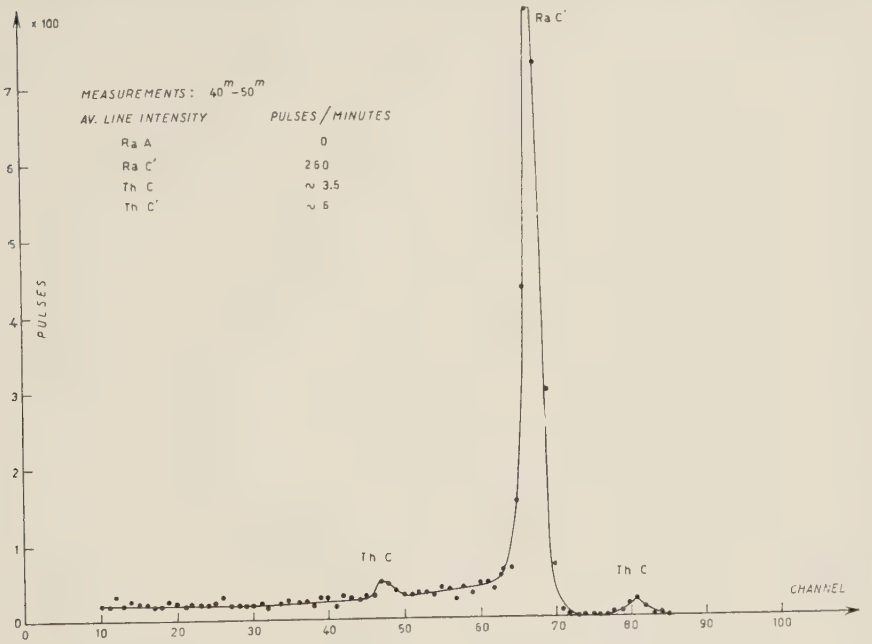

Fig. 1*a*. – α spectrum from ordinary air: air volume: 1.06 m³; time of flow 20 min; measurement: 22÷30 min.

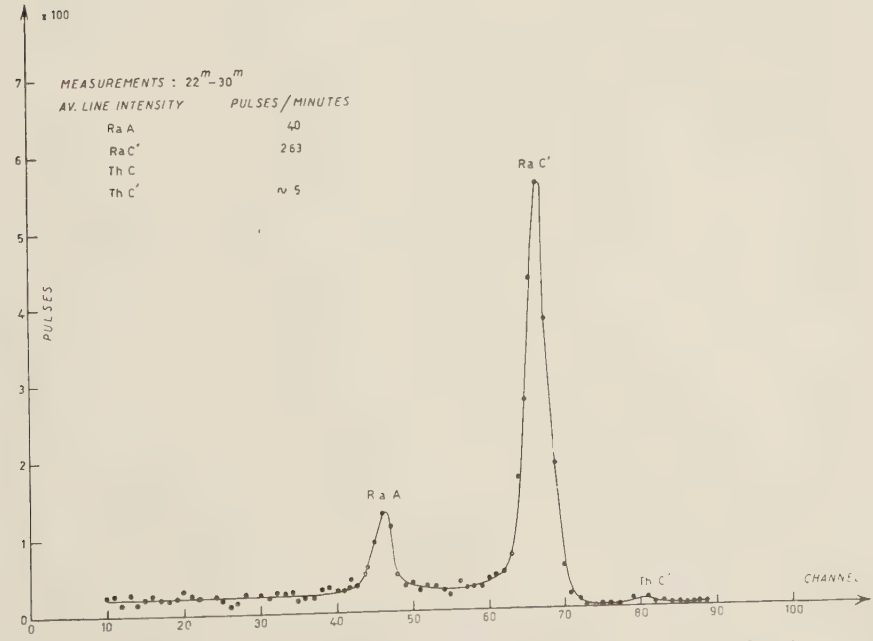

Fig. 1*b*. – α spectrum from ordinary air: air volume: 1.06 m³; time of flow 20 min; measurement: 40÷50 min.

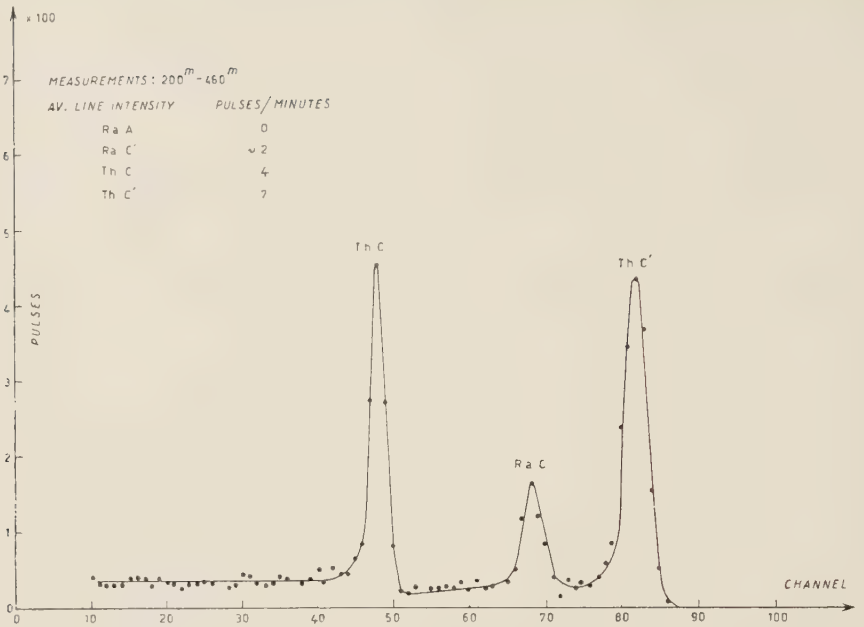

Fig. 1c. – α spectrum from ordinary air: air volume: 1.06 m³; time of flow 20 min; measurement: 200÷460 min.

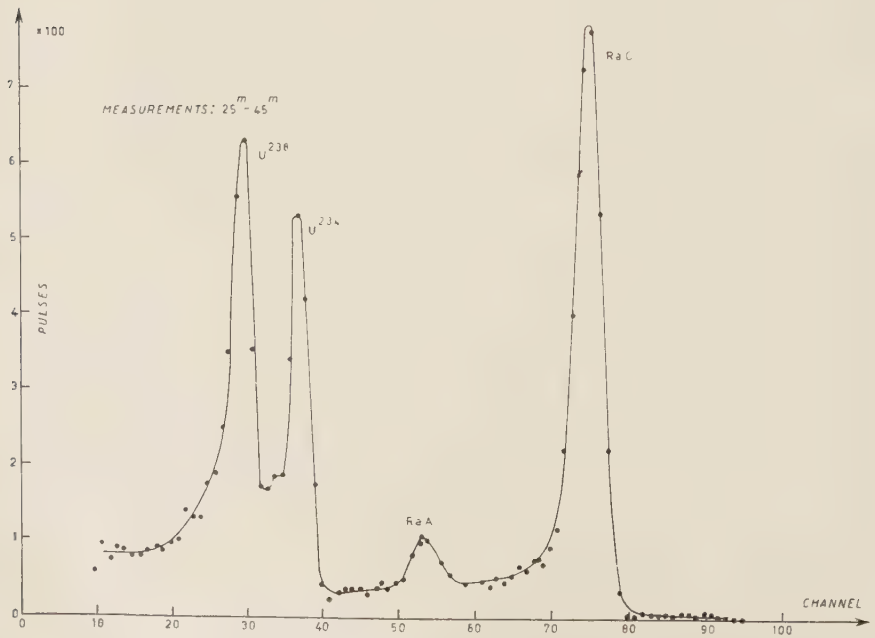

Fig. 2. – α spectrum from air contaminated with uranium: air volume: 1 m³: time of flow 20 min; measurement: 25÷45 min.

well known decay schemes of these radionuclides. Taking into account the decay time of the different nuclides it is possible to obtain their relative concentration in air. When the method is calibrated, the absolute concentrations are obtained easily.

The method described is very sensitive: ordinary air can be analyzed without any difficulty. The yield of collection of radioactive deposits is greater than 50%. The background of the ionization chamber is often less than 1 pulse per minute and depends on the cleanness of the electrodes, this background is made of pulses of different amplitude.

When an α-particle line is measured by means of a pulse analizer the pulses are collected by a certain number of channels (5-6).

The background pulses in these channels form only a small percentage of the total background; i.e. 2 to 3 pulses/hour. It is therefore possible to reveal a line of α particles when the total number of pulses on the corresponding channels is of the order of 20 pulses/hour.

When, for instance, the analyzed volume of air is 1 m^3, a radionuclide can be revealed when its concentration in the air is of the order of $5 \cdot 10^{-13}$ Curie/m^3 a very low one.

The method described above can be used for studying air contaminated with α-active elements such as Pu, U, Po, etc. This will be of interest to uranium or plutonium plants and hot laboratories where the air is contaminated. Fig. 2 shows the α-spectrum obtained from 1 m^3 of air taken in a uranium workshop.

The uranium activity can be easily and quickly measured and distinguished from the usual α-lines (RaA, RaC′, etc.) of ordinary air, without having to wait for the decay of these lines. This is also true in the case of plutonium where the method described can be even useful.

The authors thank prof. G. Bolla for his kind interest.

The Lifetime of the τ-Meson.

W. Alvarez and S. Goldhaber
Radiation Laboratory - Berkeley, California

(ricevuto il 7 Luglio 1955)

Now that K-mesons are available in large numbers from proton synchrotrons, experiments will soon yield precise values for the lifetime, or lifetimes, of the K-mesons. Exposures of emulsions to K-particles have been made by several groups at Berkeley, under quite different conditions, so far as distance from the target and magnetic resolution are concerned. If one knew the relative integrated currents on the targets for exposures with long and short flight paths, and if geometrical and resolution factors were properly taken into account, these experiments would yield a lifetime. Until recently, such an intercomparison of the results has appeared impossible. A method has now been found to tie the results of the various experiments together; this note describes the method and presents the lifetime so determined.

The earliest exposures ([1,2]) were made in a re-entrant well with no magnetic resolution, 90° to the target at a distance of about $11\frac{1}{2}$ inches. One set of exposures was carried out in a well which had a 0.1-inch aluminum window and another in a well which had a 1-inch aluminum window. Later work was done at a distance of about 106 inches from the target with magnetic resolution ([3]). The « well exposures » yielded a total of 10 τ-mesons from all groups in the laboratory. All groups tabulated the number of K_L and τ-mesons stopping at a range corresponding to a momentum of about 350 ± 15 MeV/c, and the number of all π-mesons stopping at the same range. We have also counted, in the stack exposed in the well that had a 0.1-inch aluminum window, the number of 350 ± 15 MeV/c protons and the number of π-mesons that stop at the range corresponding to 350 ± 15 MeV/c K-mesons. In the well exposures silver, lead, and brass targets were used. The ratio of stopped π mesons to protons, determined in the above exposures, was independent of the targets. The measurements of this ratio cannot be done for the exposure in the well that had the 1-inch aluminum window, since the desired protons stopped in the aluminum window. Using the π-mesons as secon-

([1]) Chupp, Goldhaber, Goldhaber, Goldsack, Lannutti, Smith and Webb: *Phys. Rev.*, to be published July 1, 1955.

([2]) Heckman, Goldhaber and Smith: *Bull. Am. Phys. Soc.*, **30**, no. 1, 63.

([3]) Kerth, Stork, Birge, Haddock and Whitehead: *Bull. Am. Phys. Soc.*, **30**, no. 3, 41.

dary standards, we can normalize the well exposures to the flux of 350 MeV/c protons.

In the magnetically resolved exposures ([4,5]), the K_L and τ-mesons were counted relative to the protons of the same momentum. These exposures yielded a total of about 60 τ-mesons from all groups in the laboratory. We then have the ratio of τ-mesons to protons of 350 MeV/c at two distances (proper time of flight + slowing-down time: $1.8 \cdot 10^{-9}$ s and $1.3 \cdot 10^{-8}$ s, respectively), which yields a mean life for the τ-mesons of

$$\tau_\tau = 1.0^{+07}_{-03} \cdot 10^{-8} \text{ s} .$$

The main contribution to the rms error comes from the small number of τ-mesons (10) found in the well exposure.

Unfortunately, the lifetime of the K_L-mesons as determined by this method is not trustworthy, even though the statistics are better. The difficulty is that we do not know the scanning efficiency for K_L-mesons for the method of scanning used in the well exposures. The efficiency for τ-mesons can be assumed to be greater than 0.9, since the τ-meson decay is so easily distinguished.

We wish to thank Dr. H. H. Heckman and the Richman group for making some of their unpublished results available to us.

This work was done under the auspices of the U. S. Atomic Energy Commission.

([4]) Birge, Haddock, Kerth, Peterson, Sandweiss, Stork and Whitehead: *Positive Heavy Mesons Produced at the Bevatron*, University of California Radiation Laboratory Report no. UCRL-3031, June 1955.

([5]) Chupp, S. Goldhaber, Goldhaber, Johnson and Webb: *K-Particle Production*, University of California Radiation Laboratory Report no. UCRL-3009, May 1955.

Further Evidence for the Existence of a Heavy K-Meson or Heavy Hyperon (*).

W. F. Fry, J. Schneps and M. S. Swami

Department of Physics, University of Wisconsin - Madison, Wisconsin

(ricevuto il 7 Luglio 1955)

A second example of a K-mesonic decay of a stopped secondary particle has been found in a pellicle stack exposed to cosmic rays (1). A photograph of the event is shown in fig. 1. In the event described in this note a slow particle (Track A) was ejected from a cosmic ray star of type (17+ 3N). After 44 μm the particle ejected a K-meson (Track B) of 42 MeV. From the general appearance of track A it is concluded that the particle stopped before ejecting the K-meson. Particle B traveled 10900 μm before it stopped. All of the track is contained in one plate. There are no associated tracks from the end of track B. The mass of particle B was determined by multiple scattering and grain density measurements. The results obtained are

constant sagitta . . $M = 1005 \pm 200\ m_e$.

grain density versus range . . . . . $M = 1024 \pm 150\ m_e$.

In addition, a measurement of the integrated gap length near the end of the range also indicates that the mass of particle B was intermediate between that of a proton and a π-meson. From the agreement of the various mass measurements we can only conclude that the particle which produced track B was a K-meson. The absence of a decay product from the stopped K-meson strongly suggests that it was captured and therefore we assume that it was negative. It is possible that a minimum track from the end of the K-meson could have been unobserved. however the probability is estimated to be no more than a few percent.

Although track A is not long the scattering along it suggests that it was produced by a singly charged particle of roughly protonic mass, as opposed to an α-particle or a heavier nuclear fragment.

The following possible interpretations have been considered; the K-meson was due to the nuclear absorption of 1) a « heavy » K-meson (track A), or 2) a « heavy » hyperon. It seems improbable that a stopped negative particle would decay before being absorbed. If particle A was captured by a heavy nucleus such as Ag or Br, the residual momentum from the K-meson might not produce an observable recoil.

It must be borne in mind that the K-meson may have decayed, with the

(*) Supported in part by the Graduate School from funds supplied by the Wisconsin Alumni Research Foundation.

Fig. 1. – A photograph is shown above of a cosmic ray star where a slow unstable particle (Track A) seems to have stopped and produced a K-meson (Track B).

decay track unobserved, and therefore the K-meson may have been a decay product of a positive particle (A). A search has been made in the opposite direction from the K-meson for the neutral unstable particle which might have been involved in the decay of particle A. No evidence for such a particle was found.

If particle A is assumed to be a « heavy » K-meson, the mass must have been greater than the rest mass of the K-meson plus the visible kinetic energy which is $965+86=1051\ m_e$, (the rest mass of the K-meson (B) is assumed to be that of a τ-meson, $965\ m_e$). On the other hand particle A may have been a hyperon which had a mass greater than $965+86+1836=2887$.

It is interesting to note that the kinetic energy of the K-meson in this event (42 MeV) is nearly the same as in the previously reported [1] event (43 MeV). It is possible that these two events are due to the same unstable particle.

All the tracks from the primary star were followed until they either left the emulsion stack or stopped. However, nothingunusual was observed.

The authors are grateful to Major D. G. Simons, USAF, fur exposing the emulsion stack in a balloon flight. Several discussions with the members of the high energy physics group, Professors R. G. Sachs and W. D. Walker have been helpful and stimulating.

[1] W. F. Fry, J. Schneps and M. S. Swami: *Phys. Rev.*, **97**, 1189 (1955).

Double Pion Production in Nucleon-Nucleon Collisions. Selection Rules for Production near the Threshold.

R. Gatto

Istituto di Fisica dell'Università - Roma
Istituto Nazionale di Fisica Nucleare - Sezione di Roma

(ricevuto l'8 Luglio 1955)

Recent experiments [1] have shown that double pion production in nucleon-nucleon collisions is a very frequent process. Its study, both experimental and theoretical, will deserve particular attention, for it could throw some light on the unknown pion-pion interaction. Present experimental data are insufficient to allow a theoretical study of double pion production along similar lines as the well known phenomenological analysis of single production due to Watson and Brueckner [2]. On the other hand it should prove useful to have a list of the transitions allowed on the basis of Pauli's principle, conservation of parity and angular momentum, and conservation of isotopic spin. The role played by these conservation theorems has appeared to be very important for the study of single pion production [2]. Moreover, conservation of total isotopic spin provides a large number of relationships between the different reactions, which should be useful in interpreting the experiments. The partial wave analysis is suitable for the study of the production process near the threshold, where it is expected that the final particles are principally produced with small relative orbital angular momenta. It may be that such a picture extends successfully up to energies far above the threshold. We shall always assume an angular momentum $l_n = 0$ for the relative motion of the two final nucleons, and angular momenta $l = 0$ or $l = 1$ for the relative motion of the two pions and $L = 0$ or $L = 1$ for the motion of the two pions relative to the nucleons. The whole analysis follows from Pauli's principle for the two nucleons, from the symmetry of the final wavefunction with respect to the two pions, and from the required invariance properties of the R-matrix with respect to spatial rotations, coordinate reflection and rotation in charge space. We classify the reactions according to whether they lead to a final triplet S-state for the two nucleons or a final singlet S-state. It is well known that the final state interaction is different for the two cases. Triplet S-state interaction being very strong, one may expect deuteron formation to occur frequently when this transition is allowed.

(1) W. B. Fowler, R. P. Shutt, A. M. Thorndike and W. L. Whittmore: *Phys. Rev.*, **95**, 1026 (1954).

(2) K. M. Watson and K. A. Brueckner: *Phys. Rev.*, **83**, 1 (1951).

a) $l = 0,\ L = 0$

	allowed transitions	matrix element
pp → pp + −	$^1S_0 \to {}^1S_0$	$\sqrt{\frac{1}{30}}\,R_1 + \sqrt{\frac{2}{3}}\,R_2$
pp → pp00	$^1S_0 \to {}^1S_0$	$\sqrt{\frac{1}{15}}\,R_1 - \sqrt{\frac{1}{3}}\,R_2$
pp → pn + 0	$^1S_0 \to {}^1S_0$	$-\sqrt{\frac{3}{10}}\,R_1$
	$\to {}^3S_1$ (forbidden)	
pp → nn + +	$^1S_0 \to {}^1S_0$	$\sqrt{\frac{3}{5}}\,R_1$
pn → pp0 —	$^1S_0 \to {}^1S_0$	$\sqrt{\frac{3}{10}}\,R_1$
pn → pn + −	$^1S_0 \to {}^1S_0$	$-\sqrt{\frac{2}{15}}\,R_1 + \sqrt{\frac{2}{3}}\,R_2$
	$^3S_1, {}^3D_1 \to {}^3S_1$	$\sqrt{\frac{2}{3}}\,R_3$
pn → pn00	$^1S_0 \to {}^1S_0$	$\sqrt{\frac{4}{15}}\,R_1 - \sqrt{\frac{1}{3}}\,R_2$
	$^3S_1, {}^3D_1 \to {}^3S_1$	$-\sqrt{\frac{1}{3}}\,R_3$

b) $l = 1,\ L = 0$

	allowed transitions	matrix element
pp → pp + −	$^3P_1 \to {}^1S_0$	$\sqrt{\frac{1}{2}}\,R_1'$
pp → pp00	forbidden	
pp → pn + 0	$^3P_1 \to {}^1S_0$	$-\sqrt{\frac{1}{2}}\,R_1'$
	$^3P_{0,1,2}, {}^3F_2 \to {}^3S_1$	$-R_2'$
pp → nn + +	forbidden	

b) $l=1$, $L=0$ *Continued:*

	allowed transitions	matrix element
$pn \to pp0$ —	${}^1P_1 \to {}^1S_0$	$-\sqrt{\frac{1}{3}}\,R_3'$
	${}^3P_1 \to {}^1S_0$	$\sqrt{\frac{1}{2}}\,R_1'$
$pn \to pn + -$	${}^1P_1 \to {}^1S_0$	$\sqrt{\frac{1}{3}}\,R_3'$
	${}^1P_1 \to {}^3S_1$	0 (forbidden)
	${}^3P_1 \to {}^1S_0$	0 (forbidden)
	${}^3P_{0,1,2}, {}^3F_2 \to {}^3S_1$	$-R_2'$
$pn \to pn00$	forbidden	

c) $l=0$, $L=1$

	allowed transitions	matrix element
$pp \to pp + -$	${}^3P_1 \to {}^1S_0$	$\sqrt{\frac{1}{30}}\,R_1'' + \sqrt{\frac{2}{3}}\,R_2''$
$pp \to pp00$	${}^3P_1 \to {}^1S_0$	$\sqrt{\frac{1}{15}}\,R_1'' \quad \sqrt{\frac{1}{3}}\,R_2''$
$pp \to pn + 0$	${}^3P_1 \to {}^1S_0$	$-\sqrt{\frac{3}{10}}\,R_1''$
	${}^3P_{0,1,2}, {}^3F_2 \to {}^3S_1$	0 (forbidden)
$pp \to nn + +$	${}^3P_1 \to {}^1S_0$	$\sqrt{\frac{3}{5}}\,R_1''$
$pn \to pp0-$	${}^1P_1 \to {}^1S_0$	0 (forbidden)
	${}^3P_1 \to {}^1S_0$	$\sqrt{\frac{3}{10}}\,R_1''$
$pn \to pn + -$	${}^1P_1 \to {}^1S_0$	0 (forbidden)
	${}^1P_1 \to {}^3S_1$	$\sqrt{\frac{2}{3}}\,R_3''$
	${}^3P_1 \to {}^1S_0$	$-\sqrt{\frac{2}{15}}\,R_1'' + \sqrt{\frac{2}{3}}\,R_2''$
	${}^3P_{0,1,2}, {}^3F_2 \to {}^3S_1$	0 (forbidden)

c) $l=0$, $L=1$ *Continued:*

	allowed transitions	matrix element
pn → pn00	${}^1P_1 \to {}^1S_0$	0 (forbidden)
	${}^1P_1 \to {}^3S_1$	$-\sqrt{\frac{1}{3}}\,R_3''$
	${}^3P_1 \to {}^1S_0$	$-\sqrt{\frac{4}{15}}\,R_1''-\sqrt{\frac{1}{3}}\,R_2''$
	${}^3P_{0,1,2}, {}^3F_2 \to {}^3S_1$	0 (forbidden)

d) $l=1$, $L=1$

	allowed transitions	matrix element
pp → pp + —	${}^1S_0, {}^1D_2 \to {}^1S_0$	$\sqrt{\frac{1}{2}}\,R_1'''$
pp → pp00	forbidden	
pp → pn + 0	${}^1S_0, {}^1D_2 \to {}^1S_0$	$\sqrt{\frac{1}{2}}\,R_1'''$
	${}^1S_0, {}^1D_2 \to {}^3S_1$	R_2'''
pp → nn + +	forbidden	
pn → pp0 —	${}^3S_1, {}^3D_{1,2} \to {}^1S_0$	$\sqrt{\frac{1}{3}}\,R_3''$
	${}^1S_0, {}^1D_2 \to {}^1S_0$	$\sqrt{\frac{1}{2}}\,R_1'''$
pn → pn + —	${}^3S_1, {}^3D_{1,2} \to {}^1S_0$	$\sqrt{\frac{1}{3}}\,R_3'''$
	${}^3S_1, {}^3D_{1,2,3}, {}^3G_3 \to {}^3S_1$	0 (forbidden)
	${}^1S_0, {}^1D_2 \to {}^1S_0$	0 (forbidden)
	${}^1S_0, {}^1D_2 \to {}^3S_1$	$-R_2''$
pn → pn00	forbidden	

Phase Shift Analysis for Negative Pion-Proton Scattering at 187 MeV.

E. Clementel, G. Poiani and C. Villi

Istituti di Fisica dell'Università di Padova e di Trieste
Istituto Nazionale di Fisica Nucleare - Sezione di Padova

(ricevuto il 9 Luglio 1955)

Recently extensive phase shift analyses of the scattering of negative pions on hydrogen have been carried out by means of electronic computers [1] and graphical methods [2], in the latter case assuming either $\alpha_{11} = \alpha_{13} = \alpha_{31} = 0$ [3] or only $\alpha_{11} = \alpha_{13} = 0$ [4]. In this note an analysis of the scattering data at 187 MeV for negative pions [5] will be carried out using the analytical method outlined in a previous paper [6].

We assume that the P-wave phase shifts for isotopic spin $\frac{1}{2}$ are zero, i.e. $\boldsymbol{b}_+ = \boldsymbol{b}_- = \boldsymbol{b}_0$ and $\boldsymbol{c}_+ = \boldsymbol{c}_- = \boldsymbol{c}_0$. Although there is no evidence that this is true, it must be stressed however that the actual experimental situation do not provide a sound contrary evidence either. In fact, from the first of the following exact relations (*a*) $C_+ = 9C_- = (9/2)C_0$ and (*b*) $B_+ = 3(B_- + B_0)$, derived from the scattering theory under the assumption $\alpha_{11} = \alpha_{13} = 0$, it follows $C_0 = 2C_-$, which is fairly well satisfied, within experimental errors, between 120 and 217 MeV. This is one of the most trivial reasons why α_{11} and α_{13} cannot be determined with any realiability at the present level of experimental errors and appear to be strongly dependent on the input coefficients.

As primary data we use [5] the following six coefficients, fitting the angular distribution observed at six angles:

$\pi^- \to \pi^-$			$\pi^- \to \pi^0$		
A_-	B_-	C_-	A_0	B_0	C_0
0.107 ± 0.017	0.046 ± 0.026	0.407 ± 0.032	0.193 ± 0.032	-0.021 ± 0.039	0.744 ± 0.116

[1] F. de Hoffman, N. Metropolis, E. F. Alei and H. A. Bethe: *Phys. Rev.*, **95**, 1586 (1954).
[2] J. Ashkin and S. H. Vosko: *Phys. Rev.*, **92**, 1248 (1953).
[3] M. Glicksman: *Phys. Rev.*, **94**, 1335 (1954).
[4] R. L. Martin: *Phys. Rev.*, **95**, 1606 (1954).
[5] M. Glicksman: *Phys. Rev.*, **95**, 1045 (1954).
[6] E. Clementel, G. Poiani and C. Villi: *Nuovo Cimento*, September 1955; here quoted as I.

At this energy the total cross-section, yielded by transmission measurements, is $\sigma_T(-) = \sigma_T(\pi^-) + \sigma_T(\pi^0) = (63.5 \pm 1.6)$ mb, in good agreement with the value interpolated from the data of ASHKIN *et al.* (7). To be consistent with the starting assumptions, from relation (a) we determine $C_+ = 3.66 \pm 0.45$. The experimental quantities B_- and B_0 are affected by very large errors: it is therefore convenient not to include them in the calculations, as it would be required using the method suggested by ASHKIN and VOSKO. The only quantities relatively well defined are A_-, A_0 and $C_- = 2C_0$: these will be assumed as input coefficients. No calculations will be developed either on the basis of the total cross-section for negative or positive scattering. The latter has the value (5) $\sigma_T(\pi^+) = (190 \pm 10)$ mb. Phase shift analysis must be carried out with some precautions in this energy region where resonance is expected to occur. It is easy to realize that the 5.3% of error on $\sigma_T(\pi^+)$ would be misleading in the determination of the contribution of $T = \frac{1}{2}$ states. In fact, since we have agreed to neglect in first approximation the contribution of $P_{\frac{1}{2}}$ states for isotopic spin $\frac{1}{2}$, we have (6) $p_-(\alpha_1) = 3$ and $q_-(\alpha_1) = 0$. Then, from Eq. (I, 8) it is found

$$\cos 2\alpha_1 = 1 + (k^2/4\pi)[\sigma_T(\pi^+) - 3\sigma_T(-)] \,. \tag{1}$$

This equation exhibits one of the most critic features of the phase shift analysis for pion-proton scattering. It is clear that no states of isotopic spin $\frac{1}{2}$ would exist ($\alpha_1 = 0$) if $\sigma_T(\pi^+) = 3\sigma_T(-)$. The actual experimental situation shows that between 130 and 217 MeV this is only approximately true. It follows that if one uses in Eq. (1) the experimental cross-sections, the determination of α_1 would be based essentially on experimental errors, which is of course not very promising. For example, at 187 MeV the only information on α_1 is $0^\circ \leqslant |\alpha_1| \leqslant 63^\circ$. This result is obviously of no practical use because the uncertainty thus introduced would spread over the phase shifts for $T = \frac{3}{2}$ states. If one uses in Eq. (1) the mean values of the cross-sections, it is found $|\alpha_1| = 9.1^\circ$, a result in principle acceptable but probably casual. In fact, using for $\sigma_T(-)$ the value consistent with Ashkin's *et al.* measurements, it is found $|\alpha_1| = 23^\circ.3$. The experimental situation therefore requires a different line of attack, and the parametrization procedure allows to overcome at least partially these difficulties.

First we express in Eq. (1) the total cross-sections in terms of the quantities A, B and C. Then, taking into account all implications of the assumption $\alpha_{11} = \alpha_{13} = 0$, we substitute A_+, given by Eq. (1), in

$$A_+ = 9A_- + \mathrm{Re}\,(\boldsymbol{a}_+) + \tfrac{1}{2}[\mathrm{Re}\,(\boldsymbol{a}_+)\mathrm{Re}\,(\boldsymbol{a}_-) - \mathrm{Im}(\boldsymbol{a}_+)\,\mathrm{Im}\,(\boldsymbol{a}_-)] \,, \tag{2}$$

derived from Eq. (I.13). In this way we can express α_1 as a function of α_3, i.e.

$$\cos 2\alpha_1^{(\pm)} = \beta \pm (\beta^2 - \gamma)^{\frac{1}{2}} = f^{(\pm)}(\alpha_3) \,,$$

where

$$\beta(\alpha_3) = \frac{(1 - r_+/2)\varphi(r_\tau)}{1 - r_+} \,, \qquad \gamma(\alpha_3) = \frac{\varphi^2(r_+) - \sin^2 2\alpha_3}{2(1 - r_+)} \,,$$

$$\varphi(r_+) = 1 + 3(A_0 - 2A_-) - r_+/2 \,. \tag{5}$$

(7) J. ASHKIN, J. P. BLASER, F. FEINER, J. GORMAN and M. O. STERN: *Phys. Rev.*, **93**, 1129 (1954).

It follows that the integrated total cross-section for positive scattering depends also on α_3 through the relation

$$A_{+}^{(\pm)}(\alpha_3) = 3(A_0 + A_-) - 1 + f^{(\pm)}(\alpha_3) . \tag{6}$$

Calculations have been made with various combinations of « up » and « down » values of the input coefficients. A close agreement with the basic experimental situation is obtained by taking « up » values of A_- and A_0 with the « down » value of C_-, and viceversa. With this choice the integrated cross-section for the process $\pi^- \to \pi^-$ is (23.5 ± 0.61) mb. All other combinations have been found unable to reproduce correctly the initial experimental situation or conflicting with the experimental value of the total cross-section for positive scattering.

The (+)-type solution, given by Eq. (3), differs substantially from the (−)-type one, both in total cross-section and angular distribution for the process $\pi^+ \to \pi^+$. The phase α_3 has been varied within the interval $-45^\circ \leqslant \alpha_3 \leqslant +45^\circ$. In this interval $f^{(+)}(\alpha_3)$ and $A_{+}^{(+)}(\alpha_3)$ are surprisingly more stable than the $f^{(-)}(\alpha_3)$ and $A_{+}^{(-)}(\alpha_3)$ against variations of α_3. A reasonable agreement with $\sigma_T(\pi^+)$ has been found for $|\alpha_3| = 18^\circ$. It follows that $A_{+}^{(+)} = 0.89 \pm 0.14$ and $|\alpha_1^{(+)}| = 3^\circ.2 \pm 0^\circ$.W. The (−)-type solution has been rejected as giving a too low total cross-section (~ 160 mb). Inspection of Eq. (2) shows that α_1 and α_3 must have the same sign. Therefore, if we rely to the physics of the problem and assume repulsion in the S-state for isotopic spin $\frac{3}{2}$, both α_1 and α_3 must be taken as negative. The value found for α_3 is consistent with a linear dependence of this phase on the relative momentum, whereas the associated value of α_1 is in agreement with the general behavior of the quantity $\Delta = (\alpha_1 - \alpha_3)/k$ versus the relative momentum. In our case it is found $\Delta = 2 \cdot 3 \cdot 10^{-14}$ cm [8].

Since A_+, C_+ and α_3 are known, we solve Eqs. (4) and (5) of I to determine the cosines of the Fermi and Yang phase shifts. At this stage we are left with a complete ambiguity for the signs of the pair $(\sin 2\alpha_{33}^{(\pm)}, \sin 2\alpha_{31}^{(\mp)})$. Neglecting causality arguments [9], it follows that four solutions and therefore eight sets of phase shifts are mathematically possible. It is found that the experimental data are consistent with the condition $\sin 2\alpha_{33}^{(\pm)} > 0$ and $\sin 2\alpha_{31}^{(\pm)} < 0$, which gives $B_- = 0.038 \pm 0.004$ and $B_0 = 0.074 \pm 0.004$, instead of the least square values given in the Table. The coefficient of the $\cos\theta$ term in the differential cross-section for positive scattering is found to be $B_+ = 0.33 \pm 0.04$, showing that constructive interference between S and P-waves is operating at this energy. The values of the experimental coefficients A, B and C are in good agreement with those calculated at 188 MeV by DE HOFFMAN *et al.* [1] by means of phase angle interpolation. It follows that the Glicksman data with the new values of B_- and B_0 are not conflicting with the evidence that the inversion point for B_+ is located somewhere between 178 and 184 MeV, where the coefficient of the asymmetric part of the angular distribution for direct and charge-exchange scattering should change from negative to positive values, if the assumption $\alpha_{11} = \alpha_{13} = 0$ were correct.

The phase shifts consistent with 187 MeV scattering data are

$$\alpha_3 = -18^\circ \qquad \alpha_1 = -3.2^\circ \pm 0.2^\circ$$

$$\alpha_{33}^{(+)} = 55.1^\circ \pm 8.2^\circ \qquad \alpha_{31}^{(+)} = 149.1^\circ \pm 19.5^\circ \qquad \text{(Yang solution)},$$

$$\alpha_{33}^{(-)} = 82.5^\circ \pm 6.1^\circ \qquad \alpha_{31}^{(-)} = -14.6^\circ \pm 7.2^\circ \qquad \text{(Fermi solution)}.$$

[8] H. A. BETHE and F. DE HOFFMAN: *Introduction to Meson Theory* (Lecture Notes, Cornell University, 1953), p. 315.

[9] R. KARPLUS and M. A. RUDERMAN: *Phys. Rev.*, **98**, 771 (1955).

The negative sign for the Fermi $\alpha_{31}^{(-)}$ is apparently required by the behavior of the $\pi^+ \to \pi^-$ cross-section; attraction in the $P_{\frac{1}{2}}$, $T = \frac{3}{2}$ state would imply a negative B_- and a sensible distorsion on the differential cross-section. This result is in agreement with the suggestion that $\alpha_{31}^{(-)}$ is negative at all energies from 120 to 217 MeV.

The more drastic assumption that also α_{31} be zero alters the previous calculation in so far as the contribution from the $P_{\frac{3}{2}}$, $T = \frac{3}{2}$ state is concerned, being the determination of α_1 and α_3 dependent only on the assumption $\alpha_{11} = \alpha_{13} = 0$. In this case the two simple relations are immediately found

$$\cos 2\alpha_{33} = \tfrac{1}{2}(p_+ - 1); \qquad \sigma_T(\pi^+) = (2\pi/k^2)(3 - 2\cos 2\alpha_{33} - \cos 2\alpha_3) \,. \tag{7}$$

At 187 MeV $\alpha_{33} \sim 90^\circ$ and the total cross-section $\sigma_T(\pi^+)$ is very near to its resonance value.

We like to thank Dr. M. GLICKSMAN for useful correspondence.

On a Mechanical Analyzer for Proton-Proton Triplet Phase Shifts.

E. Clementel and C. Villi

Istituti di Fisica dell'Università di Padova e di Trieste
Istituto Nazionale di Fisica Nucleare - Sezione di Padova

(ricevuto il 9 Luglio 1955)

In a previous note [1] the triplet phase equations have been solved by means of a parametrization procedure based on expressing δ_0 and δ_1, for a given value of the experimental quantities z_1 and z_2, as functions of δ_2 and then determining δ_2 from the known value of z_1, the coefficient of $P_2(\cos\vartheta)$ appearing in the nuclear term of the proton-proton cross-section.

Experience gathered in successive calculations for various energies has shown that this procedure is rather lengthy, mainly because a reliable selection among all sets can be performed only provided δ_0 and δ_1 are parametrized for a large number of values of δ_2: Since the analysis of scattering data implies the variation, within experimental errors, of the quantities z_i, the same procedure must be repeated several times for a given energy and many of the sets thus found must be rejected because conflicting with the continuity requirements of all phase shifts versus proton energy. It was felt therefore as highly desirable to seek for a quick method to find out « good » solutions and then apply the parametrization only to them in order to determine the phase shifts with a high degree of accuracy, avoiding in this way all solutions later to be rejected.

With this aim in view, the triplet equations were examined to see whether it would be possible to set up a graphical method allowing a straightforward determination of the δ_j, once the experimental quantities z_i are known. But, as it will be seen later, the use of graphical methods is convenient only to check the consistency of solutions or to determine two phase shifts when the third is known.

The other alternative which has been investigated was to find out the kinematics underlying the triplet phase shift equations to determine the working principle of a mechanical analyzer giving a quick answer, otherwise obtainable through tedious calculations. This at-

[1] L. Beretta, E. Clementel and C. Villi: *Nuovo Cimento*, **1**, 739 (1955). The procedure given in this note has been simplified, avoiding the fourth degree equation in $\sin K_0$ by direct use of Eqs. (1). In this way, solutions not compatible with the best fit are automatically eliminated. This new procedure will be given in a forthcoming paper concerned with the general formulation of the phase shift analysis problem in proton-proton scattering.

tempt happened to be successful and this note is devoted to it.

From the definition of z_1, z_2 and z_4 the following expressions can be easily

to the multiplicity of the total angular momentum quantum number j, whereas the points P_1 and P_2 depend on the energy at which the proton-proton

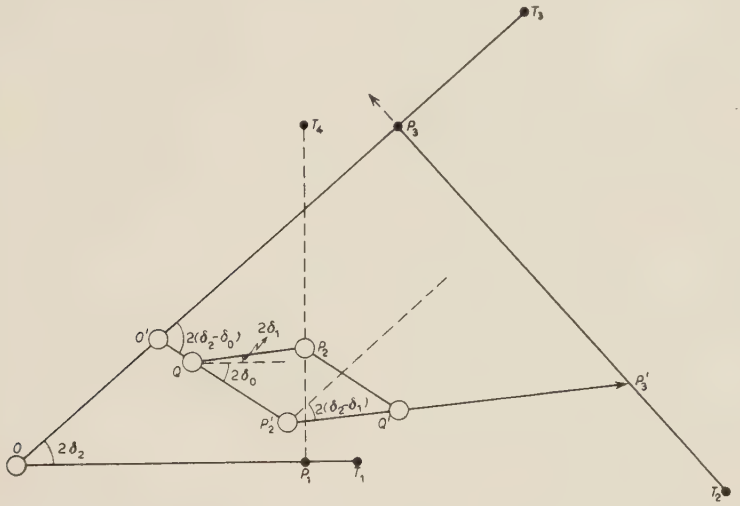

Fig. 1. – The working principle of a mechanical analyzer for proton-proton triplet phase shifts.

derived

$$(1)\qquad \begin{cases} \sum_0^2 (2j+1)\cos 2\delta_j = r_1, \\ \sum_0^2 (2j+1)\sin 2\delta_j = r_2, \end{cases}$$

$$(2)\qquad \sum_0^1 (2+j)^2 \cos 2(\delta_2 - \delta_j) = r_3,$$

where

$$(3)\qquad \begin{cases} r_1 = 9 - 2z_1, \qquad r_2 = 2z_2, \\ r_3 = 13 - 8(z_1 - z_4/2)\,. \end{cases}$$

The mechanical translation of Eqs. (1) and (2) is given in Fig. 1. At a distance r_1 from the origin O ($OT_1 = 9$) we determine the point P_1 and on the perpendicular to OT_1, at a distance r_2 from P_1, we fix the point P_2. This point is connected with the origin O through the articulated system $[OO'QP_2]$ where $OO' = 5$, $O'Q = 1$ and $QP_2 = 3$. The system $[OO'QP_2]$ is obviously related

scattering is considered. In this way Eqs. (1) are fullfilled. Since the arms OO', $O'Q$ and QP_2 are free to rotate around the junctions at O, O', Q and P_2, a limited variation of δ_0 and δ_1, as a function of δ_2, is allowed. This is the exact mechanical equivalent of the parametrization procedure used in the previous note [1]. To make things easy, we use in the mechanical scheme the geometrical properties of the parallelogram $[P_2QP_2'Q']$, all branches of which are articulated. The arm $O'QP_2' = 4$ is rigid at Q. Therefore, if we extend OO' up to the point T_3 in such a way that $OT_3 = 18$, the projection of $O'P_2'$ on OT_3 corresponds to the first term ($j = 0$) in Eq. (2). We now use the remaining experimental quantity r_3 to determine the point P_3 on the rigid axis OT_3 at a distance r_3 from O'. This distance, as well as OP_1 and P_2P_1, is kept fixed for a given energy during all operations. Then, we rigidly extend $P_2'Q'$ and connect its end-point with the axis P_3T_2 (= 13),

perpendicular to OT_3. Be P_3' the contact point. It is clear that when $P_2'P_3' = 9$ the whole system is frozen: Eqs. (1) and (2) are simultaneously satisfied and the triplet phase shifts, for a given energy, are obtained by direct reading. Since the positions of the points P_1, P_2 and P_3 depend on the energy, i.e. on the singlet phas shift ${}^1K_0$, it follows that the mechanical analyzer gives a direct answer for different energies pro vided the point P_3 is allowed to move along the axis OT_3, P_2 along P_1T_4 and P_1 along OT_1.

The kinematics of the computer shows the existence, for a given set of the experimental quantities r_i $(i = 1, 2, 3)$, of a maximum number of four resolution positions corresponding to four points of contact of the rigid arm $P_2'P_3'$ with the axis P_3T_2, two resolution positions being on one side and two on the other side of the axis OT_3. Inspection of the geometrical properties of the system reveals the existence of the following relations

$$\delta_i' - \delta_j' = \delta_j'' - \delta_i'' \quad (i, j = 0, 1, 2) \tag{4}$$

where the $\delta_{i,j}'$'s and the $\delta_{i,j}''$'s are solutions on the opposite side of the axis OT_3. As a check compare the solutions obtained in the analysis of 240 MeV proton-proton scattering [2]. The « associated » solutions are (A) and (C), (B) and (D). It is seen that the relations (4) are verified with an error of about 1.6°, which could be reduced by improving the parametrization of δ_0 and δ_1 as functions of δ_2.

For a given « good » δ_2 there exists one and only one set (δ_0, δ_1) consistent with Eqs. (1) and (2). However, if we disregard Eq. (2), two sets (δ_0, δ_1) are given by the computer for the same value of δ_2, consistent with Eqs. (1). In this case no contact exists of the axis $P_2'P_3'$ with the axis P_3T_3. This circumstance can easily be seen graphically. Suppose we fix δ_2. Then, Eqs. (1) read

$$\begin{cases} \sum_0^1 (2j+1)\cos 2\delta_j = x_1 \\ \sum_0^1 (2j+1)\sin 2\delta_j = y_1 \end{cases} \tag{5}$$

$$\begin{cases} x_1 = r_1 - 5\cos 2\delta_2 \\ y_1 = r_2 - 5\sin 2\delta_2 \,. \end{cases} \tag{6}$$

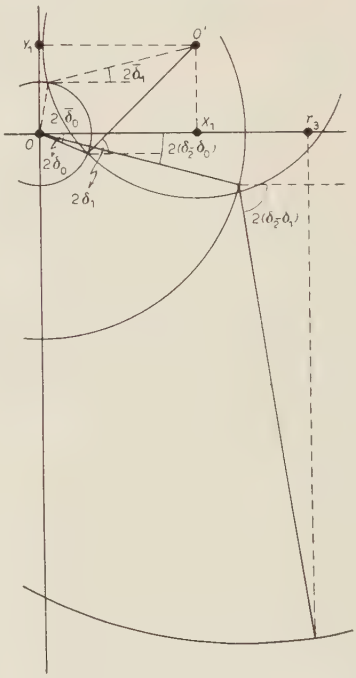

Fig. 2. – Graphical check of the set (*C*) for 240 MeV proton-proton scattering [2] ($\delta_2 = -18°.1$).

The graphical plot in Fig. 2, which may prove useful to check the consistency of any solution and can be directly derived from the mechanichal scheme, explains the situation. With some obvious changes it corresponds to the graphical check used for pion-proton scattering [3], where

[2] L. BERETTA, E. CLEMENTEL and C. VILLI: *Phys. Rev.*, **98**, 1526 (1955).

[3] E. CLEMENTEL, G. POIANI and C. VILLI: *Nuovo Cimento*, September 1955.

p^+ and s^+ correspond here to x_1 and respectively y_1, and the circle of radius 2 is substituted by a circle of radius 3. To be definite, the graph given in Fig. 2 has been drawn for the set (C) of 240 MeV proton-proton scattering ([2]), which has been also obtained by Klein at 260 MeV through a different procedure ([4]). From the graph it is clearly seen that only the solution (δ_0, δ_1) is consistent with Eq. (1) and with the experimental value of r_3, the other solution $(\bar{\delta}_0, \bar{\delta}_1)$ being consistent only with Eqs. (1). It is therefore clear that for proton-proton scattering there is nothing similar to the mechanism of « Fermi » and « Yang » solutions, characteristic of pion-proton scattering, because the third relation (Eq. (3)) is much more restrictive than the third relation of the pion-proton scattering (Eq. (3) of the paper quoted in reference ([3])), which clearly exhibits the Fermi-Yang ambiguity $\alpha_{33} - \alpha_{31} = (\frac{1}{2}) \sin^{-1} [4A_+ - r_+]^{\frac{1}{2}}$.

The mechanical computer, besides the determination of the δ_j in terms of S and P waves, may be used to solve all problems involved in a scattering analysis: the determination of one of the experimental quantities consistent with a given set of δ_j, the stability of the δ_j against variations of the z_i's, search for the continuity of the phase shifts versus the proton energy, etc.

Attempts have been made to select solutions according to polarization by limiting the mouvement of the end-point on the « polarization » axis P_3T_2. However, the complications so arising suggested as more convenient to carry on a mathematical selection, which is straightforward when the possible solutions have been found.

([4]) C. A. KLEIN: *Nuovo Cimento*, **1**, 581 (1955).

On the Dipole Selection Rule in ^{16}O.

G. Morpurgo

Istituto di Fisica dell'Università - Roma
Scuola di Perfezionamento in Fisica Nucleare - Roma

L. A. Radicati

Istituto di Fisica dell'Università - Napoli

(ricevuto il 9 Luglio 1955)

Devons [1] has recently mearused the half lives of several transitions in ^{16}O getting the following results:

$$(1) \qquad \begin{cases} \text{E1} & 7.1 \to 0 & \tau_1^{\text{exp}} \lesssim 8 \cdot 10^{-15} \\ \text{E3} & 6.19 \to 0 & 5 \cdot 10^{-12} \lesssim \tau_3^{\text{exp}} \lesssim 10^{-11} . \end{cases}$$

The purpose of the present note is to calculate τ_1 and τ_3 in order to see whether the violation of the dipole rule may simply be accounted for by Coulomb impurity [2] or whether it may give evidence of other effects [3].

Shell model in LS and JJ coupling has been used throughout [4], but in the following, we refer only to LS results which seem to give the better fit for the E3 transition.

Both the states at 6.13 MeV and 7.1 MeV have been assigned to the configuration $p^{11}d$. For the state at 7.1 MeV we have also considered the alternative possibility of a configuration $p^{11}2s$. A mixture of other configurations is probably necessary to improve the results: this is shown by the existence of the E2 transition from the 6.9 MeV state to the ground state which can be accounted for in a plausible way only by assuming configurational mixing.

However a rough calculation shows that for the transitions [1] the effect of configurational mixing does not change the results by more than a factor 2.

The calculations have been performed using oscillator wave functions

$$\psi_{n_1 n_2 n_3} \sim H_{n_1}(x) H_{n_2}(y) H_{n_3}(z) \exp[-r^2/4a^2]$$

with $a = 1.5 \cdot 10^{-13}$ cm.

---

[1] S. Devons, G. Manning and D. St. P. Bunbury: *Proc. Phys. Soc.*, A **68**, 18 (1955).
[2] L. A. Radicati: *Proc. Phys. Soc.*, A **67**, 39 (1954).
[3] G. Morpurgo: *Nuovo Cimento*, **12**, 60 (1954).
[4] A. M. Lane and L. A. Radicati: *Proc. Phys. Soc.*, A **67**, 167 (1954).

The E3 width depends on a^6 so that the value assumed for a is rather critical; on the other hand E1 depends on a^2 only. The above value of a has been chosen to give a fit up to a factor 2 of the E3 experimental width; the fit could be improved by configurational mixing and possibly by intermediate coupling.

The results for the calculated life times are:

$$\tau_3^{\text{calc}} \cong 2.5 \cdot 10^{-11} \text{ s} \qquad \begin{cases} \tau_1^{\text{calc}} \cong 0.7\ \alpha_d^{-2}\ 10^{-18} \text{ s} \ (p^{11}d) \\ \tau_1^{\text{calc}} \cong 0.7\ \alpha_s^{-2}\ 10^{-17} \text{ s} \ (p_{11}2s) \end{cases}$$

where α_d^2, α_s^2 are the Coulomb impurities for the $p^{11}d$ and $p^{11}2s$ configurations.

By comparison with the experimental value for τ_1^{exp} one gets:

$$\alpha_d^2 \gtrsim 10^{-4} \qquad \alpha_{2s}^2 \geqslant 10^{-3}\ .$$

The theoretical value ([2]) for α^2 calculated with the rame value of a as used here is

$$\alpha_{\text{calc}}^2 \cong 3 \cdot 10^{-3}\ .$$

We conclude therefore from the above figures that the violation of the dipole rule can be accounted for in terms of Coulomb impurity and nothing can be said at the moment from the experimental data about the magnitude of the mesonic effect ([3]).

Sulla efficienza di rivelazione dei fotoni a mezzo di scintillatori liquidi.

E. Beretta e G. Poiani

Istituto di Fisica dell'Università - Trieste
Istituto Nazionale di Fisica Nucleare - Sezione di Padova

(ricevuto il 14 Luglio 1955)

L'efficienza di rivelazione dei fotoni di diversa energia è stata oggetto, in questi ultimi tempi, di parecchie ricerche, volte specialmente allo scopo di determinare lo spettro energetico di emissione dei raggi X degli acceleratori (1). È evidente che sotto questo rispetto, gli scintillatori a cristallo (ad es. NaI(Tl)), presentano i maggiori vantaggi perchè la presenza di un elemento piuttosto pesante favorisce i processi di conversione dei fotoni.

Tuttavia le piccole dimensioni dei cristalli limitano l'efficienza raggiungibile; si è pensato perciò di poter superare questo limite ricorrendo agli scintillatori liquidi, che sopperiscono al minor assorbimento con la possibilità di realizzare grandi dimensioni, specialmente nella direzione di attraversamento dei fotoni.

Nella Tabella I sono stati riportati i cammini di assorbimento dei fotoni di 1, 10, 100 MeV relativi agli scintillatori liquidi e solidi più comunemente usati. Essi sono stati calcolati utilizzando i dati sulle sezioni d'urto totali, per i vari effetti, riportati da C. M. Davisson (2).

(1) M. R. Cleland, H. W. Koch: *Phys. Rev.*, **86**, 588 (1952); R. S. Foote, H. W. Koch: *Rev. Sci. Inst.*, **25**, 746 (1954).

(2) K. Siegbahn: *Beta and gamma ray spectroscopy* (Amsterdam, 1955), p. 857.

Tabella I. – *Cammini di assorbimento, in* cm, *dei fotoni di varia energia.*

	1 MeV	10 MeV	100 MeV
NaI(Tl)	4.67	7.35	4.31
Antracene . . .	11.9	26.5	39.2
Xilolo.	16.8	56.1	81.3
Toluolo	16.7	55.8	80.6
Fenilcicloesano .	15.1	51.0	70.4

Quando lo spessore attraversato dal fascio di fotoni diventa molto grande la quantità di luce raccolta diventa piccola per le scintillazioni prodotte lontano dalla superficie fotosensibile, perchè buona parte della luce o esce dallo scintillatore, o viene assorbita nella riflessione sulle pareti e nell'attraversamento del liquido; così può avvenire che si determini non solo un peggioramento nella uniformità della risposta del contatore, ma anche una saturazione nell'efficienza di rivelazione, non praticamente superabile se non con l'aumentare il numero di fotomoltiplicatori impiegati nel dispositivo.

Abbiamo voluto indagare questo punto, misurando l'efficienza di uno scintillatore liquido a colonna, di altezza

variabile. Il liquido usato per la solita soluzione di terfenile in xilolo (*), contenuta in recipienti cilindrici di altezza di 3, 6, 12, 18, 24 cm. Per esaminare l'effetto della natura delle pareti abbiamo usato contatori con superfici cilindriche dei seguenti tipi:

a) vetro comune;

b) alluminio lucidato a specchio;

c) vetro comune dipinto esternamente con una vernice contenente biossido di titanio;

d) lo stesso vetro ricoperto di una sottile lamina di alluminio lucidato;

e) vetro o metallo ricoperto internamente con una vernice costituita da biossido di titanio e gelatina di pesce: questa vernice resiste ai comuni solventi e non ha alcun effetto nocivo sulla soluzione usata per il riempimento dei contatori.

In tutti i casi il coperchio dei contatori era di alluminio lucidato a specchio ed il fondo di vetro comune. Per unire tra loro le varie parti abbiamo usato un mastice composto di vetro solubile ed ossido di zinco.

I cilindri venivano investiti, nella direzione dell'asse, da un fascio di fotoni, ottenuto schermando una sorgente di 100 mC di ^{60}Co con 30 cm di Pb e praticando nello schermo un foro di 3 mm di diametro. La rivelazione veniva effettuata con un fotomoltiplicatore E.M.I. 6260 posto sul fondo del cilindro, in contatto ottico con questo. L'area del fotocatodo era di poco superiore alla sezione dei cilindri.

Nella fig. 1 sono riportate, in funzione dell'altezza della colonna, le curve sperimentali e teorica dell'efficienza dello scintillatore liquido per la rivelazione dei fotoni di energia media di 1.25 MeV.

(*) Sostanze che si trovano in commercio con la qualifica di « pure », senza ulteriore raffinamento.

La curva teorica è ottenuta calcolando il numero dei fotoni convertiti nel liquido, nell'ipotesi di un cammino di assorbimento di 17.2 cm. Le curve sperimentali sono invece tracciate normalizzando

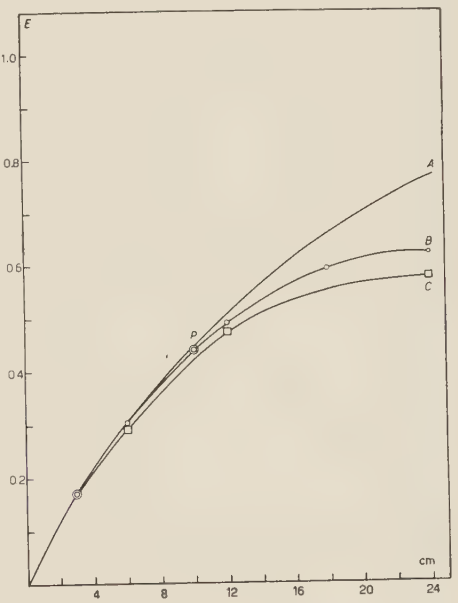

Fig. 1. – Efficienza dello scintillatore, in funzione dell'altezza della colonna liquida. *A*, curva teorica; *B*, curva sperimentale per contatori con pareti di vetro trasparente; *C*, id. con pareti di alluminio riflettente.

i valori allo spessore di 3 cm di liquido, ed ammettendo che a tale spessore tutti i fotoni convertiti vengano rivelati dal dispositivo.

Si può osservare che l'efficienza di rivelazione cresce con lo spessore del liquido, ma più lentamente del valore teorico, fino a raggiungere una saturazione verso i 20 cm, dove le perdite dovute a cattiva raccolta della luce sono ormai tali da neutralizzare il vantaggio di un aumento dello spessore. Si noti ancora come il contatore a pareti di vetro presenti un'efficienza migliore, al crescere dell'altezza del liquido, rispetto a quello con le pareti riflettenti di alluminio. Questo fatto era già stato messo

in evidenza da W. A. SCHNEIDER *et al.* [3] per scintillatori liquidi attraversati dai mesoni dei raggi cosmici, e viene qui ritrovato nel caso della rivelazione dei fotoni di energia piuttosto bassa.

Il punto P del diagramma corrisponde all'efficienza di uno scintillatore di NaI(Tl), dell'altezza di 30 mm e diametro di 28 mm; questo punto si raccorda molto bene alla curva relativa al liquido e risulta poco inferiore al valore teorico.

Nella fig. 2 sono invece riportate le curve del numero di impulsi in funzione della loro altezza per ogni tipo di parete adoperata. Esse si riferiscono ad un recipiente cilindrico dell'altezza di 12 cm, diametro di 4 cm, le cui pareti sono state successivamente cambiate, usando però sempre la stessa soluzione. Le pareti che offrono la migliore efficienza sono quelle di vetro trasparente; e se queste sono poste in una scatola a pareti bianche diffondenti, l'efficienza risulta ancora leggermente migliorata. Subito dopo vengono le pareti a superficie riflettente, mentre quelle a superficie bianca diffondente presentano il comportamento peggiore. In compenso però l'andamento della curva relativa a quest'ultimo tipo conferma il fatto già noto della migliore uniformità della risposta delle pareti bianche diffondenti. La diversità di comportamento delle diverse pareti non è di poco conto: passando dalle pareti diffondenti (curva E) a quelle formate da vetro comune trasparente (curva A) l'efficienza viene quasi raddoppiata.

Comportamento analogo si ottiene operando con contatori cilindrici di altezza diversa da quella esaminata; fa eccezione soltanto il caso del contatore di 3 cm di altezza, per il quale le pareti riflettenti di alluminio e quelle diffondenti si dimostrano di pari efficienza, maggiore però di quella delle pareti di vetro trasparente, confermando così l'osservazione già fatta da altri autori.

In conclusione si può affermare che per la rivelazione dei fotoni con scintillatori liquidi a colonna, e non avendo riguardo all'uniformità della risposta, risultano più favorevoli i recipienti di vetro trasparente e comunque è bene che l'altezza della colonna non ecceda i 20 cm. Questi risultati valgono quando si operi, come nel nostro caso, con il fotomoltiplicatore a temperatura ambiente (20 °C), per cui è necessario eseguire un « taglio » (vedi fig. 2) sull'altezza degli impulsi, ad un valore dove il fondo non sia eccessivo.

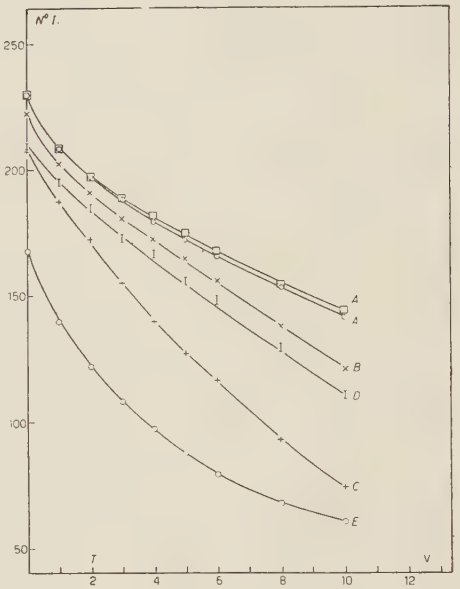

Fig. 2. – Numero d'impulsi in funzione della loro altezza in volt, all'uscita dell'amplificatore, per diverse pareti. Pareti: A, vetro trasparente; A^+, id. in scatola diffondente; B, alluminio riflettente; C, vetro verniciato esternamente; D, vetro ricoperto con lamina d'alluminio; E, alluminio o vetro verniciato internamente; T, taglio.

[3] W. A. SCHNEIDER, J. HERSHKOWITZ and H. KALLMANN: *Nucleonics*, **12**, n. 12 (1953).

A Cloud Chamber Observation of a Singly Charged Unstable Fragment.

G. Alexander, C. Ballario, R. Bizzarri, B. Brunelli, A. De Marco, A. Michelini, G. C. Moneti, E. Zavattini and A. Zichichi

Istituto di Fisica dell'Università - Roma
Istituto Nazionale di Fisica Nucleare - Sezione di Roma

J. P. Astbury

The Physics Department, University College - London

(ricevuto il 18 Luglio 1955)

Among 30000 cloud chamber photographs taken at Testa Grigia (3500 m a.s.l.) we have found about 150 V°-particles. In the same series of photographs there are 20 events in the gas which have 3 or more prongs. Eighteen of these can be interpreted without difficulty as stars produced in argon; but the remaining two, which we discuss in this letter, show certain peculiar features.

A sketch of the experimental arrangement is given in fig. 1. The chamber is triggered if *a*) at least 2 counter discharges in the top tray are associated with at least 3 discharges in the bottom tray or alternatively *b*) 4 discharges in the top tray are associated with 2 in the bottom tray. For the two events described below both conditions *a*) and *b*) were satisfied.

A photograph of event I is given in fig. 2; only the space between plates 1 and 2 is reproduced. The angles and estimated specific ionizations are given in Table I. The ionizations are the outside limits of the estimates of 4 observers; in making the estimates account has been taken of the steep inclination of several of the tracks.

The continuations of tracks 3′ and 4 intersect at a common point A, in plate 1; those of tracks 2 and 5 intersect at another point B, in the same plate. The continuations of tracks 3″ and 1 below plate 2 lie outside the illuminated volume of the chamber. There is no sign of a recoil nucleus at the intersection of tracks 1, 2, 3′ and 3″. The four tracks are coplanar to within $\pm \frac{1}{2}°$; tracks 3′ and 3″ are colinear to within $\pm \frac{1}{2}°$. Thus if this event is a nuclear interaction it is of a very unusual type. We therefore consider below the possibility that it is a decay process.

Track 2, which has an ionization of less that 2.5, can only have unit charge. It is almost certain that the charge of track 3′ is the same as that of track 3″. There is no detectable change in ionization between tracks 3′ and 3″ (the inclination of the two tracks to the camera being the same a change in the

TABLE I.

Event I

track	1	2	3′ and 3″	4	5
I/I_0	5 — 15	< 2.5	5 — 15	< 2.5	5 ÷ 15

$\theta_{13} = 21.3 \pm 0.3$ $\theta_{23} = 76.1 \pm 0.5$

$\theta_{12} = 97.4 \pm 0.5$

ionization could be estimated more nicely than the absolute ionization of either track). It is therefore reasonable to assume, from conservation of charge,

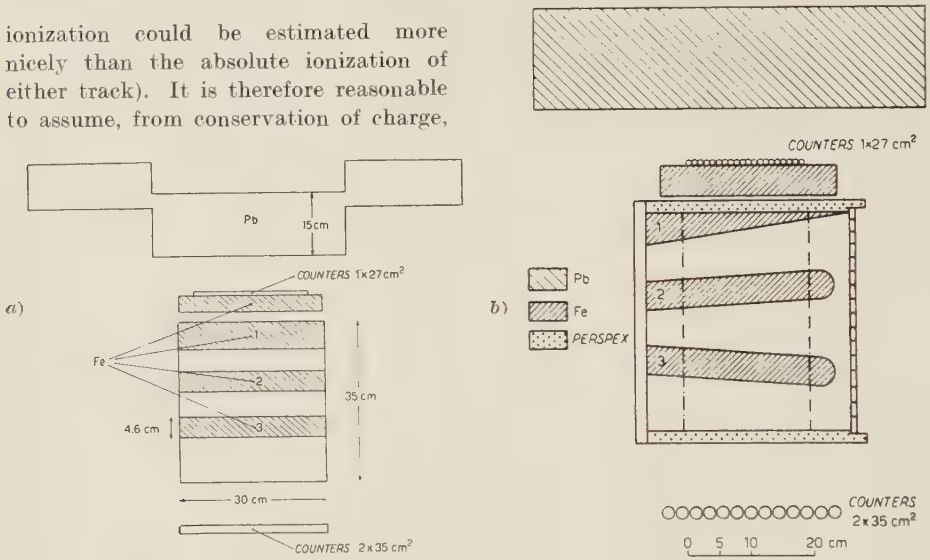

Fig. 1. – Experimental Arrangement: *a*) front view; *b*) side view.

that particle 1 has unit charge, opposite in sign to that of particle 2. We can then obtain from the ionization estimates limiting values of p/m for the particles 1 and 2. If we make the further assumption, justified by the coplanarity of the event, that no neutral secondary particles are produced we can obtain, from conservation of momentum perpendicular to track 3, a limit for the mass ratio m_2/m_1. We find, $m_2/m_1 < 0.23$.

This result indicates that the event cannot be the decay of a τ-meson. A further implication is that, unless particle 1 is heavier than a deuteron, particle 2 can only be an L-meson or an electron. The intersection of the lines of flight of particles 2 and 5 indicate that particle 2 is probably a π-meson which has produced a star in the iron plate.

If particle 2 is assumed to be a π-meson and particle 1 a proton, both secondaries of a V^0-particle travelling in the direction of track 3, the Q-estimate for the decay is from 28 to 53 MeV. These limits are derived from the limits in the ionization estimates. The event thus fits well with a Λ^0-decay. For a Λ^0-decay with a Q-value of 37 MeV the ionization of the secondary particles would be $I_1/I_0 = 7.4$, $I_2/I_0 = 2$, which

are in good agreement with the observed values. It thus appears that the most probable interpretation of this event is

is $\pi/(4\cdot 37)^2 = 1.4\cdot 10^{-4}$ sterad. In our experiment the total number of particles observed to come from the same origin

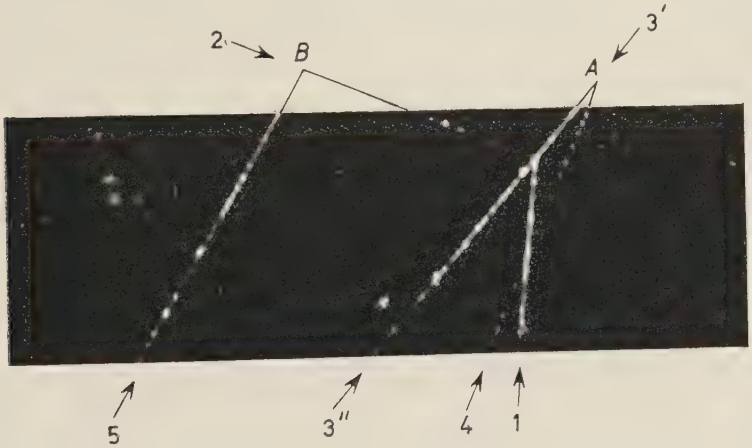

Fig. 2. – Event I. Only the space between the first and second plates is reproduced.

that particles 1 and 2 are secondaries of a Λ^0-particle coming from the same source as particle 3. If this is true then the velocity of the Λ^0-particle must be $0.24c$. A singly charged particle with this velocity would have a specific ionization of 9.5. It is remarkable that this ionization agrees very well with the estimated ionization of track 3. The estimate given in table I is 5-15; but as a result of the assumption that particles 1 and 2 are produced in a Λ^0-decay this range can be further restricted; track 1 can be taken as a standard with known ionization — 7.5. The ionization of track 3 is estimated to be very close to that of track 1. Thus not only do the directions of travel of the Λ^0 and particle 3 agree, but also their velocities (assuming that particle 3 is singly charged) must be very similar.

It is possible that this agreement is merely fortuitous. The coincidence of the V^0 and the line of flight of particle 3 can be defined to within $\pm \frac{1}{4}$ mm. The distance of the apex of the V^0 from point A is 37 mm; thus the solid angle subtended at A by the disk of uncertanty as V^0-particles is 150. This number corresponds to an average of about 1 per V^0-particle, which is much lower than that obtained in most experiments; this is mainly because most of our V^0-particles have no detectable origin. In some cases, where the V^0-particle has not yet been reprojected, the number of accompanying shower particles has been estimated from visual inspection of the two stereoscopic photographs). If these 150 shower particles were isotropically distributed the probability of our observing by chance such a coincidence in direction of flight would be $(150\cdot 1.4\cdot 10^{-4}) = 1.7\cdot 10^{-3}$. Shower particles are certainly not isotropically distributed in the laboratory system. When allowance is made for this the above figure has to be multiplied by a factor which is certainly less than 10, so that the probability becomes < 0.02 [1]. This is the probability of obtaining such

[1] If it is assumed that all the particles are emitted in the downward hemisphere and follow a $\cos^2\theta$ distribution, the factor is ≤ 6; for a $\cos^4\theta$ distribution it is ≤ 10. These figures are

a coincidence in our 30000 pictures. The probability of obtaining a coincidence in any one of the number of experiments on V^0-particles which are being conducted is evidently very much greater than this. In fact one example of a chance coincidence has already been reported [2]. It is possible that our event is another such example; but the correlation, not only in direction but also in velocity, suggests that in this case it is more reasonable to assume a physical connection between the two particles. The data are entirely consistent with the interpretation of the event as the decay of an unstable hydrogen isotope, — unstable because one of the neutrons of the stable isotope is replaced by a Λ^0-particle which is so lightly bound to the rest of the nucleus that the latter is substantially unaffected by the decay [3].

Two examples [4,5] of an excited deuteron or triton decay at rest have been observed in photographic emulsions in which almost all the available energy was taken by the Λ^0-particle. An event which has not yet been fully analyzed, but which appears very similar to that which we have reported here, has been found at Bristol [6]. The Padua group [7] have observed, again in a photographic emulsion, the decay at rest of an unstable helium nucleus yielding as the only detectable secondaries the proton and

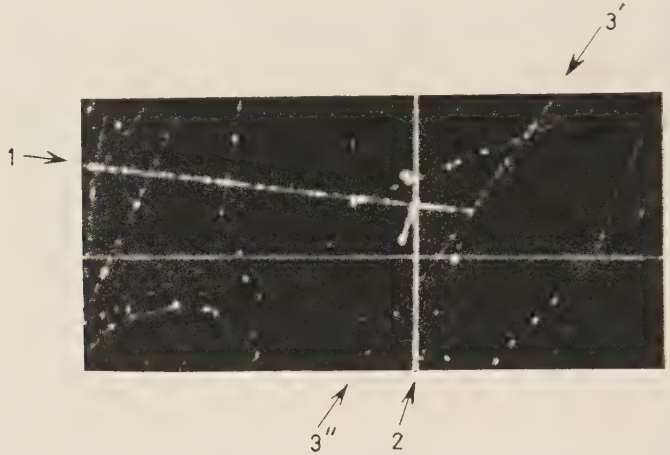

Fig. 3. - Event II. Only the space between the second and third plates is reproduced.

extreme upper limits obtained by assuming that the peak of the distribution $\theta = 0°$ is in every event defined by the direction of the V^0 particles.

[2] R. ARMENTEROS, A. ASTIER, C. D'ANDLEN, B. GREGORY, H. HENDEL, J. HENNESSY, A. LAGARRIGUE, L. LEPRINCE-RINGUET, F. MULLER, CH. PEYROU et R. RAU: Report of the Pisa Conference on Elementary Particles, June 1955, to be published in *Nuovo Cimento*.

[3] For a theoretical treatment of such problems see the following letter by R. GATTO.

[4] J. CRUSSARD, V. FOUCHÉ, T. F. HOANG, L. JAUNEAU, G. KAYAS, L. LEPRINCE-RINGUET, O. MORELLET, A. ORKIN-LECOURTOIS, F. RENARD et J. TREMBLEY: Report of the Pisa Conference on Elementary Particles, June 1955, to be published in *Nuovo Cimento*.

[5] F. ANDERSON, G. LAWLOR T. E. and NEVIN: Report of the Pisa Conference on Elementary Particles, June 1955, to be published in *Nuovo Cimento*.

[6] M. V. FRIEDLANDER; private communication.

[7] M. CECCARELLI: private communication.

π-meson of a Λ^0-decay. SORRELS *et al.* [8] have obtained the cloud chamber photograph of the decay in flight of an unstable helium nucleus; in this case the fragment was deflected at the point of decay through an angle of $3^\circ \pm 1^\circ$.

particles 3″ and 2 lie within the illuminated region below plate 3, but three is no sign of a continuation of either track. The angle between tracks 3′ and 3″ is less than 0.5°. The angle made by these tracks to the plane containing

TABLE II.

Event II				
track	1	2	3′	3″
I/I_0	3 — 8	< 2.5	< 2.5	< 2.5
Range g/cm² Fe	—	< 45	—	< 42

$\theta_{13} = 60.9 \pm 0.5$ $\theta_{23} = 33.6 \pm 0.5$

$\theta_{12} = 94.6 \pm 0.5$

Observations of the decays in flight of unstable nuclei are particularly valuable because they yield information about the mean life. In our event the length of track 3′ is 2.5 cm; that of track (3′+ 3″) is 12.5 cm. The time of flight of the Λ^0 in the illuminated volume of the chamber before decay was $3.3 \cdot 10^{-10}$ s. The potential traversal time was $17 \cdot 10^{-10}$ s. The lengths and times of flight quoted are those actually observed in the chamber and no fiducial surface corrections have been applied.

A superficially similar event is reproduced in fig. 3. The measurements for this — event II — are given in table II. Here again there is no trace of a recoil nucleus at the intersection of the four tracks. The lines of flight of tracks 1 and 2 is also less than 0.5°; but a null method of measurement indicates that this latter angle is definitely not zero.

Even disregarding the slight departure from coplanarity in event II it can be shown that the pairs of tracks, 1 and 2, in the two events cannot be examples of the same two body decay, whatever masses are assigned to the secondary particles. Event II can be interpreted as a τ-decay, but only by assuming that one of the secondary π-mesons was emitted at a very small angle (in the centre of mass system) to the line of flight of the primary; moreover an invisible low energy star in plate 3 must be postulated in order to explain the non-appearance of track 3 in the bottom part of the chamber. However, if this event is not a nuclear interaction of a very unusual type, the least unsatisfactory interpretation appears at present to be that it is a τ-decay.

[8] J. D. SORRELS, G. H. TRILLING and R. B. LEIGHTON: reported at Pisa Conference by M. GELL-MANN.

Sull'energia di legame degli iperframmenti leggeri.

E. Diana e F. Duimio

Istituto di Scienze Fisiche dell'Università - Milano
Istituto Nazionale di Fisica Nucleare - Sezione di Milano

(ricevuto il 18 Luglio 1955)

Con procedimento del tutto analogo a quello usato da uno di noi per uno schema dell'energia di legame del $^3H^*$ [1], abbiamo cercato di trarre qualche informazione anche sul sistema $^4H^*$.

L'esistenza dell'$^4H^*$, per la prima volta supposta da Dalitz [2], è ora definitivamente accertata sperimentalmente.

I punti essenziali su cui si basa il nostro calcolo che, vogliamo sottolinearlo anche qui, è estremamente semplificato, sono i seguenti:

1) l'interazione N-Λ^0, supposta mediata da mesoni pesanti, π_1 di massa $\sim 965\ m_e$, e l'ordinaria interazione N-N, mediata da mesoni π^0, possono essere rappresentate da buche di potenziale: nel presente caso si assumono buche gaussiane; riguardo al tipo delle forze si suppone siano pure forze di scambio (di Majorana).

2) indicando con α_0 e V_0, α_1 e V_1, rispettivamente il range e la profondità per i due suddetti potenziali di interazione, supporremo valide le relazioni [1]:

$$\alpha_1 \simeq \alpha_0/\beta\ ,$$

$$V_1 \simeq \beta V_0\ ,$$

con

$$\beta \simeq \frac{m\pi_1}{m\pi_0} = \sim 3.5\ .$$

[1] F. Duimio: *Nuovo Cimento*, **1**, 668 (1955).
[2] Dalitz: in corso di pubblicazione.

Scelto quindi il seguente sistema di coordinate

$$\boldsymbol{R} = \frac{M_0(\boldsymbol{r}_1 + \boldsymbol{r}_2 + \boldsymbol{r}_3) + M_1\boldsymbol{r}_4}{3M_0 + M_1} \qquad \begin{aligned} M_0 &= \text{massa del nucleone} \\ M_1 &= \text{massa della } \Lambda^0 \ (\sim 2\,185\ m_e) \end{aligned}$$

$$\boldsymbol{S}_1 = \sqrt{3}\,\boldsymbol{r}_4 - \frac{\boldsymbol{r}_1 + \boldsymbol{r}_2 + \boldsymbol{r}_3}{\sqrt{3}}$$

$$\boldsymbol{S}_2 = \boldsymbol{r}_1 - \frac{\boldsymbol{r}_2 + \boldsymbol{r}_3}{2}$$

$$\boldsymbol{S}_3 = \frac{\sqrt{3}}{2}(\boldsymbol{r}_2 - \boldsymbol{r}_3)$$

con $\boldsymbol{r}_1$, $\boldsymbol{r}_2$, $\boldsymbol{r}_3$, posizione di 3 nucleoni, $\boldsymbol{r}_4$ posizione della Λ^0, e assunta come funzione di prova la

$$\psi = \exp\left[-\mu(r_{12}^2 + r_{13}^2 + r_{23}^2) - \nu(r_{14}^2 + r_{24}^2 + r_{34}^2)\right],$$

con

$$r_{ij} = |\boldsymbol{r}_i - \boldsymbol{r}_j|\ ,$$

il valore medio dell'energia totale nel sistema del baricentro (cioè trascurando l'energia cinetica di traslazione) risulta dato dalla seguente espressione

$$(1) \qquad E = \frac{\hbar^2}{M_0}[9\mu + 3\gamma(1 + \gamma/2)] - 3V_0\left[\frac{3\mu + \nu}{3\mu + \nu + \alpha_0^{-2}}\right]^{\frac{3}{2}} - 3\beta V_0\left[\frac{2\nu(3\mu + \nu)}{(\mu + 3\nu + \beta^2\alpha_0^{-2})(\mu + \gamma)}\right]^{\frac{3}{2}},$$

con

$$\gamma = \frac{M_1 + 3M_0}{M_1}\ .$$

Con le posizioni

$$A = \frac{\hbar^2}{M_0\alpha_0^2}, \qquad \tau = \frac{3\mu + \nu}{\mu + 3\nu}, \qquad \sigma = (\mu + 3\nu)\alpha_0^2,$$

la (1) assume la forma

$$(2) \qquad E = \frac{3}{8}A\sigma[8\tau + \frac{\gamma}{2}(3 - \tau)] - 3V_0\left[\frac{\tau\sigma}{\tau\sigma + 1}\right]^{\frac{3}{2}} - 3\beta V_0\left[\tau\frac{3 - \tau}{\tau + 1}\,\frac{\sigma}{\sigma + \beta^2}\right]^{\frac{3}{2}}.$$

Si dovrebbe a questo punto procedere alla minimizzazione rispetto ai parametri σ e τ. Come già nel caso del $^3H^*$ è però opportuno, rinunciando ad ogni risultato quantitativo, che, date le approssimazioni fatte, avrebbe poco senso, limitarsi ad un confronto con l'energia di legame del tritio, che si ottiene, con lo stesso grado di approssimazione, come caso limite dalla (2) con $\theta = 3$ (cioè con $\nu = 0$): tale energia è $E_{^3H} \simeq -13.5$ MeV.

D'altronde dalla (2) con $\tau = 2.5$, $\sigma = \frac{1}{2}$, $\beta = 3$ si ha

$$E = -16.1 \text{ MeV} , \tag{3}$$

ciò che conferma che il $^4H^*$ è stabile, e che la sua energia di legame è di poco maggiore di quella del ^3H.

Volendo ora considerare il sistema $^4He^*$, basterà aggiungere all'energia (2) l'energia media di repulsione coulombiana tra i due protoni; cogli stessi parametri usati per dedurne la (3) si ha il valore di ~ 0.9 MeV. Da qui è facile concludere che anche il $^4He^*$ è stabile.

Con calcoli analoghi si ha per il $^3He^*$ un'energia di legame molto vicina allo zero, per cui non è possibile affermare che tale sistema è certamente stabile: d'altronde anche sperimentalmente è difficile accertarne l'esistenza; poichè ogni decadimento finora attribuito a $^3He^*$ può essere spiegato anche come dovuto a $^4He^*$.

Phenomenological Treatment of the Decay of Light Hyperfragments.

R. Gatto

Istituto di Fisica dell'Università - Roma
Istituto Nazionale di Fisica Nucleare - Sezione di Roma

(ricevuto il 18 Luglio 1955)

It is the purpose of this paper to point out that a number of questions exist about the decay of light hyperfragments, to which it should be possible to give an answer without requiring very detailed assumptions. At present no established theory exists of the new particles, therefore it seems highly reasonable to try to obtain as much as possible information without invoking very specific hypotheses. An event has been recently found by the cloud chamber group of Rome University, which could be interpreted as the mesonic decay of a possible bound system formed by a Λ^0 and a proton (1). It must be remarked that up to now no convincing evidence of such Λ^0-deuterons has never been reported. If the bound Λ^0-proton system exists, than one would also assume the existence of the bound Λ^0-neutron system. The possibility of a bound state Λ^0-neutron has been sometimes discussed in connection with the problem of the anomalous Q-values, and the calculations which will be reported here may be of interest also in this regard.

From a theoretical viewpoint the existence of such Λ^0-nucleon bound states would appear rather dubious, in view of the fact that the Λ^0-nucleon force seems to be weaker than the ordinary nucleon-nucleon force, and the ordinary deuteron itself is a weakly bound system. However, possible many body effects and a possible strong spin dependence of the Λ^0-nucleon force would easily invalidate such conclusions. Therefore no credit can be given to these speculations, lacking as we are of sufficient information on the nature of the binding force. An important problem in this connection, which we would like to point out to the experimentalists, is that of determining whether such a binding does exhibit a saturation effect, as the ordinary nuclear binding, or not.

A most interesting feature of the event found by the Rome group is that it must be assumed that the bound Λ^0 disintegrates as if it were nearly undisturbed by the accompanying proton, if the interpretation as a mesonic decay of a Λ^0-deuteron is accepted. The transverse momentum imparted to the residual proton after the decay is found to be less than ~ 2 MeV/c, which is of the order of the experimental error. One could ask whether to such a class of disintegration does in fact correspond a large fraction of probability, considering that the binding energy of the Λ^0-proton

(1) See preceding letter.

system is presumably small. The answer to this question, as well as to other ones which often occur in the interpretation of decays of hyperfragments, does not require very detailed hypotheses, but follows from the more general features.

The underlying physical idea is the following. The interaction which is responsible for the disintegration should be a very weak interaction, such as to be compatible with the long lifetime. The precise form of this interaction is not known. Beside such weak interaction there are a strong initial state interaction and a strong final state interaction. The strong initial state interaction produces the strong binding of the Λ^0 and the nucleons. We must postulate the form of the wavefunction of the initial bound state. The strong final state interaction is the ordinary interaction between the emitted nucleons and the possible emitted pion. Its effect is that of modifying the wavefunction of the final particles for distances smaller than the range of the forces, and of introducing appropriate phase shifts in its asymptotic expansion. It is expected that the dominant features of a wide class of problems mainly follow from the form of the initial and final wavefunctions, and that they should be rather independent from the details of the weak interaction which produces the decay.

To illustrate these remarks and to solve as well the problem posed before on the interpretation of the mentioned cloud chamber event (1), we will discuss here the case from the mesonic decay of the suggested Λ^0-deuteron. Let us consider the decay

$$(\Lambda^0, \mathrm{p}) \rightarrow \mathrm{p} + \mathrm{p} + \pi^- .$$

in the rest system of the fragment. We call $\boldsymbol{p}_1$ and $\boldsymbol{p}_2$ the momenta of the two final protons and $\boldsymbol{k}$ the momentum of the final meson. Momentum conservation gives

$$\boldsymbol{p}_1 + \boldsymbol{p}_2 + \boldsymbol{k} = 0 . \tag{2}$$

As independent momenta we take the relative momentum of the two final protons, $\boldsymbol{p} = \frac{1}{2}(\boldsymbol{p}_1 - \boldsymbol{p}_2)$, and $\boldsymbol{k}$. The momenta $\boldsymbol{p}_1$ and $\boldsymbol{p}_2$ are then given by

$$\boldsymbol{p}_1 = \boldsymbol{p} - \tfrac{1}{2}\boldsymbol{k}, \qquad -\boldsymbol{p}_2 = \boldsymbol{p} + \tfrac{1}{2}\boldsymbol{k} . \tag{3}$$

Energy conservation is expressed by the relation

$$M - m - \varepsilon = \frac{p_1^2}{2m} + \frac{p_2^2}{2m} + \sqrt{k^2 + \mu^2} = \frac{p^2}{m} + \frac{k^2}{4m} + \sqrt{k^2 + \mu^2} , \tag{4}$$

where M is the mass of the Λ^0, m the mass of the proton, ε the binding energy of the bound state (Λ^0, p), and μ the meson mass. As a convenient distribution function we shall evaluate $f(k)$, such that $f(k)^3\boldsymbol{k}$ is the probability that the meson is emitted with a momentum contained in $\mathrm{d}^3\boldsymbol{k}$. It is expected that $f(k)$ has a maximum in a region around k_0, k_0 being the value of the momentum which is taken by the meson in the center of mass system of a Λ^0 which is supposed to decay as free. In the following we shall be concerned with the evaluation of the width of this maximum. The momentum k_0 is defined by the equation

$$M - m = \frac{k_0^2}{2m} + \sqrt{k_0^2 + \mu^2} . \tag{5}$$

It will be convenient in the following to use the velocities $V_0 = k_0/m$ and $v_0 = k_0/\sqrt{k_0^2 + \mu^2}$ of the final nucleon and of the final meson. As to the exact position of the maximum of $f(k)$, it is expected that it is displaced to some value $\bar{k}_0$, smaller than k_0 for a little quantity x_0 of the order of the binding energy. If we take into account the small binding energy ε, we can write in place of (5) the equation

$$M - m - \varepsilon = \frac{\bar{k}_0^2}{2m} + \sqrt{\bar{k}_0^2 + \mu^2}\,. \tag{6}$$

If we write $\bar{k}_0 = k_0 + x_0$, we get from (5) and (6), neglecting higher order terms in ε

$$x_0 = -\frac{\varepsilon}{v_0 + V_0}\,. \tag{7}$$

For the probability $f(k)\,\mathrm{d}^3\boldsymbol{k}$ we can write

$$f(k)\,\mathrm{d}^3\boldsymbol{k} = \mathrm{d}^3\boldsymbol{k} \int S\,|T_{if}|^2\,\delta\left(\frac{p^2}{m} + \frac{k^2}{4m} + \sqrt{k^2 + \mu^2} - M + m + \varepsilon\right)\mathrm{d}^3\boldsymbol{p}\,. \tag{8}$$

where T_{if} is the element of the transition matrix for the process and S stays for an average over the initial spin states and a summation over the final spin states. For simplicity we have assumed spin $\frac{1}{2}$ for the Λ^0, although the result will be essentially independent of this assumption. For the initial wavefunction of the (Λ^0, p) bound system we take

$$\psi = \frac{1}{x}\,(e^{-\alpha x} - e^{-\beta x})\chi\,, \tag{9}$$

where x is the relative coordinate, α is a constant related to the binding energy

$$\alpha^2 = 2\,\frac{mM}{m + M}\,\varepsilon\,, \tag{10}$$

β is a constant related to the effective Λ^0-proton scattering range A by

$$\beta \cong \frac{3}{A}\,, \tag{11}$$

and χ is the spin part. The transition matrix, the general form of which is restricted by the usual invariance requirements, contains the wavefunction of the emitted meson as a factor. We first consider the case when final state interaction is neglected. The result for $f(k)$ may be approximated by

$$f(k) = XF - YG\,, \tag{12}$$

where

$$F = 2\left[\frac{1}{a^4 - q^4} - \frac{1}{(p^2 - \alpha^2)q^2}\ln\frac{\alpha^2 + q^2}{a^2 - q^2} + \frac{1}{b^4 - q^4} - \frac{1}{(\beta^2 - \alpha^2)q^2}\ln\frac{b^2 - q^2}{b^2 + q^2}\right], \tag{13}$$

$$G = \frac{\beta^2 - \alpha^2}{(a^2 + b^2)q^2}\left[\frac{1}{a^2}\ln\frac{a^2 + q^2}{a^2 - q^2} - \frac{1}{b^2}\ln\frac{b^2 + q^2}{b^2 - q^2}\right], \tag{14}$$

and a^2, b^2, q^4, are defined by $a^2 = m(M - m - \sqrt{k^2 + \mu^2} - \varepsilon) + \alpha^2$, $b^2 = m(M - m - \sqrt{k^2 + \mu^2} - \varepsilon) + \beta^2$, $q^4 = m(M - m - \sqrt{k^2 + \mu^2} - \varepsilon)k^2 - \frac{1}{4}k^4$. In (12) X and Y are assumed to be slowly varying functions of k, but it is impossible to determine their form without making explicit assumptions on the transition matrix. We have accomplished with eq. (12) the desired separation into factors X, Y, which depend on the details of the interaction, and which can not be determined at the present stage of the theory, and into form factors F and G which mainly depend on the kinematics of the disintegration and on the form of the wavefunctions.

We can simplify the expressions (13) and (14) by observing that the radius of the bound state Λ^0-proton will be much larger than the range of the Λ^0-proton force. Roughly, the radius of the bound system will be of the order of

$$R_0 \cong \frac{1}{\alpha}, \tag{15}$$

whereas the range of the force should be of the order of

$$r_1 \sim \frac{1}{m_K}, \tag{16}$$

where m_K is the mass of the K-mesons. It is expected that the Λ^0-nucleon force is mediated by some heavy meson. However, the assumption of a greater value for r_1 does not alter the conclusions. From (15) and (16) we see that for $\varepsilon \cong 1$ MeV, the range of the force is about 14 times smaller than the radius of the system, and for $\varepsilon \cong 0.1$ MeV it is about 50 times smaller. It seems that, to account for the possible existence of such Λ^0-deuterons, a very intensive force is needed, if its range must be assumed to be small. Letting $\beta \to \infty$ we can approximate F and G as

$$F \cong 2\frac{1}{a^4 - q^4} = 2\frac{1}{a^2 + q^2}\frac{1}{a^2 - q^2}, \tag{17}$$

$$G \cong \frac{1}{q^2 a^2}\ln\frac{a^2 + q^2}{a^2 - q^2}. \tag{18}$$

To obtain an approximate expression for the width of the maximum around $\bar{k}_0$ we observe that G is negligible in that region as compared to F for the values of ε which are considered. Putting $k = k_0 + x$, we can approximate $f(k)$ as

$$f(k) \cong \text{constant} \cdot \frac{1}{\alpha^2 + \beta x + \gamma x^2}.$$

and we easily find, by comparison with (17)

$$\beta = 2\varepsilon \frac{1}{V_0}\left(1 + \frac{v_0}{V_0}\right) \tag{20}$$

$$\gamma = \left(1 + \frac{v_0}{V_0}\right)^2 + \frac{\varepsilon}{m}\frac{1}{V_0^4}(3V_0^2 + 6v_0^2 + 9v_0V_0 - v_0^3V_0) \tag{21}$$

neglecting higher order terms in ε. The linear term βx in the denominator of (19) exactly accounts for the displacement of the maximum from $\bar{k}_0$ to $k_0 = k_0 + x_0$. By a displacement $x' = x - x_0$ we can write $\alpha^2 + \beta x + \gamma x^2 = (\alpha^2 + \beta x_0 + \gamma x_0^2) + (\beta + 2\gamma x_0)x' + \gamma x'^2$. If we choose x_0 to be given by

$$x_0 = -\frac{\beta}{2\gamma}, \tag{22}$$

we can write for $f(k)$

$$f(k) \cong \text{constant} \cdot \frac{1}{(\Gamma^2/4) + x'^2} = \text{constant} \cdot \frac{1}{(\Gamma^2/4) + (k - \bar{k}_0)^2}; \quad \frac{\Gamma^2}{4} = \frac{1}{\gamma}\left(\alpha^2 - \frac{\beta^2}{2\gamma}\right). \tag{23}$$

Comparing with (20) and (21) we see that x_0 here defined is the same as that given by equation (7).

We see from (23) that the width of the maximum is just given by Γ. From (20), (21), (22) and (23) we get the following figures for

$\varepsilon = 1$ MeV	$x_0 = -0.96$ MeV	$\Gamma = 7.4$ MeV
$\varepsilon = 0.5$ MeV	$x_0 = -0.57$ MeV	$\Gamma = 5.9$ MeV
$\varepsilon = 0.1$ MeV	$x_0 = -0.13$ MeV	$\Gamma = 2.7$ MeV .

We see that for a binding energy less than 0.1 MeV, which still seems a reasonable value, the width of the maximum is less than ~ 3 MeV. Of course, to compare the derived distribution with experiment many examples are needed of such decays. However, it can be concluded that in such conditions a disintegration of the kind of that observed in the cloud chamber [1] should in fact have an appreciable probability to occur, if the event is interpreted as a mesonic decay of a possible Λ^0-deuteron (a rough estimate gives a probability of the order of 20%).

We will now discuss the correction due to final state interaction. In doing this we shall neglect the final pion-nucleon interaction, that is we assume that the final pion wavefunction may still be represented as a plane wave, and moreover we shall assume that the two final protons are emitted in a $^1S_0$ state. Although the kinetic energy of the two final protons is very small, this last approximation is certainly a rough one. The reason for this is that the critical length which determines the appearance of the higher angular momentum states would be of the order of the radius of the Λ^0-deuteron, which is large. On the other hand only the phase shift of the $^1S_0$ state should be appreciably affected by the final state interaction, since for such an effect the critical length will be of the order of the range of the force.

We take the final wavefunction of the form

$$\frac{1}{kr}\left[\sin\left(kr+\delta\right)-e^{r/c}\sin\delta\right], \tag{24}$$

where δ is the phase shift. The second term inside the bracket should account for the deviation of the wavefunction, at small distances, from its asymptotic form. The phase shift may be approximately derived from the well known relation

$$k\operatorname{cotg}\delta=-\frac{1}{a}+\frac{1}{2}r_0k^2, \tag{25}$$

where a is the singlet scattering length and r_0 is the effective range. The probability $f(k)\,\mathrm{d}^3\boldsymbol{k}$ turns out to be

$$f(k)\,\mathrm{d}^3\boldsymbol{k}=Z(k)\left(M-m-\varepsilon-\sqrt{k^2+\mu^2}-\frac{k^2}{4m}\right)^{\frac{1}{2}}\cdot \tag{26}$$

$$\cdot\left\{\frac{\alpha pk\cos\delta+\frac{1}{2}k(\alpha^2+\frac{1}{4}k^2-p^2)\sin\delta}{[\alpha^2+(p-\frac{1}{2}k)^2][\alpha^2+(p+\frac{1}{2}k)^2]}-\frac{1}{2}\,\frac{k\sin\delta}{(\gamma+\alpha)^2+\frac{1}{4}k^2}\right.$$

$$\left.-\frac{\beta pk\cos\delta+\frac{1}{2}k(\beta^2+\frac{1}{4}k^2-p^2)\sin\delta}{[\beta^2+(p-\frac{1}{2}k)^2][\beta^2+(p+\frac{1}{2}k)^2]}+\frac{1}{2}\,\frac{k\sin\delta}{(\gamma+\beta)^2+\frac{1}{4}k^2}\right\}^2\mathrm{d}^3\boldsymbol{k},$$

where

$$p=\sqrt{m}\left(Q-\varepsilon-\sqrt{k^2+\mu^2}-\frac{k^2}{4m}\right)^{\frac{1}{2}}. \tag{27}$$

The last two terms in (26) can be neglected in the same zero-range approximation as before. The main contribution in the vicinity of k_0 comes from the term

$$\frac{1}{\alpha^2+(p-\frac{1}{2}k)^2}, \tag{28}$$

which similarly as for the preceding case can be written as

$$\text{constant}\cdot\frac{1}{\alpha^2+\beta x+\gamma x^2}=\text{constant}\cdot\frac{1}{(\Gamma^2/4)+(k-\bar{k}_0)^2}. \tag{29}$$

The expressions for β and γ, which can be derived from (26), are still given by (20) and (21) respectively.

We can conclude that the final state interaction does not alter very much our result. The physical reason for this is that the two final protons after the decay stay on the average at a relative distance which is larger than the range of the forces.

We have treated the example of the suggested Λ^0-deuteron mainly because it would be the most simple case of application of our general remarks on a phenomenological

treatment of the decay of hyperfragments. On the other hand, an event has been reported, which could be interpreted as the decay of a Λ^0-deuteron [1]. Of course, our calculations do not add any substantial argument in favor of this interpretation of the event. Moreover, we have remarked that at the present stage of the theory no clear-cut arguments can be given to conclude that bound states Λ^0-nucleons exist, or to exclude their existence. Particular problems on the decay of other light hyperfragments can be treated along similar lines. A fuller application of the method will be given in a next work.

* * *

I would like to thank Prof. B. Ferretti, Prof. B. Touschek, and the experimentalists of the cloud chamber group of Rome University, in particular Prof. J. P. Astbury, Prof. C. Ballario, Dr. R. Bizzarri, and Dr. G. Moneti for discussions on the subject.

Sulle funzioni d'onda configurazionali della teoria dei campi.

P. Bocchieri

Istituto di Scienze Fisiche dell'Università - Milano
Istituto Nazionale di Fisica Nucleare - Sezione di Milano

A. Loinger

Istituto di Fisica dell'Università - Pavia

(ricevuto il 23 Luglio 1955)

Nei problemi in cui non sia ragionevole fare uso del metodo perturbativo si sono dimostrate di una certa utilità le trascrizioni delle equazioni della teoria dei campi nello spazio delle configurazioni o in quello dei momenti (1).

Trascrizioni configurazionali *covarianti* si possono fare nella descrizione di Heisenberg e in quella di interazione.

Le trascrizioni nella descrizione di Heisenberg forniscono equazioni per le cosiddette « ampiezze di Feynman » , (2) le quali *non* ammettono, come è ben noto, una interpretazione probabilistica.

Poichè, d'altro canto, nella descrizione d'interazione le parti a frequenze positive o negative degli operatori di campo hanno significato, rispettivamente, di operatori di assorbimento e di emissione di particelle in punti dello spazio-tempo, si potrebbe essere indotti a ritenere che le proiezioni del vettore di stato $\Psi[\sigma]$ sugli autostati dell'operatore N, numero di particelle dei campi interagenti, forniscano senz'altro delle ampiezze di probabilità. Non è però difficile rendersi conto che un tale punto di vista non può essere, in generale, corretto.

A questo scopo basta infatti osservare che nel caso di un campo bosonico libero non si possono costruire espressioni che abbiano le proprietà di varianza di una ampiezza di probabilità (3), mentre nel caso di un campo fermionico libero la cosa è invece possibile. Segue di qui che quando si considerano, nella descrizione d'interazione, un campo fermionico e un campo bosonico accoppiati, l'unico procedimento che possa fornire delle ampiezze di probabilitè di presenza di particelle è quello di

(1) Esposizioni d'insieme della questione si trovano nei seguenti lavori: M. Jean: *Ann. de Phys.*, **8**, 338 (1953); W. Zimmermann: *Supp.* al vol. **9.** del *Nuovo Cimento*, 43, 106 (1954; A. S. Wightman e S. S. Schweber: *Phys. Rev.*, **98**, 812 (1955).

(2) V. particolarmente P. T. Matthews e A. Salam; *Proc. Roy. Soc.*, **221** A, 128 (1954).

(3) V. per es. W. Pauli : *Handbuch der Physik*, **24**/1 (Berlin, 1933), p. 216 e p. 260.

fare una trascrizione configurazionale relativa *ai soli fermioni*: si ottengono così delle funzioni d'onda che (come nella « many-time theory) sono vettori astratti rispetto al campo bosonico; affinchè tali funzioni d'onda rappresentino realmente delle ampiezze di probabilità, occorre inoltre che le coordinates pazio-temporali dei fermioni appartengano alla superficie σ *di tipo spaziale*, rispetto alla quale è definito il vettore di stato $\Psi[\sigma]$ del sistema dei due campi; e ciò per non incorrere in nonsensi fisici.

A illustrazione di queste considerazioni, vogliamo esaminare sommariamente il problema degli stati legati dell'elettrodinamica.

L'equazione cui obbedisce il vettore di stato $\Psi[\sigma]$ nella descrizione di interazione sarà ($\hbar = c = 1$):

$$\Psi[\sigma] = -e \int_{-\infty}^{\sigma} : \bar{\psi}(x')\gamma^{\mu}\psi(x') : A_{\mu}(x')\Psi[\sigma']\,\mathrm{d}^4x' \quad (3). \tag{1}$$

Il più generale vettore di stato $\Psi[\sigma]$ si potrà esprimere nel modo seguente:

$$\Psi[\sigma] = c_0[\sigma]\rangle_0 + \sum_{1}^{\infty}{}_{f,g} : c_{f,g}[\sigma]\Psi_{f,g}[\sigma]; \tag{2}$$

ove

$$\Psi_{f,g}[\sigma] = (f!g!)^{-\frac{1}{2}} \int_{\sigma}^{\cdot} \bar{\psi}^{(-)}_{\alpha_1}(z'_1) \dots \bar{\psi}^{(-)}_{\alpha_f}(z'_f) \cdot \psi^{(-)}_{\beta_1}(y'_1) \dots \psi^{(-)}_{\beta_g}(y'_g)\rangle_0 \, \gamma^{\mu_1}_{\alpha_1\delta_1} \dots \gamma^{\mu_f}_{x_f\delta_f} \gamma'^{\nu_1}_{\varepsilon_1\beta_1} \dots \gamma'^{\nu_g}_{\varepsilon_g\beta_g} \cdot \tag{3}$$

$$\cdot \Phi^{(+)}_{\delta_1 \dots \delta_f \cdot \varepsilon_1 \dots \varepsilon_g}(z'_1, \dots z'_f; y'_1, \dots y'_g)\ \mathrm{d}\sigma_{\mu_1} \dots \mathrm{d}\sigma_{\mu_f},\ \mathrm{d}\sigma_{\nu_1} \dots \mathrm{d}\sigma_{\nu_g}\ .$$

Proiettando la (1) sullo stato di vuoto, sullo stato di un elettrone, di un elettrone e un positrone, ... si ottiene un sistema S di infinite equazioni accoppiate per le ampiezze di probabilità di presenza degli elettroni e dei positroni. L'equazione che, ad es., si ottiene dalla proiezione di (1) su ${}_0\langle\bar{\psi}^{(+)}_{\eta_1}(y''_1)\psi^{(+)}_{\theta_1}(z''_1)$ è:

$$c_{1,1}[\sigma]\Phi^{(+)}_{\theta_1\eta_1}(z''_1, y''_1) = -e \int_{-\infty}^{\sigma} \mathrm{d}_1x' c_0[\sigma'] A_{\mu}(x')\gamma^{\mu}_{\alpha\beta} S^{(+)}_{\theta_1\alpha}(z''_1 - x')S^{(+)}_{\beta\eta_1}(y''_1 - x') +$$

$$+ ie \int_{\infty}^{\sigma} c_{1,1}[\sigma'] A_{\mu}(x')\gamma^{\mu}_{\alpha\beta} \cdot S^{(+)}_{\theta_1\alpha}(z''_1 - x')\Phi^{(+)}_{\beta\eta_1}(x', y''_1) -$$

$$- ie \int_{-\infty}^{\sigma} c_{1,1}[\sigma'] A_{\mu}(x')\gamma^{\mu}_{\beta\alpha} S^{(+)}_{\alpha\eta_1}(y''_1 - x')\Phi^{(+)}_{\theta_1\beta}(z''_1, x') -$$

$$- 2e \int_{-\infty}^{\sigma} c_{2,2}[\sigma'] A_{\mu}(x')\gamma^{\mu}_{\alpha\beta}\Phi^{(+)}_{\theta_1\beta\alpha\eta_1}(z''_1, x'; x', y''_1)\ .$$

(3) Questo integrale va definito con una certa cautela, se si vuole avere un'espressione matematicamente sensata; cfr. W. Glaser e W. Zimmerman: *Zeits. f. Phys.*, **134**, 346 (1953).

Per risolvere un problema particolare si estrae dal sistema S un opportuno sottosistema S', costituito anch'esso di infinite equazioni accoppiate, il quale, come è evidente dalla forma dell'interazione, è indipendente dalla parte restante $S - S'$ di S, nel senso che nessuna delle funzioni d'onda di S' figura in $S - S'$.

Ovviamente, per poter ricavare la soluzione di un dato problema occorre far ricorso ad opportune approssimazioni, per es. tipo Tamm-Dancoff.

Ringraziamo vivamente il prof. P. CALDIROLA per il suo interessamento.

C. N. Martin – *Tables numériques de Physique Nucléaire*. 1 vol. di pagg. VIII-258, Edit. Gauthier-Villars, Paris, 1954; senza indicazione di prezzo.

Il volume presenta una raccolta di valori numerici relativi a formule semiempiriche o teoriche di fisica nucleare, frutto di un enorme lavoro di calcolo del volenteroso autore, che ha preferito non servirsi di calcolatrici meccaniche. Non possiamo dubitare, sfogliando il volume, che si tratti di un fisico « plein d'enthousiasme et doué d'une grande puissance de travail », quale ce lo presenta L. de Broglie. Nell'introduzione, un attacco inneggiante alle glorie della fisica atomica, subito trattenuto come si conviene ad una raccolta di tavole numeriche (ma che già assurdo suona nella traduzione inglese di cui l'intero testo è provveduto), ci dice pure quanto controllato e razionale debba essere stato l'entusiasmo dell'autore nell'accingersi a questa fatica.

La prima parte presenta: valori numerici delle masse atomiche, in funzione di A e di Z ($10 \leqslant A \leqslant 280$, $1 \leqslant Z \leqslant 115$), secondo la nota formula semiempirica di Weizsäcker, aggiornata da Fermi; valori, calcolati attraverso la medesima via, delle energie delle transizioni β e α energeticamente permesse; valori dell'energia di legame di parecchi gruppi di particelle nei nuclei, e dei singoli termini della formula di Weizsäcker per una scelta di nuclidi.

La seconda parte tratta estesamente dei raggi nucleari, del calcolo dell'energia di soglia per le reazioni endoergiche, dell'energia di rinculo dei nuclei dopo emissione α, dei fattori per il calcolo della trasparenza nella formula di Gamow per la disintegrazione α, dell'altezza della barriera coulombiana, della sezione geometrica dei nuclei, e infine della conversione di unità di massa in unità di energia.

Ogni tavola è preceduta da una chiara spiegazione dotata di numerosi esempi numerici, tratti da situazioni attuali. Ci è spiaciuto di trovare qui alcune inesattezze e incongruenze. È augurabile che, almeno in un singolo volume, la convenzione accettata sul segno dell'energia di legame sia una: a pagg. 118 e 121, introduzione alla Tav. 5, si deducono formule non corrispondenti alle convenzioni adottate nella tavola stessa, mettendo così in imbarazzo il fisico novellino, o soltanto disattento, nel giudicare se una reazione sia esoergica o endoergica. Alcuni esempi numerici ci paiono errati: concettualmente il primo, riportato a pagg. 204 e 205, sul calcolo dell'energia di rinculo di un nucleo dopo emissione α, e di oscura interpretazione il secondo, che l'autore risolve « immediatement » e « readily », ma che a noi pare incomprensibile se non si fanno alcune approssimazioni che permettano l'uso della Tav. 10. Se si tien conto inoltre che i due esempi riportati richiedono duplice interpolazione in una tavola a due entrate, mentre sono facilmente risolubili, entro la stessa approssimazione, con due colpi di regolo, l'utilità

di questa tabulazione appare dubbia. Una svista tipografica nella tavola stessa ci ha costretti a rifare qualche calcolo per scoprire il significato di un simbolo incompleto.

Pure l'esempio a pagg. 200 e 201, sulla soglia di una reazione che porta al nucleo composto $^{113}_{49}$In, ci pare numericamente errato, oltre ad essere affetto dalla citata incongruenza sui segni dell'energia di reazione.

Quattro o cinque altre sviste tipografiche di nessun conto ci sono apparse ad una lettura superficiale; a pagg. 227 e 229 è però due volte riportato, con abbondanza di decimali, che 1 eV è pari a $1.6018 \cdot 10^{-13}$ erg; nè ci è piaciuto il modo erratico di indicare le incertezze sui valori numerici delle costanti fisiche, a pag. 252.

L'opera, pure utilissima, è appesantita talvolta da ripetizioni numeriche. Se la Tav. 2, risistemazione della Tav. 1, ci pare opportuna, non così pensiamo della disposizione della Tav. 7, sui raggi nucleari, ove, in successive estensioni, parecchi dati sono ripresentati anche tre volte. Una presentazione unica, che eventualmente lasciasse bianche le caselle non ritenute interessanti, ci parrebbe più opportuna. Anche le figg. 3, due volte ripetute per il testo francese e inglese, assomigliano da vicino a parte delle figg. 1 e 2 pure duplicate, e avrebbero potuto esservi conglobate.

L'opera risulta in complesso di grande aiuto per il fisico sperimentale, che può rapidamente valutare l'ordine di grandezza dei fenomeni in esame, e per il fisico teorico, che, dalla presentazione sistematica dei dati, può rilevare più facilmente regolarità e anomalie che portano all'interpretazione o al miglioramento di formulazioni approssimate; l'abbondanza dei dati presentati permette anche di sconfinare nel campo delle reazioni nucleari di alta energia e delle reazioni da bombardamento con nuclei medii, ancora da realizzare.

A. Rossi

H. Boerner – *Darstellungen von Gruppen, mit Berücksichtigung der Bedürfnisse der modernen Physik*, 1 vol. in-8° di pagg. XII+287 con 15 figure; Springer-Verlag, Berlin-Göttingen, Heidelberg, 1955; rilegato, Volume LXXIV della collezione *Die Grundlehren der mathematischen Wissenschaften*.

La teoria della rappresentazione dei gruppi è un ramo dell'algebra astratta che trova le sue origini in lavori di Frobenius e di Schur e che, attraverso la scuola di E. Noether, è giunto ai giorni nostri sotto forma di organica teoria che ha trovato la sua esposizione in alcuni moderni trattati di illustri algebristi. Questa di Boerner è, dopo il 1932, la prima esposizione in lingua tedesca che tenga conto delle possibilità applicative della teoria.

Il problema fondamentale della rappresentazione è, nella sua essenza, il seguente: Dato un gruppo G, rappresentare i suoi elementi mediante matrici quadrate di dato ordine, in modo che la rappresentazione sia lineare, che al prodotto di due elementi di G corrisponda il prodotto dalle rispettive matrici e che all'identità di G corrisponda la matrice diagonale unitaria. Il presente volume tratta il problema per certi tipi di gruppi che presentano particolare interesse per la fisica moderna; la trattazione si mantiene tuttavia, come l'autore stesso dichiara, nel campo puramente algebrico, cioè fornisce tutti gli elementi teorici necessari per le applicazioni, senza però passare all'applicazione effettiva. Il corpo delle costanti sul quale è costruita la teoria è in ogni caso un corpo algebricamente chiuso di caratteristica zero e, in molti tratti dell'opera, il corpo complesso. L'esposizione, in molti passi originale e quasi sempre originalmente rielaborata, è studiata in modo che il lettore interessato ad un singolo argomento possa giungervi leggendo solo le premesse strettamente necessarie; a ciò servono le prime righe

di ciascun capitolo, che chiariscono dettagliatamente la struttura logica dell'opera. Aggiungasi che parecchi argomenti sono trattati ciascuno con più metodi diversi. Le nozioni preliminari all'opera sono tutte definite ex novo, e solo per talune dimostrazioni si rinvia a trattati di Algebra. A rendere facile la lettura contribuiscono l'ordine e la chiarezza dell'esposizione, l'accurata scelta delle notazioni, non certo facile in una teoria quale quella trattata, l'ottima veste tipografica, fedele alle tradizioni sia dell'editore che della collezione cui il volume appartiene.

L'opera inizia con una *Prefazione*, nella quale sono esposti brevemente i precedenti e sono chiariti i concetti e le teorie che stanno alla base dell'esposizione. I capitoli sono: I. *Matrici* - II. *Gruppi* - III. *Teoria generale della rappresentazione* - IV. *Le rappresentazioni dei gruppi simmetrici* - V. *Le rappresentazioni dei gruppi lineari generali, dei gruppi unimodulari e dei gruppi unitari* - VI. *Caratteri dei gruppi lineari e dei gruppi di permutazioni. Il gruppo alternante* - VII. *Caratteri e rappresentazioni univoche del gruppo delle rotazioni* - VIII. *Rappresentazioni « spin », anello infinitesimale, ordinario gruppo delle rotazioni* - IX. *Il gruppo di Lorentz*. Seguono una *Bibliografia*, nella quale si rinvia ad opere precedenti per la bibliografia completa sulla teoria della rappresentazione, e un *Indice analitico e degli autori*.

Dall'indice sopra riportato risulta evidente quali sono gli argomenti trattati. A maggior chiarimento precisiamo che i gruppi menzionati sono così definiti: per gruppo lineare s'intende quello di tutte le matrici (quadrate non degeneri di dato ordine) reali o complesse; per gruppo unimodulare quello delle matrici di determinante 1; per gruppo unitario quello delle matrici che lasciano inalterata la forma $\xi_1\bar{\xi}_1 + \ldots + \xi_n\bar{\xi}_n$; per gruppo ortogonale quello delle matrici che lasciano inalterata la forma $\xi_1^2 + \ldots + \xi_n^2$; per gruppo dei movimenti il gruppo delle matrici ortogonali reali di determinante 1; per gruppo di Lorentz quello delle matrici che lasciano inalterata la forma $-\xi_1^2 - \ldots - \xi_t^2 + \xi_{t+1}^2 + \ldots + \xi_n^2$. Data la loro importanza nelle applicazioni, sono studiati in modo particolare il gruppo delle rotazioni nello spazio ordinario e l'ordinario gruppo di Lorentz ($t = 1$, $n = 4$).

M. Benedicty

E. Feenberg – *Shell Theory of the Nucleus*. Princeton University Press, Princeton, 1955, pp. 211. Serie: Investigations in Physics, n. 3.

Perchè funziona così bene il modello a *shell*? È la domanda che l'autore pone al termine del suo libro, senza quasi tentare di dare una risposta, non dico esauriente, ma neppure plausibile. Tuttavia, anche se non esistono giustificazioni teoriche molto fondate della validità di questa teoria dei nuclei, è innegabile che essa descrive bene molti fenomeni, ed è perciò un'ottima cosa che si tenti da parte di un competente come Feenberg di dare un quadro il più esauriente possibile dell'accordo (e del disaccordo) fra i dati sperimentali e le previsioni della teoria.

Nelle intenzioni dell'autore lo scopo del libro è di servire da guida a coloro che hanno già familiarità con gli elementi della meccanica quantistica e della fisica nucleare, per seguire gli sviluppi del modello ad accoppiamento spin-orbita e la sua applicazione all'interpretazione degli spin e delle parità, dei momenti magnetici e di quadrupolo elettrico, dell'isomerismo e del decadimento β di tutte le specie nucleari. Tuttavia il testo è molto succinto e la sua comprensione presuppone una preparazione abbastanza specifica, in particolare per quanto riguarda le transizioni β e il calcolo degli elementi di matrice dei relativi operatori in accoppiamento j-j.

Un'osservazione che è necessario fare è che manca una valutazione critica dei limiti di validità della teoria: l'abbon-

dante materiale è presentato senza una discussione adeguata e se ci si vuole fare un'idea di quanto le previsioni si discostino dai dati sperimentali, è necessario un paziente lavoro da parte del lettore. Sarebbe stato inoltre opportuno che il lettore fosse stato messo al corrente del fatto che in alcuni casi i dati spiegati dal modello a *shell* possono essere spiegati ugualmente bene dai modelli collettivi, i quali, inoltre talvolta rendono conto di fenomeni che il solo modello a *shell* non è sufficiente a interpretare.

Nel complesso la ricchezza dei dati, sia teorici che sperimentali, raggruppati in 82 Tabelle e 18 figure, e la abbondantissima bibliografia, aggiornata a tutto il 1953, fanno di questo libro un testo utilissimo di consultazione per il ricercatore già addentro all'argomento.

M. Cini

C. H. Bachman – *Physics, A Descriptive Interpretation*. 1 vol. in-8° di pp. VIII+497. John Wiley & Sons, New York, 1955.

Questo spiritoso testo del prof. Bachman riflette la sua notevole abilità didattica, esercitata per vari anni a favore degli studenti della Syracuse University che devono impadronirsi dei principi essenziali della fisica senza poter fare uso degli strumenti matematici. Il volume presenta molte caratteristiche originali, a parte le illustrazioni umoristiche improntate allo stesso stile dei noti disegni di Gamow: la fisica moderna è fusa con quella classica, in modo da non introdurre distinzioni che hanno senso sul piano storico, ma non su quello logico; l'ordine dell'esposizione procede dalla microfisica verso la fisica dei fenomeni macroscopici e astronomici; come fonte di esempi pratici, viene usato il corpo umano con i relativi organi motori e di senso; le applicazioni industriali della fisica sono trattate in un capitolo a parte, cui segue un panorama conclusivo dell'evoluzione storica della scienza e delle sue prospettive per il prossimo futuro. Pure originali, e scelti bene, appaiono gli esercizi di discussione posti alla fine di ogni capitolo; con soli argomenti qualitativi, essi obbligano lo studente ad approfondire numerosi punti critici, che di solito vengono trascurati nei corsi di fisica per i licei e per le facoltà di scienze mediche e naturali.

V. Somenzi

K. Hauffe – *Reaktionen in und an festen Stoffen*. Springer-Verlag, 1955. Pagg. XII-696, 427 figure.

Negli ultimi anni ha assunto sempre maggior importanza il problema della struttura dei solidi in relazione ai diversi processi ai quali essi prendono parte, come diffusione, reazioni allo stato solido, ossidazioni e riduzioni, e anche processi di assorbimento e catalisi, e ne è indice il numero di articoli e di opere monografiche che più o meno direttamente dedicano la loro attenzione a tali argomenti. Il presente libro, 2° della serie di monografie di Chimica generale e inorganica edite da G. Jander e W. Klemm, riguarda appunto questo soggetto.

Gli argomenti esposti sono i seguenti. Trattazione generale delle strutture difettive (pagg. 1-40). Comportamento elettrico dei cristalli ionici e covalenti (41-216). Problemi inerenti ai processi di chemiadsorbimento e di catalisi, in relazione alla formazione dello strato superficiale (216-259). Diffusione nei solidi (259-410). Ossidazione di metalli e leghe (411-571). Reazioni allo stato solido (571-648), e infine processi di riduzione di ossidi e solfuri (648-679). Il titolo forse lascerebbe supporre una maggiore estensione della parte che riguarda le reazioni catalitiche, ma è anche vero

che muovendo l'Autore dal punto di vista del significato delle strutture difettive nei vari processi, il campo della catalisi è ancora in uno stato così fluido che è impossibile al giorno d'oggi dargli un assestamento organico. Sono esaminati in dettaglio invece i contributi fondamentali dati dall'Autore e dai suoi collaboratori alla discussione del problema dell'adsorbimento chimico in relazione alla formazione di uno strato esterno, e il trovar riunito in un unico volume quanto era finora sparso nelle riviste scientifiche costituisce una notevole attrattiva per chi lavora su tali argomenti. Questo capitolo, e gli altri nei quali vengono applicati i principi generali dello stato solido, come i capitoli sulla ossidazione e sulla riduzione, costituiscono probabilmente le parti migliori e più utili del libro, anche se, a causa della vastità degli argomenti, in questi capitoli ha dovuto scegliere se dare una maggiore completezza panoramica del gran numero di fatti sperimentali noti, o se, viceversa, limitando gli esempi discussi, approfondire e discutere in dettaglio alcuni casi significativi. Questa seconda soluzione adottata dall'Autore risulta ben giustificabile se si considera che la maggiore difficoltà in questo campo non è tanto il compito indubbiamente complesso di informazione, facilitato del resto nel presente caso da numerosi richiami bibliografici, nonchè dall'esistenza di recenti opere monografiche e articoli di rivista che trattano gli stessi argomenti, quanto la corretta, appropriata discussione e applicazione ai casi reali di principi e di teorie. Risultano quindi di minor importanza alcune inevitabili omissioni, anche se il criterio della scelta può in alcuni casi non trovar tutti consenzienti. Così, per esempio, si sarebbe potuto augurare una maggior estensione e aggiornamento nel caso dei lavori di Volkenstein sui problemi di assorbimento e catalisi.

Il libro è molto ricco di figure e di grafici riportati dai lavori originali, cosa questa particolarmente utile in un campo nel quale l'esatta e dettagliata informazione sperimentale ha un posto di primo piano, e inoltre si presenta in una veste tipografica molto nitida.

Nell'insieme quindi il presente volume costituisce una utilissima e autorevole opera su un argomento molto attuale, ed è pertanto molto raccomandabile a quanti si occupino, direttamente o indirettamente, di problemi inerenti ai solidi.

A. Cimino

H. Faul – *Nuclear Geology. A Symposium on nuclear phenomena in the earth sciences.* John Wiley & Sons, New York, 1954, pp. 413.

Un libro che venga pubblicato come raccolta di monografie su una certa branca della scienza ha generalmente un duplice carattere. Da un lato vengono elencati i risultati raggiunti nello studio dell'argomento in questione, inquadrati per quanto è possibile in teorie coerenti, dall'altro si indicano i problemi, sperimentali e teorici, ancora parzialmente o totalmente insoluti.

Nel caso di « Nuclear Geology » si ha invece l'impressione di trovarsi di fronte a un caso un poco diverso.

L'applicazione dei risultati e delle tecniche della fisica nucleare alla geologia è infatti troppo recente perchè si siano potuti raccogliere un numero di dati sperimentali sufficiente per dare una risposta, anche di prima approssimazione, a molti degli interrogativi della geologia.

I dati sulla distribuzione delle sostanze radioattive naturali più diffuse, Uranio, Torio, Potassio, non consentono, ad esempio, di formulare una teoria coerente sulla generazione di calore all'interno della terra per effetto della radioattività.

Troveremo perciò in questo libro essenzialmente una esposizione di quelli che sono i grandi problemi della geologia, con la indicazione delle vie che

attualmente sembrano più idonee per la soluzione di essi, oltre a una esposizione aggiornata di tutti i dati sperimentali possibili.

I problemi sono essenzialmente quattro: il ruolo svolto dalle trasformazioni radioattive nella produzione di calore all'interno della terra, influenze degli elementi radioattivi sulla formazione del petrolio, determinazione dell'età delle rocce e dell'età della terra, origine della terra e del sistema solare.

Per la trattazione di questi punti è stato necessario naturalmente far precedere i capitoli ad essi specificamente dedicati da altri in cui vengono esposti i metodi sperimentali e i risultati numerici che rappresentano i punti di partenza della discussione. Così, nel caso del primo problema, si ha una serie di capitoli contenenti le misure di abbondanza, nei vari tipi di rocce, delle sostanze radioattive naturali.

La trattazione dei vari argomenti è dovuta a un numero abbastanza grande di Autori diversi, si hanno perciò fatalmente ineguaglianze di metodo nella esposizione e qualche ripetizione.

La bibliografia citata, raccolta in fondo al volume, abbraccia circa 700 lavori; inoltre alcuni capitoli sono seguiti da un elenco di libri di avviamento o di rassegna.

Il libro è dedicato soprattutto ai geologi. In esso, però, sono descritte ampiamente alcune applicazioni delle nuove tecniche della fisica nucleare, a volte fino ai limiti delle possibilità sperimentali, come, per esempio, nella misura di debolissime radioattività. Questo fa pensare che la lettura di « Nuclear Geology » possa riuscire utile anche a tutti coloro che lavorano nel campo della fisica nucleare sperimentale.

G. CORTELLESSA

Direttore responsabile: G. POLVANI Tipografia Compositori - Bologna

Questo fascicolo è stato licenziato dai torchi il 13-VIII-1955